Summer 2015

Particle gel propagation and blocking behavior through high permeability streaks and fractures

Abdulmohsin Imqam
Missouri University of Science and Technology, ahikx7@mst.edu

Department: Geosciences and Geological and Petroleum Engineering

PARTICLE GEL PROPAGATION AND BLOCKING BEHAVIOR THROUGH HIGH PERMEABILITY STREAKS AND FRACTURES

By

ABDULMOHSIN HUSSAIN IMQAM

A DISSERTATION

Presented to the Faculty of the Graduate School of the

MISSOURI UNIVERSITY OF SCIENCE AND TECHNOLOGY

In Partial Fulfillment of the Requirements for the Degree

DOCTOR OF PHILOSOPHY

in

PETROLEUM ENGINEERING

2015

Approved
Baojun Bai, Advisor
Shari Dunn-Norman
Ralph Flori
Mingzhen Wei
Mojdeh Delshad

ABSTRACT

Water channeling, one of the primary reservoir conformance problems, is caused by reservoir heterogeneities that lead to the development of high-permeability streaks and fractures. These streaks and fractures prevent large amounts of oil from being recovered. The ultimate objective of this research was to provide comprehensive insight into designing better particle gel treatments intended for use in large openings, including open fractures, high permeability streaks, and conduits to increase oil recovery and reduce water production.

An intensive laboratory study was conducted to better understand the injection and placement mechanisms of millimeter and micron size preformed particle gels (PPGs) through thief zones. Core flooding experiments were also conducted to investigate the effectiveness of micron-size PPGs to correct the heterogeneity within reservoirs. The effectiveness of combined conformance control (gel), stimulation treatments (acid), and mobility control treatments (polymer) were examined for their ability to increase oil recovery from non-cross flow heterogeneity cores.

A PPG partially blocks a large channel rather than fully blocking it. A PPG pack permeability of oil was much more than PPG pack permeability of water. The gel formed a cake on the low-permeability layers, reducing their permeability. Fully swollen gel particles had better injectivity than did partially swollen particles with a larger diameter size. The PPG was used successfully used to correct both non-cross and cross flow heterogeneity problems. Combined PPG with either acid or polymer showed promise results of increasing oil recovery.

ACKNOWLEDGMENTS

IN THE NAME OF GOD, MOST GRACIOUS, MOST MERCIFUL

First, I am eternally grateful to Allah for helping me accomplish this work.

I would like to express my sincere thanks to my advisor. Dr. Bajojun Bai. I would not have been able to complete this research without his assistance, support, and friendship.

I must also thank the Libyan Ministry of Education for supporting me during my academic studies. I am thankful for the members of my advisory committee: Dr. Shari Dunn-Norman. Dr. Ralph Flori, Dr. Mingzhen Wei, and Dr. Mojdeh Delshad for their guidance and assistance. I am a particularly grateful to Dr. Shari Dunn-Norman for allowing me serve as a teaching assistance throughout my time at Missouri University of Science and Technology.

I cannot fully express my thanks and gratitude to my mother and father. They have showered me with unlimited support and I dedicate this work to them. I am also tremendously grateful for my precious wife and my lovely kids for their support, patience, and love. I am grateful for the help I received from the department administrative staff particularly Patti Robertson, Paula Cochran, and Patti Adams. I would like also to express my appreciation to Nathaniel Inskip for his great help in lab.

Finally, I would like to thank my colleagues and friends: Dr. Mahmoud Elsharfi, Dr. Ayman Almohsin, Dr. Paul Tongwa, Dr. Farag Muhammed, Dr. Hao Zhang, and Hilary Elue.

TABLE OF CONTENTS

LIST OF ILLUSTRATIONS

Page

LIST OF TABLES

Page

NOMENCLATURE

Symbol	Description
A	Cross-sectional area (cm^2)
a	Coefficient factors, (dimensionless)
b	Coefficient factors, (dimensionless)
C_{ppg}	Gel compressibility (psi^{-1})
C_{brine}	Brine concentration, (wt. %)
C_{HCl}	Hydrochloric acid concentration, (wt. %)
D	Inner conduit diameter, (mm)
D_g/D_p	Particle opening ratio, (dimensionless)
K	Core permeability (mD)
ESC	Equilibrium swelling capacity, (ml/ml)
E	Constant coefficients, (dimensionless)
E	Plugging efficiency (%)
E_R	Total recovery efficiency (%)
E_D	Displacement efficiency (%)
E_A	Areal efficiency (%)
E_I	Vertical efficiency (%)
K	Core permeability,(mD)
Ko	Intrinsic permeability (mD)
K_{PPG}	PPG pack permeability (mD)
K_{GB}	PPG pack permeability before the load pressure (mD)
K_{GA}	PPG pack permeability after the load pressure (mD)
K_{GR}	PPG pack permeability reduction factor (%)
K_i	Initial core permeability, (mD)
K_a	Core permeability after adding PPG, (mD)
K_f	Final core permeability after adding HCl, (mD)
K_{RD}	Core permeability reduction, (%)

K_{RT}	Core permeability retained, (%)
Fr	Resistance factor, (dimensionless)
Frrw	Residual resistance factor to water, (dimensionless)
Frro	Residual resistance factor to oil, (dimensionless)
$G`$	Storage moduli, (pa)
L	Lenght of the gel in channel, (cm)
L	Core length, L, (cm)
M	Constant coefficients, (dimensionless)
n	Gel elastic index
P_{inj}	Initial stable injection pressure, (psi)
Vo	Initial PPG volume before compression, (cm^3)
V_2	Volume of PPG after compression, (cm^3)
V_p	Cumulative volume of total fluid production, (cm^3)
V_i	Cumulative volume of total water injection, (cm^3)
V_2	PPG volume after swelling, (cm^3)
V1	PPG volume before swelling, (cm^3)
Vi	Initial volume of swellable PPG, (cm^3)
Vf	Final volume of PPG volume after deswelling, (cm^3)
v	Superficial velocity, (ft/day)
q	Injection flow rate, (cm^3/s)
ϕ	Porosity, (%)
μ	Viscosity of the brine, (cp)
μ_{gel}	Gel viscosity, (cp)
Δ_P	Pressure drop, (atm)
ΔP_{PPG}	PPG injection drop, (psi)
ΔP_{brine}	Brine injection drop, (psi)
Δ_V	Change in PPG after compression, (cm^3)
Δ_{Pg}	Change in pressure across gel, (psi)
γ	Shear rate, (1/sec)
λw	Water mobility
λo	Oil mobility

λ_{gel}	Gel mobility
α	Shape parameter characteristic the pore structure
r_p	Average porous radius, (cm)
e	Adsorbed gel layer thickness
Π	Swelling pressure, (psi)
Π_{osm}	Osmotic pressure, (psi)
$\Pi_{elastic}$	Elastic pressure, (psi)
Π_{mixing}	Polymer-solvent mixing pressure, (psi)
Π_{ions}	Ionic pressure, (psi)

1. INTRODUCTION

1.1. STATEMENT AND SIGNIFICANCE OF THE PROBLEM

Excess water production has long been considered a major problem leading to the life-shortening of oil and gas wells and operational problems. An estimated average of three barrels of water are produced for each barrel of oil produced worldwide (Bailey et al., 2000). The total cost related to separating, treating, and disposing of unwanted water is approximately $50 billion per year (Hill et al., 2012). Water can flow into the wellbore as a result of either near-wellbore problems or reservoir-related problems (Seright et al., 2001). The mechanisms that contribute to this undesired water production must be fully understood before the appropriate treatment can be chosen. High permeability streaks, fractures, conduits, and fracture-like features can expedite undesirable water channeling and early water breakthrough during water flooding. As a result, large amounts of oil remain un-swept as a large water flood bypasses oil-rich un-swept zones/areas.

Gel treatments have been proven as a cost-effective chemical conformance control technology that can be used to reduce the fluid flow in these large open features. The application of this technology can assist with controlling water production, significantly increasing the oil production, extending the economic life of a reservoir. In-situ bulk gels traditionally have been used for this purpose. However, preformed particle gels have recently attracted much attention because they can solve some of the problems associated with in-situ gel systems. These problems include the dilution and dispersion of the gallant and the chromatographic separation of the gallant solution. (Chauveteau et al., 2001, 2003; Coste et al., 2000; Bai et al., 2007a, 2007b).

Commercial preformed gels currently available include millimeter-size particle gel (PPG), microgels, and submicron gels. The differences between each are primarily related to particle size, swelling ratio, and swelling time. The millimeter-size particles are not only more distinguishable but also more reliable than other types of particle gels when plugging large pore opening features (Imqam et al. 2014). It is estimated that PPGs have been used to treat more than 5,000 wells (Bai et al. 2013).

A gel treatment's success depends heavily on the gel's ability to extrude through fractures and channels during the placement process. Thus, understanding the mechanism, performance, and behavior of gel propagations and plugging efficiencies through these high permeability streaks is the key to a successful conformance control treatment.

The primary objective of this research was to provide a comprehensive study of gel treatment optimization to solve excess water production problems and increase oil recovery.

1.2. EXPECTED IMPACTS AND CONTRIBUTIONS

Results obtained from this research will promote using the PPGs for conformance control in mature reservoirs as the mechanism and the performance of PPGs extrusion through high permeability streaks and fracture were deeply investigated. Understanding the mechanism and performance of PPGs are a crucial to obtaining a better blocking efficiency and improving conformance control objectives. The results gathered from this work can be used to optimize the PPGs design as it requires for achieving a successful gel treatment and will aid to select future conformance control candidates.

The following information were provided from the research:

- The factors that could affect extrusion and placement through high-permeability zones and fractures were identified. Reservoir property factors such as permeability, fracture width, permeability contrast ratio, flow communication between layers, and pore throat size were each studied. The PPG's properties factors including brine concentration (gel strength), particle size, gel concentration, PPG injection pressure, PPG slug volume, and injection velocity were also investigated.
- The mechanisms and factors that help to reduce water cut and increase oil recovery during PPG treatments were investigated. These mechanisms include study the disproportionate permeability reductions and investigate the oil recovery incremental. Both homogenous and heterogeneity experimental models (crossflow and non-cross flow formations) were assembled to accomplish these objectives.
- Studied the mechanisms associated with PPG injection (e.g., retention and dehydration) and studied the mechanisms associated with PPG placement (e.g., washout and dehydration).
- Based on lab results data, empirical correlation models were built and inserted into a simulator for better gel optimization and performance predictions. Regression techniques were used to develop these models.

1.3. OBJECTIVES

The primary objective of this research was to develop a mechanistic understanding of particle gel systems to increase oil recovery and reduce water production. Extensive core flooding experiments were performed to better understand gel

particle extrusion mechanism, process, and performance through high permeability streaks and fracture. This research evaluated the effect of two different particle gel sizes ranges, millimeter and micron sizes. The following objectives were established for this research activity:

- Determined the factors that impact the permeability of gel pack permeability. A gel pack that has a desired permeability can be designed by selecting proper gel strength and particle sizes at reservoir pressures. Gel pack permeability is very important for gel treatment success because an optimized gel treatment design target on reducing the permeability to the degree as planned.
- During particle gel propagation into desired formations (high permeability), portion of gel formed a cake on low permeability. Therefore, this research determined what factors affect the gel cake damage to the low permeability formations and evaluated the effectiveness of using acid stimulations to remove such damage.
- The factors that impact gel extrusion and placement through conduits were investigated. Two fluid phases (oil and water) flew through the conduit were investigated to determine to what degree PPGs reduce channel water permeability as compared to its oil permeability.
- The factors that can significantly affect gel propagation through high permeability formations were explored. Thus, particle gel's mechanism and performance were evaluated in terms of gel injectivity, gel retention, gel dehydration, gel wash-out, disproportionate permeability reduction, and oil recovery incremental during gel injections.

- A particle gel's ability to correct heterogeneity formations was studied in both heterogeneity natures, cross flow and non-cross flow formations. Two experimental models were used to study a gel's ability to reduce water production and increase oil recovery from low permeability or non-swept zones.
- Based on these intensive experiments work, empirical correlations models were developed for not only better gel rheology predictions but also better gel optimizations. The results obtained from these experiments were used to build and validate a simulator developed (UT-Gel) for gel treatment purposes.
- Particle gel were combined with additional technologies (e.g., stimulation and mobility control treatments) to investigate the effectiveness of utilizing these treatments with conformance control technology. This combination then was used to gain a better oil incremental from the un-swept rich oil low permeability zones.

The results gathered from this research provide a comprehensive knowledge and insight into particle gel mechanisms and performance that increase oil recovery and generate additional revenue.

1.4. SCOPE OF THIS WORK

This research was primarily a laboratory study that was conducted to investigate factors affecting the particle gel propagation and plugging efficiency of the gel intended for use in super K formations (e.g., fractures, channels and/ or conduits, and large permeability streaks). Core flooding experiments assist in understanding the prevailing mechanism and performance of particle gel propagation through these porous media. The

experiment also provided the necessary data required to develop and validate a reservoir simulator to obtain better design and optimize gel treatment in field conformance applications. Figure1.1 shows the constructions of the main experiments performed to accomplish the research objectives.

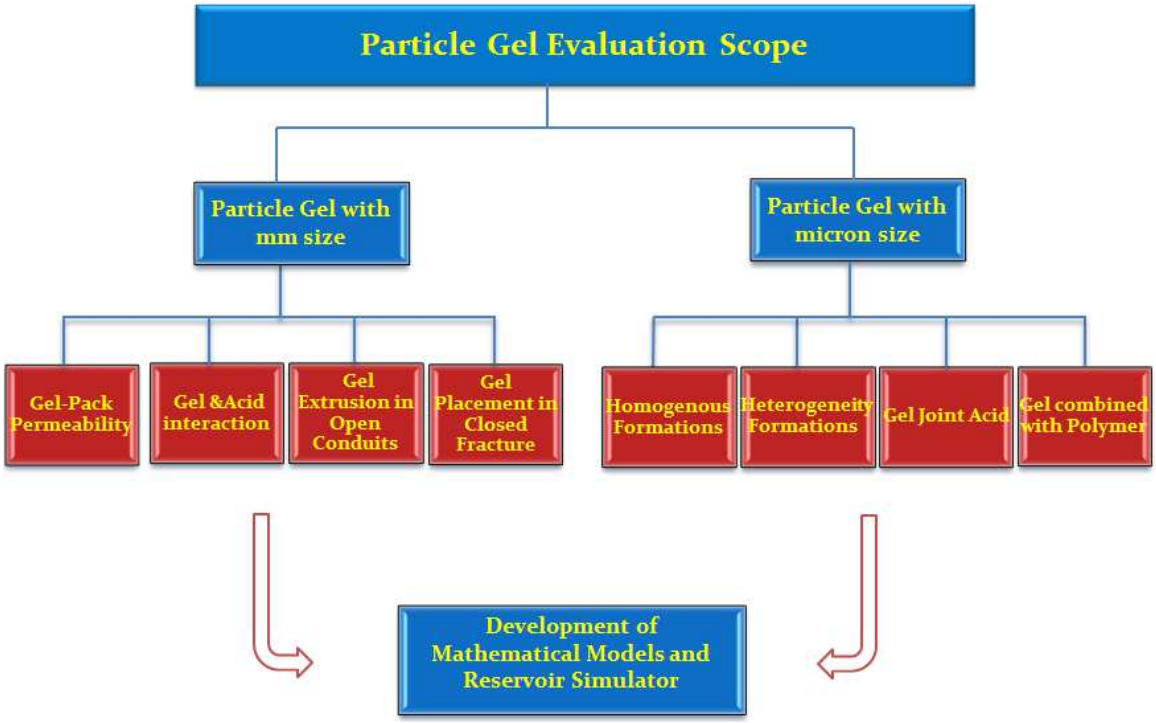

Figure 1.1—Scope of the research.

2. LITERATURE REVIEW

2.1. RECOVERY MECHANISMS

There are three main mechanisms to produce oil: primary recovery, secondary recovery, and tertiary recovery. Primary oil recovery involves naturally occurring reservoir characteristics or properties that induce the flow of oil. Such mechanisms include solution and gas cap drive, water drive, gravity drainage, and a combination of the aforementioned primary oil recovery mechanisms. Primary recovery accounts for 12-15% of the original oil in place (OIIP). The primary recovery methods become inadequate in sustaining economic production rates as oil reservoirs become depleted.

Secondary recovery mechanisms typically involve the injection of either gas or water into reservoir in an attempt to pump the oil out of the reservoir. Secondary recovery accounts for 15-20% of the OIIP. Both primary and secondary oil recovery methods can generally achieve up to 35% recovery of the original volume of oil in place. (Green & Willhite, 1998)

Heterogeneity within a reservoir is one of the primary reasons neither primary nor secondary recovery mechanisms can retrieve large amounts of hydrocarbon recovery. Reservoir heterogeneities lead to the development of high-permeability streaks. These streaks include open fractures, fracture-like features, caves, worm holes, and conduits. These high-conductivity areas inside the reservoir only occupy a small fraction of the reservoir but it captures a significant portion of injected water. As a result, large amounts of oil remain un-swept as large water injections bypass oil-rich un-swept zones/areas.

In the United States, 45% of the discovered oil reserves are unrecoverable by secondary recovery technologies. They are instead targeted by Enhanced Oil Recovery (EOR) methods. Enhanced Oil Recovery makes it possible to recover more oil by improving the efficiency of oil displacement while rehabilitating the primary recovery mechanism.

The following formulae represent the factors that are responsible for increasing oil recovery:

$$E_R = E_D \times E_A \times E_I \quad \text{..... (2.1)}$$

where E_R is the total recovery efficiency, E_D is the displacement efficiency, E_A is the areal sweep efficiency, and E_I is the vertical efficiency.

Enhanced Oil Recovery is classified into three main categories: gas injection, chemical injection, and thermal recovery. Each EOR method targets the manipulation of a reservoir force to reduce the residual oil and/or remaining oil.

Enhanced Oil Recovery methods focus on increasing either displacement efficiency by reducing residual oil saturation in swept regions or sweep efficiency by displacing the remaining oil in un-swept regions. Residual oil saturation is a function of the capillary number, which is the ratio of viscous force to capillary force. Oil in un-swept regions can be recovered by (1) increasing the viscosity of the displacing fluid, (2) reducing oil viscosity, (3) modifying permeability, and/or (4) altering wettability.

This study was conducted in an attempt to use chemical treatment to modify heterogeneity inside reservoirs. Hence, oil recovery would increase by improving sweep efficiency and reducing excessive water production.

2.2. EXCESSIVE WATER PRODUCTION

Water production associated with oil and gas production is becoming a major technical, environmental, and economical problem worldwide. Water production can shorten the productive life of oil and gas wells creating severe problems (e.g., equipment corrosions, hydrostatic load, and sand fine migrations). It is estimated that over 15 billion barrels of water are produced annually, approximately eight barrels of water are produced for each barrel of oil (Environmental Protection Agency, 2000). Worldwide, an averages of three barrels of water are produced for each barrel of oil (Bailey et al. 2000). The total cost to separate, treat, and dispose of the unwanted water is estimated to be approximately $50 billion per year **(**Hill et al. 2012).

Excessive water production becomes prevalent as reservoirs becoming more mature. This increase impacts on the profitability of hydrocarbon assets. Fully understanding the mechanisms responsible for undesired water production is crucial to designing efficient solutions to the problem.

A large number of mechanical, completion, and chemical treatment technologies are available to mitigate water related problems. These technologies decrease undesired water production. They also increase hydrocarbon productions rates significantly and extend the reservoir's economic life.

2.2.1. Mechanisms of Unwanted Water Production. Many different things contribute to unwanted water productions. Understanding the nature of water production is the primary key in controlling it. Therefore, an effective strategy can be formulated to control water productions if the water production mechanism is understood (Seright et al. 2001). The flow of water into a wellbore can occur along two types of paths. Water can flow into the wellbore through paths that is separate from hydrocarbons path. Water can also be co-produced with oil. This production typically occurs later in the life of a water flood when the reservoir becomes more mature.

The sources of co-produced water can occurs either due to water exist naturally inside reservoirs (e.g., aquifers and formation waters) or due to water injected into reservoir from external sources. For water to flow through reservoirs, water saturations should exceed the connate water saturations. The relative permeability to water increases as water saturation increase beyond the connate water saturation. Water production becomes even higher due to the reservoir heterogeneity. Reservoir heterogeneity can result in water channeling through high permeability streaks including fractures, conduits, faults, and discontinuous layers. Channeling can be further exacerbated by lower water viscosity (as compared to oil) particularly during a water flood.

2.2.2. Cause Water Production Problem. Water production problems issues are related to one of the problems: near well bore problems and/or reservoir related problems. The causes of the excessive water production are summarized in Table 2.1.

Table 2.1—A summary of the factors that lead to excessive water production.

Near-wellbore Problems	Reservoir-related Problems
Casing leaks	Coning or cresting
Channel behind pipe	High permeability streaks
Shutting- off perforations	Fracturing job went to water zone
Lost circulations while drilling/work over	Watered-out zone
Completion into water zone	Channel from injector
Temporary chemical isolation	Fractures, fissures, voids, and conduits

2.2.2.1. Near wellbore problems. They can occur as a result of either mechanical or completion problems. They tend to occur early in the well's life.

2.2.2.1.1. <u>Mechanical problems.</u> Poor mechanical integrity within the casing such as holes created by corrosion, wear/splits due to flaws, excessive pressure, and formations deformation contributes to leaks (Figure 2.1). These leaks allow unwanted water to enter the casing, causing water to rise unexpectedly. Temperature logs and water analysis comparisons may be used to locate the source of the leak.

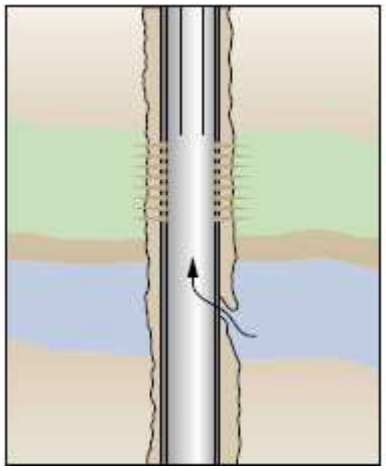

Figure 2.1—Mechanical problem (Bailey et al. 2000).

2.2.2.1.2. <u>Completion problems.</u> Common completion problems include channels behind casing, completions too close to water zone, and fracturing out of zone.

- Channels behind casing

Channel behind casing (Figure 2.2) is developed as a result of either poor cement-casing or poor cement-formation bond. This problem can occur at any time during well's life, it likely occurs just after the well is either completed or stimulated. Unexpected water production at these times strongly indicates that a channel may exist. Temperature, noise, and bond logs can verify the existence of this problem.

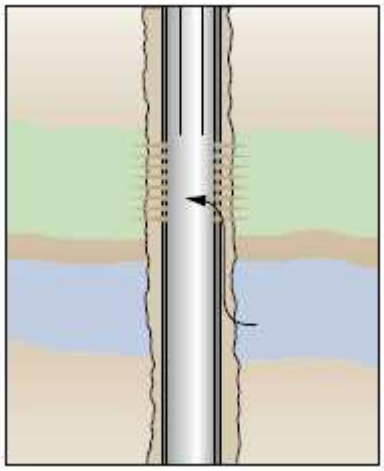

Figure 2.2—Channel behind casing (Bailey et al. 2000).

- Completions too close to water zone

Completion into undesired zones, where water saturations are higher than connate water saturations, allows for immediate water production (Figure 2.3). Perforations made above the original water-oil or water-gas contact, throughout the coning or cresting allow the water to be produced more quickly and easily. The logs, core data, and driller daily report should be reviewed to determine the cut-off point of moveable water.

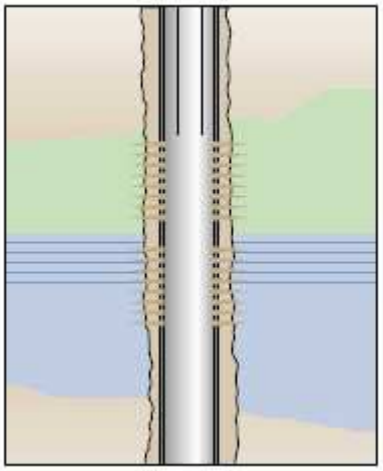

Figure 2.3—Completion close to water zone (Bailey et al. 2000).

- Barrier breakdowns

Hydraulic fractures may cause barrier breakdown near the wellbore, leading to excessive water production through the well. This barrier could be a natural barrier such as dense shale layers that separate the different fluid zones.

2.2.2.2. Reservoir-related problems. They can be the result of channeling through higher permeability zones or fractures. They can also be related to coning, cresting, reservoir depletions, and fractures out of zones. They typically occurred during the later in the well operators' life.

2.2.2.2.1. <u>Channeling through high permeability streaks or fractures.</u> Water channeling is the result of reservoir heterogeneities that lead to presence of high permeability streaks. Fractures, fractures like-features, and conduits are the most common causes of channeling. Channels can emanate via natural fractures from either a natural water drive, or induced fractures (from water flooding mechanisms), or related operations. High permeability streaks result in a premature breakthrough of water,

leaving behind large quantities of oil that remain un-swept in low permeability zones. As the driving fluid sweeps the higher permeability intervals, permeability to subsequent flow of fluid becomes even higher; which end up with increase of water-oil ratios through the life cycle of the well.

2.2.2.2.2. <u>Coning and cresting.</u> Water coning in vertical wells and water cresting in horizontal wells (Figure 2.4) both occurs when the producing formations are located above a water zones and by when pressure gradient declined near the well bore. This decline pressure draws the water from low connected zones toward the wellbore. Water can break into the perforated or open hole sections, displacing either all or part of the hydrocarbons.

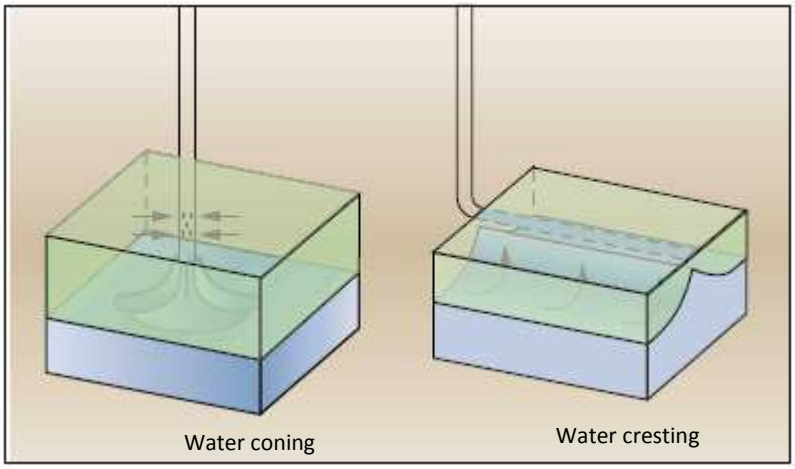

Figure 2.4—Water coning vs cresting (Bailey et al. 2000).

2.2.2.2.3. <u>Reservoir depletions.</u> If the problem is caused by reservoir depletion, there is a very little chance that can be done to reduce water productions as economical amounts of hydrocarbon must be present to produce. Generally at the later stage of

production, the focus on water control will shift from preventing to reducing water production cost.

2.2.2.2.4. <u>Fracturing out of zone.</u> When the hydraulic fracture was not designed properly, the fracture unintentionally extends and breaks into water zones. Therefore, coning or cresting through fracture can result in an early breakthrough of water. Increasing water productions substantially. A spinner survey, a tracer survey, and well testing can each be used to detect such problem.

2.3. WATER PRODUCTION DIAGNOSTIC PROBLEM

Several technologies can be used to control undesired water production. Each of these technologies requires a different approach. The appropriate selection of the water control technology is dependent on a correct diagnostic of the water production problem. Incorrect, inadequate, or incomplete diagnostics are the primary reasons that water control treatments become ineffective (Seright et al. 2001).

The nature of the problem must identified correctly before it can be treated successfully. The reasons for incorrectly identified problem include:

- Incorrect assumption that all water production problem can be effectively treated by one type of treatment
- Uncertainty about the methodology for the diagnostic,
- Lack of time or money to perform the diagnostic on marginal well.

Understanding not only fluid movement through reservoirs but also how that fluid interacts with a wellbore are the primary keys to achieving successful water treatment. Seright et al 2001 categorized the various types of water productions diagnostic based on

extensive reservoir and completion engineering studies. They proposed a gaudiness for performing effective water problem diagnostic from least to most difficult. This proposal approach is summarized in Figure 2.5.

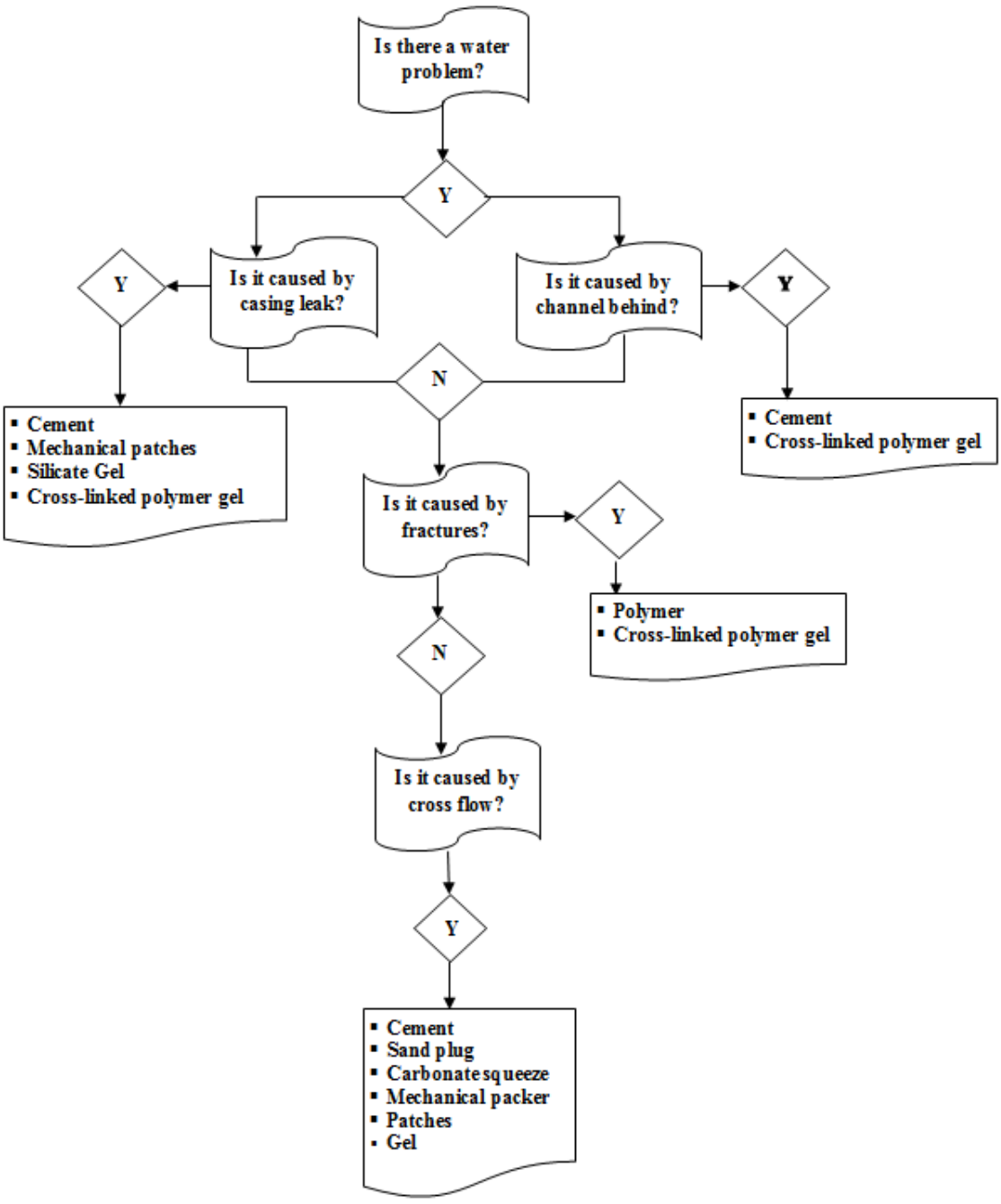

Figure 2.5—A diagnostic approach to water production.

Understanding the water production problem is the key to successfully implementing and designing a water shut-off treatment. In their proposal, they suggested that first step in the diagnostic process is to ask if water production problem is available. An unexpected increase in water cut indicates a water production problem. Plots of water oil ratio (WOR), fluid production versus time, and reservoir simulations studies can each be used to identify the development of water production problem. If water breakthrough is experienced early in the well's life, then completion problem should be examined first to determine possible reason for the development. If water entry occurs at later stage in the well's life, either mechanical or reservoir problems should be investigated first.

It must next be determined whether or not, the problem is caused by either leaks or channel behind pipe. The methods most commonly used to diagnose this problem include mechanical integrity tests, temperature surveys, production logs, cement bond logs, and noise logs. The mechanical integrity test is conducted by pressurizing up the annulus between the casing and the tubing to determine whether or not the pressure will hold. Cement bond logs are produced by several types of acoustic logging tools to evaluate the cement condition and to diagnostic the problems associated with channels behind casings. The method most commonly used to repair casing leaks involves either cement or mechanical patches. When the leak is quite small (e.g., pinhole or thread leaks) gel treatment, however, are more successful than these two applications because gel can transport easily through these small leaks and block them. Problem created by flow behind pipe can treated by cement. Cement can perform extremely well for this type of application if the channel to be plugged is not too narrow; a gel is a better solution when narrow channels are encountered.

Fluid flow around the wellbore identified either radial or linear. A linear flow is associated with channeling through fractures or fracture-like features. A radial flow is associated with flow in an un-fractured reservoir. Core and log analyses, pulse tests and pressure transient tests, and internal trace studied can be used to define this flow. Seright et al. 2001 proposed a simple and inexpensive method used to determine the flow around well bore. They proposed the injectivity/productivity calculation based on Darcy equation to identify the flow behavior:

If the flow is linear, then

$$q/\Delta p >> \sum kh \,/\, [141.2\ \mu\ ln\ (r_e/r_w)] \quad \text{.....(2-2)}$$

If the flow is radial, then

$$q/\Delta p \leq \sum kh \,/\, [\ 141.2\ \mu\ ln\ (r_e/r_w)] \quad \text{.....(2-3)}$$

This calculation will not always distinguish between a radial and a linear flow. It can, however, provide an indication of the flow geometry near the wellbore. Gel treatments can potentially correct this problem. These treatment rely on the gel's ability to reduce the water permeability much more than oil permeability.

The possibility of a cross-flow between a reservoir strata must be addressed once the fracture-like features are eliminated as the cause of water production problems. If the fluids can cross-flow between adjacent water and hydrocarbon strata, gel treatment may not be used effectively. In contrast, if fluid cannot cross-flow between adjacent strata, gel treatment can be used effectively. Several methods are used to assess whether or not

cross flow exists between strata. These methods include pressure test between zones, logs, injection/production profile, simulation, and seismic data.

The main reason for the industry failure to control unwanted water production was a lack of understanding of the different problems and the consequent application of inappropriate solutions. The key to successful water control production is the proper diagnostic of the problem. Several different analytical techniques can be used to distinguish between the different sources of unwanted water production. These techniques employ various types of information including water /oil ratio, production data, and logging measurements. The following subsections include a brief discussion on the most three commonly used diagnostic methods: diagnostic plots, logging measurements, and numerical methods.

2.3.1. Using Plots. Graphical plots of data are visual displays that assist in defining a water problem's source during the well's life. In the oilfield application, the operator can quickly identify the problem where the plots can be drawn by hand or using spreadsheet software. Many plot shapes can be used to identify and determine a water problem's source.

2.3.1.1. Water/oil ratio vs time-WOR, WOR derivative plots. A Log- log plot of the (WOR) vs time were found to be effective when attempting to identify the production trends and problem mechanisms behind water production (Chan, 1995). The derivative of the WOR vs time can be used to determine when the excessive water production is produced by water coning or multilayer channeling. Several examples use WOR vs time plots to identify water problems are shown in Figures 2.6 and 2.7. Plots

such as these can often quickly confirm other testing. They can also help illuminate other possible causes.

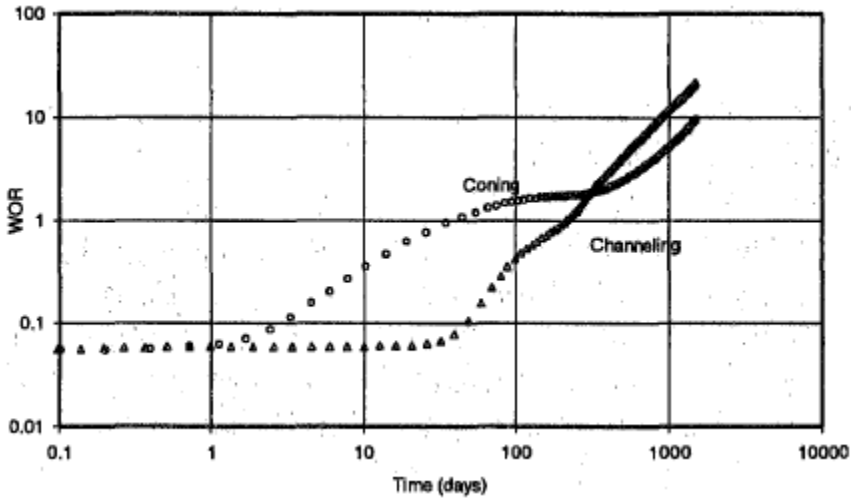

Figure 2.6—Water channeling vs water coning (Chan, K.S. 1995).

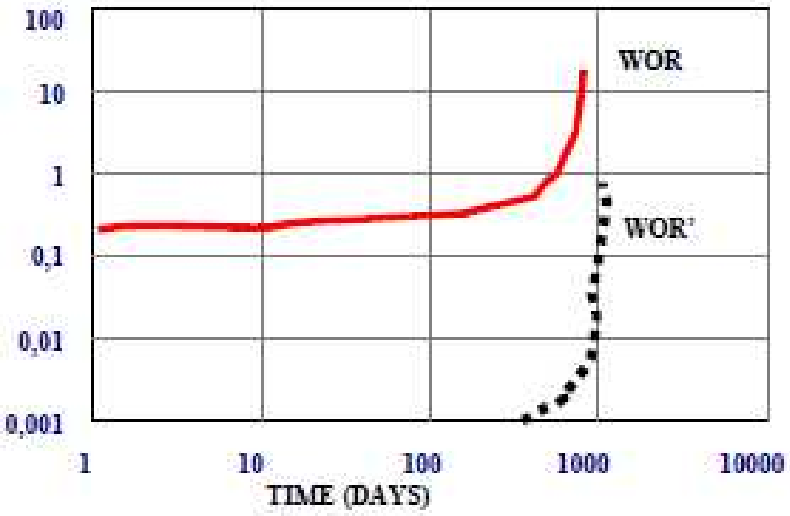

Figure 2.7—Mechanical communication (Hill et al. 2012).

2.3.1.2. Oil production versus time. Production decline curves help to observe and better understand the occurrence of water production during the well's life. This type of curves show the change in oil production over the time to determine when oil production reach peak or economic limit. They also indicate when water injection is needed.

2.3.1.3. Fluid recovery plot-WOR vs cumulative oil. A semi-log plot of WOR vs cumulative oil production shows that water production is a function of oil production. The area under the curve represents the total water production. A sharp increase in WOR can indicate a problem (e.g., casing leak or water breakthrough in the water–drive reservoir/ water flood). A high WOR associated with low cumulative oil production can indicate a channeling problem.

2.3.1.4. Hall plot-cumulative pressure vs. cumulative injection volume. The Hall plot-cumulative pressure vs. cumulative injection volume is most often used to analyze injection wells. It can also be used to analyze fluid injection treatments in production wells. These plots provide information on water channeling and formation fractures. Changes in the slop of the plotted line indicate a change in resistivity associated with fluid injection in the reservoir.

2.3.1.5. Rate vs time. A plot of various rates vs. time can assist in determining specific occurrences associated with producing wells. These rates include water production, water-oil ratio, water injection rates, and cumulative water injection. Different rates versus time are often plotted on the same graph to determine the relationship between variables.

2.3.1.6. Nodal analysis plot. Analysis of flowing wellbore and associated piping is known as NODAL analysis. It is frequently used to evaluate the effect of each component in flowing production system from bottom of well to the separator. This analysis is used to locate the excessive flow resistance that produces severe pressure losses in the tubing system.

2.3.2. Using Logs. Well logs are often used to identify water production problems. The different problems responsible for water production as well as the suggested logs that can be used to identify them are shown in Table 2.2 shows. Open hole and production logs are often used to identify both the water saturation and water source.

Table 2.2—A summary of the diagnostic logs used to identify water problems.

Problem type	Proposed Logs				
	Open hole logs	Casing Logs	Cement Evaluation logs	Pulsed Neutron Logs	Production logs
Casing leak		√		√	√
Channel behind pipe	√		√	√	√
Coning or Cresting	√				√
High permeability streaks	√				√
Water out zone	√				√
Completion near water zone	√			√	√
Fracture out of zone			√	√	√

2.3.3. Using Numerical Method. Using well test evaluations that simplify the complex results gained from numerical simulator would be beneficial. It can properly quantify the effect of treatment by determining the treatment volume, the degree of mobility reduction, and skin damage. Results obtained from the numerical simulator can be simplified into several equations including the mathematical definitions of rate, pressure, and time behavior in dimensionless forms.

2.4. CONFORMANCE CONTROL TREATMENT

2.4.1. Conformance Control Technology. Conformance control is defined as the application of processes in reservoirs and wellbores that reduce unwanted water production, enhance hydrocarbon recovery efficiency, and satisfy a broad range of reservoir and environmental objectives. It achieves these goals by either reducing or plugging water/gas produced as a result of high permeability streaks, fractures, and fracture –like features. Conformance control can improve the profitability as follows:

- Extend the well's economic life
- Reduce the well operation's maintenance cost
- Reduce the environmental concerns and cost

Conformance control treatment should be performed before serious damage occur. Input from those with varying expertise (e.g., geologists, petrophysicists, reservoir engineers, chemists, facilitators, and economists) should be sought as part of this process.

Liu et al. (2006) proposed that conformance control can be classified into six categories: unselective water shutoff, profile control, selective water shutoff, integrated

profile control treatments for multiple wells in one block, in-depth fluid diversion, and combined technology.

2.4.2. Types of Conformance Control Treatments. Any solution that is proposed to control water production must be made with a solid of understanding the options available, the working mechanisms involved pros, cons, capabilities, and limitations. Three main conformance control solutions can be used to address excess water and gas production problems: mechanical solutions, completion solutions, and chemical solutions.

2.4.2.1. Mechanical solutions. Mechanical solutions are often used to address many near wellbore problems, such as casing leak, flow behind pipe, rising bottom water, and watered out layers without cross- flow. These solutions include mechanical seal/isolation using hardware or cement. Figure 2.8 shows the using of mechanical plug back tool to shut near wellbore water shutoff.

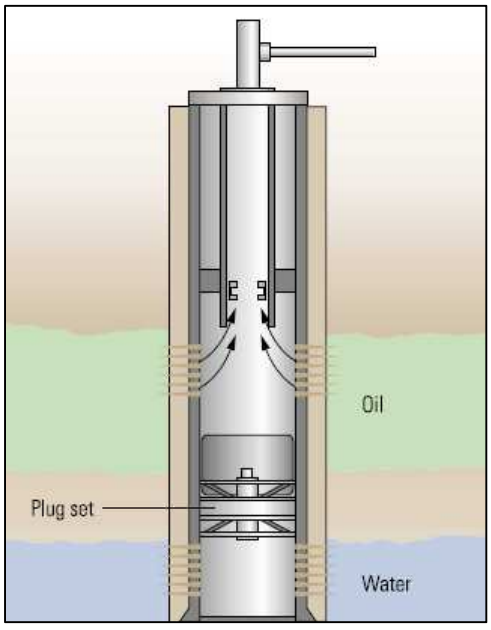

Figure 2.8—Mechanical plug back tool (Bailey et al. 2000).

2.4.2.2. Completion solutions. Alternate completions such as multilateral well, sidetracks, coiled-tubing isolation, perforation, and dual completion can be used to solve various water problems such as water coning, incomplete areal sweep, and gravity segregation. An example of using perforation and dual completion used to solve excess water production created by coning problems is illustrated in Figure 2.9.

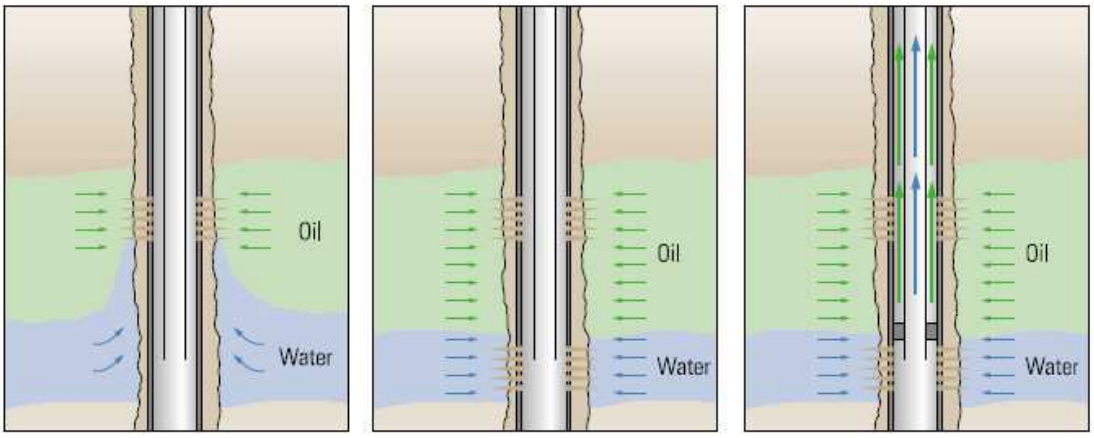

Figure 2.9—Perforation and dual completion to solve water coning (Bailey et al. 2000).

2.4.2.3. Chemical solution. Mechanical and completion solutions can provide a seal not only in the well's hardware but also in large near wellbore openings. However, there are cases where it is desirable to achieve matrix or small fissures penetration of the sealing materials. These instances could include small cement channels/fissures, natural fractures, and vertical coning through the matrix. A chemical solution is the only solution that can be applied to these problems.

Chemical solutions can be classified by either chemical type or by functionality. Chemicals classified according to type of chemical are as follow:

- In organic gels
- Resins/elastomers
- Monomer systems
- Polymer gels (sealant type, cross-linked rigid/flowing polymer gel, relative permeability modifiers, and flowing gels (cross-linked))
- Ungelled polymers/viscous systems
- Viscous flooding (with polymer, optionally foamed)

Chemicals classified according to functionality are as follow:

- Sealant (either temporary or long lasting/durable)
- Relative permeability modifiers (liquid)
- Weak sealant relative permeability modifiers
- Either mobility control or flow diverting chemical flooding system (viscous, selective plugging)

2.4.3. Chemical Placement Techniques and Equipment. Placement techniques used in treating unwanted water and/or gas production should be chosen on a well-by-well basis. The following five techniques are typically used for treatment placement: Bull heading, mechanical packer, dual-injection, Iso-flow, and transient.

2.4.3.1. Bull heading. The most simple economical treatment placement method involves operators injecting the treatment through the existing tubulars. This treatment may seal not only the intended water zone but also the oil zone. An illustration of the bull heading treatment sealed both zones is given in Figure 2.10.

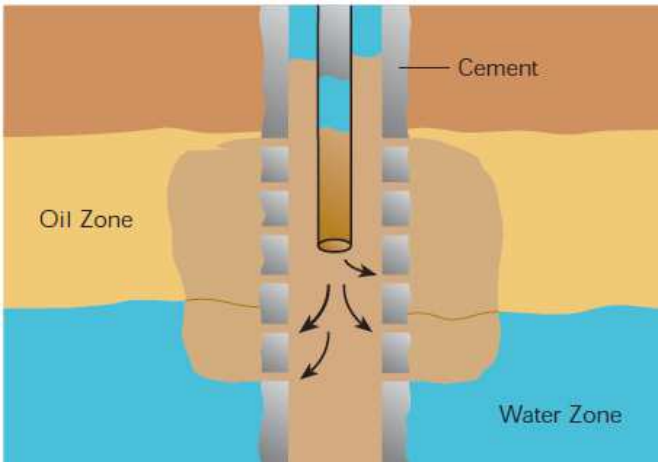

Figure 2.10—Bull heading treatment (Halliburton, 2002).

2.4.3.2. Mechanical packer placement/inflatable packer placement. An Operator can use mechanical packers, bridge plugs, or selective zone packers to isolate either the perforations or a portion of an open hole completion into which treatment will be placed. Figure 2.11 show this method can protect the critical perforation in the adjacent oil sand from sealant invasion.

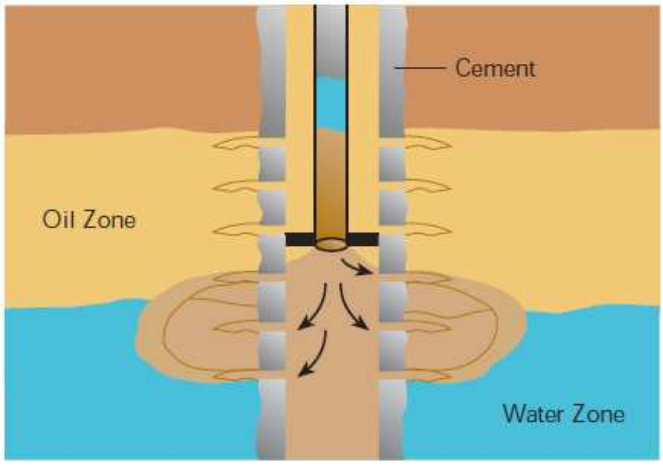

Figure 2.11—Packer placement (Halliburton, 2002).

2.4.3.3. Dual-injection placement. The dual-injection placement technique (as shown in Figure 2.12) offers efficient placement control. Operators can use the well tubular to inject treatment fluid down both the tubing and the annulus. This non-sealing fluid should be compatible with the hydrocarbon –producing zone.

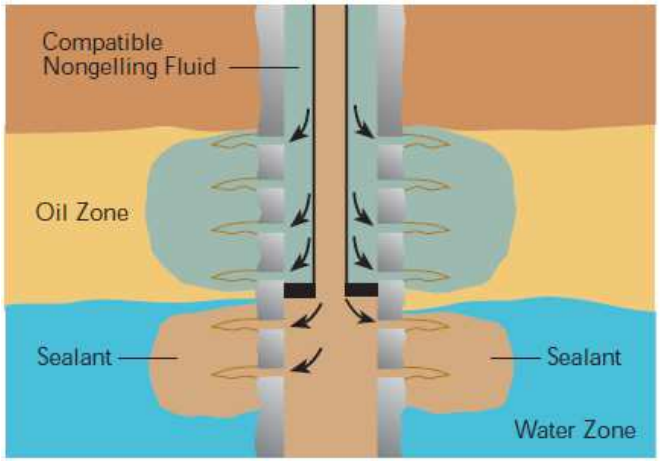

Figure 2.12—Dual-injection placement (Halliburton, 2002).

2.4.3.4. Isoflow placement. The operator direct the treatment solution into the selected interval while protecting the hydrocarbon –producing by simultaneously inject non-sealing, formation compatible fluid that contain radioactive tag down the annulus (Figure 2.13). A gamma-ray detection tool is run down the well (inside the tubing) and placed at the interface (between the upper non-sealing and lower sealing point in the well) before the treatment is run. Operator can manipulate the pump rate of the tubing and annulus fluids to adjust the location of the interface.

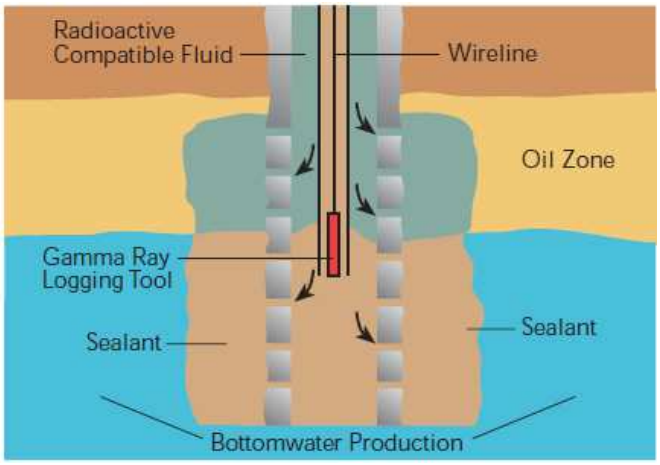

Figure 2.13—Isoflow placement (Halliburton, 2002).

2.4.3.5. Transient placement. Transient placement techniques (as illustrated in Figure 2.14) use cross- flow to help eliminate entry into unwanted intervals. These treatments are injected into the zones that will be sealed.

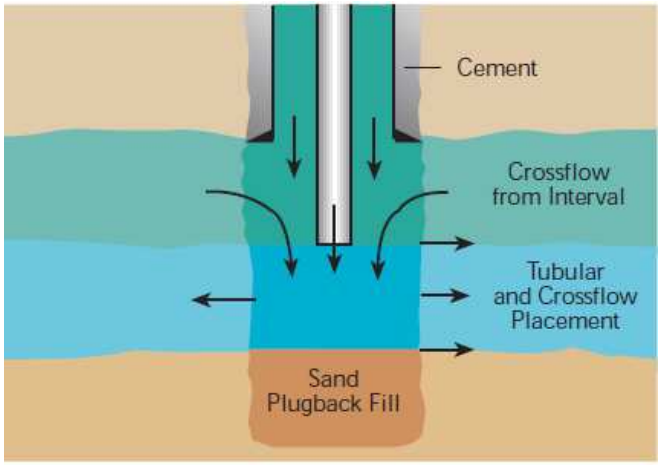

Figure 2.14—Transient placement (Halliburton, 2002).

2.5. CHEMICAL SOLUTIONS: GEL TREATMENTS AND POLYMER FLOODING APPROACHES

Water flooding is a secondary recovery mechanism that is used to displace oil not recovered during the primary recovery mechanism. Water flooding, however, is often associated with problems caused by unwanted water production. This unwanted water production becomes more severe when the reservoir becomes more mature. The heterogeneity that exists inside reservoirs is created by channeling through high permeable layers. This heterogeneity lead to unfavorable water productions. Excess water production cause a number of problems, including increased disposal costs and harsh environmental issues. Therefore, improving the reservoir's sweep efficiency is an important issue that must be addressed to minimize unwanted water production during the water flooding mechanism.

Polymer has long been used as an improved oil recovery method. Polymer flooding addresses the unfavorable mobility ratio that exists between the displaced and displacement fluids in the heterogeneity reservoirs.

Seright et al. (1994) classified polymer techniques into two categories: traditional polymer floods and gel treatments. Gel treatment are used to meet a very different objective that for the traditional polymer flooding as depicted in Figure 2.15. Both are ultimately intended to improve sweep efficiency. In the traditional polymer flood, want to the injected polymer solution penetrate as far as possible into the low permeability un-swept zones. In contrast, in gel treatment, want gallant or gel penetration to be minimized in the less-permeable oil rich zones.

A clear distinction can be also made between gel and polymer chemical composition. Gel treatments often use both a crosslinker and small gallant volume. Polymer flooding often involves relatively large banks of uncrosslinked polymer solutions.

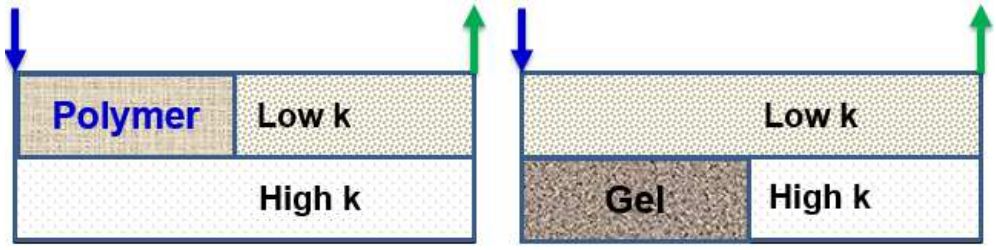

Figure 2.15—Polymer flooding vs. gel treatment functionality.

This section also discusses the most common concepts used in the polymer and gel process. It includes equations which can be used to characterize the polymer and gel processes.

2.5.1. Mobility Ratio Concept. The mobility ratio concept described by Craig (1980) is defined as the mobility of the displacing phase to the mobility of the displaced phase. In water flooding mechanism can be written as:

$$M_{w\text{-}o} = \lambda_w / \lambda_o = (k_w \mu_o)/ (k_o \mu_w) \quad (2\text{-}4)$$

If this ratio is divided by the absolute permeability, the water-oil mobility ratio can be rewritten as:

$$M_{w\text{-}o} = \lambda_w / \lambda_o = (k_{rw} \mu_o)/ (k_{ro} \mu_w) \quad (2\text{-}5)$$

where Mw-o is the mobility ratio to water and oil, λ_w is the mobility to water, λ_o is the mobility to oil, krw is the relative permeability to water and kro is the relative permeability to oil.

If the mobility ratio is greater than unity, because μ_w is less than μ_o, water flows at a higher velocity through the path of least resistance and breaks through into producing well prematurely.

Polymers are added, primarily, to increase the water viscosity so that the mobility ratio become either less than or close to unity.

2.5.2. Resistance Factor Concept. The resistance factor is used to characterize the behavior of different polymers and/ or gels in response to an increase in pressure during the polymer and/or gel injection. A resistance factor is defined as the ratio of mobility of water to the mobility of gel or polymer (Pye, 1964):

$$Fr = \lambda w / \lambda_{gel} = K_w/\mu_w / K_{gel}/\mu_{gel} \quad \text{.....(2-6)}$$

where λw and λg represent the mobility of water and gel, respectively and *kw* and *kg* represnt the water and gel, permeability.

At any given injection rate, Fr can also be expressed as the pressure drop during the gel injection to the pressure drop during water injection:

$$Fr = \Delta p_{gel}/ \Delta p_{water} \quad \text{..... (2-7)}$$

2.5.3. Shear Rate through Capillary Tubes. The maximum shear rate at the pore wall in the capillary tube can be used to calculate the shear rates on the gel flowing in tube (Zaitoun et al. 2012).

$$\gamma = 8v/D \quad \text{.....(2-8)}$$

where γ is the shear rate, v is the superficial velocity, and D is the conduit's inner diameter. This equation assumes both laminar and a single flow phase.

2.5.4. Shear Rate through Core Matrix. The shear rate on the fluids flowing through a non-fractured core can be calculated as (Lake, 1989):

$$\gamma = \frac{4\,q}{A\sqrt{8\,k\emptyset}} \quad \text{.....(2-9)}$$

where γ is the shear rate (sec^{-1}), q is the flow rate (cm^3/sec), A is the cross sectional area (cm^2), K is the permeability (cm^2), and ϕ is the porosity (dimensionless)

2.5.5. Shear Rate in an Unconsolidated Porous Media. A capillary bundle model in a porous media can be used to calculate the shear rate on the fluid flowing through sand packed cores (Chauveteau and Zaitoun. 1981).

$$r_p = \left[\frac{8\,k}{\emptyset}\right]^{0.5} \quad \text{.....(2-10)}$$

The shear rate at the wall pore in the unconsolidated porous media can be obtained via:

$$\gamma = \alpha\frac{4\,v}{r} \quad \text{.....(2-11)}$$

where r is the average porous radius (cm), k is the permeability (cm^2), ϕ is the porosity (dimensionless), γ is the shear rate (sec^{-1}), v is the superficial velocity (cm/sec), and α is the pore structure's shape parameter characteristic (α = 2.5 for a packed beds of angular grain, α = 1.7 for a pack of large spheres having same diameter).

2.5.6. Residual Resistance Factor Concept. The residual resistance factor (Frr) describes the ability of a gel to reduce the permeability to water or oil phase. It can be defined as the ratio of either water or oil phase permeability before and after particle gel treatment.

$$Frrw = (k_w/\mu_w)_{before}/(k_w/\mu_w)_{after} \quad \text{.....(2-12)}$$

$$Frro = (k_o/\mu_o)_{before}/(k_o/\mu_o)_{after} \quad \text{.....(2-13)}$$

where Frrw and Frro are the residual resistance factors to water and oil (dimensionless), respectively, Kw is the permeability to water (md), Ko is the permeability to oil (md), μo is the viscosity to oil (cp), and μw is the permeability to water (cp).

At any given injection rate, Fr can also be expressed as the pressure drop during the gel injection to the pressure drop during water injection:

$$Frrw = (\Delta p_w)_{after}/ (\Delta p_w)_{beforer} \quad \text{..... (2-14)}$$

$$Frro = (\Delta p_o)_{after}/ (\Delta p_o)_{beforer} \quad \text{.....(2-15)}$$

where $(\Delta p_w)_{after}$ is the pressure drop to water after the gel treatment (psi), $(\Delta p_w)_{before}$ is the pressure drop to water before gel treatment(psi), $(\Delta p_o)_{after}$ is the pressure drop to oil after gel treatment (psi), and $(\Delta p_o)_{before}$ is the pressure drop to oil before gel treatment (psi).

2.5.7. Gel Adsorbed Layer Thickness. The adsorbed gel layer thickness (e) is derived from the permeability reduction. It can be calculated as (Zaitoun and Kohler. 1988):

$$e = r_p\,(1 - Frrw^{-0.25}) \quad \text{.....(2-16)}$$

2.6. GEL TREATMENT FOR CONFORMANCE CONTROL TREATMENT

Gel treatment is one of the most effective and cost-effective means available to decrease the water production and improve the reservoir homogeneity in mature oil fields (Seright and Liang. 1994). Gel treatments are designed by adding a small concentration of crosslinker to the polymer solution to link polymer molecules.

In-situ gels are traditionally used to control reservoir conformance. A mixture of polymers and crosslinkers known as gallants is injected into the target formation. It forms a gel to fully or partially seal the formation at reservoir conditions (Sydansk and Moore 1992). This technology, however, has several disadvantages such as a lack of gelation time control, gelling uncertainty due to shear degradation, chromatographic separation between polymer and crosslinker, and dilution by formation water and minerals that restrict its applications for conventional reservoirs (Chauveteau et al., 1999, 2001, 2003. Coste et al. 2000. Bai et al. 2007a, 2007b).

Newer gel systems recently have been developed to overcome these drawbacks. These newer gels have a better performance than previously used gels. The new gels are formed at surface facilities and then injected into target zones with no need for gelation to occur in the reservoir conditions. These gels have different commercial product names:

Preformed Particle Gels (PPG), microgels, Bright water, and pH sensitive polymer microgels. Preformed particle gels are superabsorbent crosslinking polymer particles that can swell up to 200 times their original size when placed in brine. These PPGs are a millimeter-sized particles that are formed at the surface. They are then dried and crushed into small particles before they are injected into a reservoir (Coste et al. 2000. Bai et al. 2007a, 2007b). A micorgels is injected fully water soluble, non-toxic, soft, stable and size controlled micogels into a reservoir. It has a particle size between 10 and 1000 nm (Chauveteau et al. 1999, 2001, 2003; Rousseau et al. 2005; Zaitoun et al. 2007). Temperature sensitive polymer microgels (known as Bright water) are submicron gel particles. They are injected into the reservoir with cool injection water relative to the reservoir temperature itself. As the polymer passes through the reservoir, it gradually picks up heat from the surrounding warmer reservoir rocks. As it heats up, the polymer begins to expand to many times its original size, blocking pore throats and diverting water behind it (Pritchett et al., 2003. Frampton et al, 2004. Morgan 2007. Yanez et al, 2007. Garmeh et al. 2011) .The pH sensitive polymer microgels use pH change as an activation trigger. The gel begins to adsorb water as the pH increases, swelling up to 1000 times its initial volume (Al-Anazi et al. 2002. Huh et al. 2005. Benson et al. 2007).

Gels have traditionally been placed near the wellbore of production or injection wells, as shown in Figure 2.16 to correct interlayer heterogeneity or fractures. Near-well bore treatments are ineffective, however, if a cross-flow exists between adjacent layers. Newer trend in gel treatment was recently developed to apply in-depth diversion conformance control (Seright 2004; Frampton 2004; Sydansk 2005; Chang 2004; Rousseau 2005; Bai et al. 2007). These gels can penetrate deeply into high-permeability

streaks, channels, or fractures to create kind of resistance to water flow through these features. This water is thus diverted to recover more oil from the un-swept low permeable zones as shown as depicted in Figure 2.17.

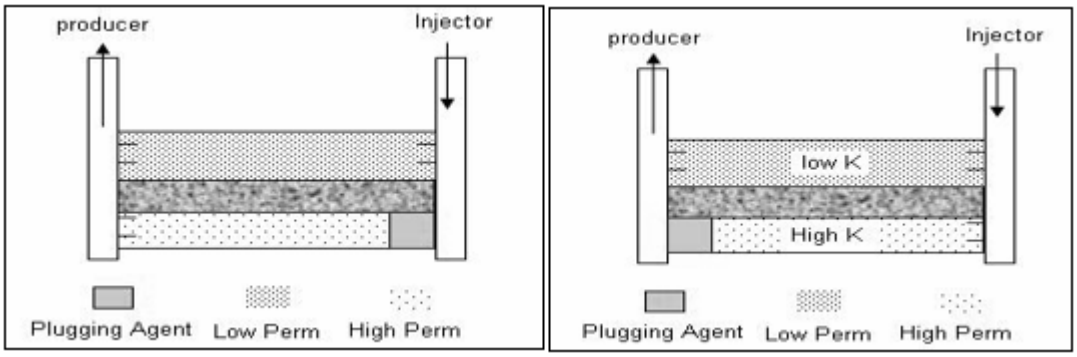

Figure 2.16—Gel treatment in heterogeneous formation without a crossflow (Liu et al. 2006).

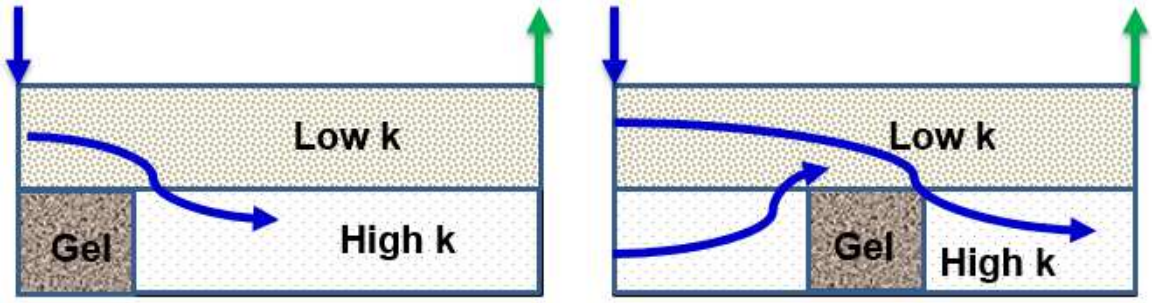

Figure 2.17—Near wellbore vs. in-depth treatment.

A gel's properties are primarily dependent on the gel's chemical composition, including the polymer concentration and the degree of crosslinking. The following describes the two main types of gels used in the oil industry.

2.6.1. In-situ Gel (Traditional Gel System). In-situ gels are crosslinked polymers composed of several chemical materials including polymers, crosslinkers, and additives. Corresponding to some internal or external stimulation, the crosslinking agent connects itself to two adjacent polymer molecules linking them together either chemically or physically. The liquid formulation of this composition is known as a gelant. The gallant in an in-situ system is injected into the formation, and the gel forms under reservoir conditions. The gelant can crosslink to form a gel under various conditions including an increasing temperature and a changing pH. Both a gelant's composition and surrounding conditions can be used to control gel strength. This strength can be either weak or very strong, as depicted in Figure 2.18. In-situ gels have been used widely to control conformance, but their crosslinking reactions are strongly affected by degradation.

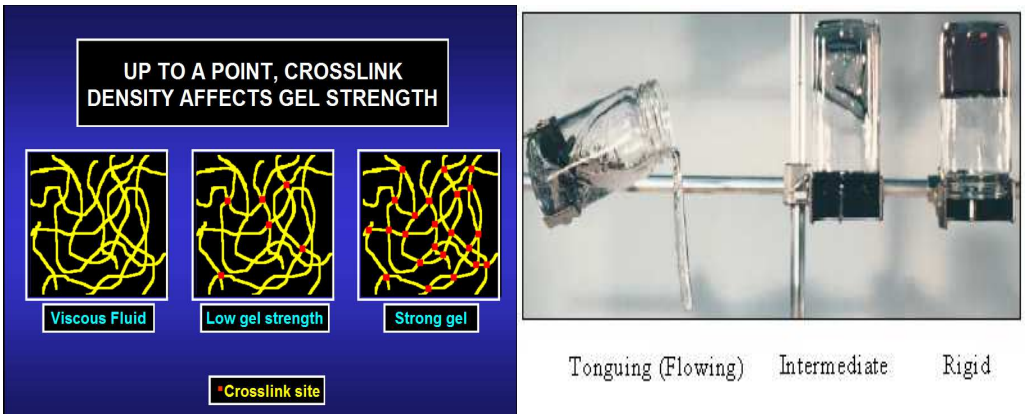

Figure 2.18—Gel composition (Seright, 1996).

2.6.2. Preformed Gel Systems. Gel is formed in surface facilities before injection. The gel is then injected into reservoirs. No gelation occurs in the reservoir. The new trend of using a preformed gel can help overcoming several of the drawbacks associated with in-suit gel systems. These drawbacks include the following:

1. Crosslinking reactions that are strongly affected by:
    - shear by pump, a wellbore, and porous media,
    - the adsorption and chromatography of chemical compositions, and
    - the dilution of formation water.
2. Possible damage on the un-swept low permeability oil zone

The different kinds of preformed gel systems used in the oil industry are listed with their respective developer and field applications in Table 2.3.

Table 2.3—A summary of preformed gel systems.

Name	Developer	Particle Size	Applications
Bright Water®	Chevron, BP and Nalco	Sub-Micro (< 1 μm)	60^+ injectors
Microgel	IFP	Micro (1-10 μm)	10^+ producers
PPG	PetroChina, MS&T, and Halliburton	Millimeter (10 μm to millimeters)	$5{,}000^+$ Injectors in China
pH Sensitive polymer	UT	Micro	Not reported

The primary differences between all of the current commercially preformed gels include particle size, swelling ratio, and swelling time.

2.6.2.1. Bright water. An industry consortium (BP, Chevron and Nalco) developed Brightwater®. It is now commercialized by Tiorco (Nalco Company). Brightwater® was first tested in Indonesia in 2001. A number of treatments have since been performed in Alaska, the North Sea, and Argentina.

Brightwater® can be defined as a sub-micron particulate chemistry that can be injected downhole with the injection water as a one-time batch. It can be deployed with conventional chemical injection equipment and requires no modification to the existing water injection system. The particle's sizes are significantly small (~0.5 micron) allowing the particles to propagate through the rock's pores with the injected water. The polymer gradually warms toward the reservoir temperature as it passes through the reservoir. It expands to many times its original volume (a factor of four to ten depending on salinity), blocking pore throats and diverting any water behind it (see Figure 2.19). Various grades of chemistry are available depending on the targeted thief zone properties, water salinity, and reservoir temperature (Roussennac et al. 2010).

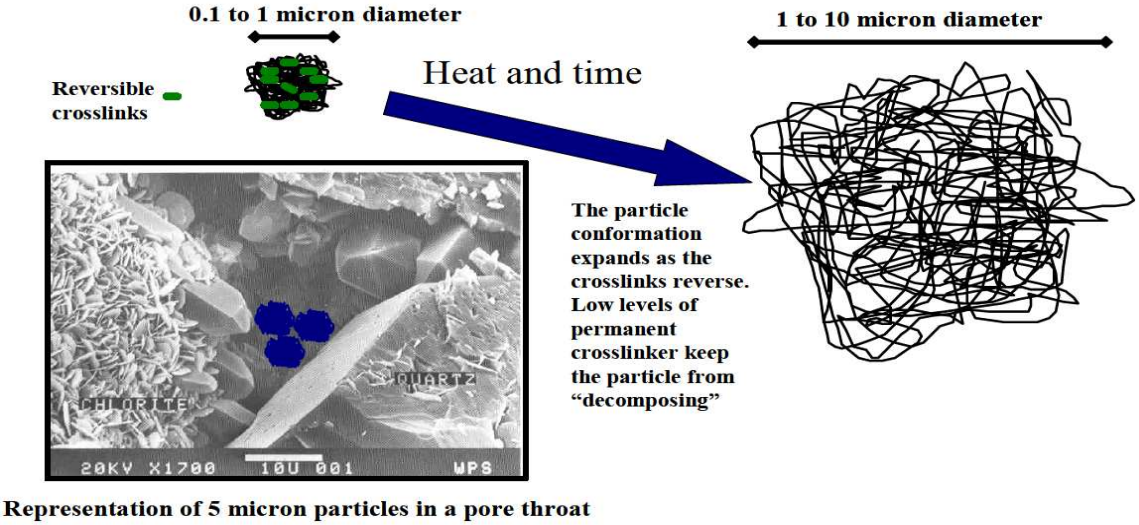

Figure 2.19—Mode of activation of the particulate reagent (Ohms et al. 2009).

2.6.2.2. Microgel. Baker coined the term "microgel" to describe cross-linked polybutadiene latex particles. The word micro referred to the gel particles size which has a diameter that is less than 1000 nm. Baker microgel referred to the ability of the particles to swell in organic solvents. Bakers emphasized that microgels have incredibly high molecular weight polymer networks. Thus, each gel particle has an individual polymer molecule. A definition of microgel has been revised and it can be defined as colloidal dispersion of gel particles. Microgels have the following features:

- Microgels fall within the particle size range of 10–1000 nm
- Microgels are dispersed in a solvent
- Microgels are swollen by the solvent
- Microgels have stable structures. Either covalent or strong physical forces stabilize the polymer network.

Chauveteau et al. (1999) introduced a new concept that consists of injecting fully water soluble, non-toxic, soft, stable, and size-controlled microgels into the reservoir. Microgels specifically designed for water shutoff (WSO) treatments do not contain toxic products and can be produced to be fully self-repulsive. They adsorb onto rock pore surface by forming soft monolayers with a thickness equal to their size. This size can be adjusted as desired during the manufacturing process. As a consequence, water permeability can be reduced as desired.

These microgels were found to reduce water permeability strongly by forming thick adsorbed layers that are so soft that oil permeability is unaffected. Microgel chemistry is chosen to be insensitive to pH and salinity variations (Chauveteau et al. 2004). Microgels are used for both water shutoff and conformance control operations.

2.6.2.3. Preformed particle gel (PPG). The gel in PPG systems is formed in a surface facility before it is injected into a reservoirs; no gelation occurs in the reservoir. They belongs to the family of superabsorbent polymers (SAP), which are different from un-swollen in situ gels. PPG can absorb a large quantity of an aqueous solution, the polymers must be only slightly cross linked so that polymer chains can be flexible enough to expand in a wide space.

PPG can be swelling over a hundred times their weight in liquids (Figure 2.20) and not easy to release the absorbed fluids under pressure.

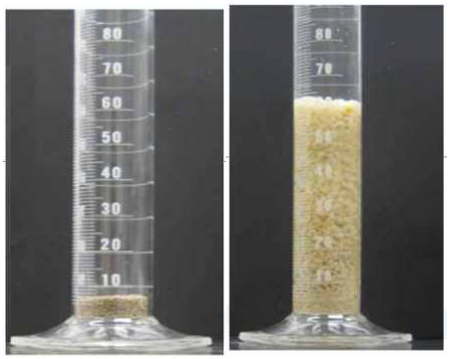

Figure 2.20—PPGs before and after swelling.

A PPG's particle size is adjustable from a scale of micrometers to millimeters. The particles have a swelling ratio of 30-200 times the original volume. The brine solutions concentration can be adjusted to control the particles size. The particle's resistance to salt permits the use of all salt types and concentrations. Particles are resistant to temperature up to 110 ºC.

2.6.2.4. pH sensitive polymer. Al-Anazi and Sharma (2002) were first proposed the use of pH sensitive polymers for conformance control purposes. They observed that swelling properties of polyelectrolytes (such as polyacrylic acid) are very sensitive to pH, ionic change, and polymer concentrations. They shrink to a low viscosity in acidic conditions. In contrast, they begin to swell and adsorb water as the pH increase. Their volume can also increase up to 1000 times its original volume. Al-Anazi and Sharma (2002) explained the chemistry theory involved when particle swell (see Figure 2.21). The interaction between the ions occurs when the carboxylic group (COOH) in the polyacrylic acid is ionized. This ionization causes negatively charged group (COO^-)

repulsion on the polymer chain. This electrostatic repulsion force causes the polymer to uncoil and stretch increasing its solution viscosity.

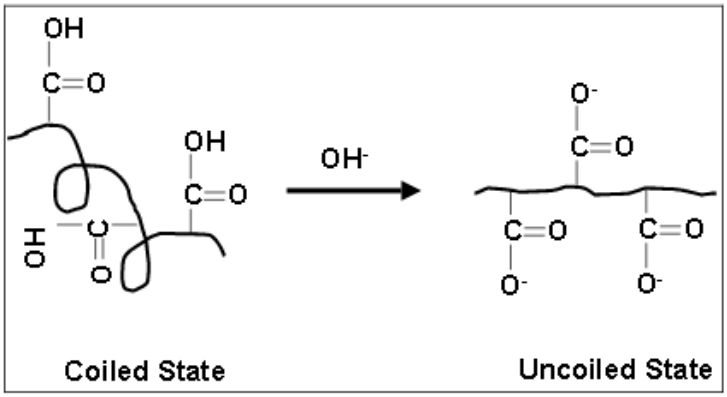

Figure 2.21—Swelling of Polyacrylic acid swelling within ionization (Al-Anazi and Sharma 2002).

2.7. PREVIOUS WORK ON GEL TREATMENT TECHNOLOGY

On water flooding process, water preferential flow through the high permeability, fractures, and large channels; cause a large amount of recycling of water without much benefit to oil production. A PPGs millimeter-sized particles (10 um~mm) make it not only more distinguishable but also more reliable than other types of particle gels in plugging large channeled features (Imqam et al. 2014). A gel treatments success depends heavily on the gel's ability to reduce the conductivity of these large channel features. Thus, understanding both the mechanism and the factors affecting the gel's ability to resist water flow through these features is the key to a successful conformance control treatment.

Many researches have been conducted to study the rheology and the factors affecting gel resistance to water flow. Grattoni et al. (2001) conducted a series of experimental studies to link polymer gel properties (such as gel strength and polymer concentrations) to flow behavior. They found that permeability is a function of both water flow rate and polymer concentration. Yang et al. (2002) developed a mathematical model for the flow of water through channels impregnated with a polymer gel. Their results indicate that a gel's intrinsic properties (such as gel reference permeability and elastic index) control water flow behavior. Zhang and Bai (2011) demonstrated that millimeter-sized particles form a permeable gel pack in opening fractures rather than form full blocking.

This research addresses the effect of brine concentration, particle size, oil viscosity, and load pressure on the permeability of PPG pack inside large channeled features. In additions, it evaluates the ability of particle gel to reduce these channel conductivity when the gel is subjected to load pressure.

Numerous studies have been conducted in an attempt to evaluate in-situ gel propagation through fractures. Seright (1995, 1997, 1998, 1999, and 2001) studied both bulk gel placement and the mechanism behind gel propagation through fracture systems. Liu and Seright (2000) identified a correlation between gel rheology and the extrusion properties of gels in fractures. Ganguly et al. (2001) conducted a series of experiments to determine the effects of fluid leak-off on gel strength when placed in fractures. Sydansk et al. (2005) characterized the transport of partially formed gels in fractures. Wang and Seright (2006) examined whether or not the use of rheology measurements to evaluate gel properties in fractures is an acceptable substitute for extrusion experiments as a way

to reduce costs. Wilton and Asghari (2007) worked to determine how to improve bulk gel placement and performance through fractures. They applied a Cr (III) acetate pre-flush to investigate whether or not a stable gel can be formed within a fracture without gallant leak-off. McCool et al. (2009) investigated the effect of shear on flow properties during the placement of gallants in fractures. No one, however, has studied either the performance or the mechanism of PPG extrusion and placement in conduit systems. Only Zhang and Bai (2011) have investigated PPG extrusion through fractures. They studied PPG injectivity and plugging efficiency when the fracture width was less than the gel particle size. The objective of this current research is to conduct an in-depth examination of several factors that can have an important impact on the PPG extrusion mechanism and placement performance in conduits system. It discusses PPG injection through fractures/conducts which have pore throat sizes equal to, less than, and larger than PPG size.

When gels are placed throughout target zones, water permeability decreases significantly and water flow into the well is minimized. However, if oil is produced from a reservoir through these zones, gel permeability will not be decreased significantly. This phenomenon is called Disproportionate Permeability Reduction (DPR). This phenomenon has examined previously and many studies have been conducted to evaluate the gel performance in presence of oil productions (Liang et al. 1993, 1995; Liang and Seright, 1997; Grattoni et al. 2001; Willhite et al. 2002; Nguyen et al. 2004; Seright, 2006; Seright, 2009). To the best of knowledge, neither of these studies or previous works had used PPG as a conformance material in their investigations, nor studied the

performance or mechanism of PPG extrusion and placement in conduit and high permeability streaks reservoirs.

This research intend to examine in-depth several factors such as particle size, gel strength, permeability of unconsolidated sand, and conduit pore size effect on DPR properties, gel extrusion, and placement through conduit and unconsolidated sandstone formations. Alternate banks of both brine and oil were used to determine the extent to which PPGs can reduce water permeability more than oil permeability within conduit and high permeability streaks.

In spite of the successful applications of PPGs in plugging large features, there is still need to combine this technology to produce more oil from the low permeable rich zones. This research studied the efficient of combining conformance control treatment using PPG and mobility control using Polymer. Conformance control combined with either CO_2 or surfactant application have been previously investigated. Few studies, however, have evaluated conformance control with mobility control. Richard et al. (2014) indicated that a large substantial benefit to use crosslinked gel treatment before introduced the polymer applications. Their field results conducted in the Buffalo Coulee reservoir shows large incremental in oil recovery reached 10 to 15%. Dong et al (2008) indicated that oil recovery could be enhanced 2-4% OIIP over the polymer flooding for some Daqing well with layers no cross flow. These field applications motivate to conduct more work to understand the mechanism and evaluate effectiveness of using PPG with mobility control to increase oil recovery from both high and low permeability zones. A new heterogonous model experiment was conducted during this research to have a better

understanding of combining these two technologies to gain more oil recovery from swept and un-swept areas.

In both cross flow and no cross flow strata, a small portion of gel still propagates into un-swept low-permeability zones in spite of the millimeter-sized gel preferentially entering into fractures or fractures features channels. Gel penetrates into un-swept zones and forms a cake on the surface of low-permeability layers. This gel cake adversely affects oil production by reducing the permeability of the near wellbore region. The extent of formation damage depends on the gel properties and the rock permeability interactions (Elsharafi and Bai, 2012).

Several laboratory studies have been conducted using oxidizers and enzymes to understand and mitigate the damage caused by using crosslinked polymer fluids. Carr and Yang (1998) introduced flow back analysis to evaluate polymer damage-removal efficiency. Crews and Huang (2010) proposed a new technique that uses nanoparticle–associated surfactant in brine that generates crosslinked-polymer-like fluid viscosity to enable the removal of residual polymer in hydraulic fractures. Sarwar et al. (2011) provided a guideline for gel degradation studies using oxidizers and enzymes to optimize the breaker type while also optimizing the concentration at specific temperatures. Reddy (2013) studied the filter cake characterization using zirconium-crosslinked fracture fluids and developed a non-oxidizer gel breaker that can actively decrosslink the crosslinked gel structure by reacting with the crosslinking agent rather than only breaking down the polymer chain. These works spend a large quantity of time and effort to optimize the breaker system for the particular well conditions and fluid requirements. Most of this work was conducted to optimize hydraulic fracturing fluid and thus obtain a better

performance. Few studies evaluated this breaker during the conformance-control treatments.

This research proposed a different method than the other applications by combining acidizing with conformance treatments to improve oil recovery from low-permeable zones and enhance the injection profile in mature oil fields. Some field applications reported promising results from combining water shutoff and stimulation technologies to improve oil recovery. Zhao et al. (2004) evaluated several acid systems to be compatible with three kinds of plugging agents to use in different reservoirs. Their results obtained from Weicheng and Mazhai oilfields show a better injection profile and better oil increase in responding wells. Turner and Zahner (2009) conducted a field study in Sockeye field, offshore California, on the applications of combining chromium crosslinked polyacrylamide gels and acid stimulation. Combining both treatments lowered water production and increased the oil rate in a manner that neither technique would yield on its own. Kosztin et al. (2012) presented a combine technology of water shut-off and acid stimulation in a mature field in North Oman. The results show a large increase in oil production and a decrease in the average water cut.

These studies did not use particle gels combined with acid stimulation. Therefore, this research examines the effectiveness of using hydrochloric acid to remove the damage caused by particle gel penetrating into low-permeability zones. Additionally, this research proposed combined gel with acid stimulation to increase oil recovery from low permeability layers, consequently a new heterogonous model will be also conducted to evaluate how much oil recovery would be obtained from combining water shutoff and acid treatments.

Gel was pumped into large permeability zones to reduce their permeability to obtain more oil from un-swept low-permeable zones. Acid was pumped to remove the gel cake formed in un-swept rich oil zones; thus, more oil can be recovered. The combined technologies increased oil production from both low and high permeable formations. During these intensive evaluations of combined gel with acid treatments, swelling ratio, deswelling ratio, effect of pH, and gel strength in acid were investigated. A core flooding experiments were carried out to more fully understand the factors affecting gel cake forming on the surface of different low-permeability cores.

In summary, this research conducted an intensive experiment work to understand and evaluate the PPG propagation and placement mechanisms in high permeability and fracture reservoirs. The research started by evaluate factors effect on gel properties and rheology by studying the concept of gel pack permeability. Numerous experiments were conducted to evaluate the PPG injection through different media, namely conduit and unconsolidated sand pack models. Several experiment were then conducted to evaluate water and oil propagation through gel after placement within conduit and unconsolidated sand pack models. Finally, a novel combination between PPG treatment, stimulation treatment, and mobility control conducted in heterogenetic experiment models to evaluate the effectiveness of using PPG with these two combination technologies.

3. EFFECT OF GEL PACK ON OIL AND WATER FLOW

3.1. INTRODUCTION

Gel pack permeability is a new concept is introduced through this study. It introduced to study factors that have a significant effect on particle gel propagation through either super-k or fracture systems. Gel was found that partially plugs undesired formations rather than fully blocking. This section investigates what factors significantly effect on particle gel pack permeability. This investigation is a crucial for a successful gel treatment because it gives an idea about how much gel pack permeability can minimize the permeability of the target zone. As the behavior of gel pack permeability was fully understood, an intensive lab work was then conducted to evaluate gel extrusion through fractures and high permeability streaks to study the mechanism and behavior of particle gel propagation through these features.

3.2. OBJECTIVES AND TECHNICAL CONTRIBUTIONS

This topic aimed to provide an intensive insight on the gel rheology properties for PPG during water and oil flow. The following are summaries of the objectives of this section and expected technical contribution gained from this investigation.

- Determine the PPG pack permeability for different fluid flow phases.
- Examine the effect of change brine concentrations, particle gel sizes, oil viscosity, and injection flow rates on PPG pack permeability.
- Study the effect of compressed gel on the blocking efficiency of PPG.
- Determine the PPG pack compressibility under the different load pressure.

- This investigation is very important for a gel treatment to be successful where gel treatment target is to reduce the undesired permeability formations to the level as we planned.
- The findings from this topic will be used to optimize a particle gel conformance control design. A gel pack with the desired permeability can be designed by selecting both gel strength and particle sizes that correspond with reservoir pressures.
- It is first time to report that gel particles usually form permeable gel pack in fluid channels rather than fully block these fluid channels.

To accomplish these objectives, this section is presenting results obtained from conducting a serious of experimental work to measure the PPG permeability for different flow phases and understand which factors significantly impact the blocking efficiency of PPG.

3.3. GEL PACK DESCRIPTIONS

Previous fracture transparent model Figure 3.1 indicates that the PPG propagated like a piston along the fracture, and gravity did not change the shape of the front of the PPG if the particle size was larger than or close to the fracture width. The fracture transparent model was constructed of two acrylic plates with a rubber O-ring between them. Bolts and nuts were used to fix the two plates and control the fracture width. On one side of the plate, a hole functioned as an inlet for the injection of the brine and PPG; on the other side, another hole provided an outlet to discharge the brine and PPG. The model was transparent so that the movement of the PPG and brine would be clearly visible. In the case of the large channeling features, such as conduits, wormholes, and

caves, understanding the gel pack permeability mechanism and determining which factors have a significant effect on the strength of the gel pack permeability is also needed to have a better PPG treatment design through these large feature systems. This section describes factors that affect the gel pack permeability inside large channels and evaluates the gel pack compressibility in the presence of load pressure. The load pressure in this study refers to the pressure developed by a piston movement to compress the gel particles inside a transparent channel model.

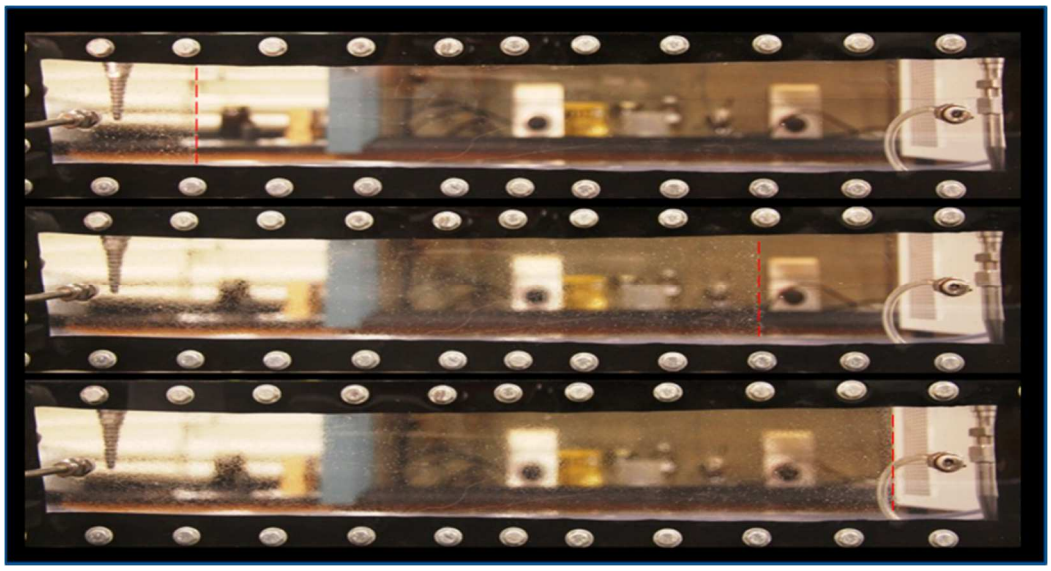

Figure 3.1—PPG propagates like a piston (Zhang and Bai, 2011).

3.3.1. Gel Pack Permeability. The PPG pack permeability was determined by measuring the differential pressures and flow rates while injecting brine through the gel pack-filled channel tube. The gel pack permeability was fitted according to the power law as follows:

$$K_{PPG} = k_o \nu^n \quad \text{.....(3.1)}$$

where K_{PPG} is the preformed particle gel pack permeability, k_o is the intrinsic permeability, v is the superficial velocity, and n is the gel elasticity index.

The permeability is a function of the flow velocity, following a nonlinear relationship. The link between velocity-dependent permeability and gel rheology has been proven experimentally, where increased brine injection flow rates enlarge the flow pathways within the PPG by elastic deformation. Power law behavior is usually observed when non-Newtonian fluid flows through a rigid porous medium. However, the brine used in this study is a Newtonian fluid, so the power law model can only be applied to the elastic properties of the PPG.

The intrinsic permeability and elasticity index are functions of fluid and gel properties. If n equals zero, the permeability would not be velocity dependent; this could be the case if the PPG acted like a rigid porous medium. The deformability/elasticity of the PPG increases when n is greater than 0.

3.3.2. Gel Pack Compressibility. Gel pack compressibility is defined as the ability of gel particles to move closer to each other when the load pressure is applied against them. PPGs swollen in different brine concentrations were used to measure compressibility. The gel pack compressibility was measured by pouring gel particles inside the transparent model. The initial volume of gel inside the model was measured before applying the load pressure. A piston was then used to compress the gel by imposing different load pressures on the gel particles. For every load pressure that was tested, the gel continued to compress until no further water loss was produced from the gel as effluent. The change in volume and the pressure drop across the gel were both

measured. This procedure was repeated for every brine concentration. In addition, the gel pack compressibility (C_{ppg}) was calculated for every load pressure based on the following equation:

$$\text{Cppg} = \frac{-1}{\text{Vo}} * \frac{\Delta \text{V}}{\Delta \text{P}_\text{g}} \quad \text{.....(3.2)}$$

where *Cppg* is the PPG pack compressibility (Psi^{-1}), V_o is the initial PPG volume before compression (cm^3), ΔV is the change in PPG volume after compression (cm^3), and ΔP_g is the change in pressure across the gel (psi).

3.4. EXPERIMENTAL MATERIALS

3.4.1. Preformed Particle Gel (PPG). A super absorbent polymer (SAP) was used as the preformed particle gel for this study. The particle was synthesized by a free radical process using acrylamide, acrylic acid, and N, N'-methylenebisacrylamide. Most PPGs reach full swelling in half an hour, but a field operation usually take a few hour to a few months, so fully swelling particles were used in experiments. The primary characteristics of the PPG used for the experiment are listed in Table 3.1.

Table 3.1—Typical characteristics of PPG.

Properties	Value
Absorption of Deionized Water (g/g)	>200
Apparent Bulk Density (g/l)	540
Moisture Content (%)	5
pH Value	5.5-6.0 (+/- 0.5; 1% gel in 0.9% NaCl)

Various sizes of PPG were selected for experiments: 18-20, 20-30, 50-60, and 80-100 mesh. Table 3.2 illustrates the PPG size distribution before and after being swollen in 1% NaCl solution.

Table 3.2—PPG size before and after being swollen in 1% NaCl.

No	PPG (mesh size)	PPG size before being swollen, µm	PPG size after being swollen, mm
1	18-20	850	42.5
2	20-30	600	30
3	50-60	250	12.5
4	80-100	150	7.5

3.4.2. Brine Concentrations. Sodium chloride (NaCl) with three concentrations (0.05, 1, and 10 wt %) was used to prepare the swollen gels. Figure 3.2 depicts the PPG before and after being swollen in different brine concentrations.

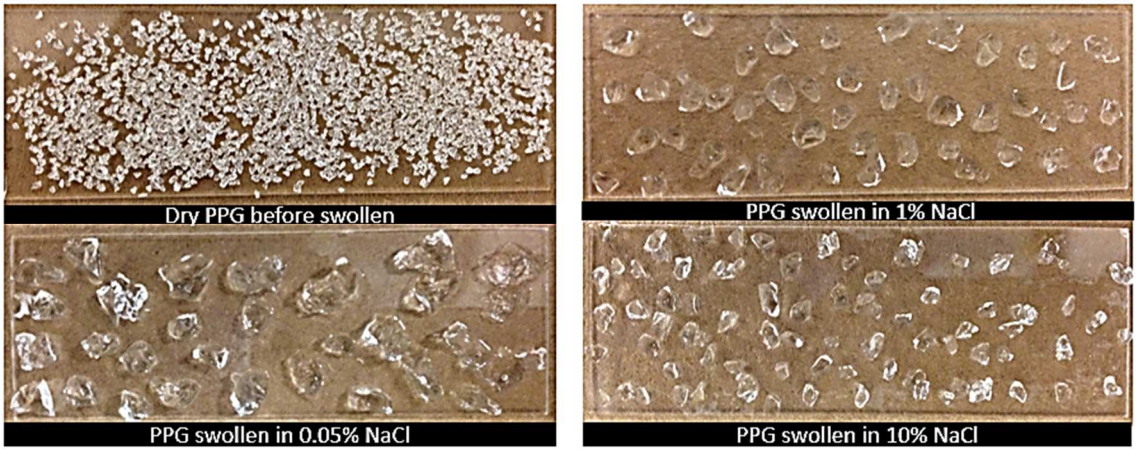

Figure 3.2—PPG (30-mesh size) before and after being swollen in different brine concentrations.

The brine concentration was carefully selected according to the gel strength and swelling ratio where the gel prepared in the low salinity brine had less strength and more swelling ratio than the gel prepared in the high salinity brine. Table 3.3 illustrates the swelling ratio and gel strength measurements for different brine concentrations. Storage moduli (G´) for the PPG prepared in different brine concentrations were measured at room temperature (23^{o}C) using a rheometer (Figure 3.3). The sensor used for measurements was PP335 TiPoLO2 016, with a gap of 0.2 mm between the sensor and the plate. G' were measured at a frequency of 1 Hz for each sample.

Table 3.3—PPG swelling ratio and strength measurements of 30 mesh size.

No	Brine concentration, % NaCl	PPG concentration, wt %	Swelling ratio	Gel strength, pa
1	0.05	0.60	165	515
2	1	2.0	50	870
3	10	4.0	25	1300

Figure 3.3—Gel strength measurement instrument.

3.4.3. Oil Viscosity. Three oils with different viscosities were used in this study. Their oil viscosities measured at certain temperatures are shown in Table 3.4

Table 3.4—Oil viscosity used for experiments.

Oil	Viscosity at 70 ^{O}F (cp)
Low Viscosity	1.5
Medium Viscosity	37
High Viscosity	195

3.5. EXPERIMENTAL SETUP

An apparatus was built to evaluate the factors impacting the permeability of the gel pack, as presented in Figure 3.4. The apparatus (simple channel) was built from an acrylic transparent tube and its square cross–section was 5.06 cm^2 and 26.5 cm long. Different brine concentrations and oil viscosities were injected into the PPG-filled transparent tube, using a syringe pump. Two caps with four stainless steel rods and nuts were used to hold the transparent tube channel. The core sample was fitted inside the tube with an O–ring to prevent any leakage of gel that might occur during brine injection. A piston made from an acrylic rod was located at the top of the tube to compress the gel inside the channel tube. A hole inside the piston was made to permit brine and oil to be injected through the gel after it was compressed. Two pressure gauges were connected, one at the inlet and the other at the bottom of the gel, to measure the differential pressure across the PPG.

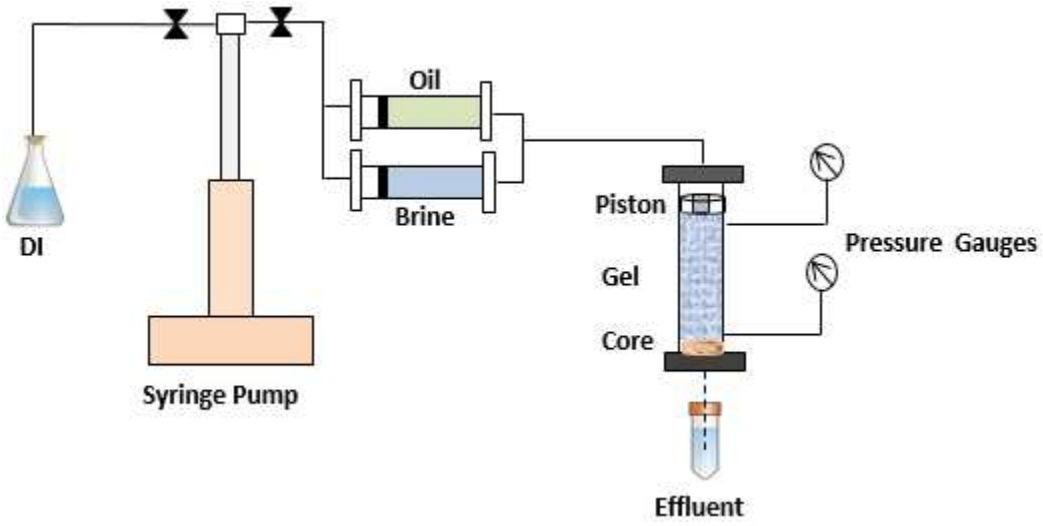

Figure 3.4—PPG pack permeability setup.

3.6. EXPERIMENTAL PROCEDURE

A consolidated sandstone core was fitted at the bottom of the channel tube model to prevent gel movement from reaching the outlet. Swollen PPG was then placed inside the transparent tube model. Six different injection fluid flow rates (0.1, 0.2, 0.3, 0.4, 0.5, and 0.6 ml/min) were used for each experiment to measure the PPG pack permeability.

A piston was then fitted inside the channel, and the gel was compressed at eight different load pressures: 75, 125, 150, 175, 200, 225, 250, and 275 psi. At each load pressure, the same injection flow rates were used to measure the gel pack permeability. The pressure drop across the PPG, the change in the length of the gel, and the fluid produced at the outlet were all recorded at the ambient temperature. In addition, to study the effect of load pressure on gel strength measurements, a sample of gel was taken before and after the gel was compressed.

3.7. RESULTS AND ANALYSIS

3.7.1. PPG Pack Permeability Measurements. This section discuss the effect of brine concentration, particle gel size, and oil viscosity on gel pack permeability measurements.

3.7.1.1. Brine concentration effect. Stabilized pressures for each concentration of brine were obtained at the different injection flow rates (Figure 3.5). The results showed that the stabilized pressure of the PPG rose as the flow rate increased. This increase, however, was significant only at a low flow rate (0.1 to 0.3 ml/min). For example, in the case of no piston effect, the stabilized pressure for the gel swollen in 10% brine started to increase from 1 psi to 2.8 psi at low flow rates (0.1 to 0.3 ml/min). At high flow rates (0.4 to 0.6 ml/min), the pressure slightly increased from 3.5 to 4.1 psi. Additionally, Figure. 3.5 provides a gel stabilized pressure comparison between the brine concentrations of 0.05% NaCl and 10% NaCl before and after the load pressure was introduced. The results showed that the pressure measurement at 0.05% did not increase significantly after the gel was compressed to 275 psi as compared to the results for the 10% solution. The pressure measurement increased almost 1 psi for the former and almost 13 psi for the latter. This behavior revealed that the permeability of a strong gel (swollen in a high brine concentrations) decreased more rapidly than that of a weak gel (swollen in a low brine concentrations) if high pressure was applied. All the measurements of gel particle compression were performed until 275 psi because it was observed that the gel pack permeability became almost at higher pressure. The results suggest that strong gel applications in an oil field will be more effective than weak gels at controlling water production.

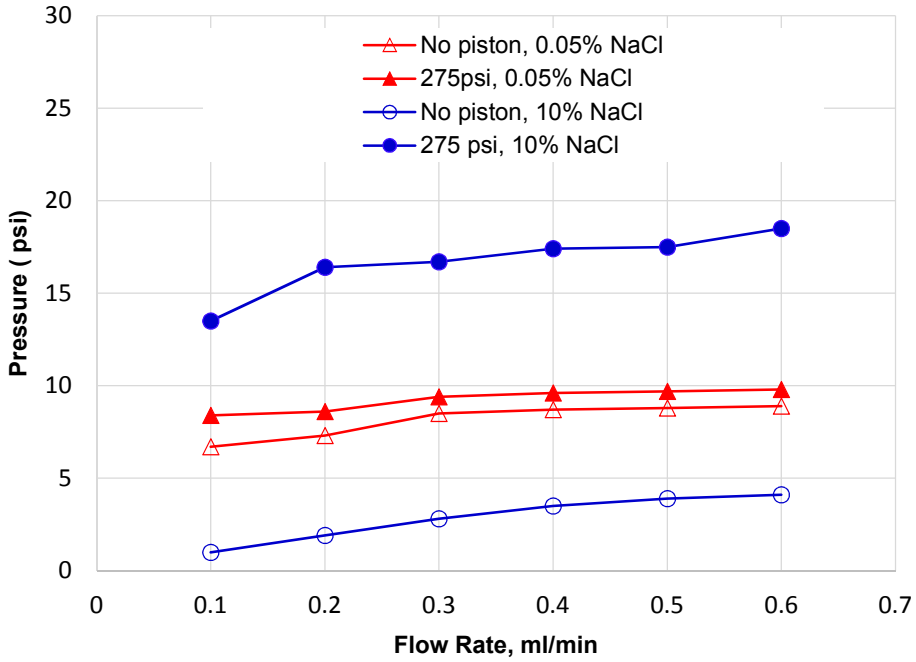

Figure 3.5—Stabilized pressure for brine concentrations before and after load pressure.

The PPG pack permeability calculated for the different brine concentrations was determined according to the power law equation and plotted as shown in Figure 3.6. At the initial load pressure, gel swollen in 10% NaCl started with a higher gel pack permeability than did gels swollen in either 0.05% NaCl or 1% NaCl. The gel pack permeability with a 10% brine concentration started at 103 md before the gel was compressed. The gel compressed gradually when the load pressure was applied. The gel pack permeability began to decrease continuously until 200 psi, it fluctuated between 5 and 7 md. The gel pack permeability with a 0.05% NaCl brine began at 20 md before the load pressure was applied. It started decreasing after the load pressure was applied. When the load pressure reached 175 psi, the gel pack permeability had a different trend. It started to form channels inside the gel, and the permeability increased to 11.8 md. When

the pressure was released, the gel network reformed and the gel pack permeability continued to decrease after the gel compressed to 200 psi.

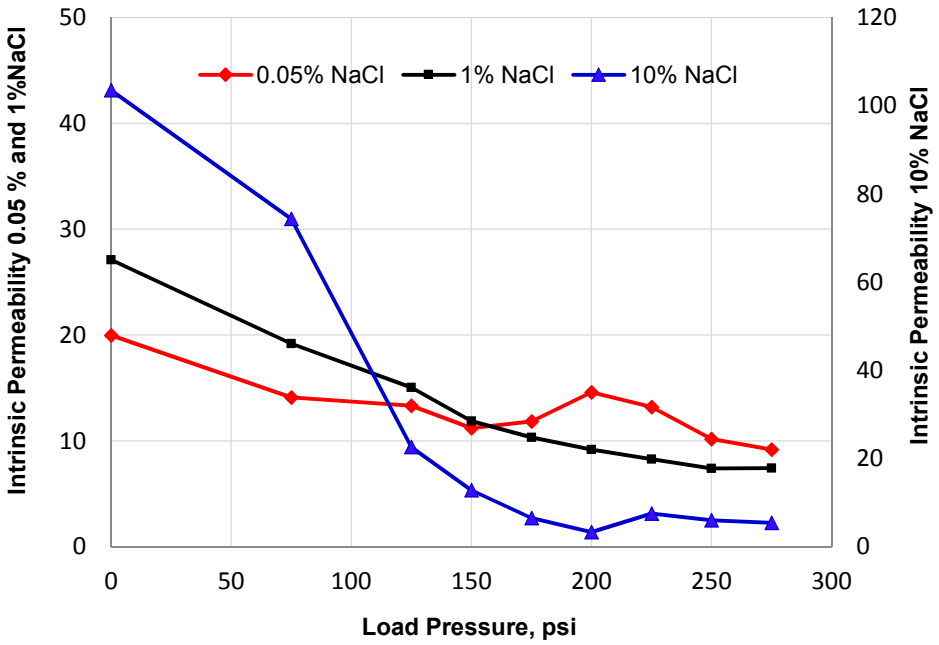

Figure 3.6—PPG pack permeabilities with different brine concentrations.

Figure 3.6 indicates also that the strong gel had a higher gel pack permeability than did a weak gel before the load pressure was introduced. At a high load pressure, however, the gel pack permeability exhibited a different trend. The decrease in the PPG pack permeability with a high gel strength was significantly less than that of the PPG pack permeability with a low gel strength.

Tables 3.5, 3.6, and 3.7 summarize both the permeability and elasticity measurements for the different brine concentrations as determined by using the power law equation. The elasticity index for the PPG varied between 0.7 and 0.9 for weak gels, while for strong gels, it varied between 0.3 and 0.8.

Table 3.5—PPG pack permeability measurements for 0.05% NaCl.

P (psi)	Intrinsic Permeability, ko (md)	Elasticity Index	R^2
No load	19.987	0.8417	0.9916
75	14.105	0.7792	0.991
125	13.316	0.7555	0.9803
150	11.196	0.9418	0.9924
175	11.856	0.9661	0.9986
200	14.594	0.7939	0.9901
225	13.201	1.381	0.9159
250	10.182	0.9003	0.9693
275	9.1823	0.9444	0.9961

Table 3.6—PPG pack permeability measurements for 1% NaCl.

P (psi)	Intrinsic Permeability, ko (md)	Elasticity Index	R^2
No load	27.114	0.8399	0.992
75	19.185	0.8464	0.9964
125	15.035	0.7729	0.9956
150	11.889	0.8575	0.9988
175	10.345	0.8055	0.9849
200	9.1845	0.8934	0.9937
225	8.2749	0.9505	0.999
250	7.4038	0.9349	0.9963
275	7.4382	0.9192	0.997

Table 3.7—PPG pack permeability measurements for 10% NaCl.

P (psi)	Intrinsic Permeability, ko (md)	Elasticity Index	R^2
No load	103.53	0.311	0.9372
75	74.323	0.1297	0.9699
125	22.643	0.4809	0.9287
150	12.809	0.6346	0.9743
175	6.4912	0.5848	0.9308
200	3.3611	0.8532	0.9963
225	7.5038	0.7202	0.9833
250	5.9863	0.6923	0.9659
275	5.4555	0.7136	0.9606

3.7.1.2. Preformed particle gel size effect. Various particle sizes were used to investigate how the PPG size affects the permeability measurements**.** Particles of all experimental sizes were swollen in the same brine concentrations (1% NaCl). Figure. 3.7 reveals that the PPG pack permeability was affected by particle size. Large particle sizes had a lower gel pack permeability than did smaller particle sizes across all of the load pressure ranges. The gel pack permeability with a particle size of 20-30 mesh was 27 md before adding the load pressure. The gel pack permeability then started to decrease gradually after the load pressure was introduced. The permeability decreased to almost 8 md at 200 psi. Gel with a particle size of 80-100 mesh had a gel pack permeability of 33 md before applying the load pressure. Permeability then decreased to almost 20 md at 200s psi.

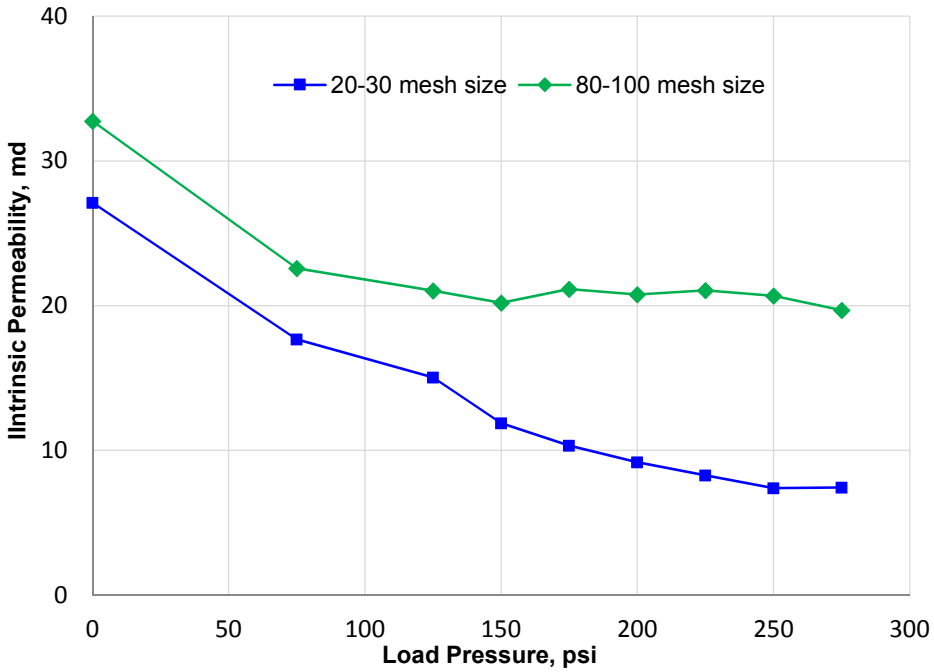

Figure 3.7—PPG pack permeabilities with different particle sizes.

In addition, the results showed that the PPG pack permeability before applying the load pressure was much larger than the PPG pack permeability after applying the load pressure. The PPG pack permeability decreased significantly when the load pressure was first applied. The permeability then became almost constant because the gel particles were compressed substantially, forcing them closer to one another during the earlier stages of the applied load pressure and less during the later stages. Similarly, this new finding indicated that the PPG pack permeability would have lower permeability at reservoir pressure conditions than it would at surface conditions. It also suggested that using smaller particles in the conformance control treatment would not result in a better gel resistance to water flow inside the high permeability channels.

3.7.1.3. Oil viscosity effect. Gels swelled at the same brine concentration (1%) and had the same particle size (30 meshes) were prepared to investigate the effect of changing oil viscosity on PG pack permeability. Figure 3.8 indicates that gel pack permeability to oil improves as oil viscosity increase. At 1 ft/day, PG pack permeability measurement for oil with 1.7 cp was 192.2 md and it improves to 2254 md when oil viscosity increase to 37 cp. Oil with high viscosity cause more deformation of gel more than oil with low viscosity, consequently easier for oil to open channel and pass through it. PG pack permeability measurement to oil was also found to be velocity dependent and permeability increased as velocity increased.

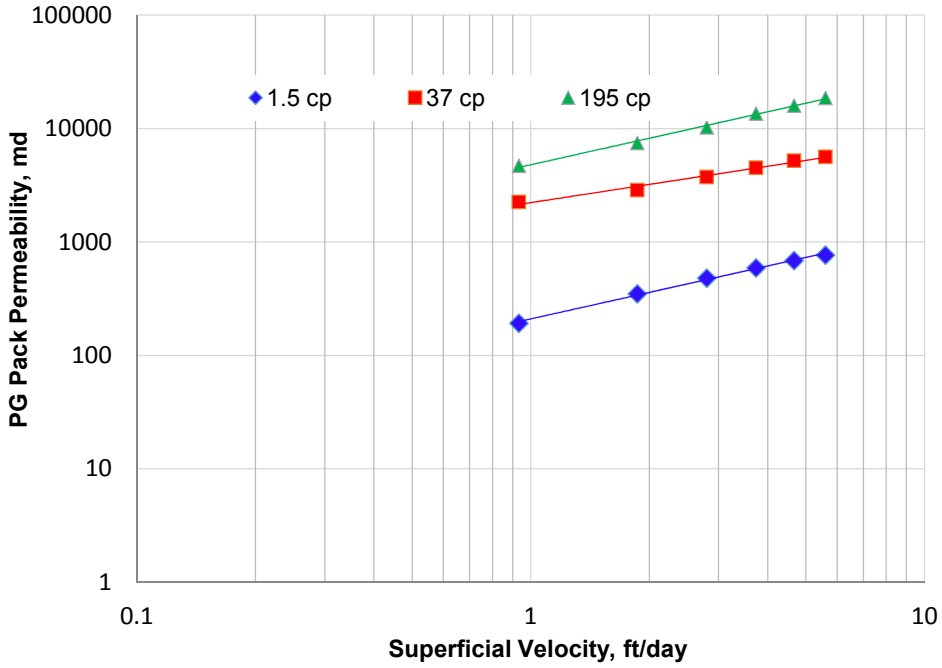

Figure 3.8—PPG permeability as a function of oil viscosity.

3.7.1.4. PPG pack permeabilities for oil viscosities and 1% brine. PPG pack permeability measured for different oil viscosities and 1% brine at the same particle size

30 mesh sizes was compared in Figure 3.9. Results indicate that PPG pack permeability to oil is much bigger than PPG pack permeability to water. PPG pack permeability for 195 cp is almost 100 times PPG pack permeability for 1% brine. PPG pack permeability was found to increase with oil viscosity and results suggest that PG has a significant potential of success in viscous oil reservoirs.

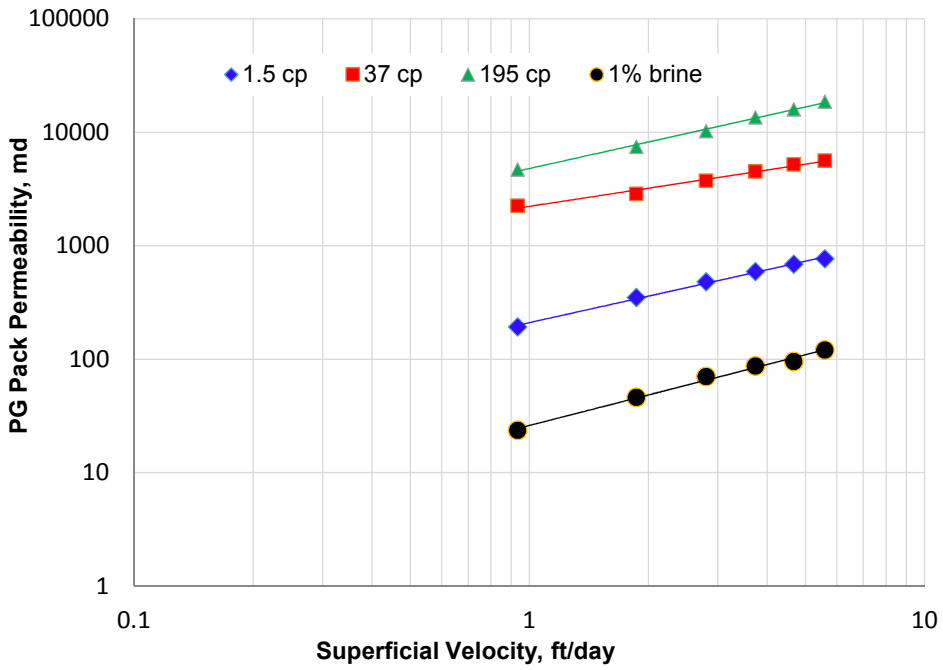

Figure 3.9—PPG pack permeabilities for brine and oil.

Results shown in Figure. 3.10 indicate that gel permeability improved as the oil viscosity increased. The Gel pack permeability measured of flowing oil with 1.5 cp had started with 209 md and decreased to 26 md when pressure load was applied. When oil viscosity increased for example to 195 cp, gel pack permeability was began at 4788 md and decreased to almost 2650 md when pressure load was applied. Thus, the more

viscous the oil, the more the PG deformed then the easier for the oil to open channel and flow through it. Based on this finding, PG has large potential of success in high viscous oil reservoir applications.

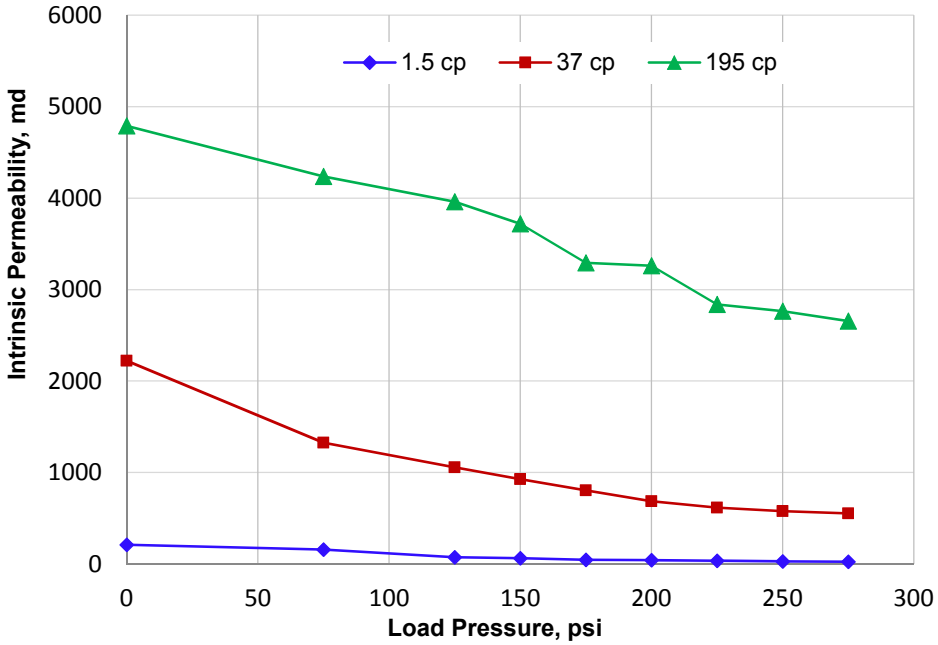

Figure 3.10—PPG pack permeabilities for different oil viscosities.

3.7.2. Gel Pack Permeability Reduction. This section presents a comparison between the gels pack permeability determined before and after load pressure for both effects of brine concentration and particle size. The results obtained from this comparison are important to quantifying the change in the gel permeability and the rheology that occurred during the PPG compression.

3.7.2.1. Reduction of PPG pack permeability for brine concentrations. The effect of brine concentration on the PPG pack permeability can be expressed using the Permeability Gel Reduction (KGR) factor. It can be defined as the ratio between the PPG

pack permeability measured after using the load pressure (KGA) and the PPG pack permeability measured before the load pressure (KGB). This concept, which is expressed in a percentage, is used to determine how much the PPG permeability can be decreased.

Table 3.8 illustrates the permeability results obtained for 30-mesh size PPG swollen in three different brine concentrations. The results indicated that the KGB increased as the brine concentration increased. When the load pressure was applied, however, the KGA decreased as the brine concentration increased. Consequently, the PPG permeability reduction (KGR %) rose as the gel strength increased. The KGR for a gel swollen in 0.05% NaCl was 54.05%; the KGR for a gel swollen in 10% NaCl was 94.73%. These results suggested that the plugging efficiency can be improved if a strong gel is selected for the conformance control treatment.

Table 3.8—Reduction of PPG pack permeability as a function of brine concentration.

Particle Size (mesh)	Brine Concentration, % NaCl	KGB	KGA@275psi	KGR (%)
30	0.05	19.987	9.1823	54.05
30	1	27.114	7.4382	72.56
30	10	103.53	5.455	94.73

3.7.2.2. Reduction of PPG pack permeability for particles sizes. Table 3.9 displays the effect of different particle sizes on the PPG pack permeability reduction. Particles of various sizes were swollen in the same brine concentration (1% NaCl). The findings show that the PPG pack permeability before and after applying the load pressure

was greater for smaller particle sizes than for larger particle sizes. The PPG permeability reduction (KGR %) did not significantly change for the experimental particle sizes. Compared with the effect of brine concentration, particle size had less effect on the KGR.

Table 3.9—Reduction of PPG pack permeability as a function of particle size.

Brine Concentration % NaCl	Particle Size (mesh)	KGB (md)	KGA@275 psi	KGR (%)
1	18-20	22.201	6.167	72.2
1	20-30	27.114	7.4382	72.56
1	50-60	27.351	16.846	38.4
1	80-100	32.756	19.592	40.1

3.7.2.3. Reduction of PPG pack permeability for oil viscosities. Reduction of particle gel permeability for different oil viscosities was also obtained in this study. Table 3.10 summarizes the PPG pack permeability results for different oil viscosities at the same particle size. PPG permeability to oil before and after applying load pressure is increasing with increasing of oil viscosity. Additionally, these results indicate that the permeability reduction (KGR %) of high oil viscosity is less than it is for less oil viscosity. For example, oil injections with 195 cp had gel permeability reduction 44.57% while oil with less viscosity (1.5cp) had gel permeability reduction 87.5%. This result is

reporting a very unique feature for PPG for controlling excess water production in high viscous oil reservoirs.

Table 3.10—Reduction of PPG pack permeability as a function of oil viscosity.

Particle size (mesh)	Oil viscosity (cp)	kGB (md)	KGA@275 psi	KGR (%)
30	1.5	209.55	26.041	87.5
30	37	2222	555.14	75
30	195	4788.4	2654.2	44.57

3.7.3. PPG Strength. A rheometer was used to measure the strength of the gel swollen in 0.05, 1, or 10% NaCl. Figure. 3.11 presents the PPG strength measurements before and after the load pressure was applied. G`A and G`B are gel strengths measured before and after the load pressure was introduced, respectively. The results suggested that the gel strength increased as the brine concentration and load pressure increased. Analogously, this result revealed that the gel strength would increase when gel is injected into the target formation under reservoir pressure conditions.

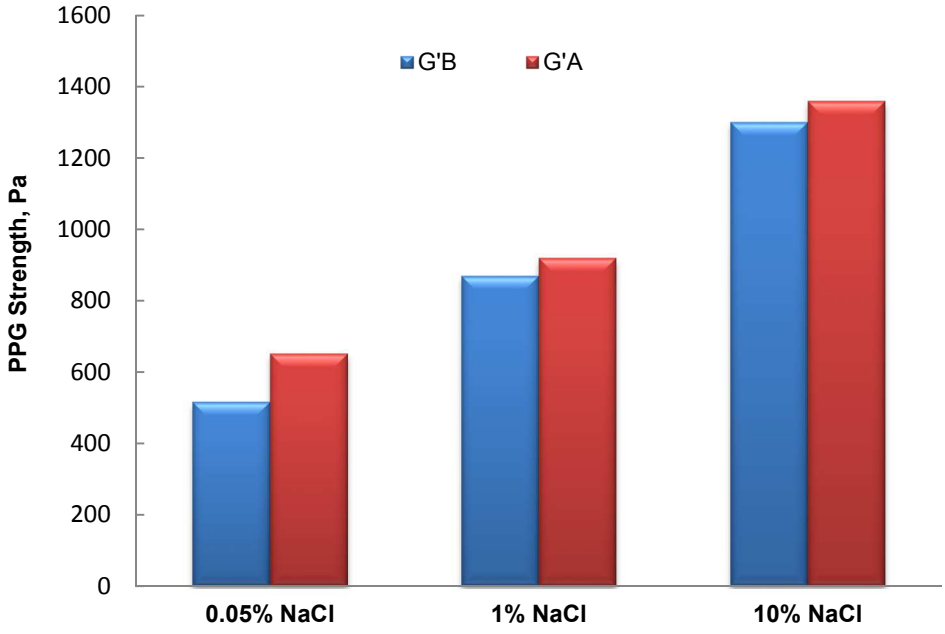

Figure 3.11—PPG strength before (G`B́) and after (G`A) load pressure.

3.7.4. PPG Compressibility Measurement. The results obtained from the experiments demonstrated that the PPG can be compressed at various values based on both different brine concentrations and load pressures. Gel compressibility was obtained and plotted in Figure 3.12 for the different brine concentrations. The PPG for all brine concentrations had a large compressibility value at the beginning of the introduced load pressure. For instance, the PPG swollen in 10% NaCl had a compressibility of 0.0037 psi^{-1} at 75 psi and then decreased gradually to 0.00172 psi^{-1} at 275 psi. The findings obtained from the compressibility measurements are consistent with data obtained from the PPG pack permeability measurements. At the initial load pressure of 75 psi, the gel

compressibility of the solution with 10% NaCl was 0.0037 psi^{-1}, while the gel compressibility of the 1% brine concentration at 75 psi load pressure was only 0.000527 psi^{-1}. The compressibility for both brine concentrations 1% NaCl and 10% NaCl is fairly fitted by Equation 3.3 and Equation 3.4**,** respectively, as follows:

$$C_{ppg} = 0.0091\ P^{-0.614} \quad \text{.....(3.3)}$$

$$C_{ppg} = 0.0437\ P^{-0.573} \quad \text{.....(3.4)}$$

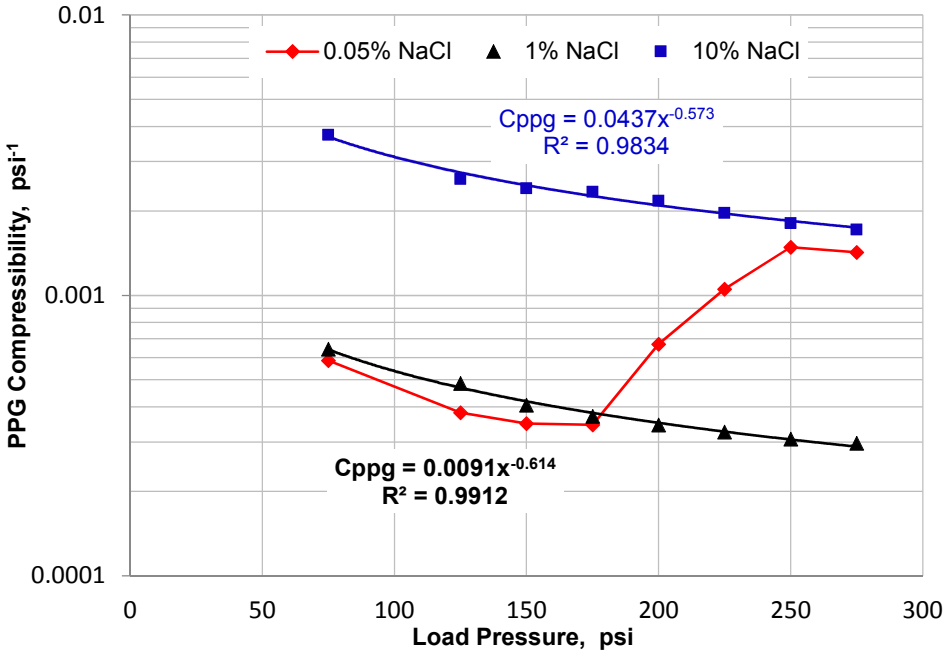

Figure 3.12—PPG compressibility (psi^{-1}) and load pressure (psi).

Additionally, the results in Figure 3.12 indicated that the compressibility for a PPG swollen in 0.05% NaCl decreased gradually and then suddenly increased at 175 psi. This increase most likely occurred due to the channel created during the PPG

permeability measurement process. Data also suggested that PPGs swollen in high brine concentrations are more compressible than PPGs swollen in low brine concentrations. The average PPG compressibility obtained for all brine concentrations ranged between 0.0003 psi^{-1} and 0.003 psi^{-1}. Table 3.11 shows the procedure for finding the compressibility in relation to the load pressure.

Table 3.11—Compressibility of 30-mesh size with1% NaCl.

P (psi)	*L*	Vo	*V2*	Delt V	Delt P	Cppg (Psi^{-1})
75	22.5	118.5093	113.9513	4.55805	73	0.000527
125	22.4	118.5093	113.4448	5.0645	123	0.000347
150	22.3	118.5093	112.9384	5.57095	147	0.00032
175	22.1	118.5093	111.9255	6.58385	173	0.000321
200	21.9	118.5093	110.9126	7.59675	198	0.000324
225	21.7	118.5093	109.8997	8.60965	223	0.000326
250	21.6	118.5093	109.3932	9.1161	250	0.000308
275	21.5	118.5093	108.8868	9.62255	273	0.000297

3.8. DISCUSSION

This section discusses four major findings: PPG pack permeability, PPG deformations, PPG compressibility, and PPG elasticity.

3.8.1. PPG Pack Permeability is Velocity Dependent. The PPG pack permeability was obtained for water flow through the gel-filled channel tube. The Darcy law for flow through porous media (Equation 3.5**)** was used to measure the PPG pack permeability:

$$\nu = \frac{\mathrm{Q}}{\mathrm{A}} = \frac{-K\Delta P}{\mu \mathrm{L}} \quad \text{.....(3.5)}$$

where Q (cm^3/s) is the flow rate, A (cm^2) is the cross-sectional area, Δ_P(atm) is the pressure drop over the length L (cm) of the gel, μ (cp) is the fluid viscosity, and K (md) is the permeability.

Because the gel is composed of shear-thinning or pseudo plastic materials, the PPG pack permeability measurements for the different brine concentrations and particle sizes were not constant. Instead, the measurements revealed that the PPG was velocity dependent, following a nonlinear relationship. Additionally, the PPG permeability was dependent not only on the velocity of the brine injected but also on the elasticity index of the gels. Therefore, all results for the PPG permeability were fitted according to the power law model. We also observed that increases in the injection flow rate caused a rise in the gel pack permeability and also deformed the gel in a manner that was proportional to the applied pressure.

3.8.2. Preformed Particle Gel Deformations. The water and oil flow through gels demonstrated a different trend in gel pack permeability measurements. This might happen due different level of gel deformation during fluid flow. The change in both PPG permeability and rheological properties can be explained as follows:

3.8.2.1. PPG strength. Results obtained from the rheometer (Figure 3.11**)** show that the gel rheology changed after the load pressure was introduced. This feature is an advantage for the PPG because the gel became stronger than it was at surface conditions. Thus, a better water flow control can be achieved in large channeled reservoirs. Also gel strength results obtained for oil flow through gel as shown in Figure 3.13 suggested that gel strength in oil have also an effect on gel pack permeability values. The gel strength for oil was less than for water; consequently gel with less strength has higher permeability than gel with high strength. This might add another reason for why gel permeability to water is decrease more than to oil.

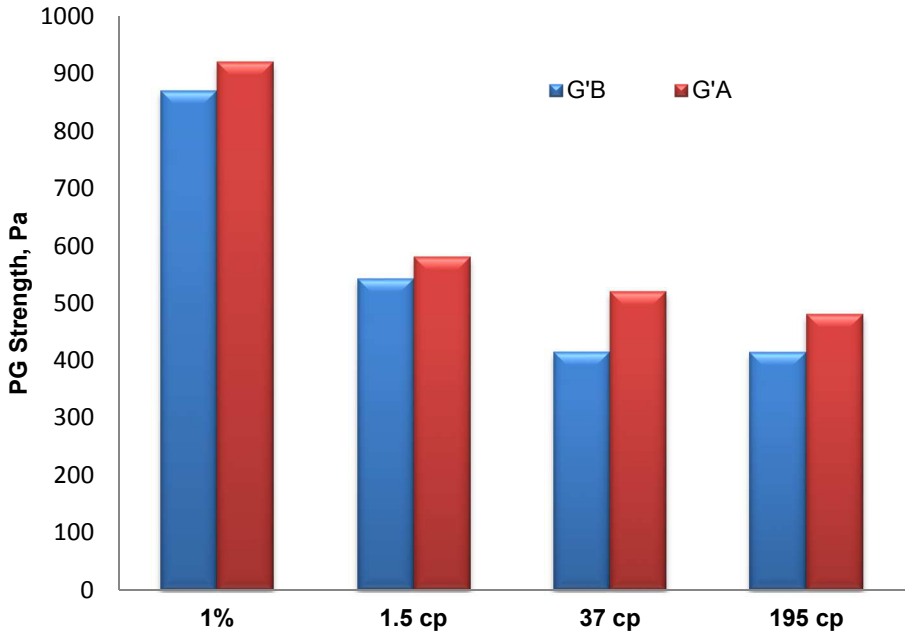

Figure 3.13—PPG strength before (G`B) and after (G`A) load pressure.

Gel strengths measured after the load pressures were correlated with the PPG pack permeability are shown in Figure. 3.14. The power law model equation for the gel

pack permeability was obtained as a function of gel strength. The gel strength for oil was less than for water; consequently gel with less strength has higher permeability than gel with high strength. This might add another reason for why gel permeability to water is decrease more than to oil. The primarily results also indicate that PG strength increased after the load pressure was applied.

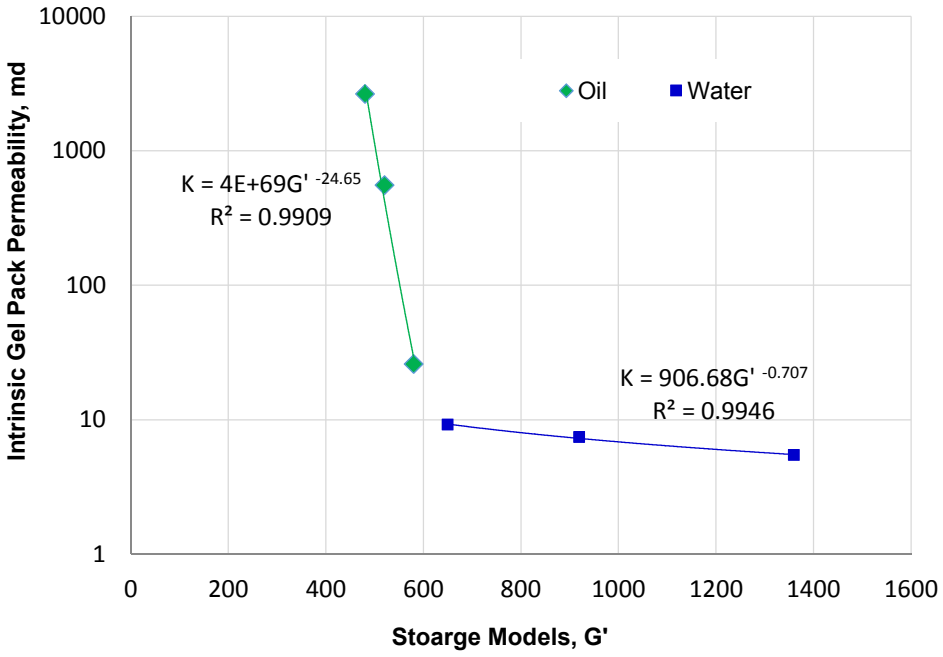

Figure 3.14—Intrinsic gel pack permeability as a function of storage modulus.

3.8.2.2. PPG compressibility. The PPG compressibility plays a crucial role in controlling water production. If the gel can be compressed using a high pressure, the plugging efficiency of the gel will be increased. This happens because the gel particles can move closer to each other and minimize the possibility that there is any open pore size during water flow. Consequently, water will be trapped behind the gel and cannot move further.

The results demonstrate that the PPGs can be compressed at different values based on the gel strength difference. This is the first study to report this feature of the PPG, and more research is needed to compare the traditional gel compressibility with the PPG.

3.8.2.3. PPG elasticity. The elasticity index for the PPG at different gel strengths was measured after applying the load pressure (Table 3.12). These findings reveal that the gel storage model (G`) increased as the elasticity index decreased. The blocking efficiency of the PPG was significantly affected by the gel strength. Gels with high storage moduli would be preferable for conformance control field applications.

Table 3.12—PPG permeability as a function of elasticity index and storage model.

Brine concentration % NaCl	Effective Permeability	Elasticity Index	Storage Moduli G´(Pa)
0.05	9.1823	0.944	650
1	7.4382	0.919	920
10	5.455	0.713	1360

Results have shown also PPG shrinks in oil and swells in water. PPG pack permeability to oil was much higher than PPG to brine. One of the reasons to this difference in permeability is that PPG intends to shrink in oil and swell in brine.

Figure 3.15*a* show dry gel can be swelled in brine many times of its original size which help to reduce the PPG pack permeability to water. However, Figure 3.15*b* show PPG water base after saturated with oil for three weeks, the gel volume decrease

dramatically to the half of original PPG volume. This decrease in gel particle size allows easily movement of oil through gel and cause gel permeability to oil increase compared to water.

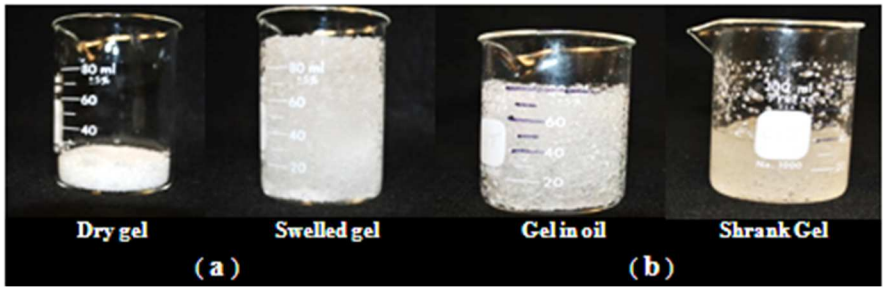

Figure 3.15—Illustrates how PPG volume shrinks in oil and swells in brine.

3.9. CONCLUSIONS

During these investigations of factors affecting the gel pack permeability formed inside large channeled features, the following are conclusions observed from the study:

- A PPG partially blocks the large channel rather than fully blocking it. The PPG will do so because the gel can formed channels for water to pass through. Therefore, we strongly recommend that operators in the field consider the effect of both particle size and brine concentration when designing PPGs for water production control purposes.
- Gel-plugging efficiency is affected by particle size selection. Our results indicated that gel resistance to water flow improved when larger particles were selected.
- Brine concentration had a significant effect on the PPG resistance to water flow. We observed that strong gels had a lower permeability than did weak gels.

Therefore, a strong PPG would be the right choice for more effectively plugging an undesired zone than a weak gel.

- Brine concentration had a more pronounced effect on the PPG pack permeability than did gel particle size.
- The gel pack permeability decreased significantly at the beginning of the compression process. Then, after the gel became slightly rigid because of the load pressure effect, the compressibility reduction became less obvious. The PPG was compressible between 0.0003 psi^{-1} and 0.003 psi^{-1}. This compressibility varied according to both brine concentration and particle size.
- The PPG strength increased as both the brine concentration and the load pressure increased. A weak gel creates internal channels more easily than a strong gel when the PPG is subjected to continuous load pressure.
- Gel pack permeability is lower at reservoir conditions compared to the gel pack permeability at surface conditions. The gel pack permeability measurements registered a few hundred *millidarcies* before the load pressure was applied; the gel permeability decreased to less than 10 md after the load pressure was introduced.
- PPG pack permeability measurements indicate that the PPG pack permeability of oil is much more than PPG pack permeability for water. PPG pack permeability of oil is increased as oil viscosity increased which imply that PPG can be applied successfully in viscous oil reservoirs.

4. EVALUATE THE EFFECTIVENESS OF USING ACID TO REMOVE GEL CAKE

4.1. INTRODUCTION

In both cross flow and no cross flow strata, a small portion of gel still propagates into un-swept low-permeability zones in spite of the millimeter-sized gel preferentially entering into fractures or fractures features channels. Gel penetrates into un-swept zones and forms a cake on the surface of low-permeability layers. This gel cake adversely affects oil production by reducing the permeability of the near wellbore region. The extent of formation damage depends on the gel properties and the rock permeability interactions (Elsharafi and Bai, 2012). This section is discussing the effective of using Hydrochloric acid to mitigate/remove gel filter cake damage anticipated on the low permeability zones.

4.2. OBJECTIVES OF AND TECHNICAL CONTRIBUTIONS

- Examines the effectiveness of using hydrochloric acid to remove the damage caused by particle gel penetrating into low-permeability zones.
- Evaluate the interaction between particle gel and hydrochloric acid. The swelling ratio, deswelling ratio, effect of pH, and gel strength is investigated.
- Establish core flooding experiments to fully understand the factors affecting gel cake formation on the surface for different low-permeability cores.
- Various concentrations of HCL along with variations in pH is used to obtain an optimum acidizing treatment.
- Results from this experiment will be used to assist to improving conformance results and improving oil recovery from low permeability rich oil zones.

4.3. EXPERIMENTAL DESCRIPTION

4.3.1. Preformed Particle Gel. Superabsorbent polymer was used as the PPG to conduct the experiments. Its main chemical component is potassium salt of crosslinked polyacrylic acid/polyacrylamide copolymer. Dry PPG with a size of 30 mesh was selected to be swollen in different brine concentrations.

4.3.2. Hydrochloric Acid (HCl). HCl from Fisher Scientific was diluted with distilled water to obtain concentrations of 5%, 10%, 15%, and 20%. A 10% HCl solution was diluted again with water to prepare solutions with pH values of 1.3, 3, and 5.5.

4.3.3. Berea Sandstone. A variety of Berea sandstone, having a diameter of 2.5 cm and length of 4.5 cm, was used for the experiments. The core was placed in the oven at around 45^{o}C for an entire night before it was vacuumed and then saturated with brine.

4.3.4. Rheometer. The storage moduli (G`) for gel swollen in brine and acid were measured at room temperature (around 23^{o}C) using a rheometer. After being swelled in brine and deswelled in acid, gel strengths were measured and compared to see if the gel strength in acid increased or decreased after acid treatment. The sensor used for measurements was PP335 TiPoLO2 016, with a gap of 0.8 mm between the sensor and the plate. G` were measured at a frequency of 1 Hz for each sample.

4.4. EXPERIMENTAL SETUP

Figure. 4.1 is a schematic model used to carry out the experiments. It is comprised of a syringe Isco-pump used to inject brine concentrations and gel through the accumulator into a Hassler core holder. Berea sandstone was placed inside the holder, and the confining pressure was adjusted to have a minimum of 500 psi difference above

the injection pressure. Spacers five cm long were placed inside the core holder in front of the core to allow gel placement at the sand face of the core. An injection pressure gauge was installed at the inlet of the core holder to measure the brine injection pressure during the experiment. Test tubes were mounted at the effluent to collect the brine produced during the injection processes.

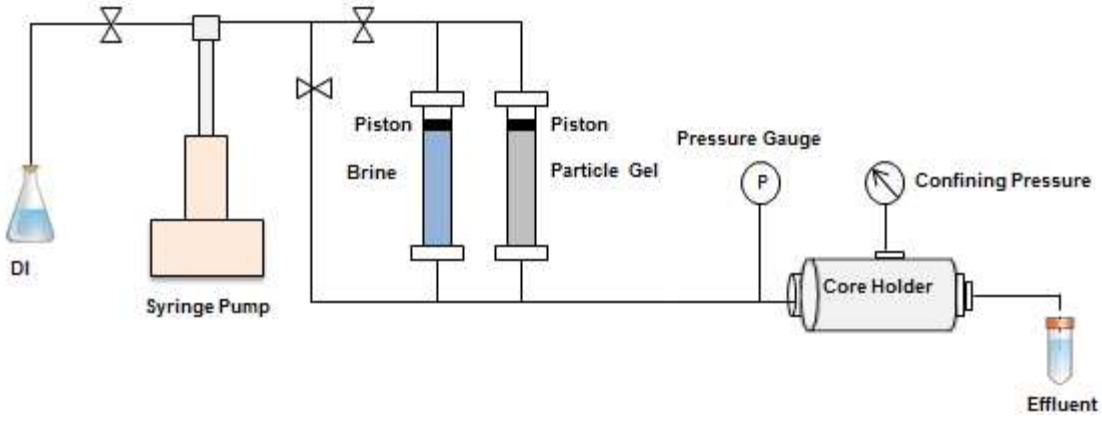

Figure 4.1—Experiment setup for gel filter cake removal.

4.5. EXPERIMETAL PROCEDURE

The experimental procedure was divided into two main steps. The first step was to investigate the interaction between HCl and the PPG. The second step was to evaluate the gel cake damage that occurred during the gel treatments and assess the gel cake-removal efficiency after the acid treatments.

4.5.1. Interaction between the Hydrochloric Acid and the PPG. A 0.5 ml of 600 μm dry gel was immersed in 49.5 ml of different brine concentrations (0.05%, 0.25%, 1%, and 10%) of NaCl at room temperature to determine the swelling capacity of the PPG with time. The swelling ratios of the PPG in different brine solutions were obtained using this equation:

$$\text{Swelling capacity} = \frac{V_2 - V_1}{V_1} \quad \text{.....(4.1)}$$

where V_2 is the final volume of the gel sample after swelling and V_1 is the initial volume of the gel sample before swelling.

To measure the swelling capacity of the same dry PPG size (600 μm) in relation to the acid concentration, solutions of 49.5 ml were prepared using different HCl concentrations (5%, 10%, 15%, and 20% by volume). In addition, the 10% HCl concentration was used to prepare varying pH values to examine the effect of pH on the swelling capacity measurement. The pH values of these solutions were adjusted by adding water and precisely checked using a pH meter. Samples of gel were collected after swelling in brine and after deswelling in acid and were placed on the disc of the rheometer to measure their strength.

Samples of fully swollen gels from different brine solutions were collected and placed in test tubes to measure the gel deswelling in different acid concentrations and at different pH levels. The deswelling capacity was measured against time, and the volume change was visibly monitored. The deswelling capacity of the PPG can be calculated using this equation:

$$\text{Deswelling capacity} = \frac{V_i - V_f}{V_i} \times 100 \quad \text{.....(4.2)}$$

where V_i is the initial volume of the swellable gel sample and V_f is the final volume of the gel sample after deswelling.

Finally, after measuring the deswelling capacity of the gel in acid, the gel inside the tubes was flushed with ten cycles of the same brine composition to test if the gel could be swelled again when it contacted the same brine solution.

4.5.2. Evaluation of Gel Cake Damage and HCl Performance. Core flooding was carried out to evaluate the damage caused by the gel cake and the effectiveness of using HCl to remove this damage. Core flooding started by performing filtration test experiments to monitor and assess the buildup of the gel cake and ended by evaluating the performance of HCl in mitigating the formation of the gel cake. The procedure used for the filtration test experiment is briefly described below:

1) The Berea sandstone with a permeability range of 4 to 65 md was placed in the oven at around 45^{o}C for an entire night before it was vacuumed and then saturated with 1% NaCl.
2) The core was put in a Hassler core holder and subjected to a confining pressure. The average absolute permeability of the core was measured using flow rates of 0.5, 0.75, 1, 1.25, 1.5, 1.75, 2, and 3 ml/min.
3) A 60-ml solution of completely swellable PPG in brine was injected through a 5-cm spacer and placed facing the core. Saline water was injected again, with flow rates of 0.5, 0.75, 0.5, 1, 0.5, 1.25, 0.5, 1.5, 0.5, 1.75, 0.5, 2, 0.5, 3, and 0.5 ml per

min. The rationale for repeating the 0.5 ml per minute flow rate after each other flow rate was to determine whether or not the core was damaged further when the flow rate was increased.

4) A filtration curve was constructed by recording the cumulative brine produced as effluent as a function of time for every injection brine flow rate.
5) The gel was removed from the core holder, and the permeability of the core was measured again to determine the effect of the gel cake on the core permeability reduction.

Finally, after completing the filtration test experiments, the core was soaked in 65 gm of HCl for 12 hrs and replaced in the holder to measure the permeability after the acid treatments.

4.5.3. Evaluation of the Gel Cake Formed and Removed. Gel that was swelled in brine concentrations of 0.05%, 1%, and 10% was used to evaluate the gel cake strength for each core permeability range. Different cycles of the same brine solution were flooded to demonstrate if the gel cake would damage the core further when the flow rate was increased. For each flow rate, the brine produced as the effluent was collected every two minutes to monitor the gel cake-buildup during the injection process.

Darcy's law was applied to calculate the core permeability before and after treatments. The permeability can be obtained using Equation 4.3.

$$k = \frac{q\,\mu\,L}{A\,\Delta P} \quad \text{.....(4.3)}$$

where q is the flow rate (ml/sec), μ is the brine viscosity (cp), L is the length of the core (cm), A is the cross-sectional area (cm^2), and Δp is the pressure drop across the core (atm).

The core permeability after the introduction of the gel can be expressed as the core permeability reduction, which is defined as the relationship between the initial permeability and the permeability after the introduction of the gel, and can be calculated using Equation 4.4.

$$k_{RD} = \frac{ki-ka}{ki} \times 100 \quad \text{.....(4.4)}$$

where k_{RD} is the core permeability reduction (%), k_i is the initial core permeability (md), and k_a is the core permeability after adding the gel (md).

The core sample was removed carefully from the holder, and only one centimeter of the core face was submersed within the HCl. The core permeability was measured to observe the change in permeability after the acid treatments. Equation 4.5 was used to calculate the retained permeability obtained after soaking for various times in acid.

$$k_{RT} = \frac{k_f}{k_i} \times 100 \quad \text{.....(4.5)}$$

where k_{RT} is the core permeability retained (%), k_i is the initial core permeability (md), and k_f is the final core permeability after applying the acid (md).

4.6. RESULTS AND ANALYSIS

To investigate which factors caused more damage to the core and to make the HCl stimulation more efficient, we first studied the interaction between the PPG and the acid in terms of the swelling ratio, gel strength, and deswelling ratio. The information obtained from this interaction provided a deep understanding of the factors that caused more damage to the core and the factors that would help to mitigate such damage. Core flooding was then performed to confirm the results obtained from the interaction study and to quantitatively evaluate the core damage and the HCl efficiency.

4.6.1. Interaction between HCl and PPG Measurement. The swelling ratio, gel strength, deswelling measurements for PPG in brine and acid are discussed in the following subsections.

4.6.1.1. Swelling capacity measurement. Superabsorbent polymers are lightly crosslinked networks of hydrophilic polymer chains. Polymer networks carrying dissociated, ionic functional groups help substantially to hold a large amount of water and swell while maintaining the physical dimension structure. PPG can swell and contract in response to structural factors and properties of the swelling medium. Structural factors include charge, degree of ionization, crosslink density, and hydrophobicity, while the swelling medium properties include pH, ionic strength, and the counter ion and its valency. This section will focus more on discussing the effect of the medium properties on the degree of PPG swelling than on the structural factors.

Dry PPG was placed separately in test tubes filled with different brine concentrations and different HCl concentrations. The stable swelling ratio was computed for each concentration. Figure 4.2 shows the influence of the brine concentration and acid

concentration on the swelling capacity. The PPG showed normal swelling ratio behavior; its swelling capacity initially increased with time and then attained equilibrium swelling capacity (ESC). The swelling degree is generally determined as a balance between water absorption (due to the hydrophobicity of polymer chains) and network elasticity (proportional to crosslink density).

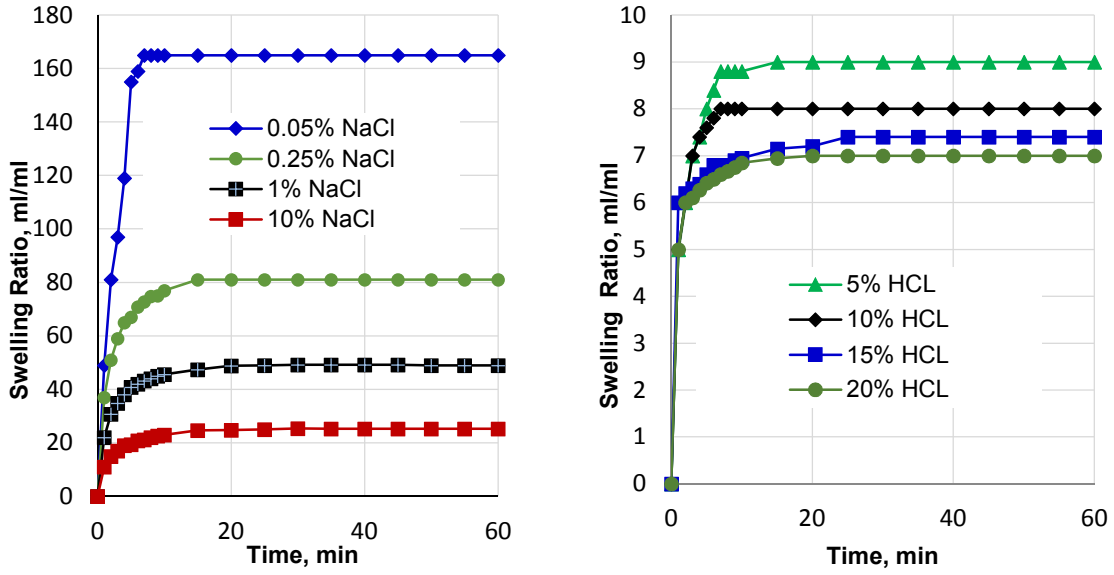

Figure 4.2—Swelling ratio of gel in different brine and HCl concentrations.

The swelling pressure of PPG (Π) is determined by a summation of the osmotic pressure Π_{osm} and the elastic pressure $\Pi_{elastic}$ (Rubinstein et al., 1996)

$$\Pi = \Pi_{osm} + \Pi_{elastic} \quad \text{..... (4.6)}$$

The osmotic pressure acts to swell the gel, while the elastic pressure (shear modules) restricts the swelling. The osmotic pressure consists of two contributions, one

from polymer-solvent mixing (Π_{mixing}) and the other from the mobile ion concentration (Π_{ions}).

$$\Pi_{osm} = \Pi_{mixing} + \Pi_{ions} \quad \text{..... (4.7)}$$

The results indicate that the particles swelled much more in brine compared to acid. The swelling ratio for the PPG swollen in brine reached 165 ml/ml when it was swollen in a 0.05% brine concentration. In contrast, the swelling ratio for the PPG swollen in acid reached only 9 when it was swollen in 5% HCl. The swelling ratio for the gel particles swollen in both brine and acid increased as the concentrations for both decreased. The concentration change had a very clear effect on the swelling ratio for brine compared to acid. The swelling ratio rose by a factor of two (from 81 to 165 ml/ml) when the brine concentrations decreased from 0.25% to 0.05%. However, the swelling ratio increased 1.2 times (from 7 to 9 ml/ml) when the acid concentrations decreased from 20% to 5%. As the brine concentration decreased, the PPG swelled more, became weaker, and began to soften. This decrease in gel strength is likely the result of the gel absorbing a large amount of water and also presumably due to the static electric repulsive force and charge balance. At low salt concentrations, the electric repulsive force will separate the gel molecules and create more space for water to enter (Bai et al., 2007a).

The ESC data obtained from Figure 4.2 was used in Figure 4.3 to show how brine and HCl concentration correlations can be applied to predict the ESC values of both concentrations. Figure 4.3 illustrates that the higher the concentration, the smaller the ESC value. Equation 4.8 is the correlation obtained to predict the ESC of the gel swollen

in brine, while Equation 4.9 is the correlation to predict the ESC of gel swollen in HCl. Both correlations were fitted with the power law model, with high R^2 accuracy.

$$ESC = 53.084 \times C_{brine}^{-0.352} \quad \text{.....(4.8)}$$

$$ESC = 12.077 \times C_{HCl}^{-0.181} \quad \text{.....(4.9)}$$

where ESC is the equilibrium swelling capacity, C_{brine} is the sodium chloride concentration in wt. %, and C_{HCl} is the HCl concentration in vol. %.

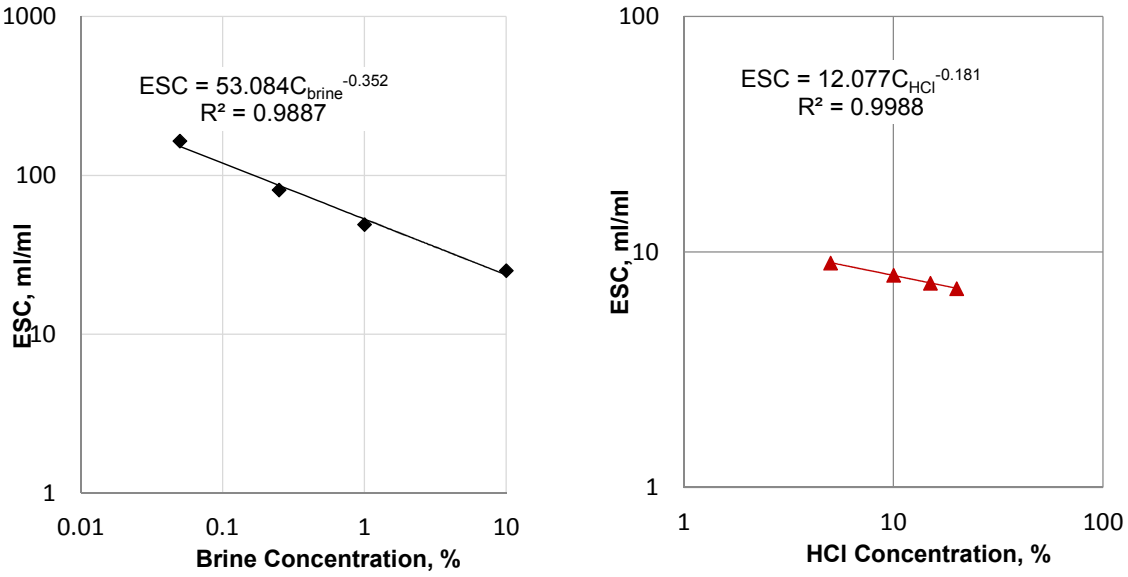

Figure 4.3—Effect of brine concentration and HCl concentration on the ESC.

A 10% HCl concentration was diluted to get three buffer solutions with pH values of 1.3, 3, and 5.5. The swelling ratio of the PPG composite in the different pH solutions was determined according to Equation 4. 1. Figure 4.4 shows that the swelling rate of the PPG reached its highest value within 10 minutes; later, the swelling rate decreased and

the curves became flatter. The solutions of varying pH had a pronounced effect on the swelling capacity. The swelling ratio of the PPG decreased significantly when the pH decreased to 1.3. The high repulsive of $–NH_2^+–$ and $–NH_3^+–$ groups in the acidic media increased the swelling ratio of the PPG as a result of an increase in the separation between the molecules in the gel, which created more space for water to enter; however, after the pH decreased too much, a screening effect of the counter ions (i.e., Cl^-) shielded the charge of the cations and prevented an efficient repulsion. The concomitant release of ions sharply reduced the internal osmotic pressure, thus reducing the water absorbency (Mahdavinia et al., 2004; Zhao et al., 2005).

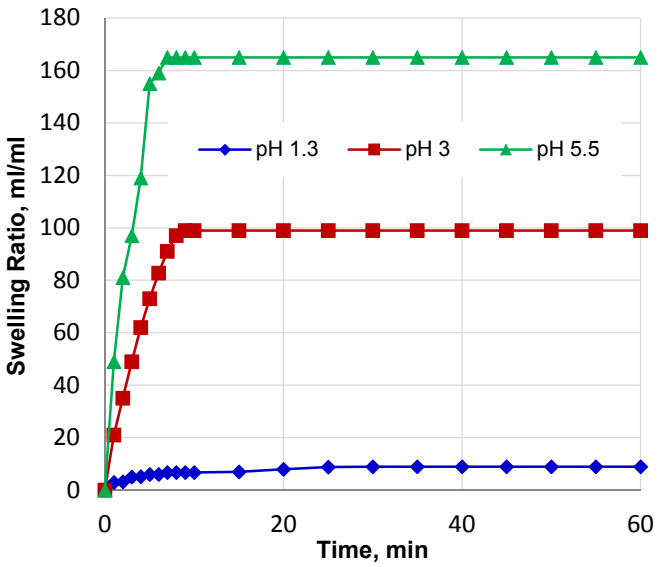

Figure 4.4—Swelling ratio of the PPG as a function of pH.

Figure 4.5 provides a comparison of the effects of brine concentration, acid concentration, and pH on the swelling degree as a function of ionic strength. The ESCs obtained at each brine and HCl concentration level were plotted against the ionic

strength. The results indicated that the ESC decreased as the ionic strength increased. The ESC was less affected by a change in acid concentration/pH than by a change in NaCl concentration. The swelling degree started to slow down when the ionic strength of the solution approached 1 M. The swelling ratio remained almost constant or changed only slightly when the ionic strength was larger than 1 M.

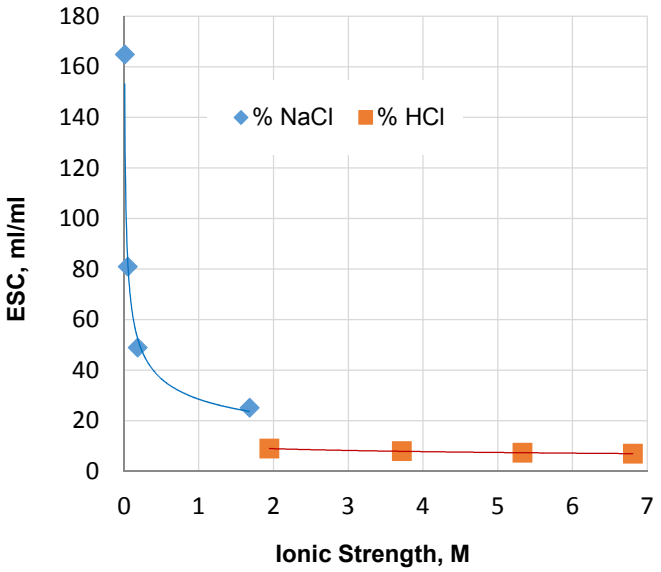

Figure 4.5—Swelling ratio of the PPG as a function of ionic strength.

4.6.1.2. Gel strength measurements. To investigate the influence of acid on the PPG strength, a rheometer was used to measure the strength of the PPG before and after introducing the acid. Figure 4.6 shows the measurement of the PPG storage modulus for gels swollen in different brine concentrations and compared with the same gels deswelled in 10% acid concentrations. The results show a significant increase in gel strength for all brine concentrations after acid treatment compared to the gel before it was treated with acid.

The gel strength measured for the 10% brine concentration increased to five times more than it had been before acid treatments. In addition, the PPG swollen in higher salt concentrations was much stronger than the PPG swollen in lower salt concentrations, both before and after applying acid. There are two possible reasons for this increase in gel strength. First, the elastic pressure of the PPG was more dominant than the osmotic pressure for the PPG swollen in high brine concentrations, as shown in Figure 4.2 and Equation 4.6. Hence, the swelling ratio was restricted, which caused an increase in gel strength. Second, the screen effect reduced efficient water absorbency, which resulted in the PPG shrinking and its strength increasing.

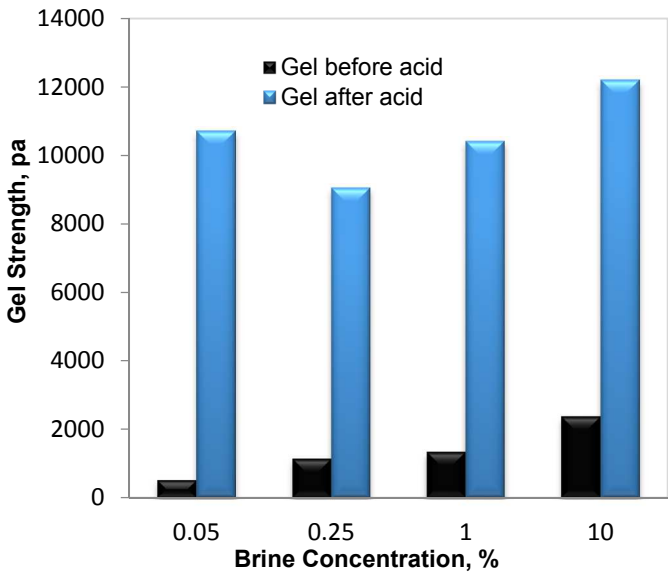

Figure 4.6—Gel strength measurements before and after introducing HCl.

4.6.1.3. Deswelling capacity measurement. The deswelling of the PPG is an important effect that should be considered in designing a gel breaker so that the gel cake formed on the low-permeability zones can be mitigated. PPG, after being fully swollen in

different brine concentrations, was placed inside test tubes filled with acid to observe the acid's ability to deswell the gel. Figure 4.7 illustrates the gel deswelling in four HCl concentrations for gels swollen in different brine concentrations. The results suggest that gel deswelling is highly dependent on the brine concentration. The PPG swollen in the lower salt concentrations deswelled more in the HCl than the PPG swollen in the higher salt concentrations. The deswelling ability reached approximately 85% on average when the gel was swollen in 0.05%, 0.25%, and 1% salt concentrations. This overall percentage, however, decreased to around 60% when the gel was swollen using a 10% salt concentration. This decrease is likely because the PPG swollen in the lower salt concentration has low gel strength while the PPG swollen in the higher salt concentration has high gel strength. The gel deswelled in different HCl concentrations exhibited a similar deswelling ability to the gel swollen in the same brine concentrations. It is likely that this occurred because the acid concentrations had almost the same pH.

Several additional measurements were also performed using the same brine concentration but employing 10% acid with pH values of both 3 and 5. The PPG did not deswell in a medium of pH 3 and above; instead, the PPG swelled to more than its initial volume.

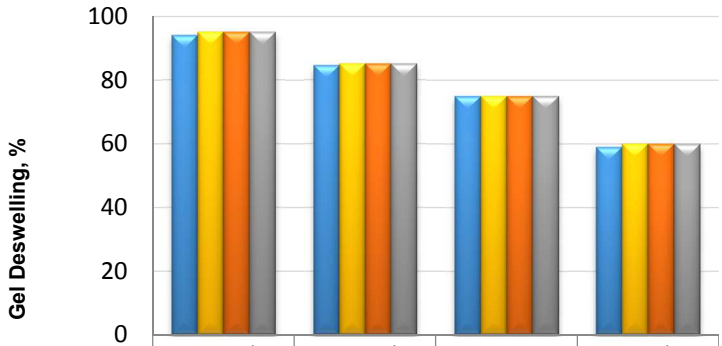

	0.05% NaCl	0.25% NaCl	1% NaCl	10% NaCl
5% HCL	94	84.5	75	59
10% HCL	95	85	75	60
15% HCL	95	85	75	60
20% HCL	95	85	75	60

Figure 4.7—PPG deswelling as a function of acid and brine concentration.

4.6.1.4. Gel swollen capacity in brine after the deswelling process. After the gel deswelling in acid was completed, we further investigated to determine whether the gel would still absorb water when it again contacted water with the same salinity. After the acid application process, the deswellable PPGs in the 10% HCl solution were again placed in test tubes filled with the same brine composition as the gel. The PPG was washed with a variety of brine cycles, and for each cycle, the pH was measured precisely. The PPG was washed with the same composition of brine until the PPG reached the original pH of the brine, which was 5.5. When no change in volume was observed after the pH of the PPG reached 5.5, the PPG was left to swell overnight. The volume changed for each cycle; the equilibrium swelling capacity ratio for each brine concentration is listed in Table 4. 1. The results show that the PPG swelled slightly, and its swelling ratio increased as the brine concentration decreased. The lack of swelling could be due to the substantial decrease in repulsion between polymer chains in an acidic solution medium.

And under such an acidic condition, the anionic carboxylate groups were protonated, which might cause a negligible polymeric network collapse, resulting in a polymer residue in solution. For the purpose of the swelling ratio calculations, V_1 is the final gel volume after deswelling in 10% HCl. The PPG swollen in the 0.05% brine solution reached an ESC value of 3.1, compared to 0.08 for the PPG swollen in a 10% brine concentration.

Table 4.1—Measure of the swelling ratio after the PPG was immersed in 10% HCl.

Brine concentrations,%	Initial volume of swellable PPG, ml	Volume of PPG after deswelling in 10% acid, ml	PPG after being re-immersed in the same brine solution			
			Flushed cycles	pH change	Gel volume, ml	Equilibrium swelling capacity ratio
0.05	20	1	1st	1	1	3.1
			2nd	3	1	
			3rd	5	1	
			4th	5	1.5	
			5th	5	1.5	
			6th	5.2	1.9	
			7th	5.5	3	
			8th	5.5	4	
			9th	5.5	4	
			10th, kept overnight	5.5	4.1	
0.25	20	3	1st	1	3	0.53
			2nd	3	3	
			3rd	3.5	3	
			4th	5	3	
			5th	5.3	3	
			6th	5.3	3.7	
			7th	5.5	4	
			8th	5.5	4.3	
			9th	5.5	4.5	
			10th, kept overnight	5.5	4.6	
1	20	5	1st	1	5	0.18
			2nd	3	5	
			3rd	4	5	
			4th	4.5	5	
			5th	5	5	
			6th	5	5	
			7th	5.3	5.5	
			8th	5.5	5.7	
			9th	5.5	5.8	
			10th, kept overnight	5.5	5.9	
10	20	8	1st	1	8	0.08
			2nd	2.5	8	
			3rd	3	8	
			4th	3.5	8	
			5th	4.5	8	
			6th	4.8	8.4	
			7th	5	8.5	
			8th	5.5	8.7	
			9th	5.5	8.7	
			10th, kept overnight	5.5	8.7	

4.6.2. Evaluation of the Gel Cake Damage and HCl Performance. The results obtained from the interaction between the PPG and the brine as shown in Figures 4.2 and 4.6 indicated that the PPG swollen in high brine concentrations had a lower swelling ratio and a higher gel strength than the gel swollen in low brine concentrations. Consequently, we predict that the gel swollen in the low brine concentrations (low gel strength) might cause more damage to rock due to the gel's softness and its ability to penetrate into small pores.

In terms of HCl performance, the first investigations showed that the PPG did not swell much in acid compared to brine, and its strength could increase as much as 95%, as did the gel swollen in 0.05% solution. This result, which was obtained from the acid interaction with the gel, provides a clue about the ability of HCl to mitigate gel damage, especially (as shown in Table 4.1) that the PPG could not swell again significantly after being treated with acid.

To have a better understanding of the interaction between the gel and the acid, core flooding experiments were performed to confirm and validate the results obtained from the interaction process. Experiments investigated the effect of brine concentration, injection flow rates, and core permeability on the gel cake formed. The effect of acid concentration and pH was examined to evaluate the impact of these two factors on the efficiency of acid in removing the gel cake. The two parameters used to evaluate both effects were the permeability reduction as a result of the gel cake formation and the retained permeability as a result of the HCl acid treatment.

4.6.2.1. Filtration measurement results. This section discusses the filtration test results obtained to test brine concentration and core permeability effects. Filtration is defined as the relationship between the cumulative filtration brine volume and the time during which the brine injection took place. Fifteen injection flow rates were used to create the filtration curves. Filtration tests were performed to determine if it were possible to form an external or an internal gel cake (or both) on the surface of the core during the brine-injection process. If the relationship between cumulative water filtration and time was nonlinear, it meant that a gel cake had formed.

4.6.2.1.1. Effect of brine concentration and core permeability. Nine core flooding experiments were conducted to evaluate gel cake/HCl performance. Figure 4.8 depicts filtration results obtained for the PPG swollen in 0.05% NaCl and 10% NaCl concentrations. A 21.8 md of core permeability was used for the PPG swollen in 0.05% brine, and a 42 md was used for the PPG swollen in 10% brine.

Figures 4.8a and 4.8b summarize the results obtained for the cumulative filtration brine volume as a function of time using the various injection brine flow rates. Results of the repeated injection flow rate (0.5 ml/min) clearly indicated that three regions occurred during the filtration test. The first region, gel cake formation occurred early in the brine-injection process. This can be determined by the nonlinear increasing trend shown in the cumulative filtration brine volume with time. The second region is the transition region, which occurred for only a short specific time. The third is the flow through already gel cake formed region, which identified by the linear increasing trend shown in the cumulative filtration curves. This linear trend indicated that the gel cake would not grow in size with increased injection flow rates and time.

Figure 4.8a shows the results for the gel swollen in the 0.05% brine solution, where a nonlinear trend continued to increase until around 20 minutes, and then the trend became linear for all flow rates. This trend signaled that a severe gel cake had formed during the early injection process. For the purpose of making filtration results more visible and clear, the findings for the repeated flow rate of 0.5 ml/min are drawn separately on the top left side of the Figure. In addition, a comparison was made between the results obtained from the repeated flow rates after the gel treatment with the results obtained from the initial brine injection flow rate of 0.5ml/min before gel treatment (shown in the line of connected dots).

All of the repeated 0.5 ml/min flow rates showed a nonlinear relationship at the beginning of the filtration process**.** There was not a big discrepency in filteration curve trends for the repeated flow rates, which implies that the rise in the injection flow rates during the filtration test did not signifcantly increase/decrease gel cake formation. Additionally, the difference in the filtration result trend between the repeated (0.5 ml/min) injection flow rates and the initial injection flow rate (0.5ml/min) could be used to assess the core damage percentage.

Figure 4.8b shows the results for the gel swollen in the 10% brine solution, where a nonlinear relationship between the cumulative volume and the injection time was only seen during the first 0.5 ml/min after the gel was first introduced. The first flow rate (0.5 ml/min) after the gel treatment showed that the gel cake formed at the beginning of the gel treatment process; after the flow rates increased, the repeated 0.5 ml/min curves changed to become linear.

Similarly to the gel swolen in 0.05% brine, an increase in injection flow rates for the gel swollen in 10% brine, did not substantially increase/decrese the gel cake damage. The filtration curves obtained from the repeated injection rates were closer to the original filtration curve obtained from the initial 0.5 ml/min, indicating a low percentage of damage to the core.

Comparing Figures 8a and 8b, reveals that gel swollen in 0.05% brine caused more gel cake damage to the core than gel swollen in 10% brine. This conclusion was inferred by comparing the nonlinear filtration curves obtained from the repeated brine injection flow rate of 0.5 ml/min for both gels.

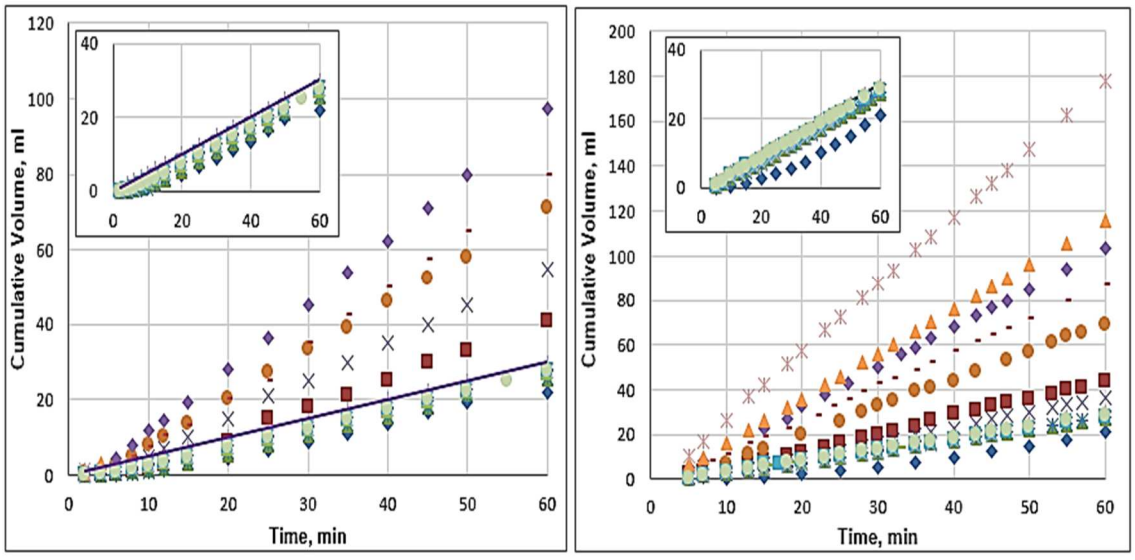

(a) Gel swollen in 0.05% NaCl.

(b) Gel swollen in 10% NaCl.

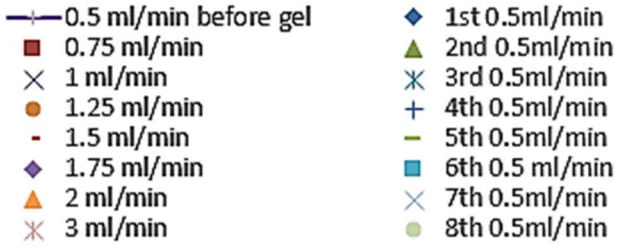

Figure 4.8—Filtration results for PPG swollen: 0.05%, and 10%.

Figure 4.9 shows a comparison between the brine injection stable pressure measured during the filtration process for both salinities. The injection pressure for the gel swollen in the 0.05% NaCl concentration rose signifcantly with the flow rates when compared to the gel swollen in the 10% NaCl concentration. This high injection pressure, which reached 2500 psi, indicates how the gel cake could create a large back pressure during the treatments. For example, during the filtration test experiment, this high injection pressure reached the upper limit of the pump pressure, which prevented obtaining the cumulative volume data for the injection rate of 3 ml/min, as shown in Figure. 4.8a.

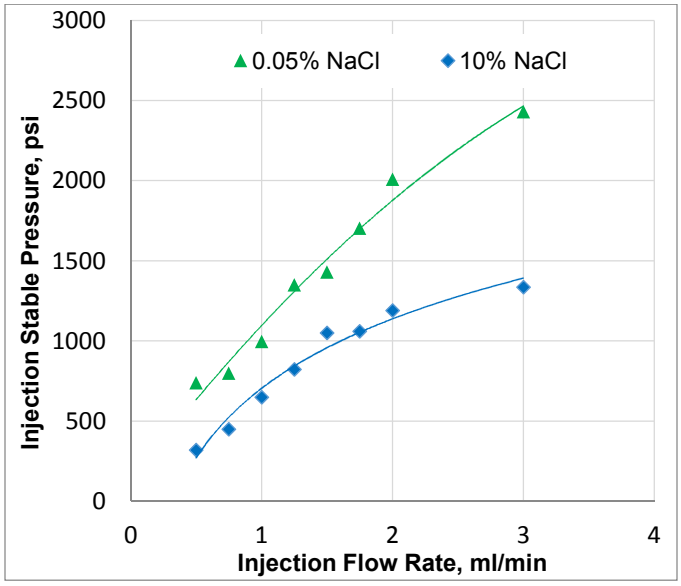

Figure 4.9—Injection pressure for two salinities during the filtration test.

The filtration test results displayed in Figurs 4.8 and 4.9 show that an external or an internal gel cake was formed and that its strength and damage percentage to the core varied and depended on the brine concentration range. The gel swollen in the low brine

concentration exhibited more of a tendency to damage the core compared to the gel swollen in the high brine concentration.

4.6.2.1.2. <u>Effect of injection flow rates.</u> Referring to the filtration measurement results shown in Figure 4.8, damage was only observed in the first few gel injection flow rates. Thus, increasing the gel injection flow rate did not cause further damage to the core. It is believed that channels were created that allowed the brine to flow easily through the gel. Figure 4.10 is a simple sketch illustrating four sequences of the effect of injecting brine through the PPG: (1) The "*static" sequence* occurs when the gel is first placed on the surface of the core sample. The sorting of the PPGs is controlled by the gel strength and particle size. Gel particles are not unlike other solid particles in terms of retaining uniformity of shape. (2) The "*particle compresses and penetrates" sequence* occurs when the brine is first injected through the particles; at this time, the particles compress by moving closer to each other, and some of the gel penetrates a little bit into the cores. The degree of penetration is dependent on the ratio of the PPG size to the pore throat size. If the gel penetrates into the core, an internal gel cake is formed in addition to an external gel cake. If the PPGs do not penetrate, then only an external cake is formed. Depending on the strength of the gel cake, back pressure can occur as a result of restricting the fluid propagation. The back pressure is likely to cause the gel to be more rigid and can lead to high injection pressure. (3) The "*initiate channel" sequence* occurs as the brine begins to form internal microchannels inside the PPG network. The pressure required to create these microchannels depends on the gel strength. As the injection flow rates increase, the brine filtered at the outlet also increases as a result of creating these microchannels. (4) The "*channel formed" sequence* occurs because as the injection flow

rates increase, the channel becomes a little larger; this explains linear relationship that was observed during filtration measurements when the injection flow rates increased. The network inside the gel reforms, and the channel closes when the driving force becomes less than the bending force between the particles.

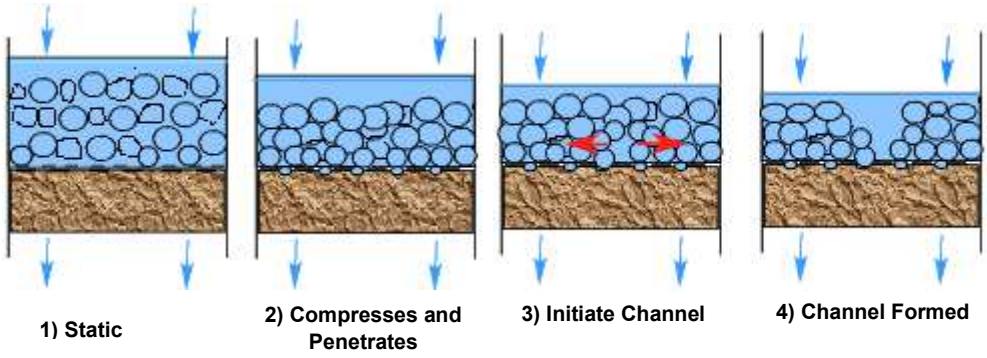

Figure 4.10—The four sequences occur when brine is injected through PPGs.

4.6.2.2. Results for permeability reduction and permeability retained. To quantitatively determine the gel damage caused by the gel cake, the permeability reduction was used to express the damage. The gel cake-removal efficiency caused by the acid stimulation was expressed as the permeability retained. After the gel was removed from the core holder, different cycles of water having the same composition as the gel were injected through the cores, and the stabilized injection pressures were obtained for each flow rate. Two ranges of core permeabilities (Figures 4.11 and 4.12) were used to observe the permeability change on the permeability reduction caused by the gel cake. Figure 4.11a shows the injection stable pressure results obtained for the range of permeability from 3 to 4.5 md. The brine injection pressure rose as the salt concentration decreased. The injection pressure increased approximately five times (from 50 to 250 psi) as the salt concentration decreased from 10% to 0.05%. This increase is likely due to the

formation of clay minerals on the surface of the core as a result of the lower salt content used. Also, the softness and deformability of the swollen PPG in the lower salt concentration enabled the gel to invade a short distance into the pore throat. Figure 4.11b illustrates how the brine concentration affects the permeability reduction. The permeability reduction rose as the brine concentration decreased. Almost a 90 percent permeability reduction was observed when the gel was placed in the lower brine concentration; however, only a 29.5 percent permeability reduction was observed for the high brine concentration. Results from these two Figures suggest that gel swollen in high brine concentration exhibited less ability to damage the core than gel swollen in low brine concentration.

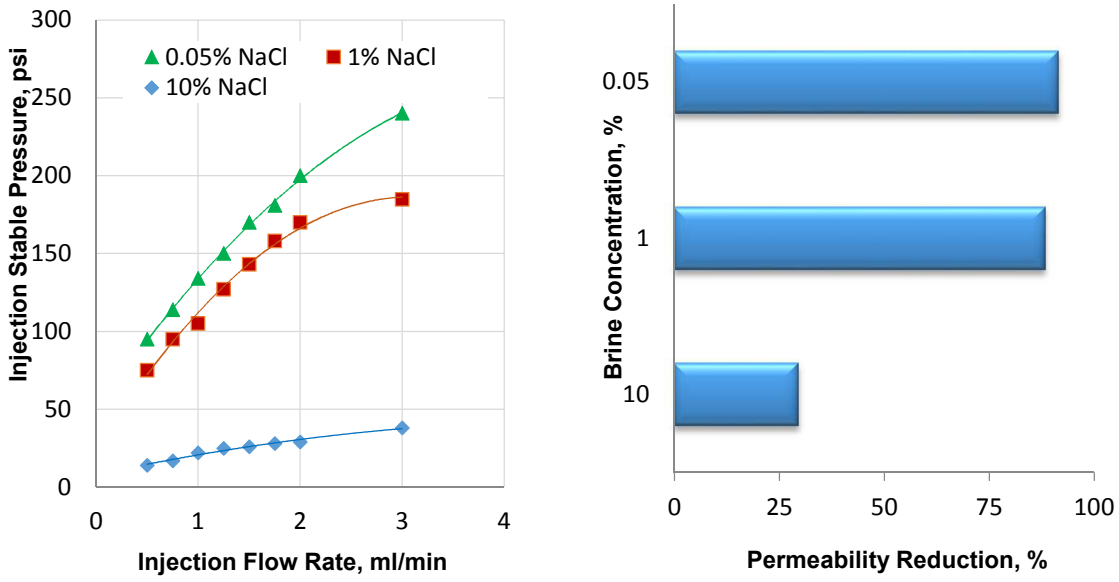

Figure 4.11— Injection pressure and permeability reduction of permeability range 3 to 4.5 md.

Figure 4.12a shows the injection stable pressure results obtained for the range of permeability from 21.8 to 27.2 mD. The injection pressure rose significantly as the brine concentration decreased. Higher injection pressure occurred in this range of permeability compared to the permeability range in Figure 4.11a. This increase reveals that gel can penetrate into areas with high core permeability more deeply than if it is placed into areas of low core permeability. As a result, Figure 4.12b shows that the decrease in core permeability is more significant in high-permeability cores than it is in low-permeability cores.

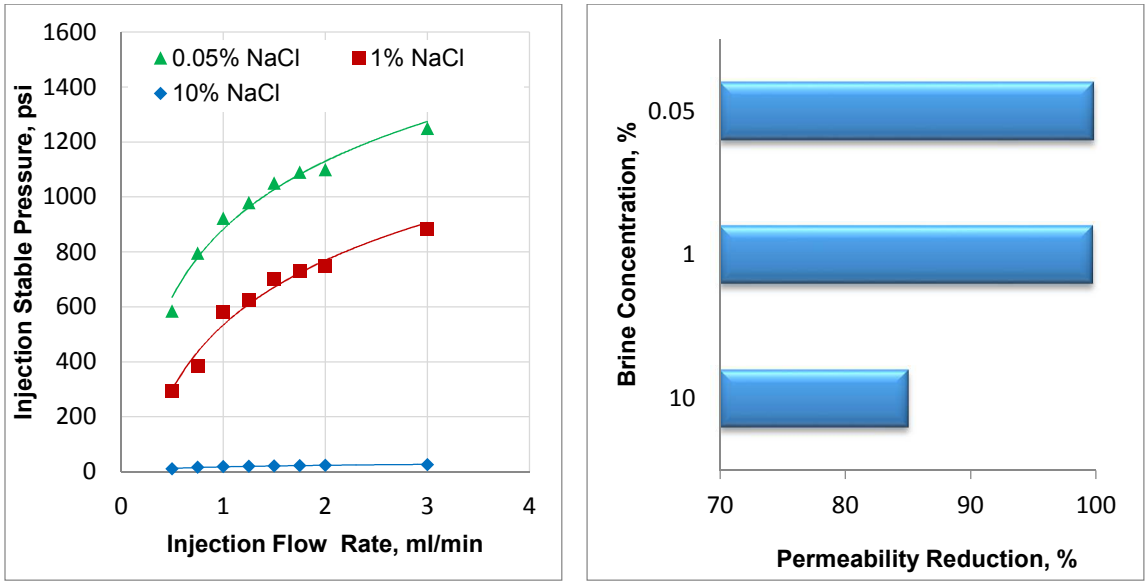

(a) **(b)**

Figure 4.12— Injection pressure and permeability reduction of permeability range 21.8 md to 27.2 md.

Comparing the two ranges of permeability shown in Figures 4.11 and 4.12 the gel swollen in 0.05% brine exhibited significant damage as both ranges of permeability

reached above 90%. When the permeability increased to a range of 21.8 to 27.2 md, the permeability reduction rose from 29.5% to 85% for the gel swollen in the 10% brine. Consequently, the brine injection pressure increased significantly as the gel cake caused more damage to the core. The injection stable pressure increased as the brine concentration decreased, and the injection stable pressure rose more significantly as the permeability of the core increased.

Elsharafi and Bai (2012), reported that the invasion of low-strength PPG into low-permeability rocks was usually less than 3 mm. Therefore, samples of the face-damaged cores were immersed into less than 1 cm in length of 10% acid concentrations to remove the gel cake of this expected length. Table 4.2 lists the results obtained for the effect of the brine concentration on the core permeability reduction and retention. Permeability after the soaking time was retained with greater than approximately 94 percent for all brine concentrations and permeability ranges. These results from the core flooding process are consistent with findings observed in the interaction process as shown in Table 4.1. Results from the interaction show that the gel did not swell again significantly after being flushed with the same brine compositions; consequently, a higher percentage of retained permeability was expected. These findings suggest that acid can be used effectively to retain low-permeability formations during the conformance-control treatments.

Two HCl concentrations were evaluated during the core flooding measurements to investigate how much the retained permeability could be increased after the acid treatments. The retained permeability that was gained after the acid treatments did not result in a significant difference in the gel-removal efficiency. For a permeability of 7.8

md, acid treatment only retained 98.7% when the acid concentration was 5%; it increased only slightly, to 104.5%, when the concentration increased to 10% for the same range of permeability (4.4 md). This suggests that both concentrations could be effectively used to mitigate gel cake formation. This is an advantage because engineers would not have to be concerned about corrosion and adding an inhibitor to prevent the problems associated with the use of high acid concentrations.

Changes in pH were also investigated to observe the effect on the core-retained permeability. Table 4.2 also provides the results obtained for pH values of 1.3 and 5.5 for gel swollen in a 10% brine concentration. The pH had a pronounced effect on the amount of core permeability retained. Solutions with lower pH values had a stronger effect on the amount of permeability retained than those with a higher pH. At a pH of 1.3, the retained permeability reached 108.6% compared to a very small retained permeability (0.5%) for a pH of 5.5. It can be inferred that the pH has a significant effect on removing damage and should be carefully selected during acid treatment process.

Table 4.2—Permeability reduction and retention for gel swollen in different brine concentrations treated with different HCl concentrations and pH.

Core	Brine Concentration %	HCl Concentration %	pH	Permeability, md			Permeability Reduction, %	Permeability Retained, %
				Absolute	After Gel	After Acid		
A	10	10	1.3	25.5	3.80	27.7	85	108.6
B	10	-	5.5	42	0.24	0.23	99.4	0.5
C	0.05	10	1.3	3.5	0.3	3.3	91.4	94.2
D	1	10	1.3	4.3	0.5	4.1	88.3	95.3
E	10	10	1.3	4.4	3.1	4.6	29.5	104.5
F	0.05	10	1.3	21.8	0.08	20.87	99.8	95.7
G	10	5	1.3	7.8	0.7	7.7	91	98.7

X-Ray Diffraction (XRD) quantitative analysis was performed on all core samples to gain knowledge about the core mineralogy before used them. Analysis revealed that some cores were composed of kaolinite and ankerite (carbonate cement) with quartz, while others were not. Table 4.2 shows that the retained permeability for some core samples exceeded 100%. This significant improvement in core permeability occurred because the HCl reacted with both the gel cake and rock. The presence of ankerite in core samples *A* and *E* increased the retained permeability above 100% because it easily dissolved when it reacted with the HCl. This dissolved solution created more spaces and increased the original porosity and permeability of the cores. The results also showed that the retained permeability for some core samples was less than 100%. The mineral content of these core samples only included quartz and kaolinite. Quartz and kaolinite are inert or

insoluble in most geochemical environments; this explains the retained permeability being less than 100%.

4.7. DISCUSSION

This work was designed to understand the interaction between preformed particle gels and hydrochloric acid. We also conducted core flooding experiments to determine the effect of the gel strength and core permeability on both the degree of damage and on the stimulation process. We observed that acid stimulation can be used successfully to mitigate the damage in un-swept, low-permeability formations that are rich in oil. This finding can significantly assist in optimizing the design of PPG treatments.

This work sought to find a method to treat the possible gel cake formed on the surface of low-permeability formations when injecting PPG using the bullhead placement technique. We proposed using hydrochloric acid to mitigate the adverse consequences of the gel cake being formed on the surface of low-permeability zones. Our findings showed that a very small amount of acid was required to remove the gel cake because the millimeter-sized PPG tends to form a limited gel cake on middle- and low-permeability porous media. Therefore, for field applications, we only recommend injecting a very small volume of acid (e.g., 0.5 m^3) to soak the near wellbore. In practice, a large amount of PPG is usually used for conformance control. If even a small amount of acid enters the high-permeability zone where a large amount of PPG is injected, it will not affect the conformance-control treatment result.

Additional work was conducted (see section 8) to investigate the performance of combining these two technologies to gain more oil from low-permeability formations. To

evaluate how much oil recovery would be obtained from combining water shutoff and acid treatments, in future studies, a new model was tested by investigating two parallel formations having low and high permeabilities. Section 8 assess also the possible side effect of acid treatment reducing the gel-blocking effectiveness in high-permeability zones/pathways. The heterogeneity model was developed as shown in Figure. 4.13 to emulate the case when there is no crossflow between layers. It is proposed that the gel be pumped into large permeability zones (thief zones) to reduce their permeability so as to obtain more oil from un-swept low-permeable zones. Pumping acid to remove the gel cake formed in un-swept zones that are rich in oil allows more oil to be recovered. The combined technologies will then increase oil production from both low- and high-permeable formations.

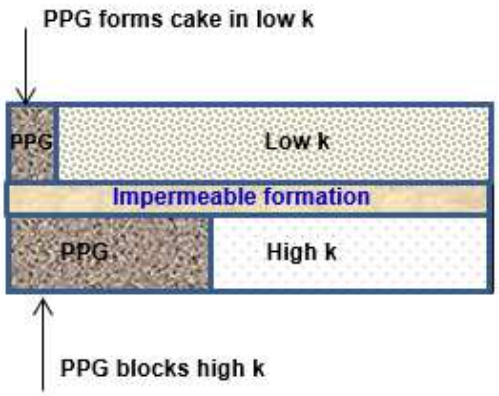

Figure 4.13—Schematic for non-crossflow experiment.

4.8. CONCLUSION

The main objective of this study was to conduct a comprehensive evaluation of the effectiveness of combining the use of hydrochloric acid and preformed particle gel to

gain a better conformance control. The interaction between the HCl and the PPG was investigated in terms of the swelling ratio, deswelling ratio, and gel strength. Core flooding was conducted simultaneously to evaluate the gel cake formed and the performance of HCl in mitigating this cake formation. The following conclusions can be drawn:

- The gel and acid interaction demonstrated that the PPG swelling capacity decreased as the brine concentration and acid concentration increased. A change in acid concentration did not correlate with a difference in the PPG deswelling for the same brine concentrations. Solutions with a change in pH had a significant effect on gel deswelling, where a pH above 1 was correlated with an ineffective gel deswelling ability.
- The gel strength increased as both brine concentration and acid concentration rose. The gel strength measured after the acid treatment was stronger than it was before the acid was introduced.
- The PPG did not swell significantly after the HCl treatment when it was flushed with different cycles of brine. This low swelling ratio decreased the chance of the PPG damaging low-permeable cores.
- The filtration test results indicated that the PPG formed a permeable surface gel cake on the low-permeability cores. The cake formed was strongly dependent on both the brine concentration and the rock permeability. The formation of a gel cake reduced the permeability to a significant degree if the brine concentration was low and the rock permeability was high.

- The filtration test results showed that no further damage would occur as the injection flow rates increased. Four sequences were observed during brine injection through the gel: static, compress and penetrate, initiate channel, and channel formed.
- The amount of permeability retained was calculated after stimulation treatments and, on average, reached more than 95 percent of the original permeability for all the various brine concentrations and rock permeability ranges. Additionally, core-damaged permeability was effectively removed when the pH was around 1.
- Hydrochloric acid showed promising results when joined with gel treatments as an effective technique to remove the gel cake formed on low-permeability zones, and hence, to improve the conformance-control objectives.

5. PARTICLE GEL PROPAGATION THROUGH OPEN CONDUIT

5.1. INTRODUCTION

The success of gel treatments depends heavily on the gel's ability to extrude through fractures and channels during the placement process (Seright, 1999a and 1999b). Thus, understanding both the mechanism and the behavior of gel extrusion is the key to a successful conformance control treatment.

5.2. OBJECTIVES AND TECHNICAL CONTRIBUTIONS

The objective of this work is to conduct an in-depth examination of several factors that can have an important impact on the PPG extrusion mechanism and placement performance in opening conduits. The following summarizes the detailed objectives and expected technical outcomes of this work.

- Examines the effect of the conduit's opening size and brine concentration (PPG strength) on the injectivity index, resistance factor, gel dehydration, particle opening ratio, gel wash-out, and plugging efficiency.
- Determine the matching ratio measured between gel particle size and conduit opening size.
- Study the effect of gel strength on the blocking efficiency of PPG.
- Determine the residual resistance factor (*Frr*) for water flow through PPG filled the conduit.

- This work will provide a significant guidance about how to better design millimeter-size particle gel treatments for large openings, like open fractures, cave, worm hole and conduits.
- Based on the laboratory data, correlation models were developed to quantitatively calculate the resistance factor as a function of particle strength, passing ratio, and shear rate. The two developed models will be embedded into an existing reservoir simulator (UT-gel) for particle gel treatment optimization design and performance prediction.

5.3. EXPERIMENTAL DESCRIPTION

5.3.1. Preformed Particle Gel. A superabsorbent polymer was used as a PPG to conduct the experiments. The particle was synthesized using acrylamide, acrylic acid and N, N'-methylenebisacrylamide by a free radical process. Dry particles with a mesh size of 30 were swollen in different concentrations of NaCl brine (0.05%, 0.25%, 1%, and 10%). The brine concentration was carefully selected based on the swelling ratio and the gel strength after swelling, as shown in Table 5.1.

Table 5.1—Summary effect of brine concentration on PPG.

No	Brine concentration, %NaCl	PPG concentration, wt %	Swelling ratio	Gel strength, pa
1	0.05	0.60	165	515
2	0.25	1.25	80	657
3	1	2.0	50	870
4	10	4.0	25	1300

PPG swollen in low NaCl concentrations will have high swelling ratio and low gel strength. PPG concentration was determined using the initial weight of dry gel divided by the final weight of completely swollen gel. PPG concentration is changed as a result of the brine concentration effect.

5.3.2. Tubes. Tubes five feet (1.5 meter) long with varying internal diameters (10.922, 3.048, 1.752, and 0.774 millimeters) were used to emulate different conduit sizes. Three pressure taps were mounted along the tube to monitor PPG propagation performances. The internal diameters were carefully selected to be larger than, equal to, and smaller than the swollen particles.

5.3.3. Microscope. A microscope as shown in Figure 5.1 was used to determine the particle size before and after particle extrusion through the conduit models. An image analysis technique was used to obtain the particle gel size distribution.

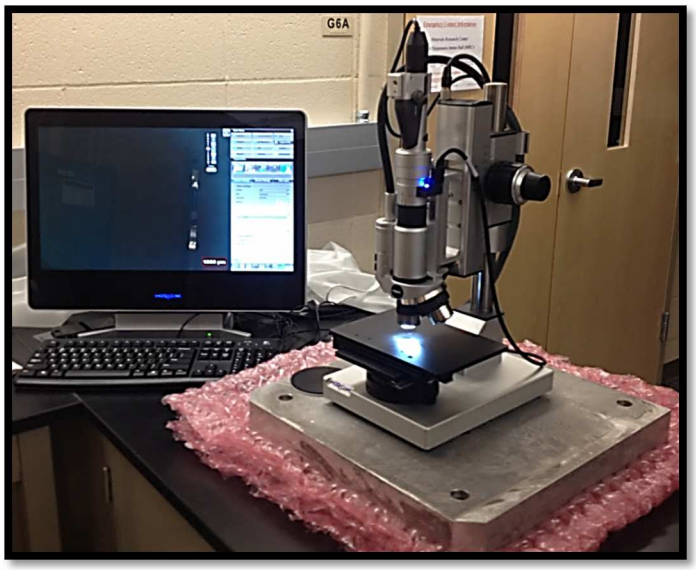

Figure 5.1—Microscopic instrument.

5.3.4. RheoScope Device. Storage moduli (G´) for PPG prepared in different brine concentrations were measured at room temperature (23 ^{o}C) using a rheoscope. The PPG strength was measured before and after gel propagation into the conduit to determine the effect of the extrusion process on strength. The sensor used for measurements is PP335 TiPoLO2 016 with a gap of 0.2 mm between the sensor and the plate. G' were measured at a frequency of 1 Hz for each sample.

5.4. EXPERIMENTAL SETUP

Figure 5.2 provides the schematic of the conduit model used to conduct the experiments. This model contained a syringe pump that was used to inject brine and gel through the accumulator into a five-foot tube. The tube was divided into three sections, the first two of which were two feet long, with last section being one foot long. Effluent gel and brine were both collected to evaluate the gel's properties after the extrusion.

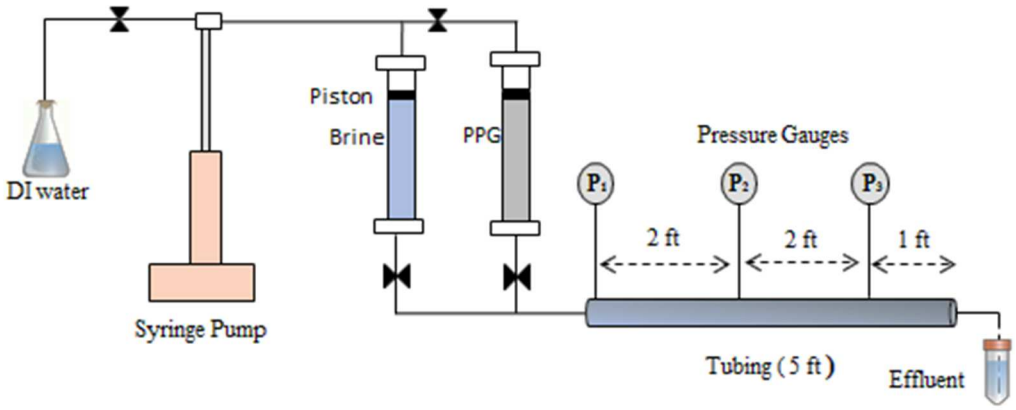

Figure 5.2—Schematic of the conduit model.

5.5. EXPERIMENTAL PROCEDURE

Dry PPG's of 30 mesh size were placed in different concentration brines and left overnight to swell fully. A sieve was used to allow the swollen gel to separate from the excess brine solution. The gel then was packed into a stainless steel accumulator so that it could be injected into a conduit model. The gel injection process at the ambient temperature is summarized as follows:

The PPGs were injected into different internal tubes at the same designed velocity. Table 5.2 summarizes the velocities used for the different inner diameters. The gel initially was injected at a high velocity, which then was reduced gradually for all experiments. The pressure needed to be stable for each gel injection velocity. Following pressure stabilization, gel samples were taken for each gel injection velocity to measure gel strength and particle size. Finally, when the gel injection process was complete, the same concentration brine was injected into the tube filled with particles from a low to a high velocity to determine gel resistance to water flow.

Table 5.2—Gel velocities designed for each conduit inner diameter.

Conduit inner diameter, mm	Injection flow rate, ml/min	Injection velocity, ft/day
10.922	39.2	1979
	29.2	1476
	19.2	970
	9.8	495
	4.9	247
	3.9	198
	1.9	99
	1	49
	0.2	10
3.048	3	1928
	2.3	1446
	1.5	964
	0.75	482
	0.37	241
	0.30	193
	0.15	96
	0.07	48
	0.01	10
1.752	1	1931
	0.75	1448
	0.5	966
	0.25	483
	0.125	241
	0.1	193
	0.05	96
	0.025	48
	0.005	10

5.6. RESULTS AND ANALYSIS

PPGs swollen in four different concentration brines were injected into three sizes of conduits at various injection velocities to investigate the effect of brine concentration (related to gel strength) on injectivity, the resistance factor, and the threshold pressure. The resistance factor and gel injection pressure data were used to develop new correlation models for PPG to predict the resistance factor and the initial stable injection pressure during gel extrusion in conduits.

5.6.1. Injectivity Index Calculation. An injectivity index was obtained as a function of the brine concentration, injection velocity, and conduit inner diameter to observe the behavior of PPG that had extruded through the conduit systems. Figure 5.3

shows the effect of the brine concentrations and gel injection velocity on the gel injection pressure through three different sizes of conduits. At the same injection velocity, the gel injection pressure increased as the brine concentration increased. This occurred because PPG swollen in low brine concentration swelled more and became weaker than the PPG swollen in high brine concentration. The gel injection volume required to achieve stable pressure is varied; it depends on the brine concentration and the conduit inner diameter size. Large volume of gel was injected as the gel become stronger and the conduit inner diameter become smaller. In conduit inner diameter 1.752 mm for gel injected at velocity 1931.26 ft/day, PPG injected pore volume required to get stable pressure increased from 11.5 PV to 33.9 PV when brine concentration increased from 0.05% NaCl to 10% NaCl.

The results also show that the gel injection pressure increased as the injection velocity increased. This increase in the gel injection pressure became insignificant when the gel injection velocity exceeded 500 ft/day. This suggests that the gel injection pressure did not increase linearly through all of the gel injection velocities, but rather tended to reach a plateau after a certain injection velocity. This insignificant increase most likely occurred because of the gel slip that can occur when extruding through conduits at a high velocity (Seright, 1997). Our results were consistent with Seright (1997, 1998) for gel extrusion through tubes where he observed that gel injection pressure became independent of injection velocity after a specific velocity value.

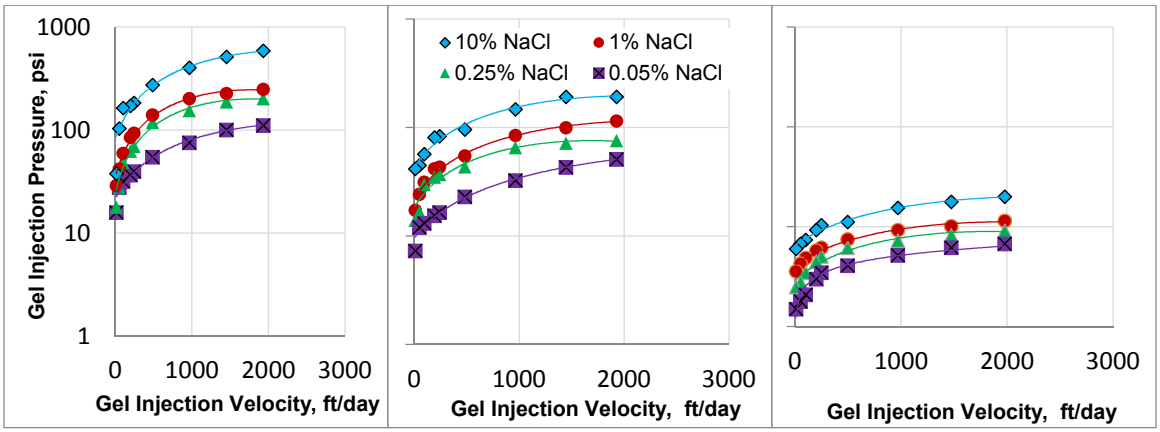

Figure 5.3—PPG injection pressure as a function of brine concentration and conduit diameter.

The data from Figure 5.3 were used to obtain the gel injectivity index through the conduit systems. PPGs with a high injectivity index required a lower injection pressure to be propagated through the conduit. In this study, the injectivity index increased as the brine concentrations decreased, as shown in Figure 5.4. This likely occurred as a result of the swelling ratio effect. PPGs swollen in low brine concentrations contain a high percentage of aqueous phase and a low percentage of solid phase. This composition allows PPGs swollen in low brine concentrations to be more injectable than PPGs swollen in high brine concentrations. These results also indicate that the injectivity index increased as both the conduit inner diameter and the velocity increased. For the conduit size, this behavior is easy to understand, but for the velocity, this occurred because the gel followed the shear thinning or pseudo plastic behavior in the conduit systems.

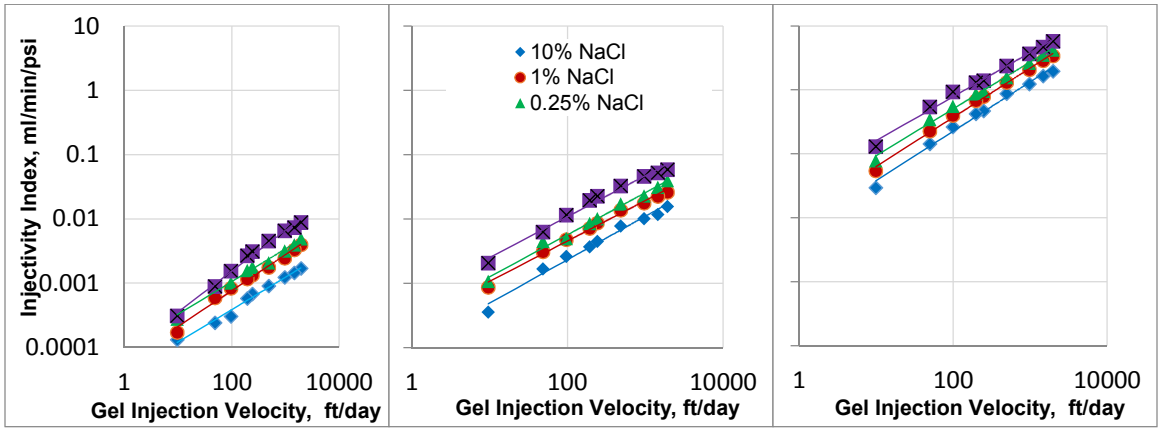

Figure 5.4—Injectivity index results.

5.6.2. Resistance Factor Calculation. In analogy to porous media experiment, resistance factor (Fr) was estimated from the injectivity index and geometry of the conduit, namely QL/AΔP for the brine and the gel injection. It can be defined as the ratio of the particle gel injection pressure drop to the brine injection pressure drop at the same flow rate and can be calculated from the following equation:

$$Fr = \Delta p_{PPG} / \Delta p_{brine} \quad \text{.....(5.1)}$$

where Δp_{PPG} is the PPG injection pressure drop and Δp_{brine} is the brine injection pressure drop before PPG placement.

PPGs swollen in four different concentrations of brines were injected into three conduits at various injection velocities to determine the effect of brine concentration and conduit inner diameter on the resistance factor. The injection began with the highest

injection velocity until the injection pressure became stable. Then the injection continued at reduced velocities. A stable pressure was recorded at each injection velocity. Figure 5.5 indicates that for all gel velocity injections, Fr increased as the brine concentration and conduit inner diameter increased. The Fr measured across all three conduits became an independent factor on velocity when it exceeded 500 ft/day. The Fr value for the gel swollen in 10% NaCl extruded in 10.922 mm was 99133; it then decreased substantially to 3364 as the velocity increased from 10 ft/day to 500 ft/day. However, as the velocity increased above 500 ft/day, the Fr values decreased only slightly during the gel injection process.

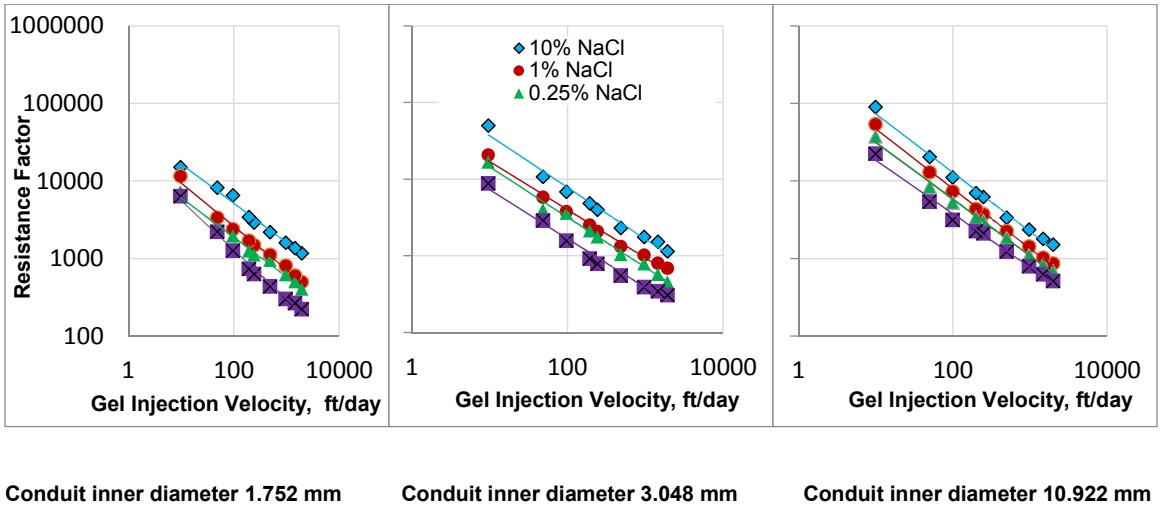

Figure 5.5—Resistance factor as a function of brine concentration and conduit inner diameter.

5.6.3. Gel Threshold Pressure vs Particle Opening Ratio. *The particle opening ratio* is defined as the ratio of the gel particle diameter (Dg) before the extrusion to the pore opening conduit diameter (Dp). The 30-mesh PPGs swollen in different concentration brines had different sizes and strengths, as shown in Table 5.1. *The gel*

threshold pressure (Pt) is the minimum pressure required to initiate gel flow through the conduit. Figure 5.6 illustrates the relationship between the threshold pressure and the particle opening ratio. Strong gel requires a higher threshold pressure than weak gel in order for it to pass through an opening. The result obtained agrees with Seright (1997, 1998) who observed that some threshold pressure was required before the gel would extrude through a given opening size. The data also suggest that when the particle opening ratio exceeded two, the threshold pressure for both strong and weak gel increased much less compared to when the ratio was below two. This may have occurred for two reasons. First, the swollen particle dehydration during extrusion process may have reduced the size of the particles as the ratio increased. Secondly, the gel particles broke into small pieces, which may lead to smaller increases in the threshold pressure with increasing particle opening ratio.

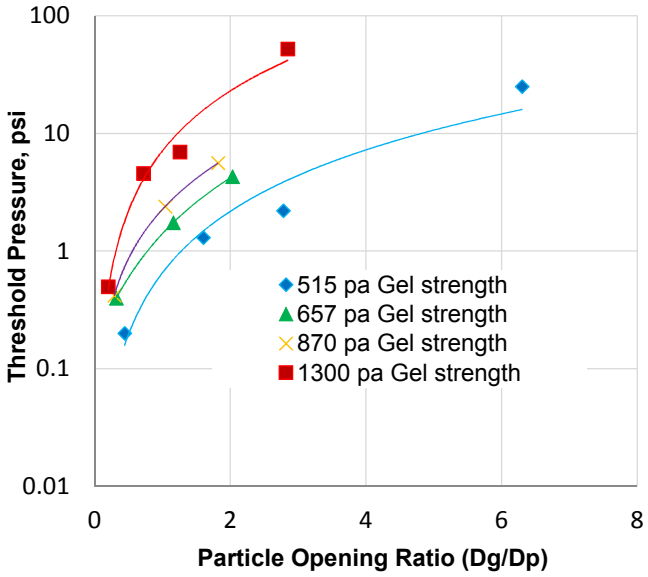

Figure 5.6—Effect of particle opening ratio on threshold pressure.

5.6.4. Stabilized Gel Injection Pressure vs Particle Opening Ratio. After the PPGs passed through the conduit, gel was injected continuously until the injection pressure stabilized. The injection pressure of the stable gel was measured as a function of the gel strength and particle opening ratio, as shown in Figure 5.7. The results show that the stable injection pressure increased with the gel strength and particle opening ratio. The gel strength had a significant effect on the stability of the injection pressure, more than did the particle opening ratio. The gel injection pressure increased by around ten times (100 to 1320 psi) when the gel strength approximately doubled from 515 to 1300 pa. The injection pressure only tripled (191.7 to 590 psi) when the particle opening ratio approximately doubled from 0.72 to 1.26 at the gel strength of 1300 pa.

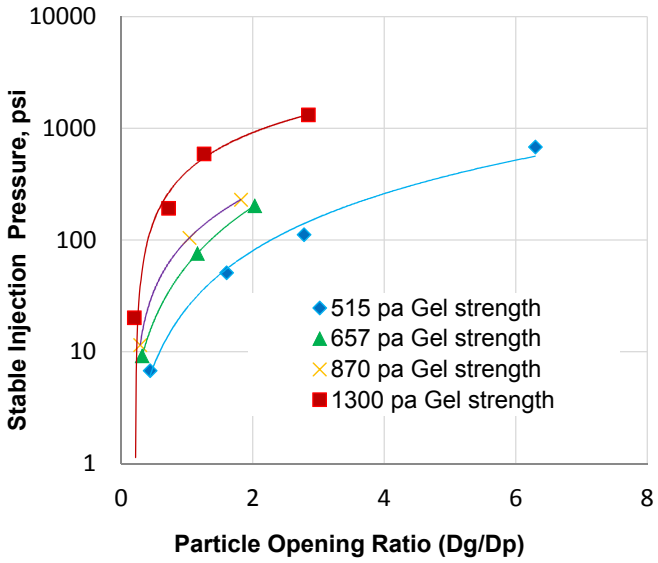

Figure 5.7—Stabilized injection pressure as a function of particle opening ratio and gel strength.

5.6.5. Correlation Models. Having correlation models that can predict the resistance factor (apparent viscosity) and stabilized injection pressure for PPGs during gel treatments is important to quantify gel transport process. Such models not only can be inserted into a simulator to yield better predictions of PPG performance, but also can provide results more quickly, as conducting all of these experiments in the lab would be time consuming and would require a great amount of effort to achieve reliable results.

5.6.5.1. PPG resistance factor model. Polymer or polymer gel viscosity is often expressed as a function of shear rate; therefore, we tried to correlate the resistance factor with shear rate. In the paper, we use the maximum shear rate at the pore wall to obtain shear rate values and the equation is given as follows (Zaitoun et al 2012):

$$\gamma = 8v/D \quad \text{..... (5.2)}$$

where γ is the shear rate, v is the superficial velocity, and D is the conduit inner diameter.

The data in Figure 5.5 was reorganized to Figure 5.8 after converting velocity to shear rate. It can be seen that all data is in the same line for the particle prepared by the same concentration brine even though their particle opening ratios are different, indicating that Fr was independent of conduit inner diameter. This phenomenon is not very surprising because we know the polymer gel viscosity is a function of shear rate but does not depend on the gap between cylinder and spindle when we measure the bulk gel viscosity.

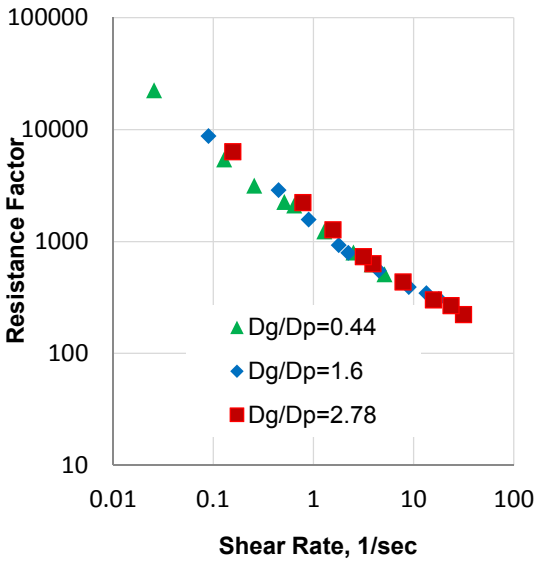

0.05% brine concentration

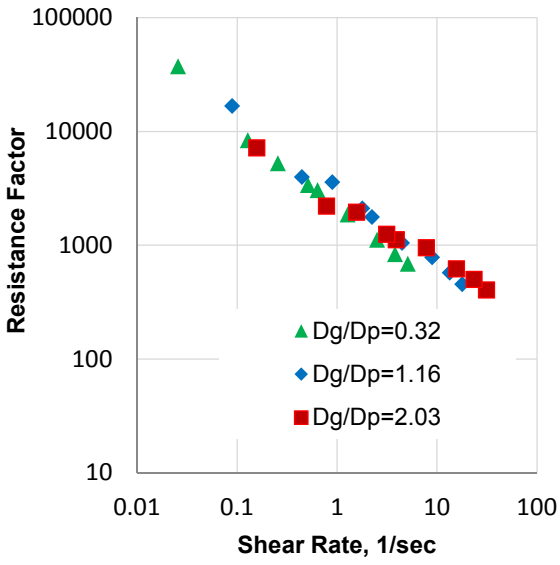

0.25% brine concntrations

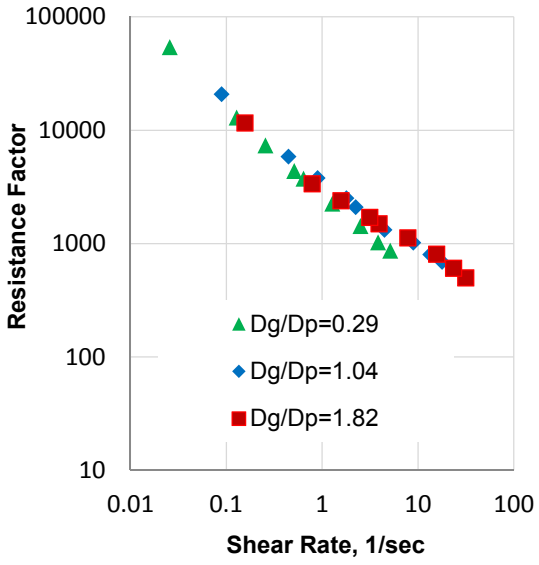

1% brine concentration

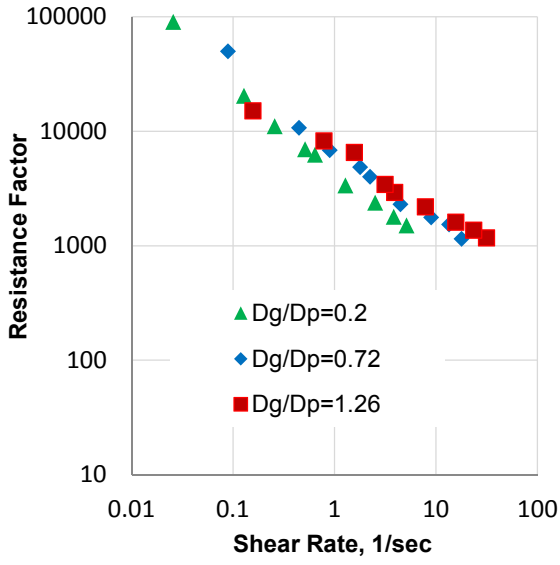

10% brine concentration

Figure 5.8—Resistance factor for gel swollen in brine concentrations as a function of both shear rate and particle opening ratio.

A good fit was noticed using power law equation for resistance factor results plotted against shear rate. The fit is even better with a particle opening ratio greater than one or equal to one. Therefore, the developed model will includes the data for particle opening ratios greater than and equal to one. The resistance factor obtained as a function of the shear rate can be expressed as:

$$Fr = M\,\gamma^{-E} \quad \text{.....(5.3)}$$

where M and E are constant coefficients related to brine concentration and particle opening ratio, both were obtained from gel extrusion through conduits. Table 5.3 summarizes the results obtained for both M and E for each brine concentration.

Table 5.3—Fitting equations for resistance factor for each brine concentration.

Brine concentration, %NaCl	*M*	*E*	R^2
0.05	1618.4	0.62	0.98
0.25	2917.9	0.61	0.97
1	3643.7	0.596	0.98
10	7128.5	0.588	0.96

To develop a general correlation that can be used to predict the resistance factor for all brine concentrations, both constant coefficients M and E need to be determined. Table 5.3 indicates that E was not affected very much by brine concentration but M was strongly affected. To obtain these coefficients, both constants were plotted as a function of the brine concentration(C), as shown in Figure 5.9. Power-law equation was used again to obtain the proper fitting correlation for the coefficients.

The constant coefficient (M) was fitted with goodness of fit of 99%:

$$M = 3831.3\ C^{0.2709} \quad \text{..... (5.4)}$$

The constant coefficient (E) was fitted with goodness of fit of 96%:

$$E = 0.6001\ C^{-0.01} \quad \text{.....(5.5)}$$

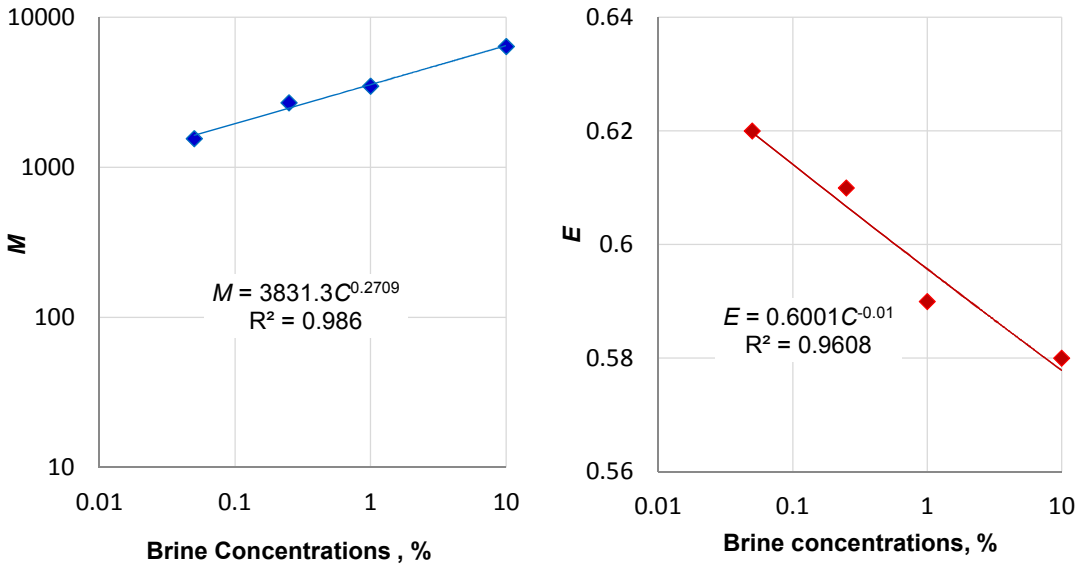

Figure 5.9—The constant coefficients as a function of brine concentration.

Then, the general form of the correlation (which can be used to predict the resistance factor in conduit systems) can be written as:

$$\mathrm{Fr} = 3831.3\ C^{0.2709}\gamma^{-0.6001\,C^{-0.01}} \quad \text{..... (5.6)}$$

The obtained correlation also can be expressed as a function of the gel strength. Table 5.1 clearly indicates that the gel strength depends heavily on the brine

concentrations; the following correlation was fitted with goodness of fit of 99.7% to expresses the relationship between brine concentrations and gel strength:

$$C = 3\times10^{-17}\, G'^{\,5.6391} \quad \text{..... (5.7)}$$

Then, the correlation can be modified to be a function of gel strength (G´):

$$\mathrm{Fr} = 3831.3 \times (3\times10^{-17}\, G'^{5.6391})^{0.2709}\gamma^{-0.6001\,(3\times10^{-17}\, G`^{\,5.6391})^{-0.01}} \quad \text{....(5.8)}$$

External data that were not included in the newly developed model were used to not only validate but also ensure the accuracy of the correlation**.** Figure 5.10 provides a comparison between the Fr obtained from the new model and the measured data obtained from lab measurements. The Fr measurements from external lab experiments were for gel extruded through different particle opening ratios ranging from 1.02 to 6.29. There was good agreement over the entire resistance factor, which indicates that the newly developed correlation can be used successfully to predict the resistance factor of PPGs extruded through open conduit systems.

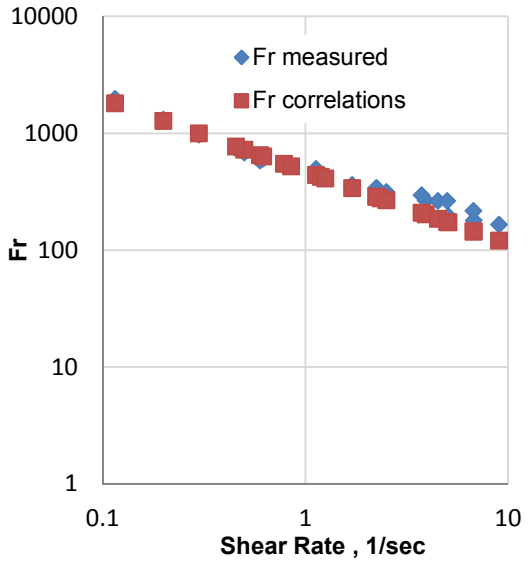

Gel swollen in 0.05%

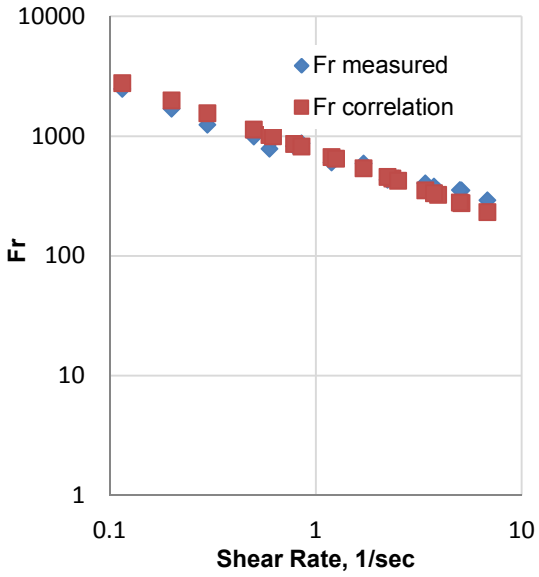

Gel swollen in 0.25%

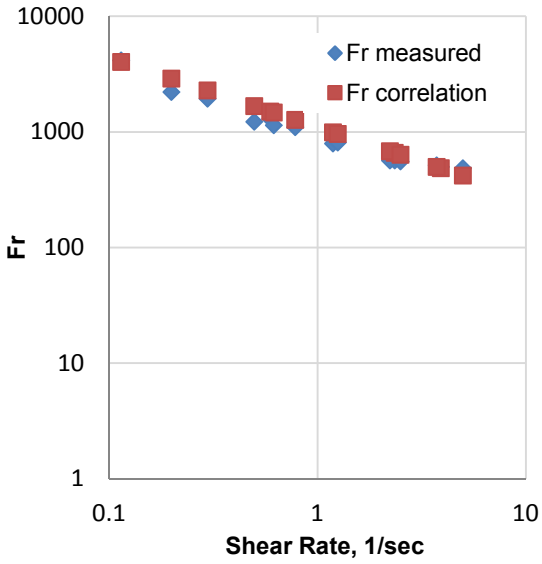

Gel swollen in 1%

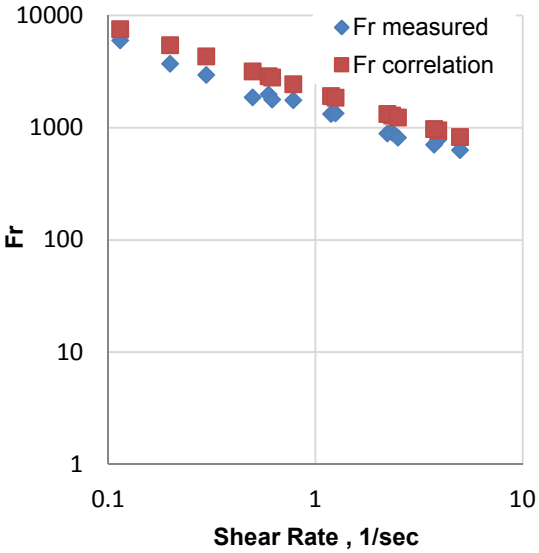

Gel swollen in 10%

Figure 5.10—Comparison between resistance factors measured in the lab and data obtained from the correlations.

5.6.5.2. PPG stabilized injection pressure model. The data in Figure. 5.7 were drawn in log-log scale as shown in Figure 5.11, and were fitted well using the following power law equation:

$$P_{inj} = a(Dg/Dp)^b \quad \text{..... (5.9)}$$

where P_{inj} is the initial stable injection pressure in psi, and *a* and *b* are coefficient factors obtained for PPGs extruded through different particle opening ratios. Table 5.4 shows the results obtained for these two factors for the different gel strengths.

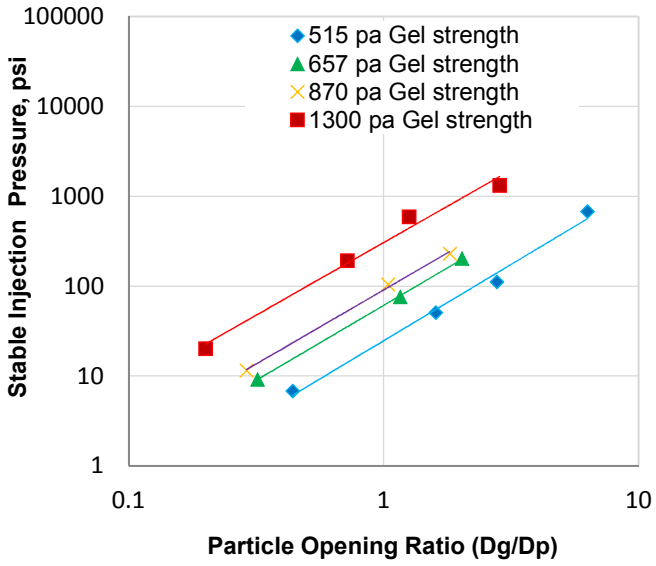

Figure 5.11—Stable injection pressure as a function of particle opening ratio and gel strength.

With fitting equations obtained for the various particle opening ratios and gel strengths, PPG's stable injection pressure can be evaluated quantitatively to obtain a better prediction of the PPG injection pressure in conduit systems.

Table 5.4—Fitting equations for stable injection pressure.

Gel strength, pa	*a*	*b*	R^2
515	24.669	1.6987	0.99
657	61.055	1.6686	0.99
870	90.713	1.6484	0.99
1300	305.49	1.6156	0.98

To develop a general correlation that can predict the PPG's stable injection pressure for all gel strengths, another regression analysis was performed to correlate these two coefficients with the gel strengths, as shown in Figure 5.12. Then, *a* and *b* were substituted into the new general fitting equations.

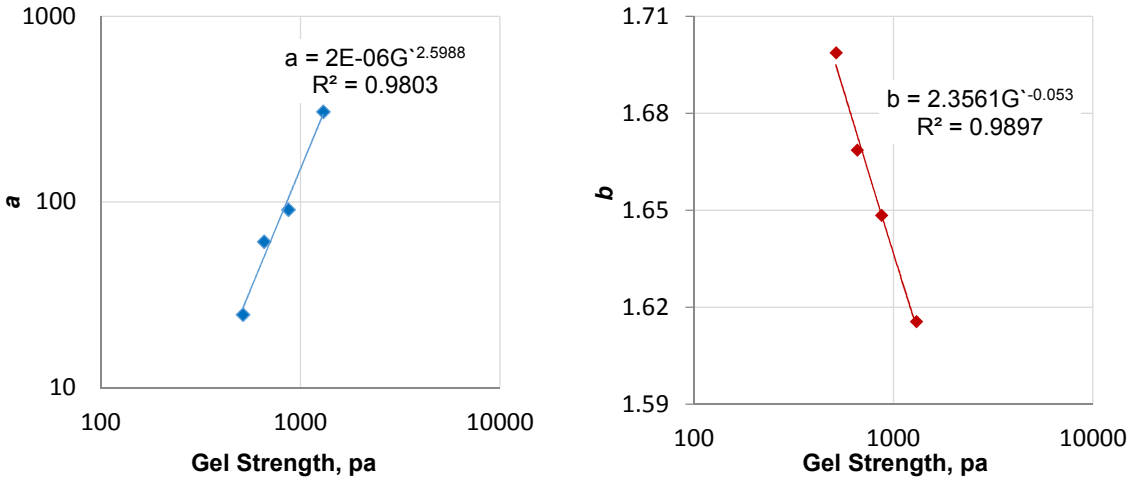

Figure 5.12—The correlation coefficients (*a*) and (*b*) as a function of gel strength.

Finally, the general form of the new correlation that can be used to predict the initial stable injection pressure in conduit systems can be written as:

$$P_{inj} = 2 \times 10^{-6}\, G'^{2.5988}\, (Dg/Dp)^{2.3561\, G'^{-0.053}} \quad \text{..... (5.10)}$$

A validation test, as described in Table 5.5, was performed to ensure the accuracy of the new model. Various ranges of particle opening ratios were not included in the developed correlation used to test the model. The initial injection pressures measured in the lab for four gel strengths in different particle opening ratios were compared with values obtained from the correlation. The relative error indicates that the new correlation can be used with relatively negligible error to determine the stable injection pressure for gel strengths of 515, 657, and 870 pa. While the correlation can be used for a gel strength of 1300 pa, the relative error is higher.

Table 5.5—New developed model validation for initial stable injection pressure.

Gel strength (pa)	Dg/Dp	Initial stable injection pressure (psi)		Relative Error (%)
		Measured	Calculated	
515	2.78	120	125	-4.1
	4.74	326	311	4.6
	3.49	184.3	184.9	-0.3
657	2.03	153	137	10.4
	3.46	375	334	10.9
870	1.82	218	233.5	-7.1
	2.29	339.5	340.8	0.38
1300	0.72	183.3	145	20.8
	1.58	440	517	-17.5

5.6.6. Resistance to Water Flow after Gel Placement in Conduits. After gel placement within the conduit system, brine was injected with different velocities, from low to high, to extrude the gel inside a conduit. In this way, four parameters were systematically obtained to characterize particle blocking behavior to water. These four sequence parameters include the pressure gradient peak, critical water breakthrough pressure, residual resistance factor, and plugging efficiency.

5.6.6.1. Pressure gradient peak (PGP). *PGP* is defined as the pressure gradient at which the gel began to move and washout from the conduit as a result of brine injection. Figure 5.13 provides an example of the brine injection pressure gradient at each section through the gel swollen in 0.05% concentration brine within a conduit inner diameter of 10.922 mm. Brine was injected through the gel at a velocity of 9.89 ft/day. Gel washout and water movement were measured by observing the pressure changes in all three sections and monitoring both the effluent produced gel and brine. In all experiments, we noticed that the injection pressure gradient in all sections increased sharply until reaching a certain peak, at which point it began to decline. This peak indicates the point at which gel failure and washout began to occur in each section (Seright, 2003). After each peak, the pressure gradient declined significantly before becoming stable in all sections. In the first section, the peak occurred at 1.85 psi/ft after 0.03 PV of brine was injected. While in the second section, the pressure gradient peak occurred at 1.05 psi/ft after injecting 0.04 PV of brine. In the last section, the peak occurred at 0.53 psi/ft after injecting 0.05 PV of brine. Then after injecting 0.15PV of brine, the water pressure gradient in all sections became stable. The pressure gradient

variations in all three sections exhibited a difference in gel movement and washout along the conduit systems.

The conduit inner diameter was checked visibly after the brine injection process was complete. For gel swollen in 0.05% NaCl, about 20% of gel was found remaining inside the conduit while for gel swollen in 10% NaCl about 70% of gel was found remaining inside the same conduit inner diameter size. This remaining volume suggests that the conduit was filled with a concentrated immobile gel.

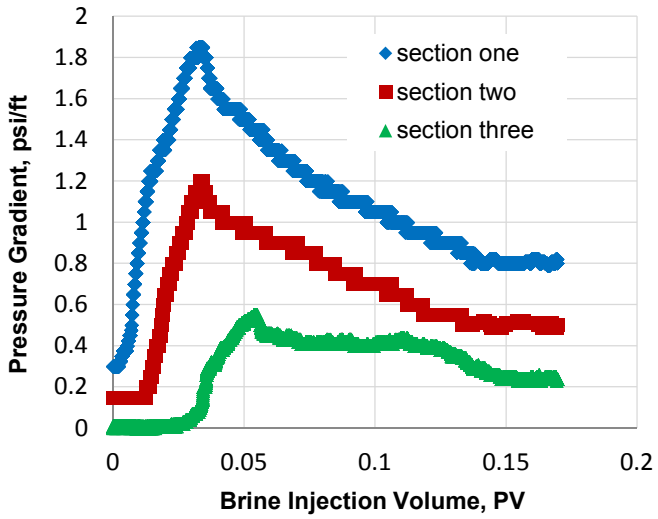

Figure 5.13—Brine injection gradient through gel in three sections for 10.922 mm conduit.

Table 5.6 provides a summary and comparison of the results obtained from the first section for all of the concentration brines. These results include the brine volume injected, as associated with its pressure gradients, for gels placed inside a conduit within an opening size of 3.0488 mm. The results suggest that gel swollen in high brine

concentrations exhibit more stability inside the conduit than gel swollen in low brine concentrations when subjected to the same injection velocity.

Table 5.6—Brine concentrations effect on gel movement at 9.62 ft/day.

Brine concentration, %NaCl	Brine injected volume for peak, PV	Pressure gradient peak through brine injection, psi/ft
0.05	0.12	4.25
0.25	0.31	7.85
1	0.52	12.05
10	0.67	25.6

Table 5.7 summarizes the results obtained from the injection of brine through gel swollen in 10% brine for three conduit inner diameters. Differing from the results obtained in large conduit opening, these results indicate that gel washout began to occur in a small conduit inner diameter when both a high injection pressure gradient and large volume of water were applied. Gel washout began to occur through an opening of 1.752 mm when 1.17 PV of brine was injected and the pressure gradient reached 245.3 psi/ft. In contrast, the gel injected through a larger opening size (10.922 mm) began to move when 0.16 PV of brine was injected and the pressure gradient was only 4.9 psi/ft. These findings indicate that less gel movement occurred in smaller conduit diameters than in larger conduit diameters.

Table 5.7—Conduit diameter effect on gel extrusion for gel swollen in 10% NaCl.

Inner diameter, mm	Brine injected volume for peak, PV	Pressure gradient peak through water injection, psi/ft
10.922	0.16	4.9
3.048	0.67	25.6
1.752	1.17	245.3

5.6.6.2. Critical water breakthrough pressure (PCW). *PCW* is defined as the pressure at which the first drop of water can be seen from the outlet. Figure 5.14 provides information about this variable as a function of both the brine concentration and conduit inner diameter. The small water breakthrough pressure indicates that water could start propagate easily through the gel. This result suggests that as the gel became stronger (swollen in high brine concentration), the water breakthrough pressure increased. Differences in water breakthrough are clear when comparing weak gel (swollen in low brine concentrations) against strong gel. Figure 5.14*a* shows the water breakthrough measurement for gel swollen in different concentration brines when gel was placed within a 3.0488 mm opening. When gel was swollen in 0.05% brine, water was able to pass through it at 8.8 psi. Water could not pass through gel swollen in 10% brine until the pressure reached 46 psi. Figure 5.14*b* shows the results obtained for water breakthrough through gel swollen in 0.05% brine concentration as a function of different conduit sizes. Water was less likely to pass through a smaller pore opening than a larger opening. Water passed through a 10.922 mm opening at a pressure of 2.1 psi, and through a 1.752 mm opening at a pressure of 60.2 psi.

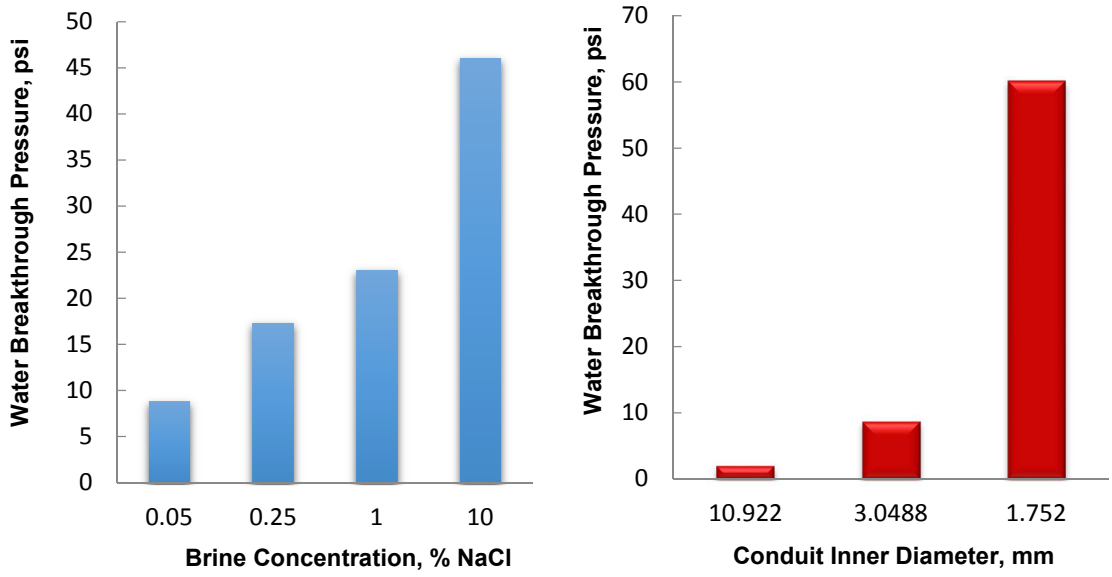

a. Conduit inner diameter 3.0488 mm

b. Gel swollen in 0.05% brine concentration

Figure 5.14—Critical water breakthrough pressure as a function of brine concentration and conduit inner diameter.

5.6.6.3. Residual resistance factor and plugging efficiency (E). *Frrw* is defined as the ratio of water phase permeability before and after particle gel treatment and (E) refers to the percentage of permeability reduction, which can be calculated from the following equation E (%) = [1- (1 / Frrw)]*100. The stabilized water injection pressures at different velocities were used to calculate *Frrw* and *E*. Figure 5.15 shows the residual resistance factor as a function of brine concentration and brine velocity. *Frrw* increased as the gel strength and conduit inner diameter increased. Figure 5.16 shows the gel plugging efficiency as a function of the brine concentration and brine velocity. The PPG plugging efficiency increased when a strong gel was selected as a plugging agent for large conduit sizes. The results suggest that gel swollen in 10% brine can provide a 97% plugging, as compared to 76% plugging for gel swollen in 0.05% brine for a conduit with

inner diameter of 1.752 mm. This percentage increased to 98% for the former and 93% for the latter when gel was placed into a large opening (10.922 mm). These findings indicate that the plugging efficiency of the PPG did not decrease significantly in spite of the gel washout occurring after gel placement.

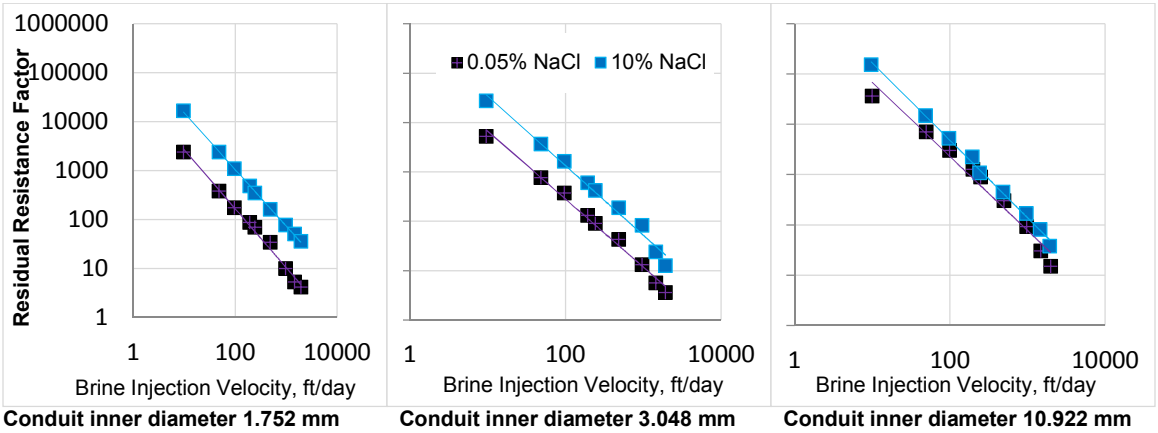

Figure 5.15—Residual resistance factor as a function of brine concentration and conduit inner diameter.

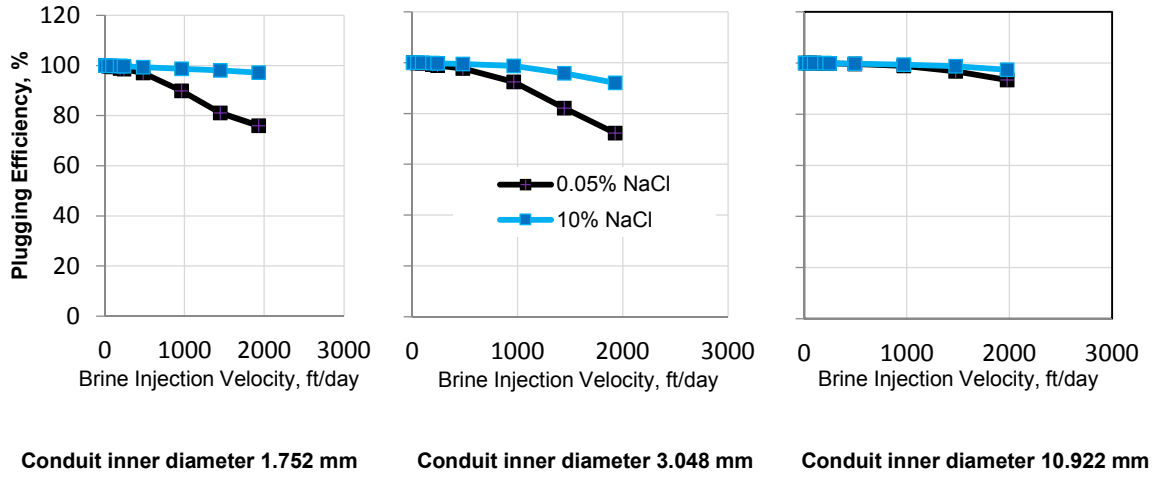

Figure 5.16—Plugging efficiency as a function of brine concentration and conduit inner diameter.

5.7. DISCUSSION

When investigating particle injection, many researchers are interested in the passing ratio, which is the ratio of the particle size to the pore throat size at which the particle can pass through a constriction. For stiff, hard particle, this question is easy to answer. Extensive experimental results have shown that stiff particles can pass through pore throats only if their particle sizes are less than 1/9 of the pore size. However, swollen gel particles are deformable and breakable, so they can pass through porous media much easier than stiff particles. Swollen gel particle transport mechanism through porous media exhibit different patterns of behavior (Bai et al., 2007). Table 5.8 provides the ratio of particle size to opening size (Dg/Dp), as well as the particle size before and after extrusion. Weak particles still were able to transport through the opening when the Dg/Dp was as high as 6.3 but required a relatively high injection pressure gradient of 12.5 psi/ft in order to do so. These results are consistent with Seright (1997) where he observed that pressure gradient increased significantly with decreased tube diameter.

Table 5.8—Particle opening ratio measurements results.

Gel strength, Pa	Particle gel size before extrusion, mm	Pore opening size, mm	Dg/Dp	Gel particle size after extrusion, mm	Gel Particle size decrease, %	Gel threshold pressure gradient, psi/ft	Gel Injection stable pressure, psi
515	4.88	10.922	0.44	3.57	26.8	0.1	6.8
		3.048	1.60	2.58	47.13	0.65	51
		1.752	2.78	2.391	51	1.1	112
		0.774	6.3	0.902	81.51	12.5	680
657	3.56	10.922	0.32	2.90	18.5	0.2	9.2
		3.048	1.16	2.17	39.04	0.85	76
		1.752	2.03	2.19	38.4	2.1	203
870	3.2	10.922	0.29	2.30	28.1	0.21	11.5
		3.048	1.04	1.99	37.81	1.2	105
		1.752	1.82	1.87	41.5	2.8	230
1300	2.21	10.922	0.20	1.945	11.99	0.25	20.1
		3.048	0.72	1.808	18.19	2.3	191.7
		1.752	1.26	1.923	12.98	3.5	590
		0.774	2.85	1.73	21.7	26.2	1320

The results shown in Table 5.8 indicate that gel particle size was reduced after extrusion when Dg/Dp larger than, equal to, and even smaller than one. Figure 5.17 shows particle sizes measurement before and after extrusion for the sample with gel strength of 515 pa. The weak gel particles experienced a significant decrease in particle size, up to 81.5%, when they moved through conduit with a 0.774 mm opening for Dg/Dp equal to 6.3. However, a strong gel decreased only by 21.7% when moving through the same conduit size but with Dg/Dp equal to 2.85. Based on previous knowledge (Bai et al., 2007), this particle size reduction could be explained by two reasons: breakdown, dehydration or both. To determine if the particle size reduction was caused by gel dehydration, we collected effluent particle gel samples from 3.048 mm conduit, where Dg/Dp have smaller than and equal to one, measured their strength and also placed them in the same concentration brine to observe their reswelling. Figure 5.18 shows how much the gel volume increased at different injection rates for four different strength gels. The results show that the weakest particles can regain 50% of water, while the strong gels can regain only approximately 20% of water, indicating that weak gel can be dehydrated more than strong gel during conformance control treatments. In another words, the weakest particles shrunk 50% of its original volume while the strongest one shrunk 20% when they passed through the conduit. The strength measurement taken after extrusion, shown in Figure 5.19 also indicates that the gel became more concentrated due to water loss from its cluster. When we compared the significant reduction in particle size to the gel particle volume shrunk, we observed that gel particle size reduction was caused by both particle breakdown and dehydration.

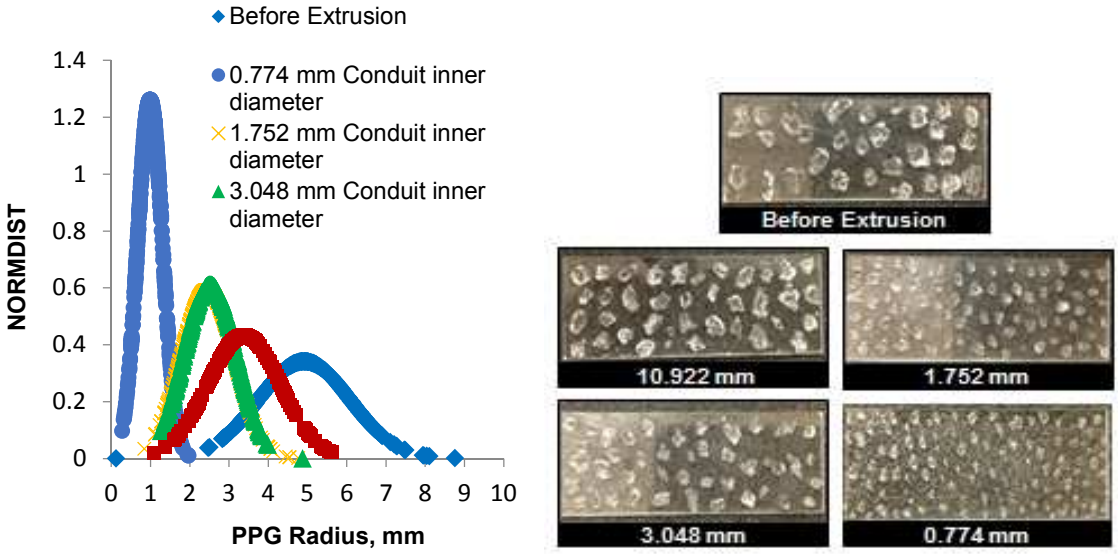

Figure 5.17—PPG size distributions and images for gel with strength of 515 pa before and after extrusion.

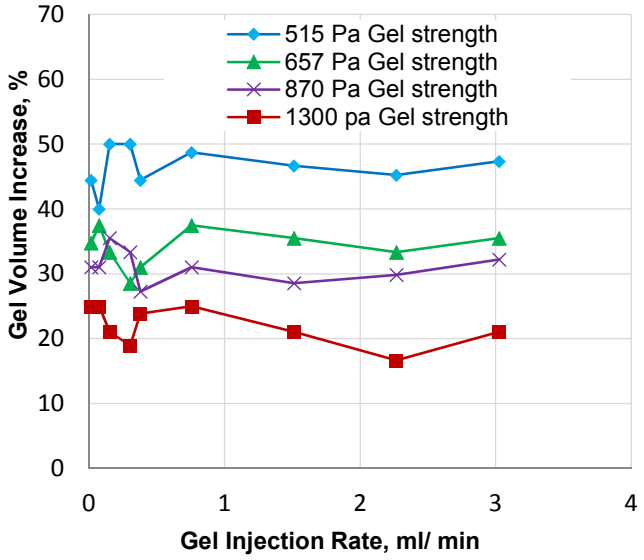

Figure 5.18—Particle volume increased after soaking in same brine.

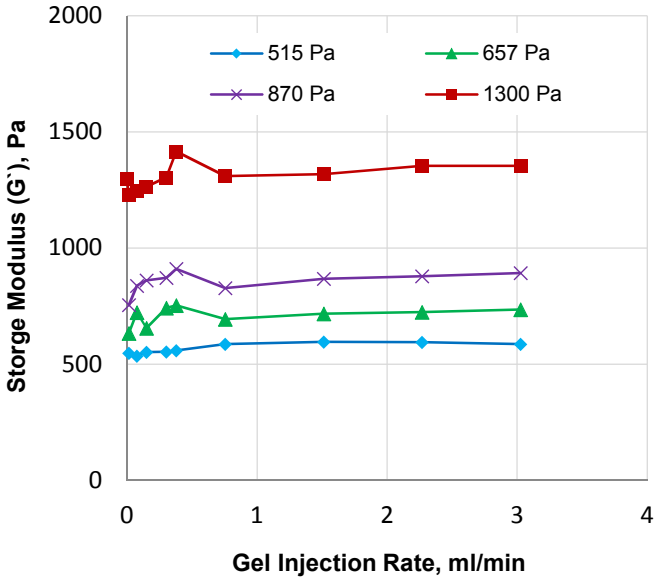

Figure 5.19—Particle storage moduli (G`) after extrusion.

5.8. CONCLUSION

A number of factors that affect PPG extrusion and blocking efficiency through conduit systems were intensively examined in this study. The mechanisms associated with gel propagation and placement, such as dehydration and gel washout, were investigated during the experiments. The following conclusions can be drawn from the research:

- PPG injection pressure increased as the brine concentration and injection velocity increased. This increase, however, after a certain velocity became unsubstantial.
- The resistance factor increased when the gel strength increased and/or when the conduit inner diameter becomes wider but it decreased if the velocity increased.
- Both the gel threshold pressure and the stable injection pressure increased as the particle opening ratio increased. Both pressures, however, would not increase

significantly after a specific ratio. Additionally, the gel strength impacted the gel injection pressure more than did the particle opening ratio.

- Two new empirical correlation models were successfully developed to predict both PPG resistance factor and stable injection pressure.
- The resistance factor measurements are not dependent on the particle opening ratio when it is measured against shear rate.
- PPG blocking performance increased as the gel strength and conduit inner diameter increased. This finding reveals that the conduit size conductivity can significantly decrease if a strong gel is selected for the conformance treatment.
- Weak gels can be injected into large particle opening ratio with relative small increase in injection pressure compared to strong gels. Weak gels break into small sizes so it could pass through.
- Weak gels tend to dehydrate more than strong gels. The gel becomes stronger after the extrusion process, as a result of the dehydration mechanism.
- PPG size can be reduced during transportation through conduits due to dehydration and breakdown.

6. DISPROPORTIONATE PERMEABILITY REDUCTION THROUGH FRACTURE

6.1. INTRODUCTION

When gels are placed throughout the fracture or conduit, water permeability decreases significantly and water flow into the well is minimized. However, if oil is produced from reservoir through conduit, oil permeability will not be significantly decreased.

6.2. OBJECTIVES AND TECHNICAL CONTRIBUTIONS

This work intends to examine in-depth several factors such as particle size, gel strength, and conduit pore size effects on DPR properties and gel extrusion through conduit systems.

- Alternate banks of both brine and oil were used to determine the extent to which PPGs can reduce water permeability more than oil permeability within conduit systems.
- Examine the effect of brine concentrations, particle gel sizes, and injection flow rates on PPG injection pressure.
- Determine the residual resistance factor (*Frr*) for oil and water during the different multiple injection cycles.
- Evaluate different DPR mechanisms using PPG as a diver agent materials
- The results obtained from this work can be used to provide a better understanding of preformed particle gel performance when two phase fluids propagate through

fractures filled with gel. It could also use for better selections of particle gel placement through fractures or conduits.

6.3. EXPERIMENTAL DESCRIPTION

6.3.1. Preformed Particle Gel. Super-absorbent polymer (SAP) was used as a PPG sample. PPG is comprised primarily of potassium salts with crosslinked polyacrylic acid / polyacrylamide copolymer.

Two sizes of particle gels, 20-30 and 100-120 mesh size, were selected for the experiments. Table 6.2 illustrates the size distribution of the PPG before swelling, as determined by a sieving test.

Table 6.1—Size distribution of particle gel.

Sieves (mesh)	Size (microns)
20-30	850-600
100-120	150-125

6.3.2. Brine Concentrations and Oil Viscosities. Sodium chloride (NaCl) with four concentrations (0.05, 0.25, 1, and 10 wt% NaCl) was used to prepare the swelling gels. The brine concentration was selected carefully according to both the swelling ratio and the gel strength; the high-salinity brine resulted in high gel strength and a low swelling ratio, as presented in Table 5.1. Two oils with viscosities of 37 and 195cp were used in the study.

6.3.3. Tubes. In this experiment, stainless steel tubes with internal diameters of 0.12 inches and 0.069 inches were used to represent fractures. These tubes were originally 20 ft long and were cut into 5 ft in lengths.

6.4. EXPERIMENTAL SETUP

Figure 6.1 presents the experimental apparatus, which consisted of a syringe pump used to inject brine, gel, and oil through the accumulator into a fracture model. The fracture model was essentially five long tubes with two different internal diameters. A check valve was used at the inlet of the fracture model to ensure that no back flow of gel occurred when pressure was released from the pump. A 0.5-micron filter was installed at the outlet of the tube to ensure that no gel washout occurred during either the brine or the oil injection process. Pressure sensors were connected at both the inlet and the outlet to measure the differential pressure across the gel.

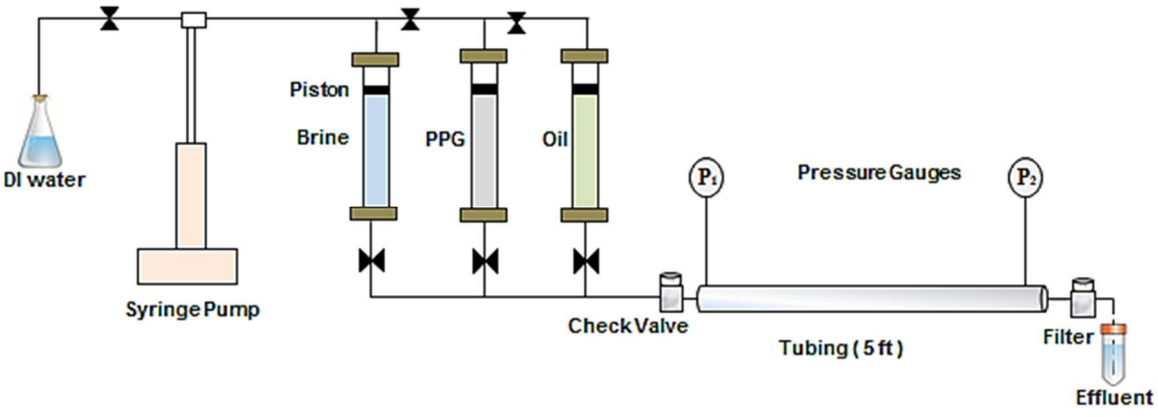

Figure 6.1—Schematic diagram of PPG placement in fractures.

6.5. EXPERIMENTAL PROCEDURES

First, we obtained the effects of brine concentrations (gel strength), particle size, and fracture width on the gel extrusion and DPR behavior through fractures. PPGs with mesh sizes of 20-30 swollen in 0.05%, 0.25%, 1%, and 10% brine solution were extruded through tubes with internal diameters of 0.069 inches. From high to low, nine flow rates, 3.0246, 2.2684, 1.5123, 0.7561, 0.3781, 0.3025, 0.1512, 0.0756, and 0.0151ml/min, were used to extrude the PPG. Stable PPG injection pressures were achieved and resistance factors determined for each flow rate. Then, a filter was installed at the outlet, and PPG was injected again and compressed through the tube until the injection pressure reached 100 psi. The same type of brine used to prepare the swollen PPG then was injected. Oil with a 37 cp viscosity was injected after each injected brine concentration. Residual resistance factors for both water and oil were determined during the experiments.

The second objective of this study was to understand gel performance under a sequence of brine and oil cycles. PPGs with mesh sizes of 20-30 swollen in 1% NaCl were extruded through a tube with a diameter of 0.12 inches using the nine different flow rates. Stable pressure was achieved for each gel injection rate. After a filter was installed and the PPG was compressed, brine and oil cycles were alternated in sequence. Both brine and oil were injected through the tube model with seven flow rates starting from low to high: 0.0151, 0.0756, 0.1512, 0.3025, 0.3781, 0.7561, and 1.5123 ml/ min. This sequence can be summarized in the following steps:

1) Concentration of 1% NaCl (first cycle) was injected with seven flow rates through PPG-filled tubes. Stable pressure was achieved for each flow rate, and the residual resistance factors for water (*Frrw*) were determined.

2) Oil with a 37 cp viscosity was injected to displace water inside the gel. Residual resistance factors for oil (*Frro*) were obtained for the seven flow rates.
3) Oil with a 195 cp viscosity was injected, and the *Frro* were again obtained for each flow rate.
4) 1% NaCl brine (second cycle) was injected after the injection of oils with same flow rates, and *Frrw* was calculated.
5) After the second cycle of brine injection, oil with a 37 cp viscosity was injected again to obtain the *Frro*.
6) High-viscosity (195 cp) oil was injected, and the *Frro* were determined.
7) Finally, 1% NaCl brine (third cycle) was injected in the same model with the same flow rates to determine the *Frrw*.

The above seven steps were repeated using PPG with a mesh size of 100-120 swollen in the same NaCl concentrations (1%).

6.6. RESULTS AND ANALYSIS

Data showing the effects of the gel particle size, gel strength, and fracture width on gel extrusions and placements were obtained. These data include the PPG injection pressure, resistance factor, residual resistance factors, and results for the brine and oil cycles.

6.6.1. PPG Injections and Residual Resistance Factor. This section presents and discusses the results obtained for the injection pressure and residual resistance factors for the effects of gel strength, particle gel size, and fracture width.

6.6.1.1. Stabilized PPG injection pressure versus injection rate. The stable pressure measurements obtained during the gel extrusion process were recorded and plotted against the PPG injection flow rate for each different gel strength and particle size. Figure 6.2 *a* illustrates the stable injection pressure of the gels for gel storage moduli of 515, 657, 870, and 1300 pa injected through a tube with an internal diameter of 0.069 inches. Figure 6.2 *b* presents the measurements taken for both 20-30 mesh size and 100-120 mesh size injected through a fracture 0.12 inches wide. The results show that the stable injection pressure for each flow rate increased as the gel strength and particle size increased. For instance, a particle gel with a 100-120 mesh size had a stable pressure of 65 psi at a gel injection rate of 3.0256 ml/min, while a particle gel with a 20-30 mesh size had a stable pressure of 71 psi at the same injection flow rate. This increase in pressure occurred because larger particles are more resistant to flow through fractures than smaller particles. This behavior, however, was most pronounced at low flow rates. This finding could imply that at a high injection rate, the stable pressure for both particle sizes is an independent factor.

The stable pressure for all of the gel strengths and particle sizes increased significantly as the injection rate increased. Though to an insignificant extent, the pressure continued to build up as the PPG injection rate increased. The results also indicate that as the gel strength increased, reaching the stable pressure for each injection rate required more time.

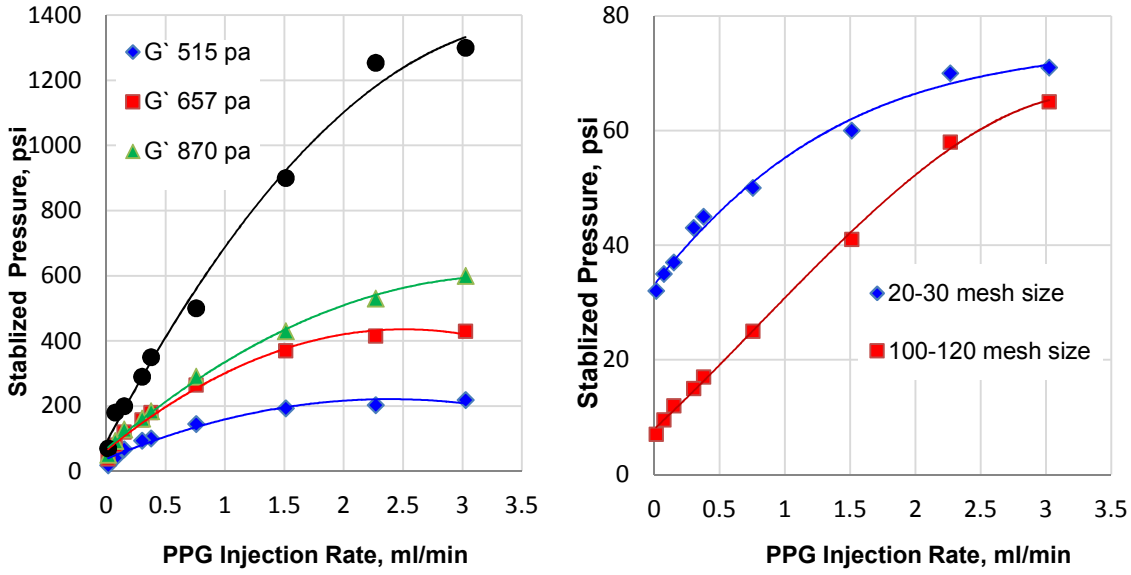

(a) 20-30 mesh size PPG

(b) PPG swollen in 1% NaCl

Figure 6.2—Stable pressures versus injection rate for gel strengths and particle sizes.

6.6.1.2. Resistance factor calculation. PPG is a shear thinning or pseudo plastic material. The resistance factor (Fr) is used to measure PPG resistance to flow when it extrudes through fractures. Similar to the porous media experiment, Fr was estimated from the injectivity index and geometry of the fracture. It can be defined as the ratio of the particle gel injection pressure drop to the brine injection pressure drop at the same flow rate.

The resistance factor was calculated during the gel extrusion process against the velocity for each different gel strength and particle size. Figures 6.3*a* and 6.3*b* illustrate the resistance factor results obtained for different gel strengths and gel particle sizes, respectively. The PPG resistance factor increased as the gel strength and gel particle size increased. For example, at a velocity of 29 ft/day, the Fr of gel strengths 515, 657, 870, and 1300 pa were 74981, 158294, 208282, and 291595, respectively. The Fr determined

for each PPG strength decreased sharply as the superficial velocity increased. For instance, the resistance factor for 100-120 mesh size was 8750 at a velocity of 10 ft/day. When the velocity was doubled, the resistance factor decreased substantially to 1683.

The data in Figure 6.3 were fitted according to the power law equations. Table 6.2 lists the fitting equations for the resistance factors obtained for both effects. The elasticity index (n) measured for the effects of gel strength were plotted against the storage moduli, as presented in Figure 6.4. As the gel strength increased, the gel elastic value decreased.

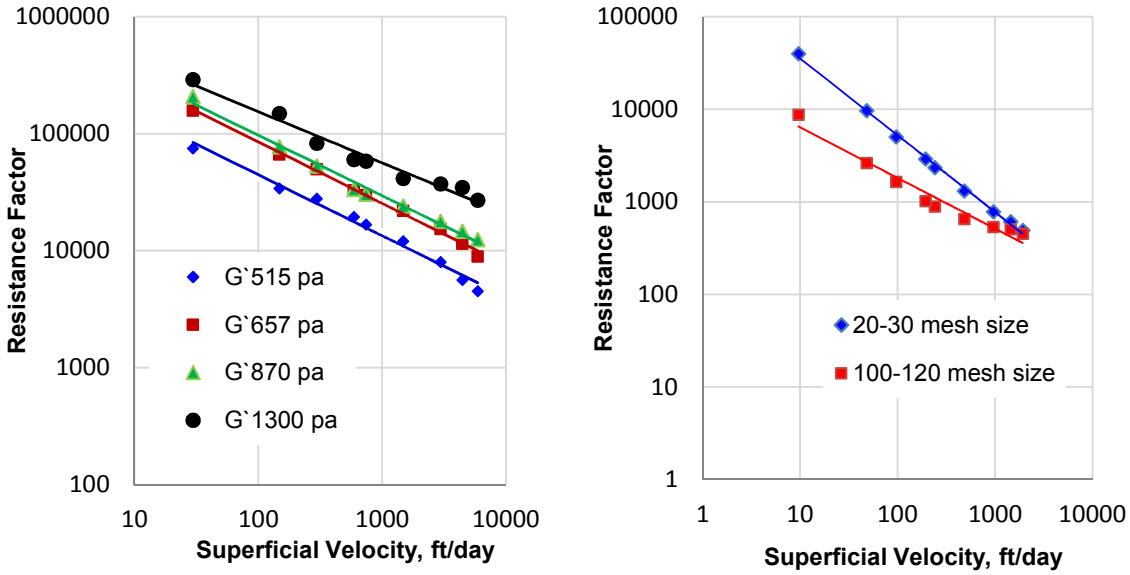

(a) 20-30 mesh size PPG *(b)* PPG swollen in 1 % NaCl

Figure 6.3—Resistance factor calculated for both gel strength and gel particle size in a log-log scale.

Table 6.2—Summary of fitting equations for resistance factor measurements.

Storage Moduli G´(Pa)	Particle Size(mesh)	Fitting Equations	Elasticity Index (n)	R^2
515	20-30	FR = 490150 u $^{-0.530}$	0.530	0.986
657		FR = 955622 u $^{-0.525}$	0.525	0.996
870		FR = 1E+06 u $^{-0.50}$	0.50	0.988
1300		FR = 1E+06 u $^{-0.437}$	0.437	0.981
870	20-30	FR = 238927 u $^{-0.829}$	0.829	0.997
	100-120	FR = 22514 u $^{-0.547}$	0.547	0.957

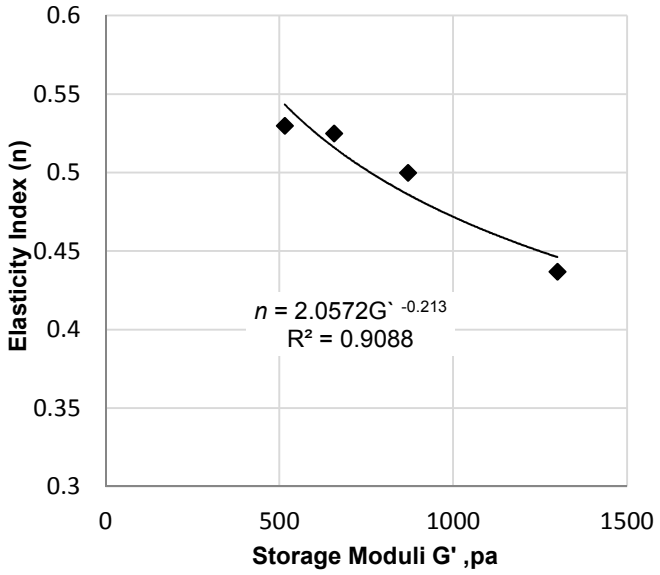

Figure 6.4—Elasticity index as a function of gel strengths.

6.6.1.3. Residual resistance factor to brine and oil. Residual resistance factors were determined by dividing the pressure drop of the injection of either brine or oil into the fracture after gel placement by the pressure drop of the injection of either brine or oil into the fracture before gel placement.

6.6.1.3.1. <u>Effect of gel strength on DPR.</u> Figure 6.5*a* illustrates the *Frrw* determined for brine injected through different strength PPGs. The results indicate that the gel strength does affect the *Frrw*; the *Frrw* increased as the gel strength increased. As the gel strength increased from 515 pa to 1300 pa, the increase in the *Frrw* became significant. After determining the *Frrw*, oil was injected through the same internal diameter with the same velocity to obtain the *Frro*. Figure 6.5 *b* depicts the measurements of oil with a viscosity of 37 cp injected through swollen PPGs. The results indicate that the gel strength also affects the *Frro*; the Frro increased as the gel strength increased. For all of the gel strengths, the *Frro* was less than the *Frrw*.

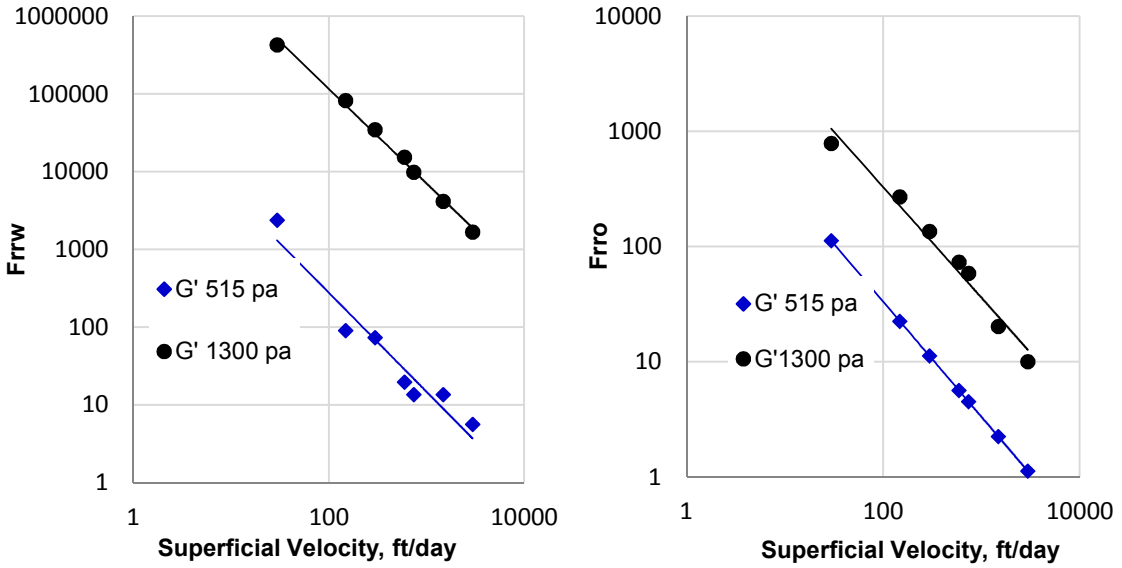

(a) (b)

Figure 6.5—Residual resistance factor for brine and oil.

6.6.1.3.2. <u>Effect of opening size on DPR.</u> PPGs with a mesh size of 20-30 swollen in a 1% NaCl solution were used to observe the effect of the fracture width on the residual resistance factors. Figure 6.6 *a* and *b* presents the results obtained from injecting a 1% NaCl solution and 37 cp oil through gel placed in fractures 0.069 and 0.12 inches wide. These data suggest that *Frrw* and *Frro* increased as the fracture widened. *Frro* was less than *Frrw* regardless of the fracture width.

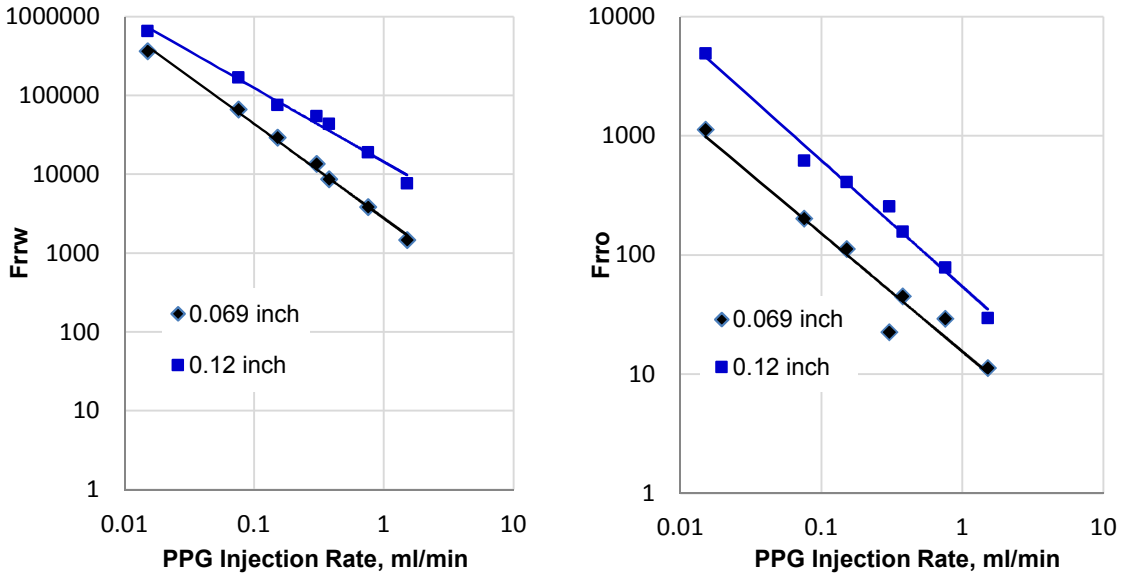

(a) Inject 1% brine *(b)* inject 37 cp oil

Figure 6.6—Residual resistance factor for brine and oil as a function of both flow rate and fracture width.

6.6.2. Brine and Oil Cycles Measurements. This section discusses the results obtained from injecting different cycles of brine and oils through gel-filled fractures. During these several cycles, the residual resistance factors to brine and oil for each cycle were determined to evaluate PPG performance.

Seven velocities were used to inject brine, and the stable pressure was observed at each. Figure 6.7*a* illustrates the *Frrw* determined for the two particle sizes as a function of superficial velocity. The *Frrw* for both particle sizes decreased as the velocity increased. This decrease was significant at a low velocity. For example, the *Frrw* value at 100-120 mesh size decreased from almost 200,000 to 50,000 as the velocity increased from 10 to 50 ft/day. The results also suggest that the *Frrw* was greater for larger than for smaller particle sizes. The power law equation was used to fit data for the *Frrw*. The following are equations that fit well for the two particle sizes:

$$Frrw = 6E+06\ u^{-0.936} \quad \text{for 20-30 mesh size} \ldots\ldots\ldots\ldots \quad (6.1)$$

$$Frrw = 2E+06\ u^{-0.995} \quad \text{for 100-120 mesh size} \ldots\ldots\ldots \quad (6.2)$$

After the *Frrw* values were determined, oils with different viscosities (37 cp and 195 cp) were injected consecutively to determine the *Frro*. Figures 6.7*b* and *c* illustrate the *Frro* measurements for both particle sizes at different oil viscosities. Both figures indicate that the *Frro* determined for the two PPG mesh sizes decreased as the superficial velocity increased. The change in particle size does not appear to have a significant effect on the *Frro* when compared to the first cycle of brine. For the oil with a viscosity of 37cp injected with a velocity of 10 ft/day, the *Frro* measurements for both 20-30 mesh and 100-120 mesh particle sizes was 4900 and 3400, respectively. The results also indicate that the *Frro* decreased as the oil viscosity (at the same given particle size) increased. The power law equation was used to fit the results obtained for the *Frro* values. The *Frro* for

the different oil viscosities and particle sizes are described using Equations 6.3, 6.4, 6.5, and 6.6:

Residual resistance factor equations for 37 cp:

$$Frro=50498u^{-1.059} \quad \text{for 20-30 mesh size} \quad \text{.....(6.3)}$$

$$Frro=19606u^{-1.004} \quad \text{for100-120 mesh size} \quad \text{..... (6.4)}$$

Residual resistance factor equations for 195 cp:

$$Frro = 11283\ u^{-1.083} \quad \text{for 20-30 mesh size..... (6.5)}$$

$$Frro = 3720\ u^{-1.004} \quad \text{for 100-120 mesh size .....(6.6)}$$

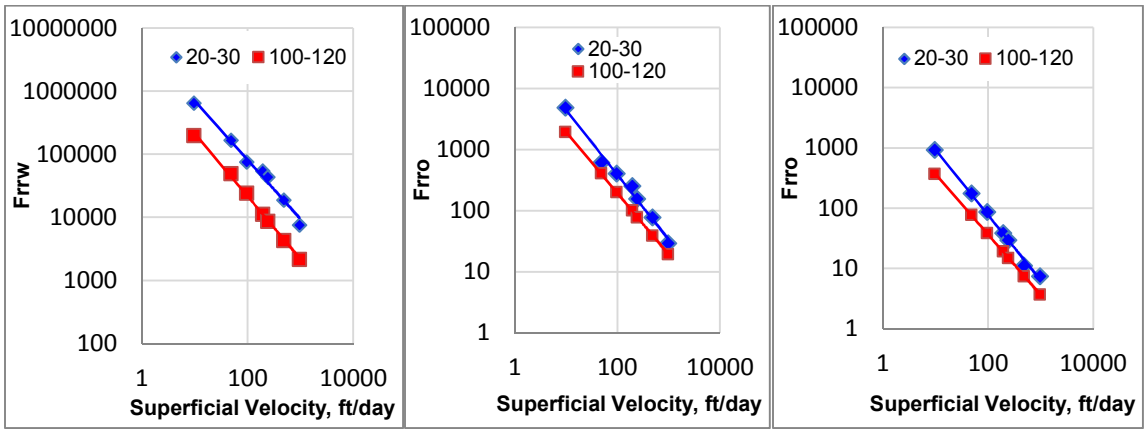

a). First 1% brine cycle *b).* First 37cp oil cycle *c).* First 195 cp oil cycle

Figure 6.7—*Frrw* and *Frro* determined for the first cycles.

The water loss (dehydration) from PPG and the injection pressure were both obtained during the process of injecting 37cp oil through 20-30 mesh. Figure 6.8 illustrates that a significant gel breakdown occurred during the oil injection process. Oil

was injected at a constant flow rate of 0.3025 ml/min. The differential pressures (stable pressure) across the gel and the water loss from the gel were measured. The pressure began to build during the early stages of oil injection, eventually reaching 53 psi before falling and finally fluctuating between 3 and 7 psi. When compared to the first water cycle injection process, the differential pressure at the same flow rate (0.3025ml/min) was 29 psi. This significant drop in pressure suggests that gel could fail during the oil injection process.

Cumulative water loss data from the gel during the oil injection process were collected. Figure 6.8 shows that the cumulative water loss from the gel began to build rapidly until the cumulative oil injected reached approximately 150s ml. The cumulative water loss then began to level off at 14 ml. We continued to inject oil until observing a stable pressure across the gel to ensure that no more water loss would occur.

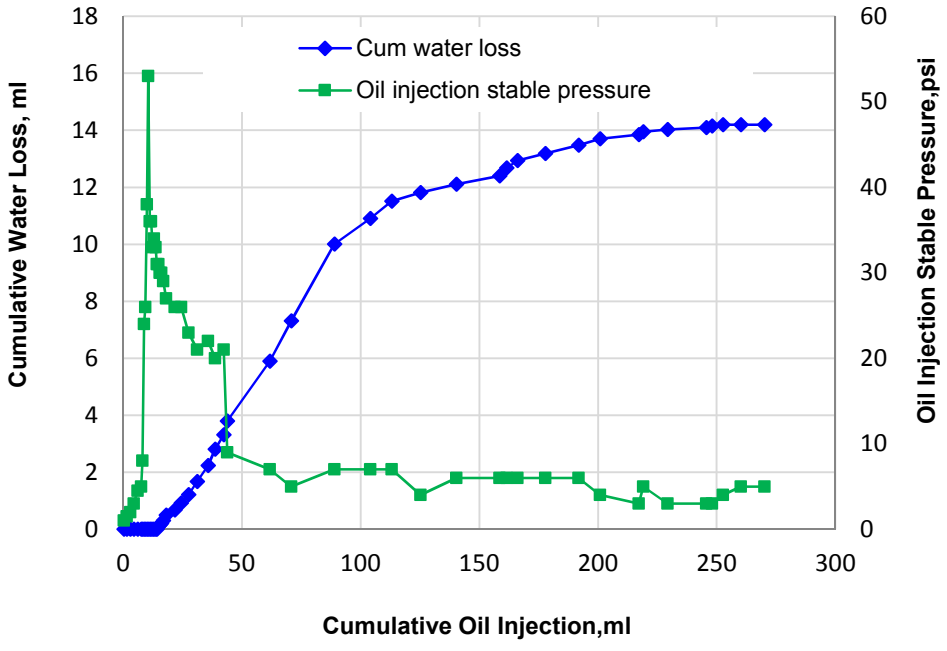

Figure 6.8—PPG breakdown during two-phase flow.

6.6.2.1. Frro and Frrw obtained from first cycle. Figure 6.9 depicts the comparison of the first cycle of 1% brine with the first cycle of two oil viscosities to identify the extent to which gel can reduce permeability to water more than to oil.

The results show that the residual resistance factor was much lower during oil injection than during water injection. At a velocity of 10 ft/day, the *Frrw* to water was 653414, and the *Frro* for oil with a viscosity of 195cp was 930, which means that the *Frro* decreased by around 700 times. A number of reasons may exist for this phenomenon; some of the reasons observed in our experiments will be explained in the Discussion section.

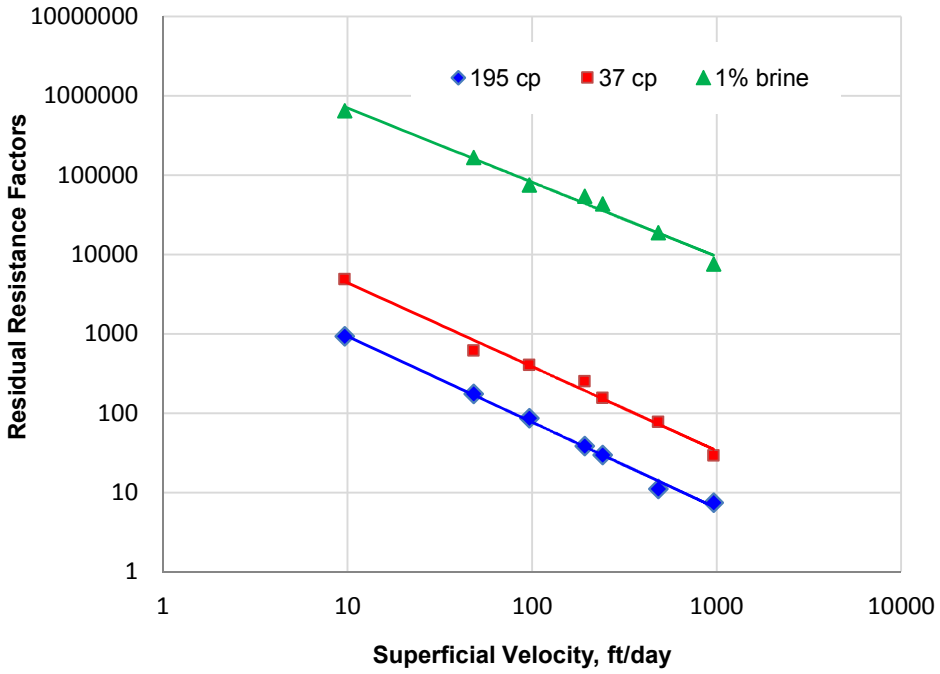

Figure 6.9—Comparisons between *Frrw* and *Frro* during the first cycle of flooding.

6.6.2.2. Brine and oil reinjection measurements. After the first cycles of brine and oil injections were completed, we continued to inject multiple cycles of brine and oil through the same gel sizes. Figure 6.10*a* shows the results obtained for the second brine cycles. The *Frrw* measurements observed during the second water injection cycle were almost the same for both particle sizes. For instance, the *Frrw* measurements for particle sizes 20-30 and 100-120 were 544.5 and 726, respectively, at the same velocity (964 ft/day). In this example, the oil may have dehydrated both particle sizes to the same extent. The effect of different particle sizes on the *Frrw* was not significant after oil was injected through the gel. The following *Frrw* measurements were taken during the second water injection cycle for both particle sizes:

$$Frrw = 2E+06\ u^{-1.216} \quad \text{for} \quad \text{20-30 mesh size} \quad \text{.....(6.7)}$$

$$Frrw = 7.25E+05\ u^{-1.004} \quad \text{for} \quad \text{100-120 mesh size} \quad \text{.....(6.8)}$$

Comparing Equations (6.1) and (6.2) with (6.7) and (6.8), respectively, indicates that the residual resistance factor for brine decreased substantially after the oil injection cycle was complete.

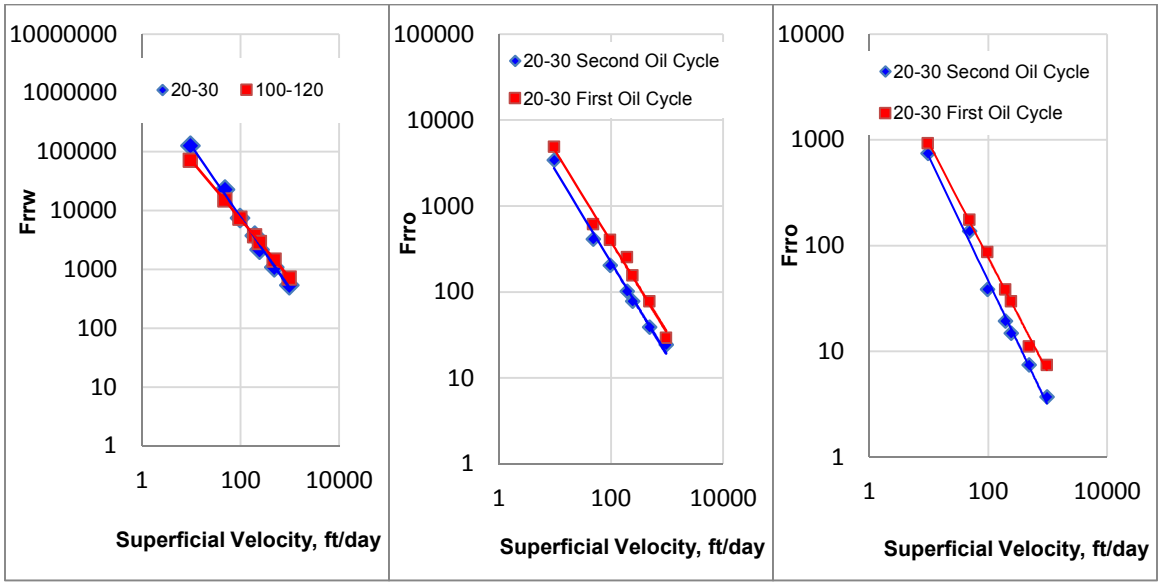

a) Second 1% brine cycle *b).* Second & First 37cp oil cycle*).* C) Second & First 195cp oil cycle

Figure 6.10—*Frrw* and *Frro* determined for the second cycles.

Figures 6.10 *b* and *c* provides a comparison of the *Frro* determined during the first and second oil injection cycles, respectively. The results obtained during the second oil injection cycle for both oil viscosities suggest a decrease in the *Frro*, even when compared to the first cycle. This decrease indicates further gel breakdown, thus continuously increasing the gel's permeability during oil injection. For example, the *Frro* determined for oil with a viscosity of 37 cp at the same velocity (100 ft/day) decreased almost two times less than the *Frro* measured during the first oil injection cycle. The *Frro* was 407 for the first oil injection cycle and 203 for the second. *Frro* measurements were taken during the second oil injection cycle for both oil viscosities, as follows:

Residual resistance factor for 37 cp:

$$Frro = 31743\ u^{-1.079} \quad \text{..... (6.9)}$$

Residual resistance factor for 195 cp:

$$Frro = 10434\ u^{-1.177} \quad \text{.....(6.10)}$$

The effect of oil viscosity on the *Frro* was noticeable when comparing Equation (6.5) with Equation (6.3) and Equation (6.10) with Equation (6.9). The *Frro* with a high oil viscosity was less than the *Frro* with a low oil viscosity for both cycles. These results indicate that gel has great potential for success in heavy oil field applications.

6.6.2.3. Comparing the Frrw obtained for all three brine cycles. Figure 6.11 compares the results from the first, second, and third water cycles for the same particle size. A third water cycle was injected after the second oil cycles. The *Frrw* measurements taken during the third brine cycle indicate a slight decrease when compared to the *Frrw* measured during the second brine cycle. For instance, at a velocity of 10 ft/day, the *Frrw* for the second cycle was 127052; it decreased slightly to 108902 during the third cycle. A comparison of all three water cycles indicates that *Frrw* decreased substantially after the first oil injection. The *Frrw* for both the second and third cycles were very similar. These measurements indicate further particle gel breakdown but to a lesser extent than during the second cycle. The *Frrw* measurement obtained during the third water injection cycle was:

$$Frrw = 2E{+}06\ u^{-1.212} \quad \text{..... (6.12)}$$

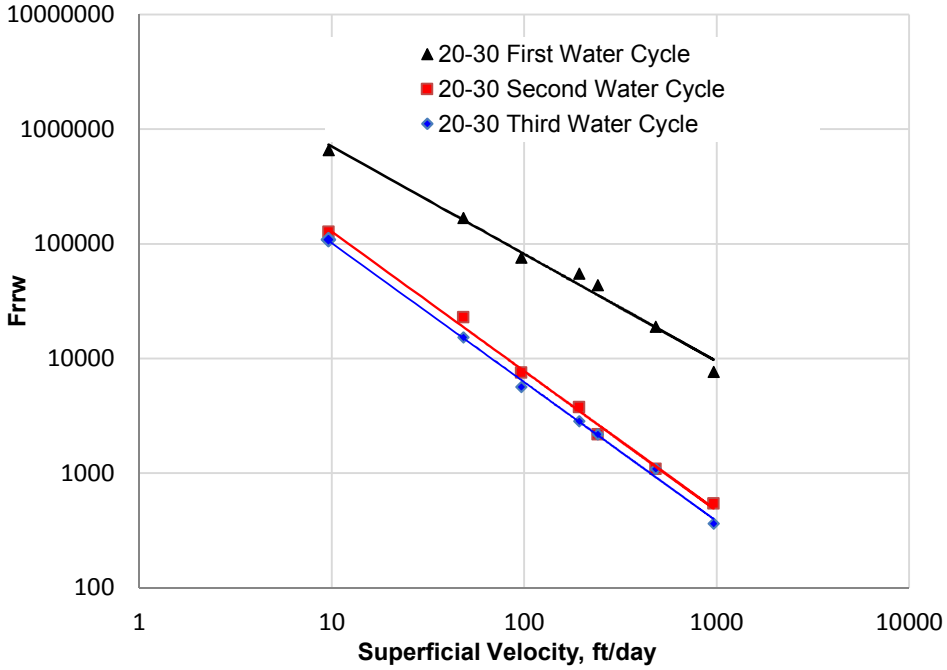

Figure 6.11—*Frrw* determined for the different 1% brine cycles.

6.6.3. Injection Pressure over DPR Processes. The alternative injection pressures for both brine and oil were recorded during their injection through the gel-filled fracture. Figure 6.12 illustrates the injection pressure for cycles of 1% NaCl and 195 cp oil through PPG with a size of 20-30. These injection pressures built up during the flooding cycles. The results also indicate that the injection pressure for water increased as more cycles of water were performed. These injection pressure increases, however, were insignificant at different oil cycles. The injection pressure recorded during the first water cycle peaked at approximately 2227 psi, while after a cumulative volume of 700 ml of oil was injected, the pressure dropped slightly to 2135 psi. Sequential cycles of brine, oil, and brine were injected with almost the same volume into PPG. After injecting 700 ml, the pressure peaked at approximately 2590 psi for the second brine cycle, 2290 psi for the second oil cycle, and 2860 psi for the third water cycle.

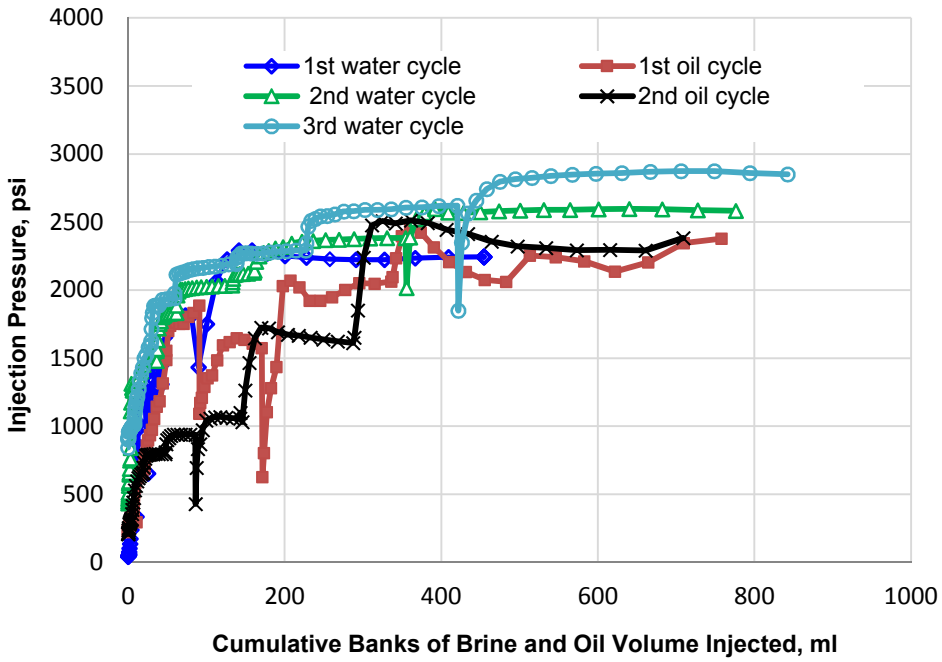

Figure 6.12—Injection pressure over oil and water flood cycle.

6.7. DISCUSSION

The study presented in this paper investigated the behavior of PPG extruded through a fracture during two-phase flow. The DPR mechanisms have been investigated extensively by several researchers. Table 6.3 summarizes the DPR mechanisms, gels, and investigators in the relevant literature. The following is a summary of the mechanisms observed during PPG placement inside a fracture.

Mechanism 1 in Table 6.3 considers gels that swell when they come into contact with brine and shrink when they come into contact with oil. In their visualization studies, Liang et al. (1995) did not observe any volume changes in the gel at atmospheric pressure. They conducted the same experiment at 1500 psi and still found no significant macroscopic changes during alternating exposures of the gels to brine, oil, and

compressed CO2. However, PPG showed a different trend. In visualization studies with PPG at atmospheric pressure, a significant volume changes was observed. In brine, dry gel swelled to many times its original size, which helps to increase the residual resistance factor for water. However, when swollen particle gel was placed in a glass container filled with oil for three weeks, the gel volume decreased dramatically to half of its original PPG volume. This shrinkage of the gel particle size volume allows oil to move easily through gel and causes the residual resistance factor to oil to decrease compared to water.

Many researchers have investigated the effect of capillary forces and gel elasticity (Mechanism 5). Al-Sharji et al. (1999) found that the flow of water and oil through gel was controlled by the elasticity of polymer gels. The results for the flow of oil and water through PPG showed the same trend. The flow of oil through gel had a different elasticity index than the flow of water through gel. The effect of dehydration (Mechanism 8) was observed when the first cycle of oil was injected through PPG (see Figure. 6.8). The pressure began to decrease substantially during the oil injection process. The experimental data suggest that the oil dehydrated the PPG by displacing water from the gel structures and creating new flow channels inside the gel.

Table 6.3—Mechanisms proposed for disproportionate permeability reductions.

No	Mechanism	Gel	Investigators
1	Gel swells in water but shrinks in oil	Cr(III)–acetate-HPAM; Xanthan gum-Cr(III) gels; polyacrylamide polymers; PPG	Liang et al.; Dawe and Zhang; Gales et al.;Sparlin and Hagen; Imqam et al.
2	Wall effects	polyacrylamide polymers; water and oil based gels	Zaitoun et al.; Liang and Seright; Liang et al.
3	Gravity affects gel locations in pores	Glyoxal / cationic polyacrylamide (CPAM)	Liang et al.
4	Gels change rock wettability	Nonionic polyacrylamide (PAM); resorcinol-formaldehyd; Cr^{3+} (chloride)-xanthan; Cr^{3+}(acetate)-polyacrylamide; colloidal silica	Zaitoun et al.; Liang et al
5	Effect of capillary forces and gel elasticity	Cr (III)-acetate-HPAM; bulk polymer gel; PPG	Liang and Seright; Al-Sharji et al.; Imqam et al.
6	Segregated pathway theory	Polymer; water and oil based gels; HPAM & crosslinker	White et al.; Liang and Seright; Nilson et al.
7	Lubrication effect	PAM and polysaccharide polymers; polyacrylamide polymers	Zaitoun and Kohler; Sparlin and Hagen
8	Gel dehydration	PPG; acetate/HPAM	Imqam et al; Dawe and Zhang; Willhite et al
9	During brine injection, polymer leaches from the gel and significantly decreases the brine mobility	Cr (III)-acetate-HPAM	Liang and Seright
10	Pore blocking by gel droplets	water and oil based gels	Liang and Seright

In this study, gel strength was established as an important factor/mechanism for PPG that greatly affects the DPR. Results obtained from rheometer measurements, as shown in Figure 6.13 suggest that gel strength measurements taken after the oil and water flowed through PPG also affected the DPR mechanism. The results indicate that the gel strength for oil was much less than for water; consequently, gel with less strength has a lower residual resistance factor than gel with high strength.

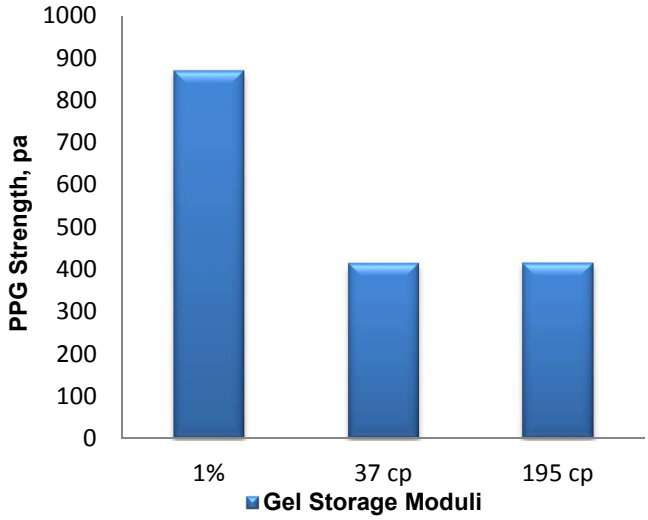

Figure 6.13—Particle gel strength as a function of oil and brine flow.

6.8. CONCLUSION

This work investigated the characterization of disproportionate permeability reduction for PPG placed in closed fractures. The following conclusions were drawn from this investigations:

- The particle gel injection pressure increased as the particle size, gel strength, and flow rate increased but decreased as the fracture width increased.
- Elasticity indices (n) were successfully obtained and fitted as a function with gel strength. The results indicated that as the gel strength increased, the gel elastic value decreased.
- The results also indicated that the greater the gel strength, the more time is needed to achieve a stable pressure for each injection rate. Additionally, wider fractures require less time to reach a stable pressure than do narrower fractures for each injection flow rate.

- The *Frro* was always much less than the *Frrw* during all alternating water and oil floods. The DPR also increased with increases in the oil viscosity, particle size, gel strength, and fracture width.
- The first oil injection (first cycle of oil) can significantly degrade the gel properties. This finding explains why the residual resistance factor *Frrw* obtained from the second brine cycle decreased significantly compared with the *Frrw* obtained from the third brine cycle.
- The injection pressure for different water cycles increased as more water cycles were performed. However, these injection pressure increases were not significant at different oil cycles.
- A different disproportionate permeability reduction mechanism of the particle gel was investigated. The gel strength greatly affected the DPR and is an important parameter that should be considered.

7. MICRON-SIZE PARTICLE GEL PROPAGATION THROUGH SUPER K PERMEABILITY STREAKS

7.1. INTRODUCTION

In the absence of profile modification, injection water transports into high permeability zones bypassing the rich saturated oil in low permeability zones. As a result, a considerable portion of oil remained un-swept, adversely impacting oil recovery. In an attempt to evaluate PPG effectiveness as a diversion materials, systematic intensive experimental studies were performed not only on homogenous sand cores but also on heterogeneity cores including non-cross flow and cross flow heterogeneities sand cores. The results obtained from the study of homogenous super K sand cores are discussed in the following section. Those obtained from the study of heterogeneity are discussed in Sections 8 and 9.

The experiments results and developed correlation models obtained from the study of homogenous super k will aid to select future conformance control candidates and optimize the particle gel treatment design for large scale field projects.

7.2. OBJECTIVES AND TECHNICAL CONTRIBUTIONS

The experiments conducted as part of this study were used to investigate the PPG injection process and the effects of PPG to water and oil permeability. They were also used to evaluate a PPG's ability to improve oil recovery. The objectives of this section were organized in three sub-sections as follows:

7.2.1. Study PPG Injection Process. PPG swollen in different brine concentrations were injected into two ranges of sand permeability to determine the following:

- Examine the effect of unconsolidated sand pack permeability, gel strength, gel size, and gel concentrations on the gel injection pressure.
- Study the effect of injection flow rate on the PPG injection pressure.
- Determine the gel threshold pressure (defined as the minimum pressure required to enable gel to propagate through high permeability streaks).
- Study associated mechanisms with PPG injections (e.g., retention and adsorption).
- Numerous studies have been conducted to evaluate commercial gels transport through super K sand permeability but none of these previous studies investigated either the performance or the mechanism of PPGs transport and placement.

7.2.2. Study Disproportionate Permeability Reduction. Cycles of brine and oil were injected sequentially after PPG injection and placement in sand cores to:

- Determine the effect of unconsolidated sand pack permeability, gel strength, gel size, and gel concentrations on the DPR.
- Examine the effect of sand pack permeability, gel strength, and gel concentrations on the gel blocking behavior.
- Study the mechanisms (e.g., dehydration and washout) associated with water and oil flow through a PPG.

7.2.3. Study PPGs Ability to Improve Oil Recovery. Sand cores were saturated with oil and then flushed with water until they reached residual oil saturations to:

- Explore which factors significantly affect the use of micron-size particle gels to reduce water channeling and enhance oil recovery from super-K sand permeability formations.
- Compare water cut and oil recovery results obtained during water flooding with the results obtained after PPG treatments were introduced.
- Study the effect of unconsolidated sand pack permeability, gel strength, gel size, and gel concentration on the oil recovery improvement.
- Evaluate the decrease in remaining oil saturation during the water flooding cycles and PPG treatments.
- Numerous studies have been conducted to evaluate commercial gels transport through super K sand permeability but this study is the only work investigated the performance and the mechanism of PPGs to increase oil recovery.

7.3. EXPERIMENTAL DESCRIPTION

7.3.1. Preformed Particle Gel. A superabsorbent polymer was used as a PPG to conduct the experiments. Dry particles with mesh sizes of 170-200 and 80-100 were swollen in a 1% NaCl brine concentration. Gel concentrations of 800 and 2000 ppm were used.

7.3.2. Brine Concentration and Oil Viscosity. Both 0.05 and 1 wt% Sodium Chloride (NaCl) were used for brine flooding and to prepare the swollen PPGs. Oil with a viscosity of 37 cp at 70 °F was used to saturate the sand pack model.

7.3.3. Magnetic Stirring Vessel. An accumulator with a1200 ml capacity and a maximum adjusted impeller speed of 1800 r/min (Figure 7.1) was used to inject PPGs into a high permeability sand pack model. The impeller was placed at the bottom of the

accumulator so that the PPGs remained dispersed in brine before they were injected into the model.

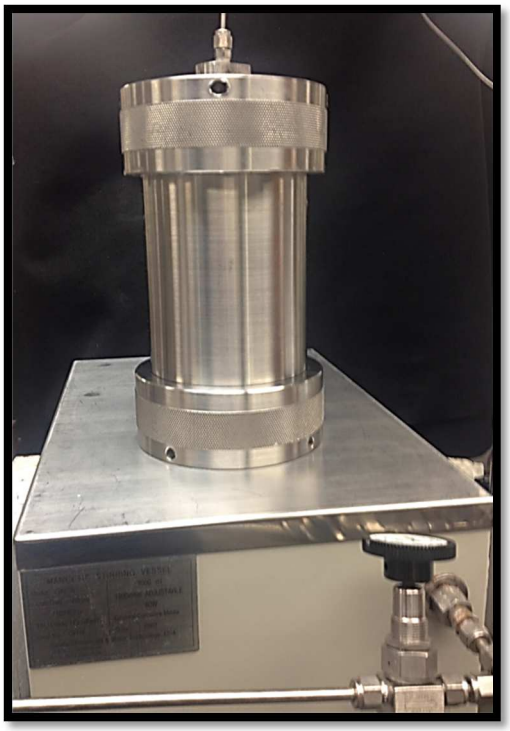

Figure 7.1—Stirring vessel accumulator.

7.3.4. Sand Packs. Silica sand were used to obtain different permeability sand packs. A Vibrator machine (see Figure 7.2) was used to pack the sand carefully to obtain the desired permeability. A mesh size of 10-18 and 20-30 were used to obtain approximately 65.4 and 26.5 Darcy, respectively. The size distribution of the silica sand used in the experiments, as determined in a sieving test are listed in Table 7.1.

Figure 7.2—Vibrator machine.

Table 7.1—Size distribution of silica sand.

Sieves (mesh)	Size (microns)
10-18	1000
20-30	600

7.4. EXPERIMENTAL SETUP

The experimental setup used in this study (see Figure 7.3) constructed from a stainless steel tube 91.4 cm in length and 2.5 cm in diameter. It was packed with different sand grains to test the effect of various Super-K permeabilities on PPG injection process. A syringe pump was used to inject suspension PPG, brine, and oil from an accumulator to the sand pack model. Four pressure transducers were mounted on both the inlet and along sand pack to monitor the pressure behavior during the brine flooding and gel treatment

processes. Test tubes mounted at the model outlet were used to record the PPGs and oil/brine production volumes at effluent.

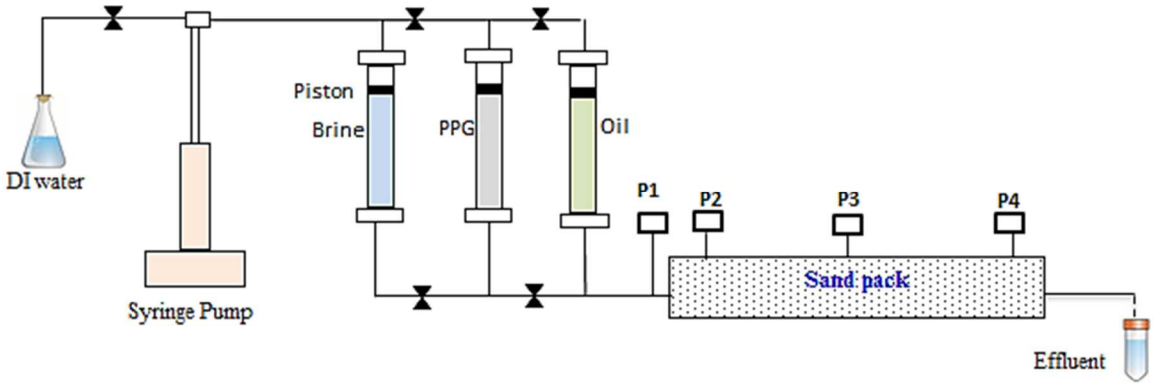

Figure 7.3—A micron size PPG injection apparatus.

7.5. EXPERIMENTAL PROCEDURES

Several procedures were followed when conducting the water flooding and PPG treatment processes. These procedures are described briefly below:

7.5.1. Preparing and Saturating Sand Pack Models. A vibrator machine was used to prepare different sizes of silica sand so that the desired sand pack permeability could be obtained. Sand grains poured inside the tube after fastened the tube's end with a screen filter to prevent migrating sand during the flooding processes. San was poured at a regular rate, then vibration was kept constant until the entire tube was filled with sand. The sand pack models were then vacuumed for at least 1 hr before being fully saturated with 1% NaCl to determine pore volume, porosity, and permeability. The sand pack model was next flushed with brine at different injection flow rates (1, 2, 3, 4, 5, 6, and 7 ml/min) to ensure that the model 100% was saturated with brine.

Oil viscosity with a 37 cp was injected from the accumulator into the sand pack at 2 ml/min to determine both the oil initial in place and the connate water saturation. Oil was injected until no water was produced and the injection pressure became stable. A variety of oil injection flow rates (1, 3, 4, 5, 6, and 7 ml/min) was then injected to determine the effective oil permeability at connate water saturation.

7.5.2. First Water Flooding. Brine was injected into super-K permeability at a rate of 2 ml/min to simulate secondary oil recovery conditions. Oil and water productions at effluent were recorded every 3 ml. The brine was injected into the sand packs until no oil was produced and the brine injection pressure became stable. Both oil recovery and water cut were determined during the first water flooding. Super-K permeability was flushed again with brine at flow rates of 1, 3, 4, 5, 6, and 7 ml/min to determine the effective water permeability at residual oil saturation.

7.5.3. PPG Treatment. Swollen suspended PPGs were injected into sand packs at a rate of 2 ml/min after the first water flooding processes were completed. The PPG was injected until began produced in effluent and the PPG injection pressure became stable in all four pressure sensors. The gel injection pressure, gel threshold pressure, and gel breakthrough pressure were all recorded so that the gel propagation's mechanisms through super-K permeability at different injection conditions could be diagnosed. The PPG injection was then resumed at different flow rates (1, 3, 4, 5, 6, and 7 ml/min) to study the effect of injection flow rates and calculate the gel resistance factor. The volume of oil and water productions at the outlet were collected to determine the oil recovery increase or water cut decrease during gel treatment.

7.5.4. Second Water Flooding. Brine was injected at 2 ml/min after the PPG treatment was complete to test the gel's resistance to water flow. Brine was injected also at different cycles to determine if there was any oil left unproduced after the gel treatment. The injection started from low to high flow rates and the repeated injection cycles were from high to low flow rates. The rational of these brine cycles was to determine the gel strength effect on water flow resistance. A series of brine cycles was run until no discrepancies occurred between the repeated cycles.

7.5.5. Second Oil Injection. Oil was injected again into Super-K permeability at a rate of 2 ml/min to determine how PPG reduced the permeability to water more than oil. Oil was injected into sand packs to ensure that no water was produced and the oil injection pressure remained stable. Both water production and injection pressure were measured during the second oil injection. Super-K sand permeability was flushed again with variety cycles of oil at flow rates of 1, 3, 4, 5, 6, and 7 ml/min to determine the effective oil permeability at residual water saturation.

7.5.6. Final Water Flooding. Brine was injected at the same injection rates (2ml/min) to determine the gel blocking behavior to water after the oil was transported through the PPG. Brine was injected until no oil was produced and the pressure became stable in all of the pressure sensors.

The above procedures were repeated for each experiment. The oil recovery factor, water cut, resistance factor, residual resistance factor to water and oil, and injection pressures were all determined for the Super-K permeability sand pack models.

7.6. RESULTS AND ANALYSIS

This section presents results obtained for the effects of sand pack permeability, gel concentration, brine concentration, and particle size. For each of these effects, the injection pressure, passing measurements, resistance factors, PPG blocking to water flow, oil recovery and water cut measurements, and PPG resistance to water and oil flow were all determined.

7.6.1. PPG Injection Pressure Measurements. The effects of sand pack permeability, gel concentration, brine concentration, and gel size on PPG injection pressure are discussed as follow:

7.6.1.1. Effect of unconsolidated sandstone permeability. Preformed particle gels were injected through the sand pack until they were produced at effluent and the injection pressure became stable. Figures 7.4 and 7.5 show the injection pressure recorded at the different sections of the sand pack for both permeability of 26.5 and 65.4 Darcy. Injection pressure was recorded during PPG injection at injection rate of 2 ml/min. The injection pressure recorded at the first section (P1) indicates the pressure increased gradually and fluctuated during the injection process. More than 15 PV of PPG was injected before injection pressure became stable for both permeabilities. As the PPG began to produce at effluent, the PPG injection continued until the injection pressure became stable at each section.

The PPG injection pressure increased as the sand permeability decreased. The injection pressure became stable at approximately 1600 psi for a permeability of 26.5 Darcy. It decreased significantly to approximately 25 psi for a permeability of 65.4 Darcy. The PPG injection pressure became stable for each section of the sand pack

though it did so with different pressure drops (see Figures 7.4 and 7.5). A significant pressure drop was observed between the measured pressure at P1 and pressures in the remaining sections. The injection pressure drop was not as significant between the last sections as it was in the first section. In a permeability of 26.5 Darcy, the injection pressure recorded at P1 became stable at approximately 1600 psi while at P2, P3, and P4 were 600 psi, 450 and 30 psi, respectively. Similarly, in the permeability of 65.4 Darcy, the injection pressure recorded at P1 got stable at around 25 psi, while at P2, P3, and P4 were 10 psi, 7 psi, and 4 psi respectively. The differences in injection pressure measured at the sand face, P1, and pressure measured in other sections, indicated a significant pressure drop at the sand face compared to the other sections. The pressure drop between sections decreased as PPG deeply transported into sand cores. Additionally, pressure drop measured for the last sand sections pressure change decreased less when the sand permeability increased.

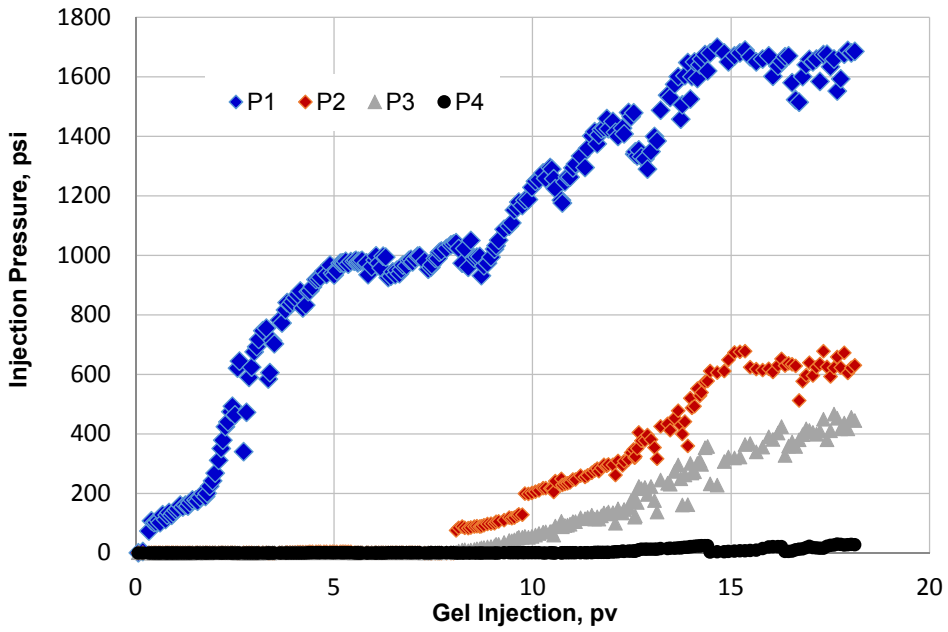

Figure 7.4—Gel injection pressure for k=26.5 Darcy.

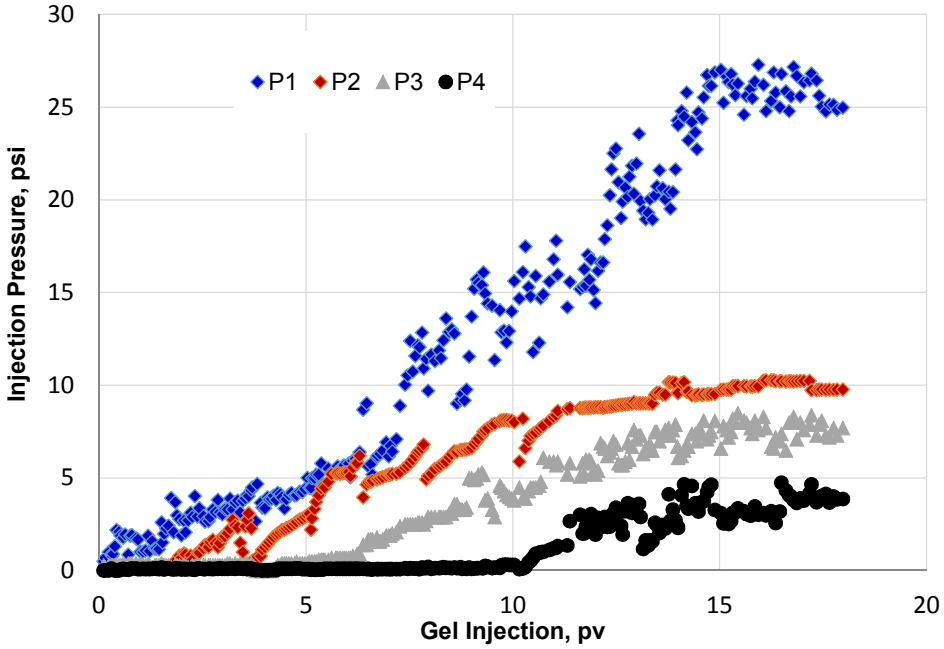

Figure 7.5—Gel injection pressure for k=65.4 Darcy.

7.6.1.1.1. <u>Effect of permeability on injection pressure.</u> The injection pressure recorded at the sand face for both permeabilities were drawn separately in Figure 7.6. The injection pressure was greater at a low permeability than it was at a high sand permeability. Injection pressure might be got stable early during the PPG injection process. This finding, however, neither indicate that the PPG began producing at effluent nor indicated that PPG injection reached the final stable pressure. The pressure became stable at 1000 psi in permeability of 26.5 Darcy, after 5 PV of PPG was injected. The injection pressure increased, however, after PPG injection increased above 5 PV. Thus, the PPG injection pressure should be monitored through all sections to determine when the stable pressure will occur. Either retention or PPG accumulation during the injection process may have a role in this mechanism at this stage.

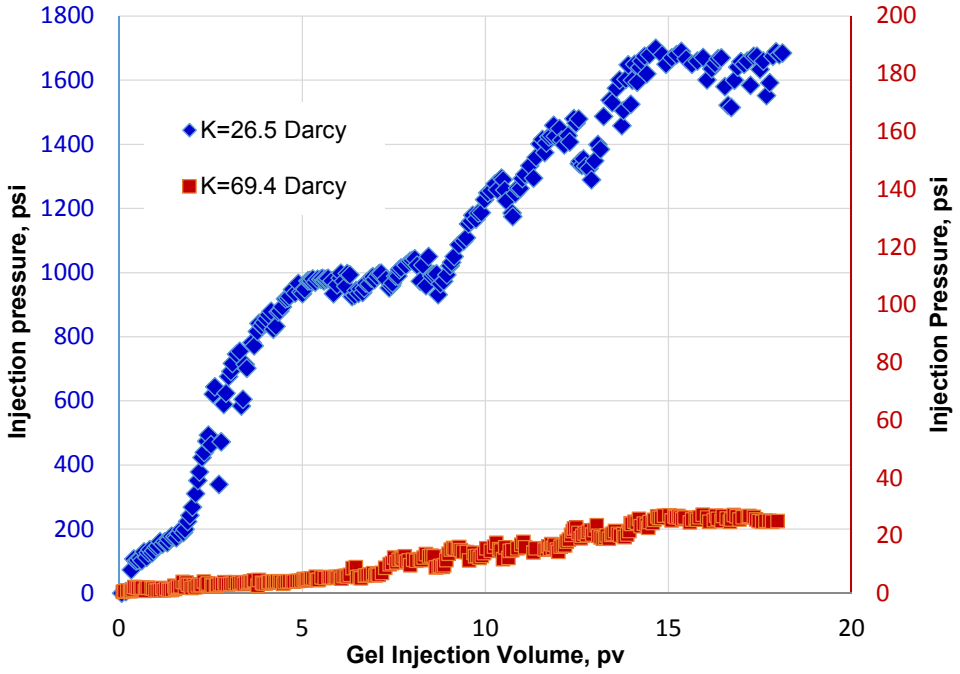

Figure 7.6—Effect of sand permeability on the sand face injection pressure.

7.6.1.1.2. <u>Effect of injection flow rates.</u> As the PPG visibly produced at effluent and pressure got stable at all the different sections, PPG was continued to inject through sand pack but at different injection rates (Figure 7.7). The PPG was injected initially at low flow rate. This rate was increased gradually. A stable pressure occurred at each injection rate. The PPG injection pressure was increased as the injection rate increased. The injection pressure recorded at a low permeability was much greater than that recorded at a high permeability for each flow rate. Seven flow rates were used to inject the PPG through the sand pack. A sharp increase in PPG injection pressure was noticed for permeability of 26.5 Darcy. This sharp increased, allowed only to use four injection flow rates (only flow rates less than 4ml/min). The injection pressure at 4 ml/min

increased significantly and got stable at around 2500 psi. The injection pressure recorded for each permeability fit the power law equations relatively well.

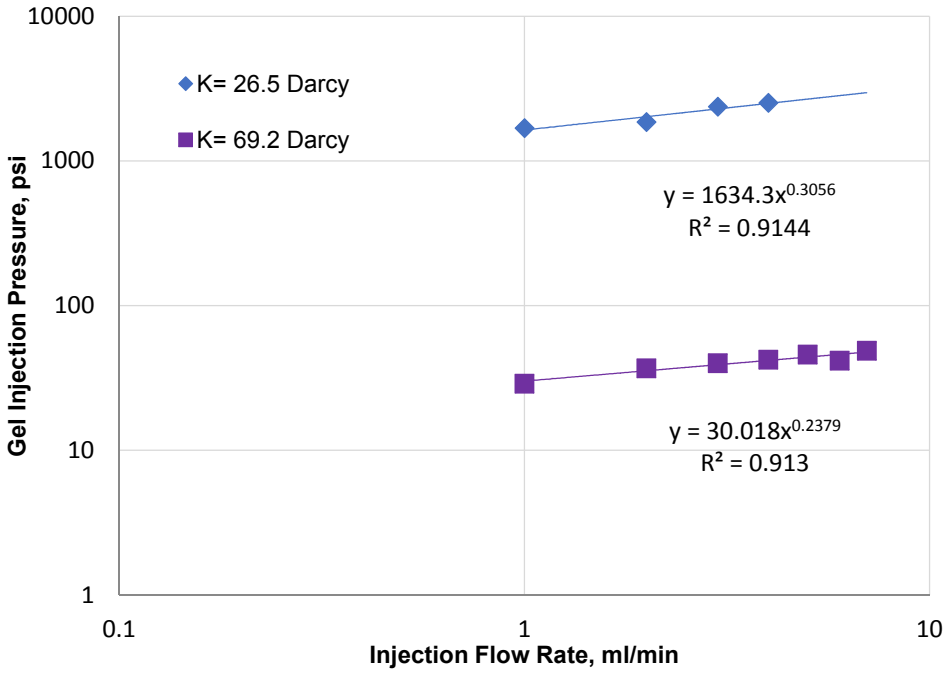

Figure 7.7—The effect of the injection flow rate on the PPG injection pressure.

7.6.1.2. Effect of gel concentrations. PPG at concentrations of 800 and 2000ppm was injected into the sand pack permeability of 26.5 Darcy to examine the effect of PPG concentration on PPG injection. The PPG injection pressure measurements for the two gel concentrations at the same injection rate (2 ml/min) are illustrated in Figures 7.8 and 7.9. PPG injection was continued until it produced at effluent and pressure became stable in each sand pack section. The injection pressure for a PPG concentration of 2000 ppm was much greater than that for a PPG concentration of 800 ppm for all of the sand pack sections. The PPG injection pressure recorded for a concentration of 2000 ppm was

approximately 1600 psi, while the injection pressure recorded for a concentration of 800 ppm was approximately 170 psi. The pressure drop across the sand pack section was nearly similar for both concentrations because the PPG was injected in the same sand permeability nearly. A considerable pressure drop was noticed for both gel concentrations for the pressure recorded in the sand face. A smaller pressure drop between sections was recorded for the last sections. The gel injection pore volume required to produce the gel at effluent and obtain a stable pressure for both gel concentrations was varied according to the PPG concentration. The PPG that was prepared with a low concentration required a significantly larger amount of gel pore volume than did the PPG prepared with a high concentration. The PPG produced at effluent and the pressure got stable after approximately 37 PV of PPG injection for 800 ppm. In contrast, less than 17 PV of PPG injection was required for the PPG prepared with a high concentration.

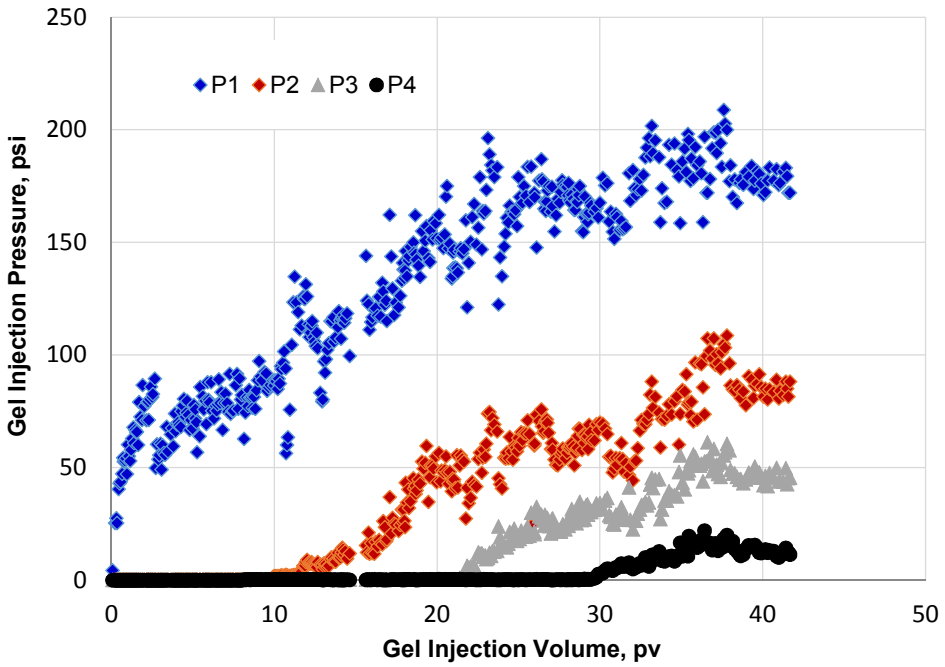

Figure 7.8—The gel injection pressure for a PPG concentration of 800 ppm.

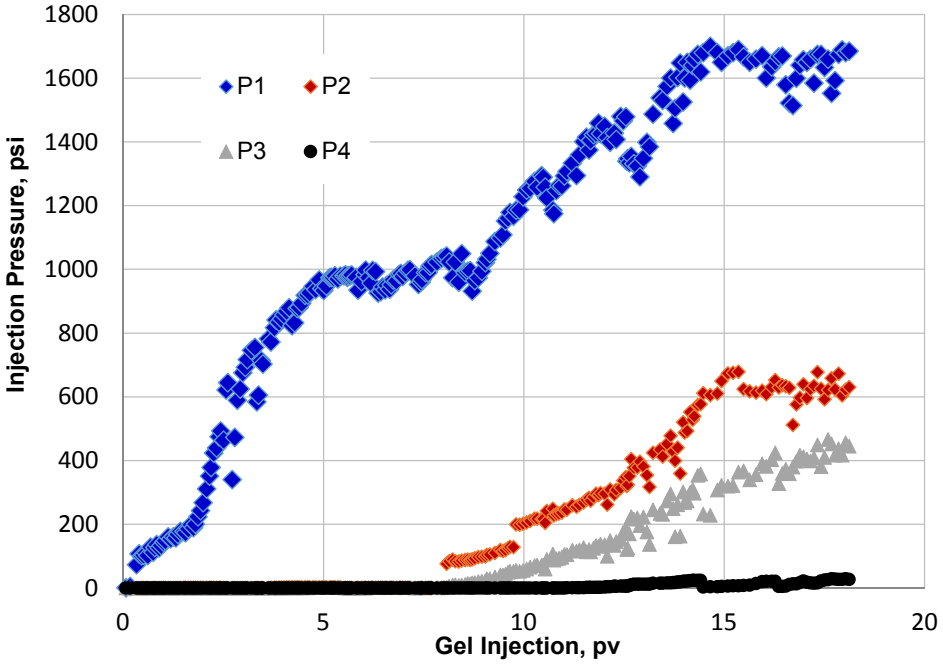

Figure 7.9—The gel injection pressure for a PPG concentration of 2000 ppm.

7.6.1.2.1. <u>Effect of gel concentrations on injection pressure.</u> The injection pressures at the sand face recorded for both gel concentrations (800 and 2000 ppm) is illustrated in the Figure 7.10. A significant difference in the PPG injection pressure and PPG injection volume measurements were noticed for the both gel concentrations. This finding reveled that a smaller gel concentration is more efficient than larger concentration in terms of the PPG injectivity. But smaller PPG concentration required larger PPG volume to propagate deeply. Stable pressure should be monitored carefully, and the injection should not be stopped until the pressure stability is detected in other sensors.

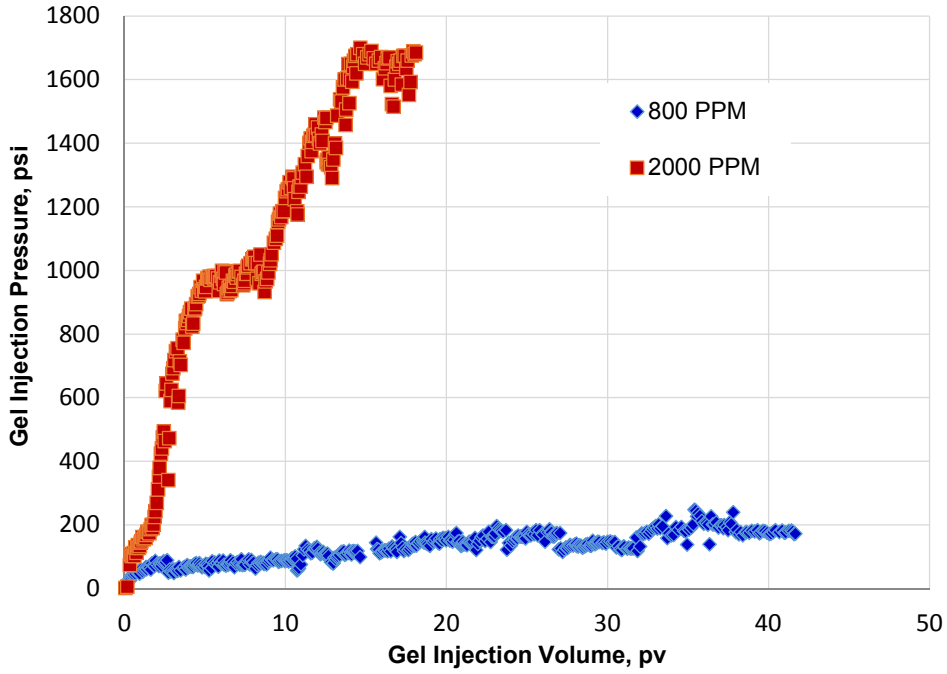

Figure 7.10—The effect of the PPG concentration on the sand face injection pressure.

7.6.1.2.2. <u>Effect of injection flow rates.</u> The PPG continued to inject after the PPG breakthrough at effluent and the pressure became stable in all sections, but at different flow rates (Figure 7.11). PPG was injected at different flow rates to test the effect of the injection rate on the PPG's injectivity. The gel injection pressure for all of the injection flow rates was higher in the large PPG concentrations than in was in the low gel concentrations; the low PPG concentrations were more injectable than large PPG concentrations. The injection pressure was increased linearly in the early injection flow rates. The gel injection pressure increased a great deal during the early flow rates. A smaller increase range occurred at higher flow rates. The gel injection pressure in a gel concentration of 800 ppm, increased approximately1.5 fold (180 psi to 250 psi) when the injection rate increased from 1 to 3 ml/min. However, when the injection rate increased

from 5 to 7 ml/min, injection pressure increased only by 1 fold. The power law equation was successfully used to fit the injection pressure data as a function of the injection flow rates.

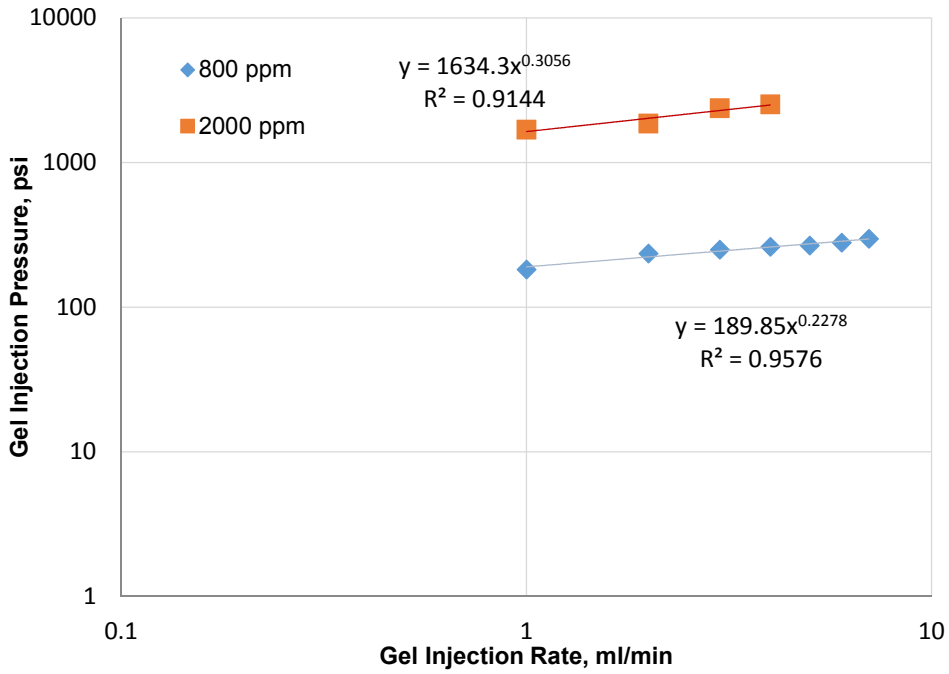

Figure 7.11—The effect of the injection flow rate on the PPG injection pressure.

7.6.1.3. Effect of brine concentration. The brine concentration used in this study was selected carefully according to the swelling ratio and gel strength. The PPGs that swollen in a low brine concentration had a larger swelling ratio and a smaller gel strength than did PPGs swollen in a high brine concentration.

The PPG injection pressure measurements for the gel swollen in 0.05% and 1% are given in Figures 7.12 and 7.13, respectively. The PPG was injected through nearly the same permeability (26.5 Darcy) at an injection rate of 2 ml/min. This injection continued

until discharged at the effluent and pressure became stable in all of the sand pack sections. The gel swollen in 1% NaCl was stronger than gel swollen in 0.05%. Thus, the gel injection pressure in the former was twice that in the latter. The gel injection pressure for the gel swollen in 1% NaCl reached approximately 1600 psi. The gel swollen in 0.05% NaCl reached approximately 800 psi.

A significant drop in injection pressure occurred between the injection pressure measured in the sand face and the other sections. The injection pressure recorded in the last sections for the gel swollen in a 1% NaCl solution was higher and more visible than pressure drops recorded for gel swollen in a 0.05%. A very small pressure change was recorded between the last sections in the 0.05% solution. This small change in pressure could be explained by the gel rheology of gels swollen in different NaCl concentrations. The gel swollen in the 1% solution was stronger than the gel swollen in 0.05%. Thus, the strong PPG needed larger driving forces to push it along the sand packs than the weak gel needed. Also the monitored gel production at effluent showed that gel swollen in 0.05% solution broken into very small tiny pieces less than gel swollen in 1% solution. As a result, small change in pressure during PPG propagated along the sand packs was noticed for gel swollen in lower brine concentration.

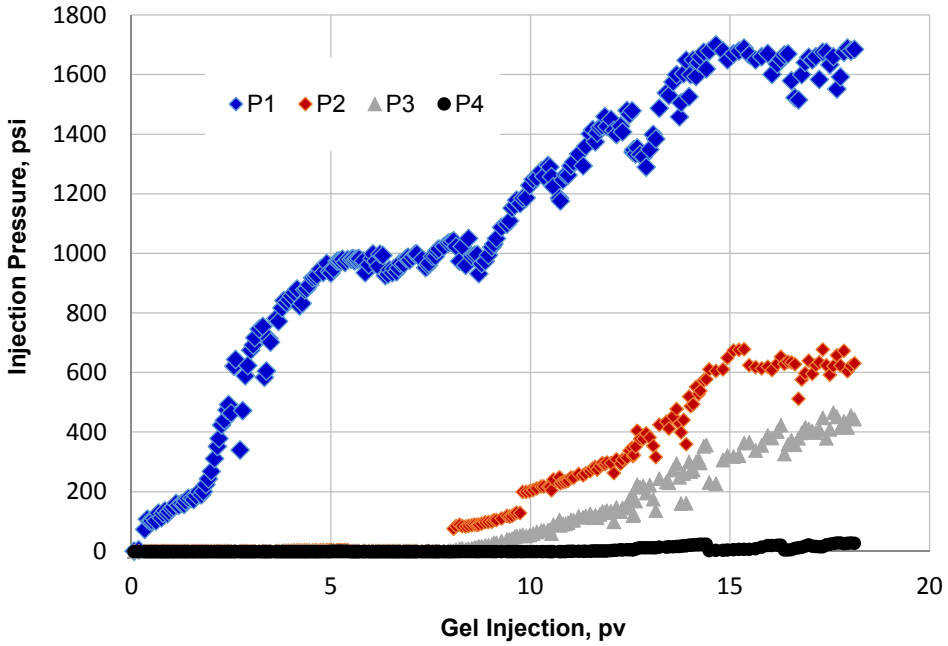

Figure 7.12—The gel injection pressure of the PPG swollen in a 1% NaCl.

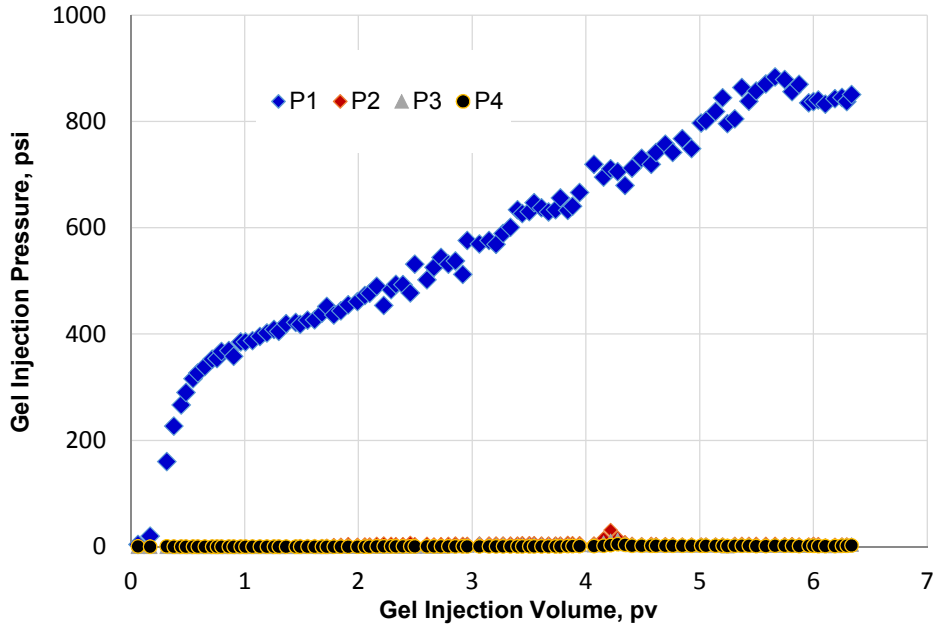

Figure 7.13—The gel injection pressure of the PPG swollen in a 0.05% NaCl.

7.6.1.3.1. <u>Effect of brine concentrations on injection pressure.</u> The injection pressures measured at the sand face for gels swollen in 0.05 and 1% NaCl solutions are plotted in Figure 7.14. The injection pressure measured for the gel swollen in 1% was twice as high as that swollen in 0.05%. This finding indicates that gels swollen in a small NaCl brine concentration have better injectivity than gels swollen in a large brine concentrations. Results also show that less gel pore volume was required to reach injection stable pressure for gel swollen in low brine concentration than gel swollen in high brine concentration. Approximately 5 PV was used for gels swollen in 0.05% while approximately greater than 15 PV was used for gel swollen in 1%.

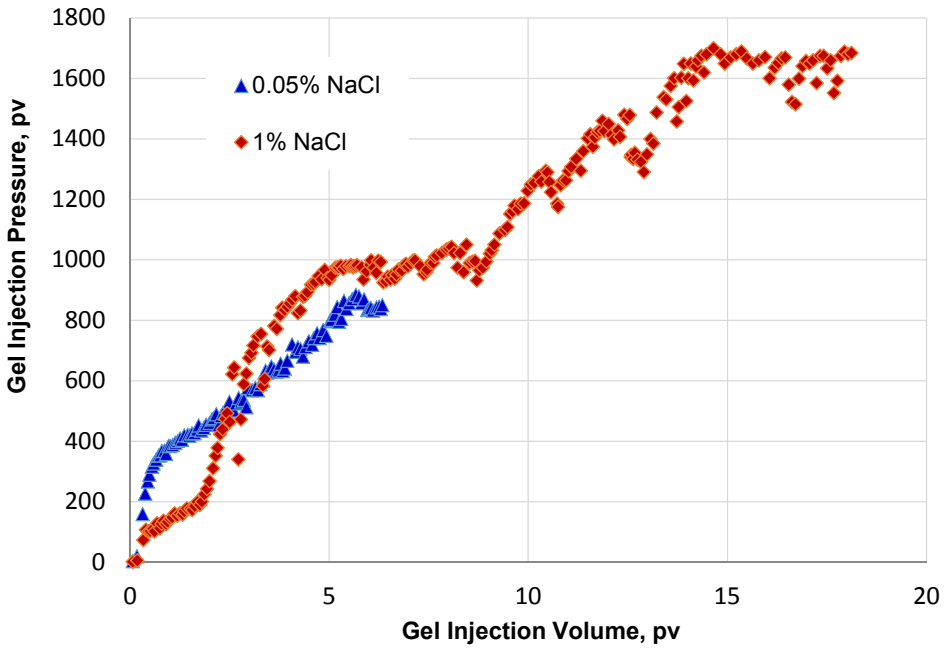

Figure 7.14—Brine concentration effect on sand face injection pressure.

7.6.1.3.2. <u>Effect of injection flow rates.</u> The PPG injection pressure measurements at different flow rates for the two brine concentrations are plotted in the Figure 7.15. Stable pressures were obtained for each injection flow rate. The injection pressure increased as the injection flow rate increased. This increase was significant and obvious at the early injection flow rates. It was less significant when the injection flow rates exceeded 4 ml/min. Injection pressures for gels swollen in high brine concentrations were greater than gels swollen in low brine concentrations for all of the injection flow rates. The power law equation was used to fit the injection pressure measurement as a function of flow rate. A very good fit was obtained for both brine concentrations.

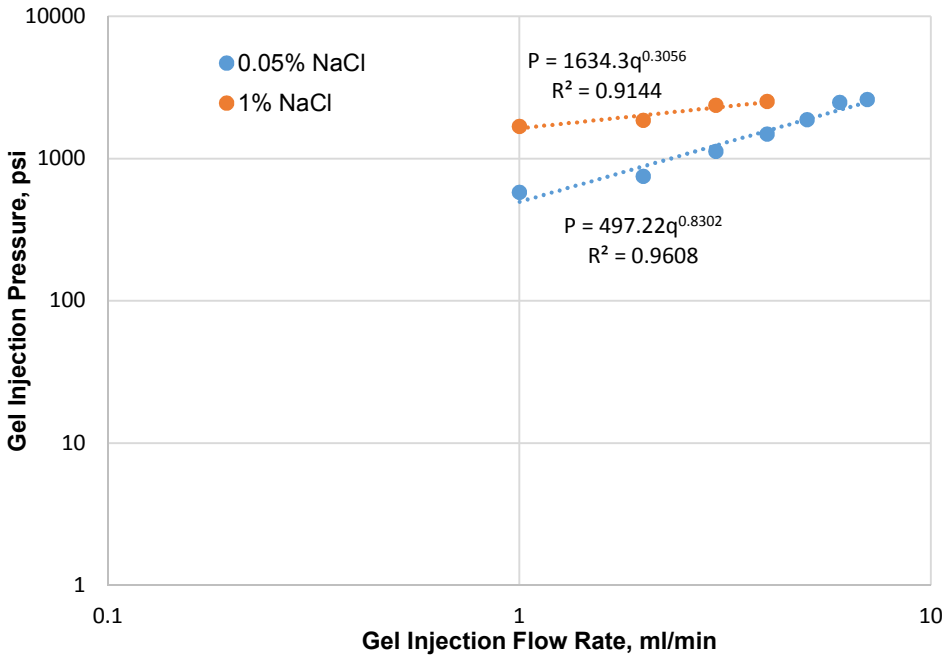

Figure 7.15—The effect of the injection flow rate on the PPG injection pressure.

7.6.1.4. Effect of particle size. Two particle sizes of PPGs were used to investigate the effect of particle size on PPG injection pressure behavior. The first particle size was 75 microns before swollen; the second was 150 microns before swollen. Both gel sizes were swollen in the same NaCl concentration (1%) and injected into the same sand pack permeability (26.5 Darcy). Two gel particle sizes were injected at the same injection flow rate (2 ml/min) as illustrated in Figures 7.16 and 7.17. The PPG was injected until produced at effluent and the pressure became stable at each sand pack section.

The injection pressure rose sharply as the injection pore volume increased. It continued to fluctuate, finally becoming stable after it began to produce effluent. The injection pressures measured at the sand face for 150 micron size was much greater than that for the PPG 75 micron size. The injection pressures became stable at approximately 2500 psi for the former and approximately 1600 psi for the latter. The larger particle size required a larger injection pore volume than did the smaller particle size before it could enter the production side. PPG with larger particle size required approximately twice injection pore volume greater than it required for small particle size. The PPG that was 150 microns used approximately 34 PV of injection volume. The PPG that was 75 microns required a smaller injection pore volume (17 PV). A large injection pressure drop occurred at the sand face for both particle sizes (as compared to the last sections of the sand pack). The pressure drop change along the sand pack when small particle sizes were used was greater than the pressure change along the sand pack when larger particle sizes were used.

The results gathered also indicated that the pressure drop in the last sand pack sections changed little when large particle size were used. This insignificant change in the last sections was attributed to the gel's size. The 150 microns needed a substantial injection pressure at the sand face to enable PPG propagation through the sand pack. This high injection pressure caused PPG to break into small pieces. As result, a small change in pressure drop occurred along the sand pack. Additionally, large entrapment of PPG at the sand face allowed only a small amount of PPGs to be transported through the sand pack.

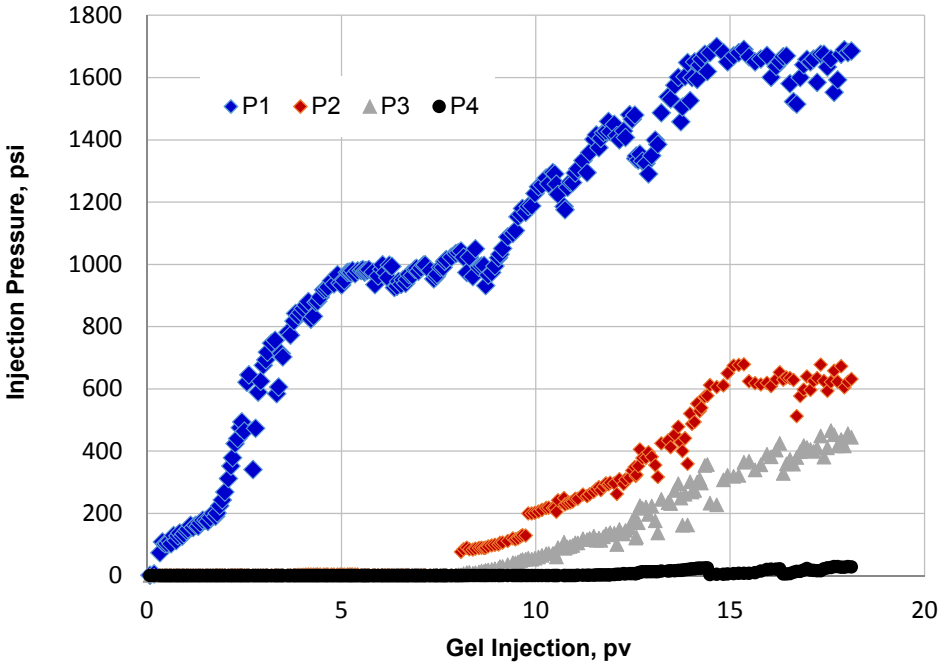

Figure 7.16—The gel injection pressure for a 75 micron PPG.

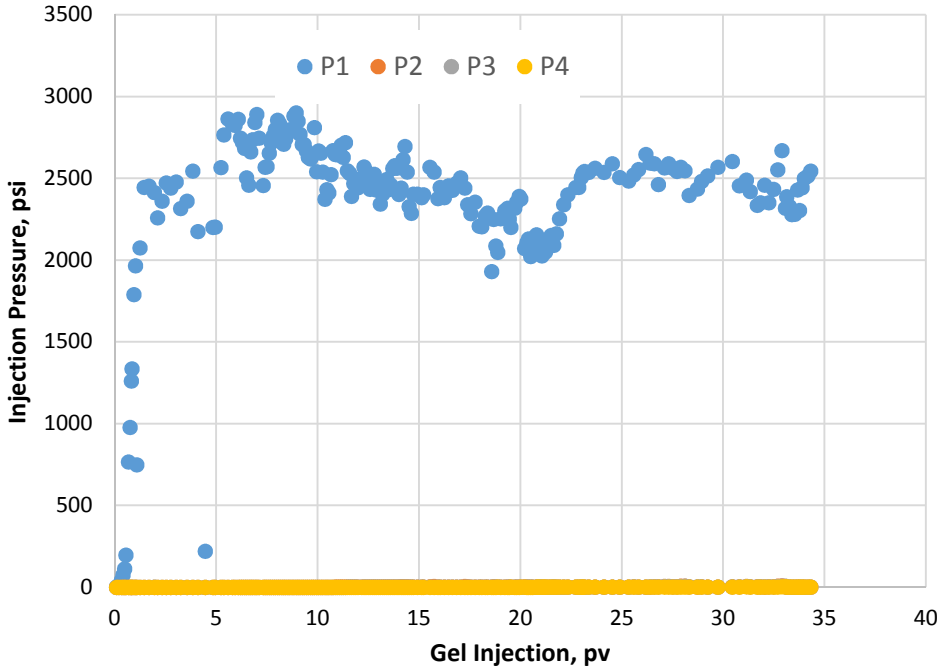

Figure 7.17—The gel injection pressure for a 150 micron PPG.

7.6.1.4.1. <u>Effect of particle size on injection pressure.</u> The injection pressure measured at the sand face was drawn for the two gel particle sizes as a function of the injection pore volume as illustrated in Figure 7.18. These results indicate the effects of gel particle size and gel injection pressure was increased approximately twice when the gel size was doubled to 150 microns.

The injection pressure fluctuated and typically, became stable early. This stable pressure, however, should not be considered the final stability. PPG should be either seen produced at the outlet or injection pressure should be achieved for all sand sections. This results suggests that a reasonable particle size should be selected for the PPG injection to avoid a large injection pressure that could exceed the formation's fracture pressure.

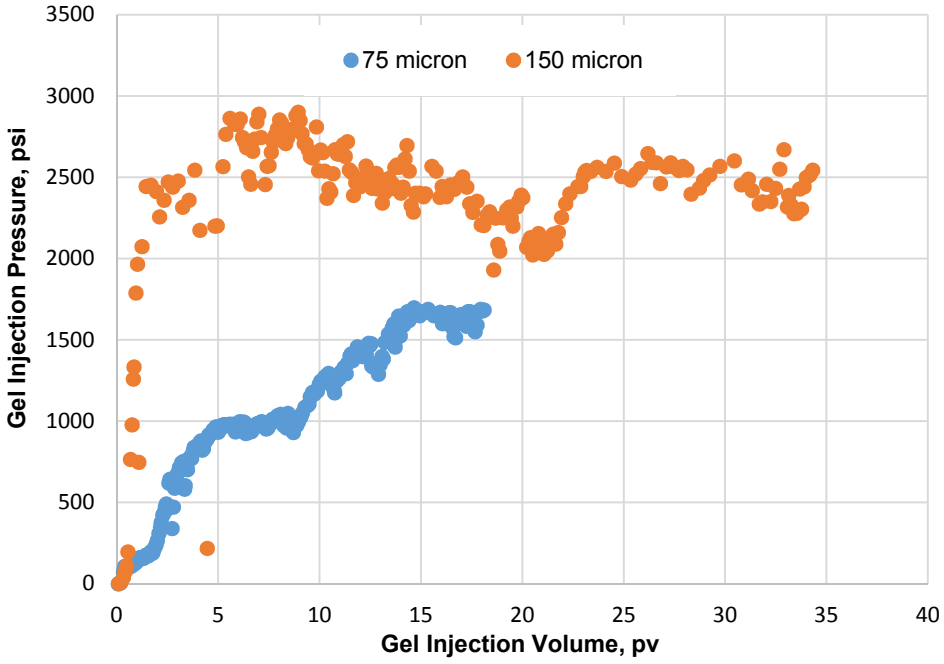

Figure 7.18—The effect of brine concentration on sand face injection pressure.

7.6.1.4.2. <u>Effect of injection flow rates.</u> As the PPG got stable in all the sand pack sections, a variety of PPG injection flow rates were used as illustrated in Figure 7.19. The injection pressure increased sharply as the injection flow rates increased. The injection pressure for 75 micron PPG reached 2375 psi and a 150 micron reached 2829 psi at injection flow rates of 3 ml/min. A large significant increase in injection pressure occurred, approaching the injection pump's upper limit pressure when the injection flow rates exceed 3 ml/min. However, the injection pressure would not change too much with particle sizes if the injection rate increase. If the injection pressure trend was extended the pressure lines may come close to each other. As a result, this trend show insignificant effect of particle size on injection pressure.

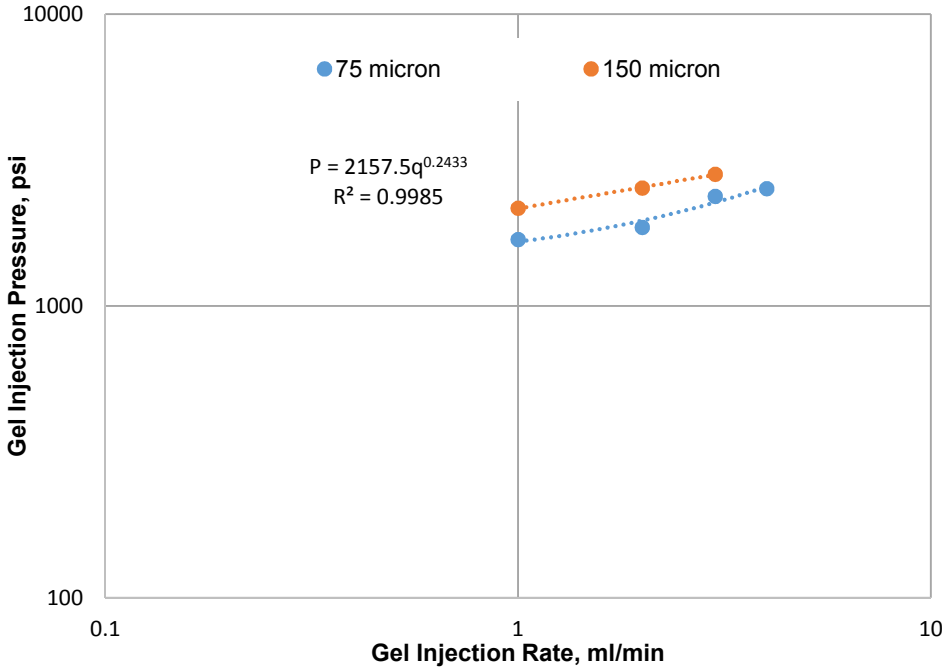

Figure 7.19—The effect of the injection flow rate on the PPG injection pressure.

The fitting equations for the pressure injection measurements obtained from the power law equation are summarized in Table 7.2.

Table 7.2—Fitting equations for injection pressure as a function of injection flow rate.

Effects		Fitting Equation	R^2
Permeability (Darcy)	26.5	$P= 1634.3\ q^{0.3056}$	0.91
	65.4	$P=30.018\ q^{0.2379}$	0.91
PPG Concentration (ppm)	800	$P= 189.85\ q^{0.2278}$	0.95
	2000	$P= 1634.3\ q^{0.3056}$	0.91
NaCl Concentration (%)	0.05	$P= 497.2\ q^{0.8302}$	0.96
	1	$P= 1634.3\ q^{0.3056}$	0.91
PPG Size (micron)	75	$P= 1634.3\ q^{0.3056}$	0.91
	150	$P= 2157.5\ q^{0.2433}$	0.99

7.6.2. PPG Passing Measurement. Both a threshold pressure and a breakthrough pressure were determined for each experiment during the PPG injection process. The threshold pressure is the minimum pressure required to initiate PPG propagation through sand. The breakthrough pressure is the initial pressure at which pressure begins to produce at the outlet. The evaluation of these two pressure is crucial to understanding PPG propagation mechanisms and injection performance through Super- K sand formations. PPG is not like other solid materials due to its elasticity and deformability. The results gathered during this study indicate the PPG injection pressure increased during three periods of injection. The injection pressure phases can be summarized as follow: the threshold pressure phase, the breakthrough pressure phase, and the stable injection pressure phase. These phases are detailed in Table 7.3.

The pore volume associated with these three pressures was also measured. The particle to pore throat ratio (d_{PPG}/d_p) was used to evaluate the passing ratio criteria for the PPG injection processes.

The threshold pressure was significantly affected by the particle pore throat ratio and the gel concentration. The threshold pressure was increased significantly as d_{PPG}/d_p and the PPG concentration increased. Four patterns were observed during the PPG-initiated propagation. These patterns were determined according to the threshold pressure measurement and the pressure drop between the sand face injection pressure and other sections pressure. First pattern, PPG pass pattern and this was observed at low threshold pressure measured for permeability of 65.4 Darcy and low gel concentration of 800 ppm. Second pattern, PPG broke and pass and this was observed for permeability of 26.5 Darcy and brine concentration of 0.05%. Third pattern, PPG broke, entrapment, and pass,

this pattern similar to the second pattern but a larger accumulation of PPG was observed at the sand face before a small portion of PPG transport through sand. PPG broke, entrapment, and pass could be concluded from the results gathered from the test that employed 150 micron PPGs. The last pattern was PPG plug pattern as shown in Figure 7.20 where PPG was not able to propagate through sand. The threshold pressure was approaching the upper limit of injection pump (>=2500 psi). PPG plug pattern is discussed in more details in Section 7.2.6.1.

Table 7.3—A summary of the passing ratio criteria for the PPG injection processes.

Effects	Threshold pressure, psi		Volume at threshold, PV	Breakthrough pressure, psi	Volume at breakthrough, PV	Stable pressure, psi	Volume at stable pressure, PV
Permeability (Darcy)	26.5	817	3.68	983	7.34	1680	14.07
	65.4	6.7	1.83	26.6	15.17	27.18	17.9
PPG Concentration (ppm)	800	88.6	9.91	184.2	38.02	183.5	40.3
	2000	817	3.68	953	7.34	1680	14.07
NaCl Concentration (%)	0.05	421.7	1.47	666.8	3.94	856	5.01
	1	817	3.68	953	7.34	1680	14.07
PPG Size (micron)	75	817	3.68	953	7.34	1680	14.07
	150	2646	10.8	2670.9	32.9	2545.4	34.3

The calculated pore volume indicated a smaller PPG volume was required when the threshold pressure was small. In contrast, larger PPG volume was required for gel concentration effect. The PPG volume injected increased as the PPG concentration

decreased. The variation in PPG injection pore volume was created by the PPG retention level during the injection process.

The PPG injection pressure increased as the PPG propagated deeply into the sand cores, as indicated by the breakthrough pressure measurements. This data also indicates the PPG reached the outlet at a pressure greater than the threshold pressure. The breakthrough pressure increased significantly as both d_{PPG}/d_p and the PPG concentration increased. Most of the results indicate the injection pressure continued increase until it became stable at rate higher that was than the breakthrough pressures.

A similar experiment were used PPG swollen in 1% brine with a concentration of 800 ppm but the sand pack model was not saturated with oil. The purpose was to test the effect of residual oil saturation on the PPG injection process. Sand pack permeability of 27 Darcy was prepared for the experiment. Figure 7.20 shows PPG injection pressure measured at different sand pack sections as a function of PPG injection pore volume. Injection pressure measured at sand face (P1) was increased without any change/response in the other sections. More than 20 PV of PPG was injected and still no response in other segment. The injection process was stopped when injection pressure approach 2500 psi which is upper limit for pump pressure. The sharp linear increased in sand face injection pressure imply that gel particles were not able to transport through sand pack cores. This kind of patterns indicate that PPG was accumulated in the sand face and only plug sand face cores.

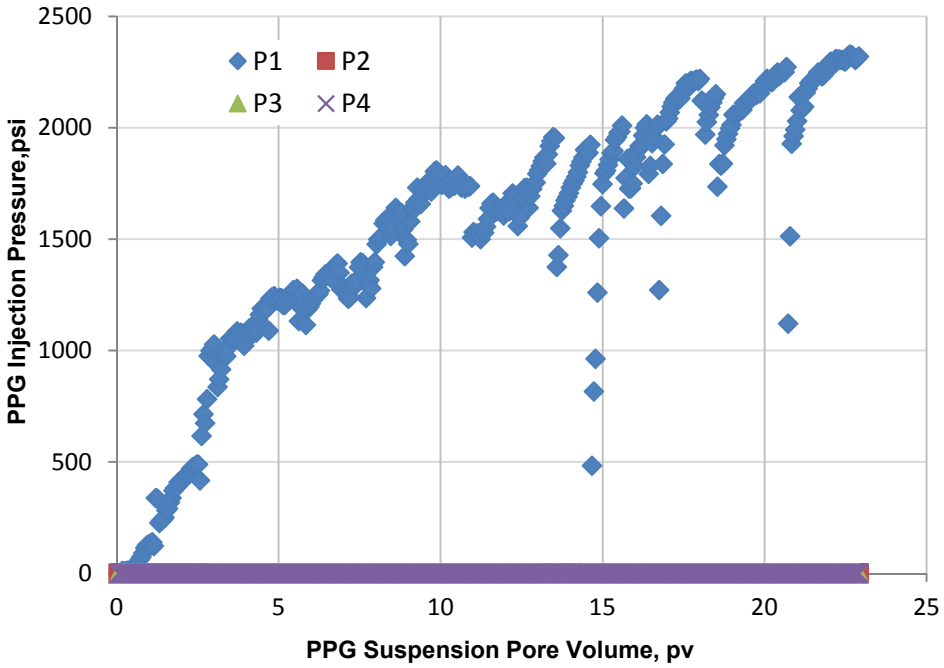

Figure 7.20—The PPG plug pattern.

To have deep understand of the effect of residual oil saturation on PPG injection, a comparison was listed as shown in Table 7.4 between sand pack had residual oil before PPG injection and this case without residual oil saturation. Both sand rocks have same permeability and flushed with same brine concentration. A 75 micron size of PPG with concentration of 800 ppm was injected for both sand at injection flow rate of 2 ml/min.

When PPG was injected into sand was previously flushed with oil, PPG was started to transport deep into sand at pressure of 90 psi after injected 10 PV of PPG. However, injection pressure was reached approximately 2400 psi and 22 PV was injected but no pressure change was noticed for sand pack without residual oil saturation.

Despite the clear effect of residual oil saturation on PPG injection for these two experiments but more experiments are needed to test other factors and verify the current conclusion.

Table 7.4—Sand permeability 27 Darcy with and without residual oil saturation.

Sand rock	Pattern	Threshold pressure, psi	Volume injected at threshold pressure, PV
With Sor	Pass	90	10
With no Sor	Plug	—	—

7.6.3. Resistance Factor Calculations. Sand permeability, PPG concentration, brine concentration, and gel size effects on resistance factors are discussed in the following sub sections.

7.6.3.1. Effect of unconsolidated sandstone permeability. The resistance factor (Fr) was determined for permeabilities of 26.5 and 65.4 Darcy; it is plotted in Figure 7.21 as a function of the injection flow rate. These results indicate that the resistance factor decreased as the injection flow rates increased. The decrease in Fr was significant at the early injection flow rates. The level of reduction became insignificant, however, when the injection flow rates exceeded 4 ml/min. In the permeability of 65.4 Darcy, Fr significantly decreased from 361 to 245 when the injection flow rate increased from 1 to 2 ml/min. It decreased insignificantly from 134 to 113 when the injection flow rates increased from 5 to 6 ml/min. These results also indicate the Fr increased as the sand permeability decreased. Fr determined for a 26.5 Darcy was substantially greater than the Fr determined for a 65.4 Darcy for all of the injection rates. Fr determined for a permeability of 26.5 Darcy was 3380 at the same injection rate of 1 ml/min; it was 361

for a permeability of 65.4 Darcy. The power law equation as a function of the injection flow rates was used to fit the Fr results for both permeabilities.

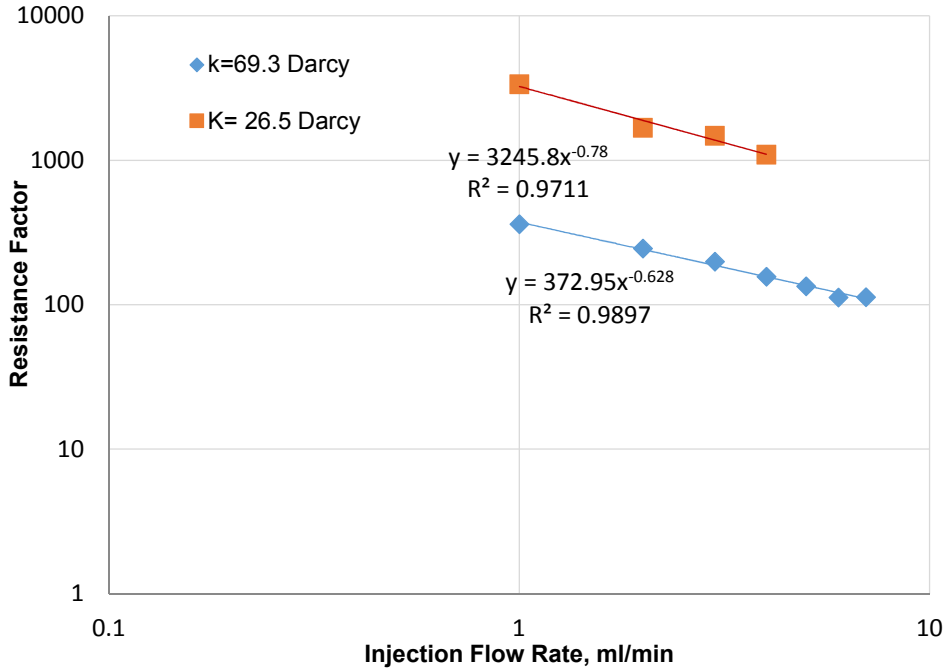

Figure 7.21—Resistance factors for the permeability affect.

7.6.3.2. Effect of PPG concentrations. The resistance factor determined for gel concentrations of 800 and 2000 ppm were plotted against the injection flow rate as illustrated in Figure 7.22. This resistance factor decreased significantly at the early injection flow rates. It became less dependent on the injection flow rates when injection rates increased above 4 ml/min. The Fr increased as the PPG concentration increased. The Fr determined for a PPG concentration of 2000 ppm was larger than the Fr calculated for a PPG concentration of 800 ppm. The Fr determined for 2000 ppm was 3380 at the injection rate of 1 ml/min; it was 1215for 800 ppm.

The power law equation was used to fit the Fr results for both PPG concentrations. These results were fairly fitted as functions of flow rates with a highly accuracy (R^2).

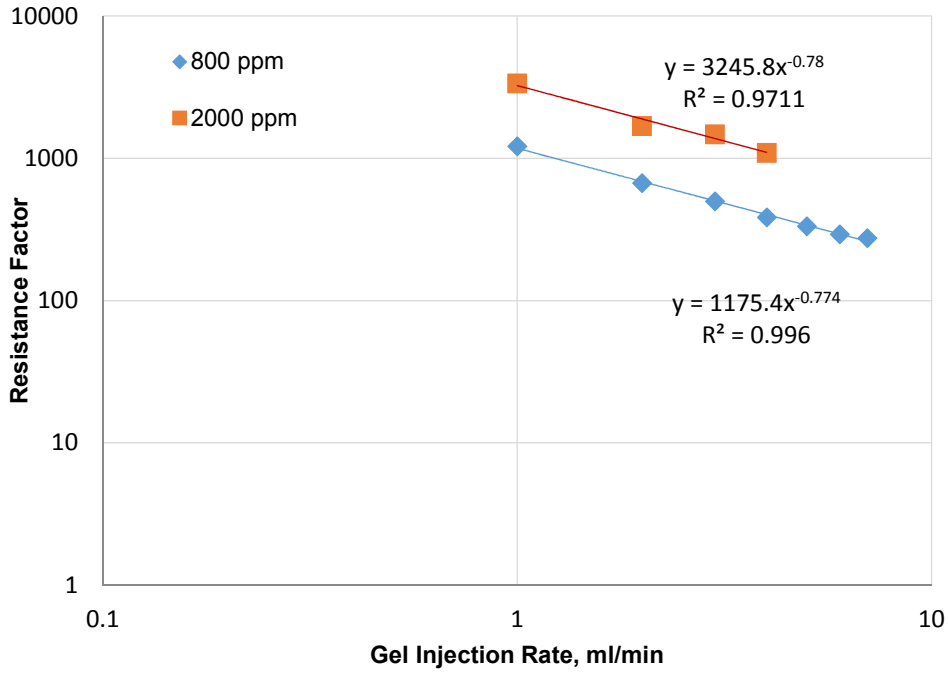

Figure 7.22—The resistance factors for the PPG concentration affect.

7.6.3.3. Effect of brine concentration. The resistance factor was determined for a PPG swollen in both 0.05 and 1% NaCl solutions; it was plotted as a function of the injection flow rate as illustrated in Figure 7.23. The Fr decreased sharply during the injection's early stages. It became less sensitive to injection flow rates as those rates increased. The Fr increased as the brine solution's concentration increased. The Fr determined for all of the injection flow rates for a 1% NaCl solution was larger than the Fr determined for a 0.05% NaCl solution. This increase in Fr occurred because the gels swollen in a high brine concentration had a low swelling ratio and large gel strength.

Thus, gels swollen in a low brine concentration are much weaker and more deformable than gels swollen in a high brine concentration. The power law equation as a function of the injection flow rates was used to fit the Fr data.

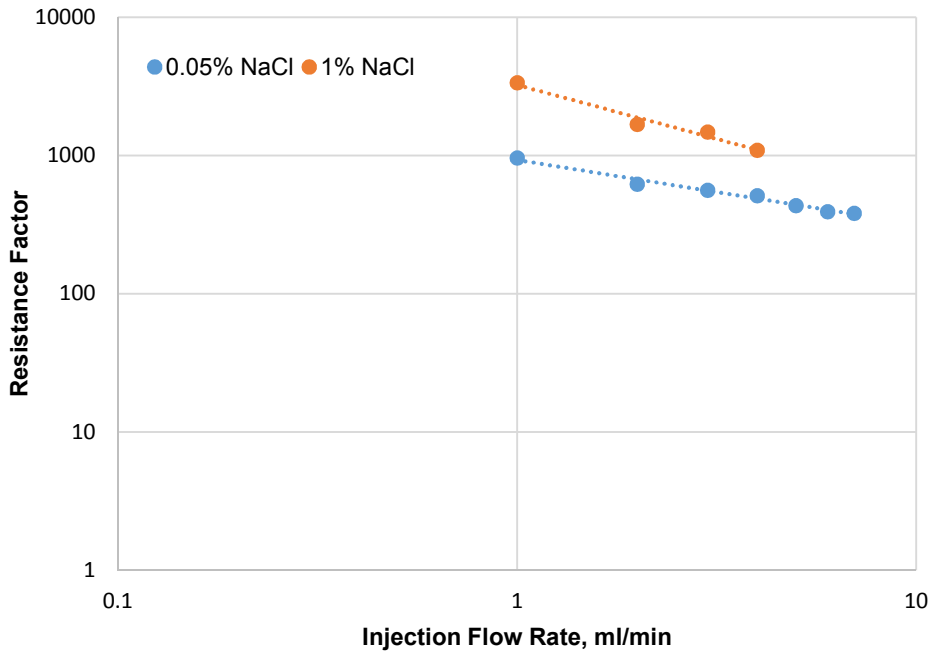

Figure 7.23—The resistance factors for the brine concentration affect.

7.6.3.4. Effect of gel particle size. Two dry particle sizes were used to determine how changes in gel particle's size impact resistance factor measurements. Both 75 and 150 PPGs were dispersed and swollen in the same brine concentration (1% NaCl). The resistance factor determined for the particle sizes changed little, despite the particle's tremendous difference in size. (Figure 7.24). The Fr determined for a 150 micron was slightly larger than the Fr determined for a 75 micron. The Fr determined for a 75 micron was 3379 at the injection flow rate of 1 ml/min; it was 4324 for a 150 micron.

The power law equation as a function of flow rates was used to successfully fir the Fr results. These equations revel the Fr for both brine concentrations decreased when the injection flow rates increased.

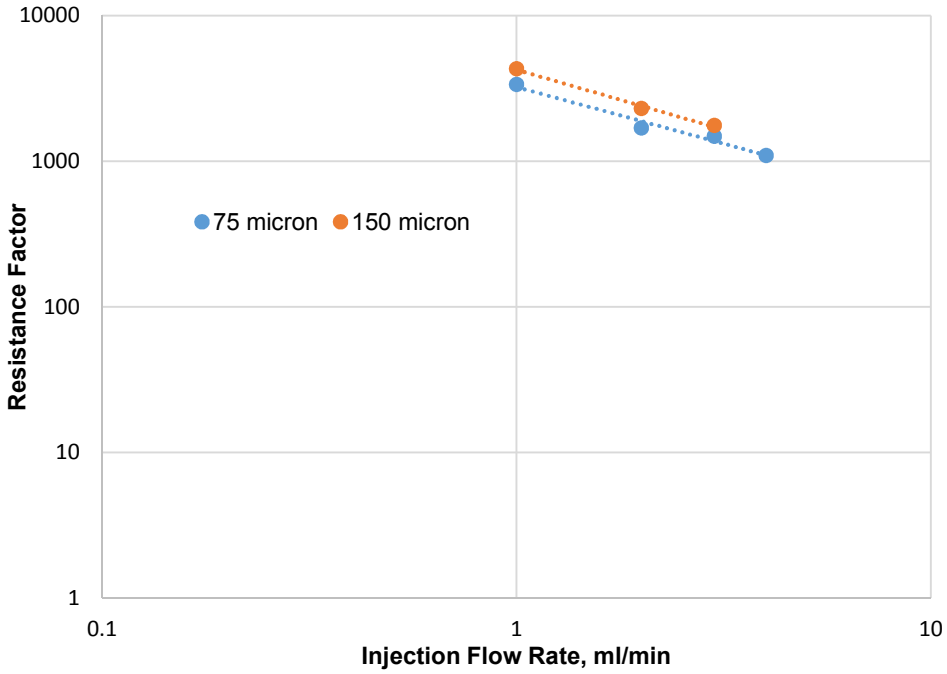

Figure 7.24—The resistance factors for the gel size affect.

Particle size had a slightly effect on Fr results than effects of permeability, PPG concentration, and brine concentration. Fr results indicate that brine concentration is more dominate factor than dry particle size. Therefore, fully swollen PPG has more injectivity than a partially swollen PPG, regardless of the original dry size.

7.6.3.5. Empirical correlation for resistance factor. The resistance factors shown in Figures 7-21, 7-22, 7-23, and 7-24 have a very good relationship with injection flow rates when they were plotted on log-log plots. This relationship was expressed using the power law equation and listed in the Table 7.5.

Table 7.5—Empirical correlation for resistance factor.

Effect	Value	Fitting Equations	R^2
Effect of K	K=26.5 Darcy	$Fr= 3245.8\ q^{-0.78}$	0.97
	K=65.4 Darcy	$Fr= 372.95\ q^{-0.628}$	0.99
Gel Concentration	800 ppm	$Fr= 1175.4\ q^{-0.774}$	0.99
	2000 ppm	$Fr= 3245.8\ q^{-0.78}$	0.97
Brine Concentrations	0.05% NaCl	$Fr= 932.45\ q^{-0.466}$	0.98
	1%NaCl	$Fr= 3245.8\ q^{-0.78}$	0.97
Effect of Particle Size	150 micron	$Fr= 4258.6\ q^{-0.824}$	0.99
	75 micron	$Fr= 3245.8\ q^{-0.78}$	0.97

7.6.4. Preformed Particle Gel Resistance to Water Flow. Cycles of NaCl concentrations were injected into the sand packs not only to test the PPG's resistance to water flow but also evaluate the pore throats blocking efficiency. A low-to-high injection rate procedure was used to inject the water through the sand pack. A stable pressure was required for each flow rate. Water was next injected into the sand packs at high-to-low injection rate to determine whether or not the gel was washed out of the pore throat as result of the increased injection rate. If the injection pressure measured from the repeated injection rate process overlapped the previous injection pressure results from the previous

injection rates, the gel did not move from the pore throat. The injection cycles stopped when the injection pressure did not change with repeated injections cycles. The final residual resistance factor (Frrw) to water was calculated at this stage, and the blocking degree of PPG to water was determined.

7.6.4.1. Effect of unconsolidated sandstone permeability. Brine concentration with a 1% NaCl was injected at different injection rate to test PPG resistance to water flow. Water was injected at seven different flow rates. These injections were made from low-to- high (see Figures 7.25 and 7.26) and again from high-to-low. The repeated injection rates began at the previous end injection rates and continued until no change in injection pressure occurred between repeated cycles.

In the permeability of 26.5 Darcy (Figure 7.25), water injection processes started at flow rate of 1 ml/min. A sharp increase in injection pressure was noticed before it declined and fluctuated when injection rate increased. The stable pressure continued to fluctuate until an injection rate of 7 ml/min was reached. The injection pressure then dropped suddenly. Water injection cycle began again from 7 ml/min. The injection rate decreased gradually and the injection's stable pressure was measured for each flow rate. Repeated results revealed a large discrepancy between the first and second injection flow rates. The water injection was continued until the fourth water cycle. At this cycle, the injection pressure measured at each flow rates matched the injection pressure measured at previous water injection. The injection pressure at the forth cycle increased as the injection flow rate increased. This increased intend to be less affected by increasing injection rate when injection rate exceeded 4 ml/min.

The injection pressure continued to increase with the injection flow rate in a permeability of 65.4 Darcy (see Figure 7.26). A large difference occurred between the injection pressure at the repeated injection flow rate and the injection pressure results taken from the first water flooding. A matched pressure reading occurred during the fourth water cycle. The injection pressure increased with the injection flow rates at this final water flooding stage.

The water injection pressure for the low permeability (26.5 Darcy) remained higher than the injection pressure for high permeability (65.4 Darcy). The pressure reduction percentage for both permeabilities due to water injection, however, seemed similar to each other. The pressure declined with approximately 80% less than PPG injection pressure.

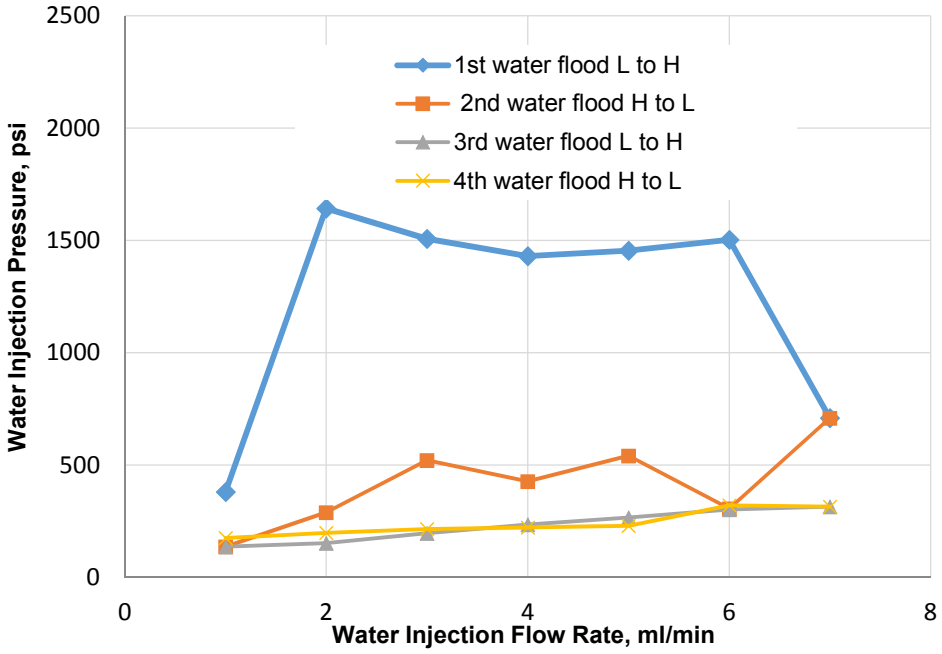

Figure 7.25—Water injection pressure for a permeability of 26.5 Darcy.

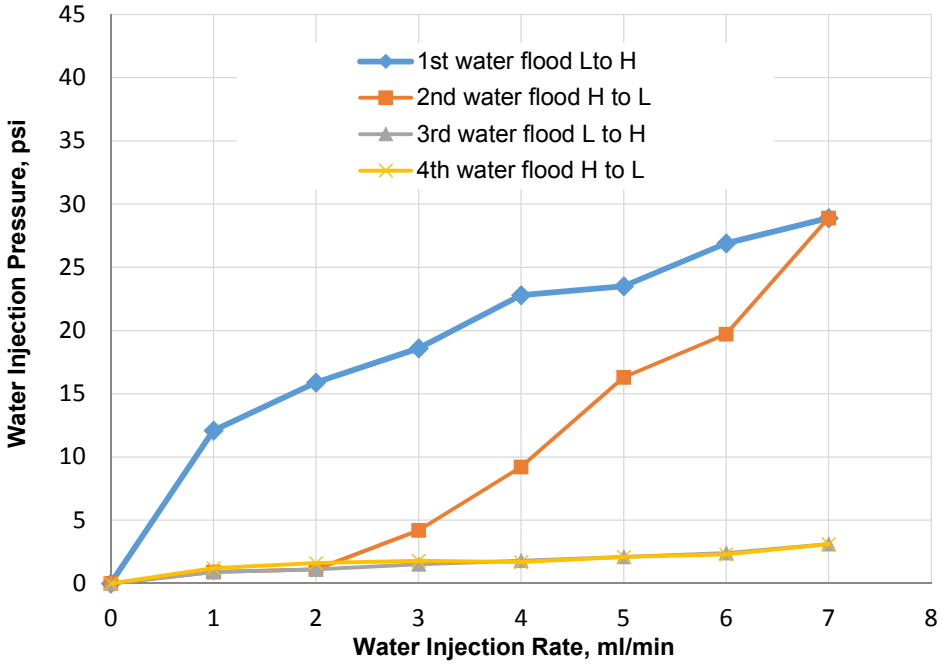

Figure 7.26—Water injection pressure for a permeability of 65.4 Darcy.

Residual resistance factors determined for the permeability of 26.5 and 65.4 Darcy were plotted as shown in Figures 7.27 and 7.28. The Frrw results did not decrease systematically with the injection flow rates as a result of the gel washout/diversion's path effects. The Frrw at the forth cycles decreased significantly at the early injection rate. After the injection flow rate exceed 4 mm/min, however, the Frrw intend to be independent to the increased injection flow rates. Therefore, the Frrw did not change too much with flow rates. The Frrw decreased from 351 to 179 when the injection rate increased from 1 to 2 ml/min in a permeability of 26.5 Darcy. It only decreased from 89 to 75 when the injection rate increased from 6 to 7 ml/min. The Frrw determined for a permeability of 26.5 Darcy was much greater than that for permeability of 65.4 Darcy during all of the water injection rates. The power law equation was used fairly to fit the FFRW as a function of the injection flow rates.

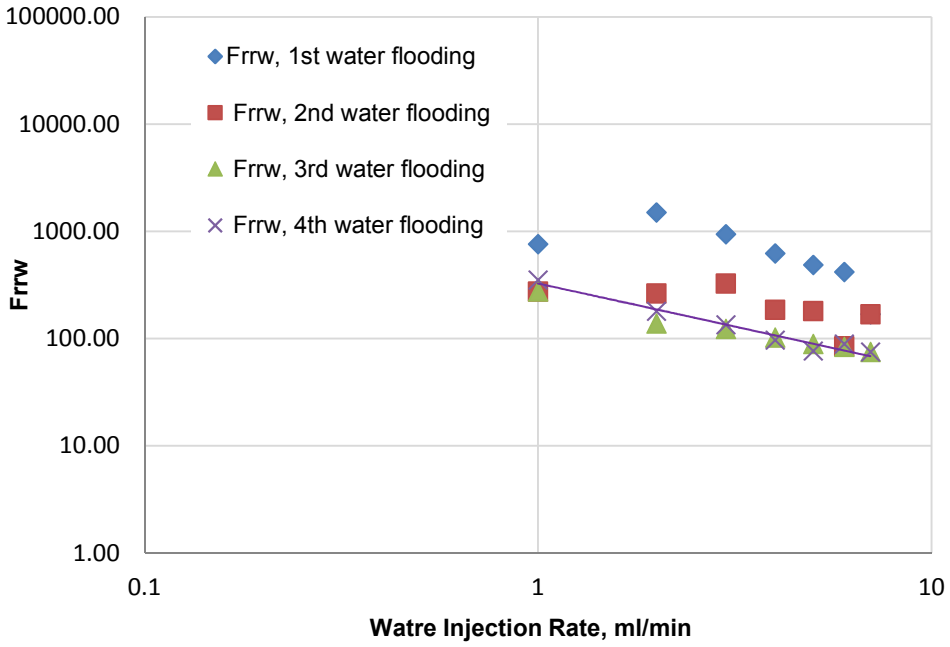

Figure 7.27—The residual resistance factor for a permeability of 26.5 Darcy.

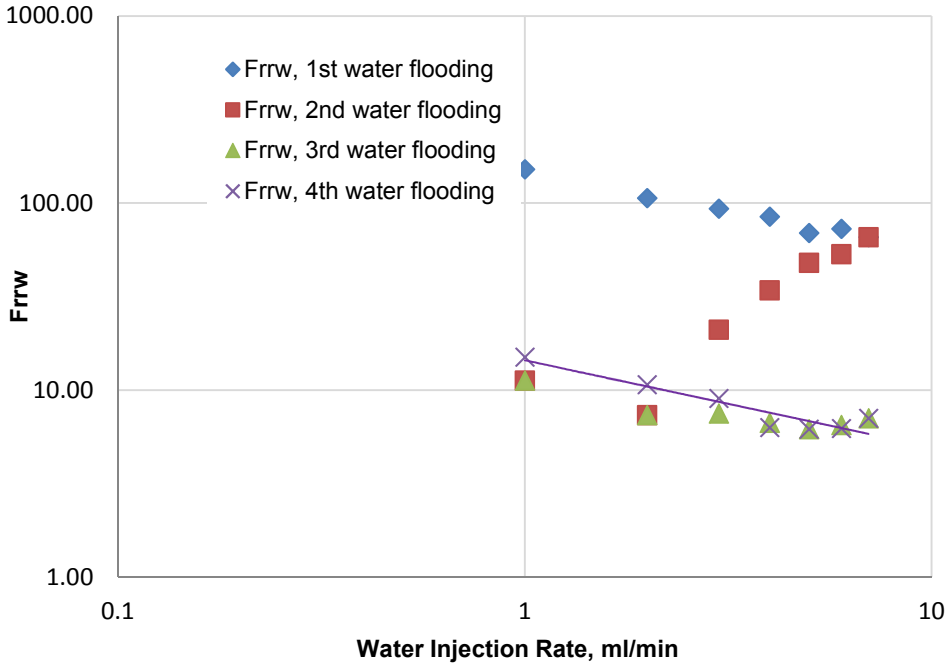

Figure 7.28—The residual resistance factor for a permeability of 65.4 Darcy.

7.6.4.2. Effect of gel concentrations. Water was injected into the sand pack after the PPG injection process was complete to determine the effect of gel concentration on PPG's resistance to water flow. Water injection flow rate again increased from low-to-high and then from high-to-low as it had for the study of permeability effect. The water injection stable pressures at the 7 injection flow rates determined for PPG concentrations of 800 and 2000 ppm are illustrated in Figures 7.29 and 7.30, respectively.

A seven cycles of a1% NaCl were injected into a sand pack model in an 800 ppm concentration until the injection and repeated measured pressures matched each other. The injection pressure increased during the first water cycles, fluctuating at times. The injection pressure continued to increase until it reached an injection flow rate of 4 ml/min, where it declined and then increased again. The second water cycle was performed and the injection rate decreased gradually until reaching 1 ml/min. The injection pressure measured from a second water injection revealed a considerable discrepancies with previously measured pressure. These discrepancies continued to occur during the water cycles. They decreased and becoming negligible as additional water injection cycle were run. A similar trend was observed for the PPG concentration of 2000 ppm. The injection pressures measured from different water cycles did not approach to each other until the fourth water cycle was performed.

The injection pressure measured for PPGs of 2000 ppm was maintained higher than the injection pressure measured for PPGs of 800 ppm after the water injection cycles ended. The injection pressure for PPGs of 2000 ppm was 314 psi at the same injection rate (7 ml/min); the injection pressure for PPGs of 800 ppm was 44 psi.

Fewer injection water cycles were performed, however, to reach final pressures for PPGs of 2000 ppm than it were performed for PPGs of 800 ppm. Four injection water cycles were injected for the former and seven for the latter.

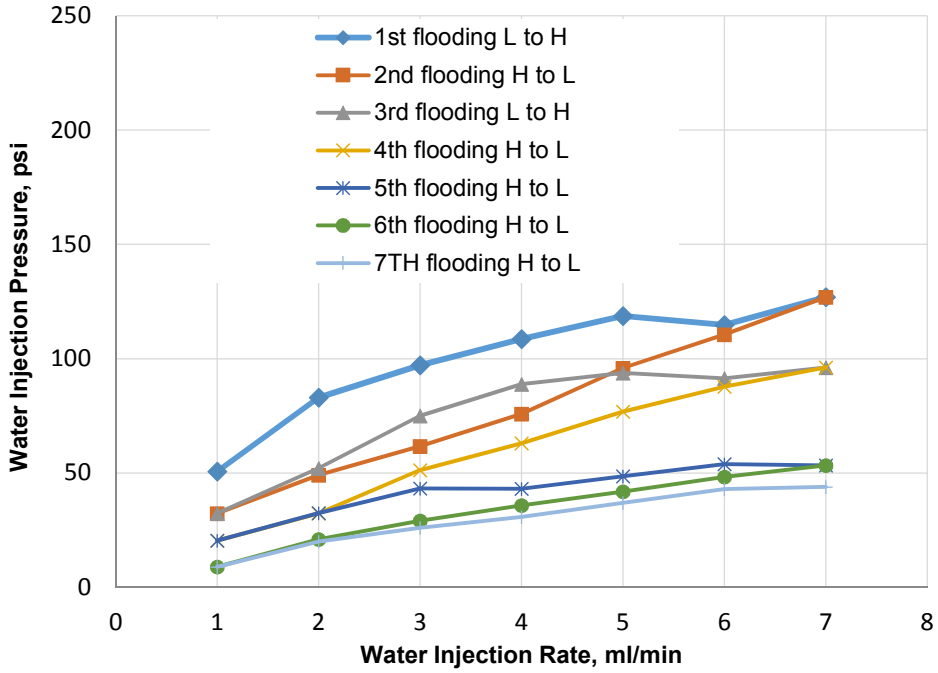

Figure 7.29—The water injection pressure for a PPG concentration of 800 ppm.

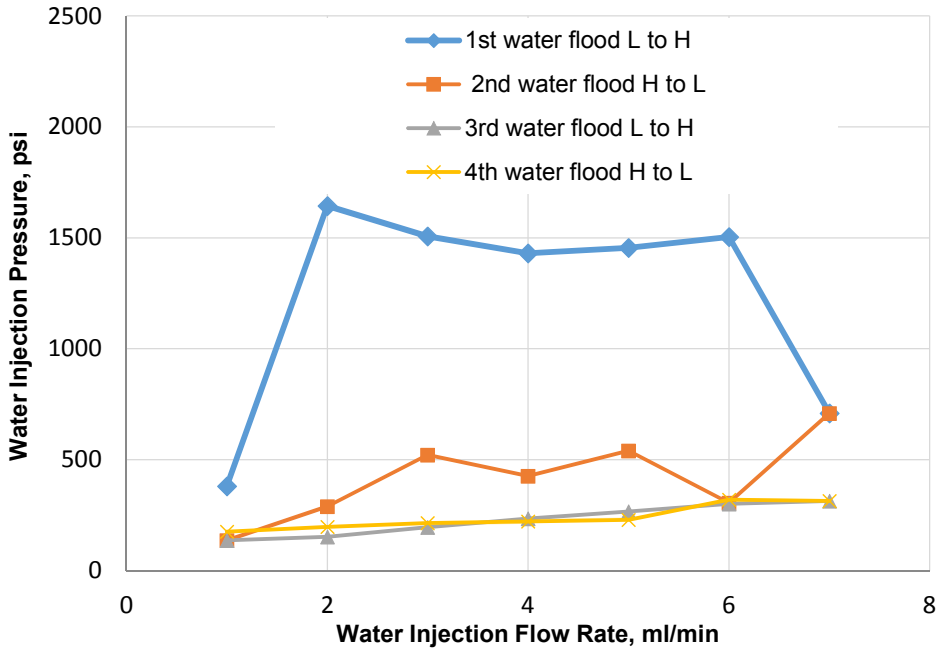

Figure 7.30—The water injection pressure for a PPG concentration of 2000 ppm.

The residual resistance factor as a function of the water injection flow rate was determined for PPG concentrations of 800 and 2000 ppm (see Figures 7.31 and 7.32, respectively). Different cycles of water were injected into sand packs at different flow rates. The Frrw did not decrease uniformly with the increasing injection flow rates during the first water cycles. The power law equation was used to fit the Frrw when the discrepancies between the Frrw results obtained from the repeated cycles became negligible. The Frrw decreased substantially at the early injection flow rates. It became less affected by the increasing injection rate when the injection rate exceeded 4 ml/min. The Frrw determined for PPG concentration of 2000 ppm was much greater than the Frrw determined for a PPG concentration of 800 ppm during all of the water injection rates.

The Frrw determined for a PPG concentration of 2000 ppm was 75 at the injection flow of 7 ml/min; it was 40 for 800 ppm.

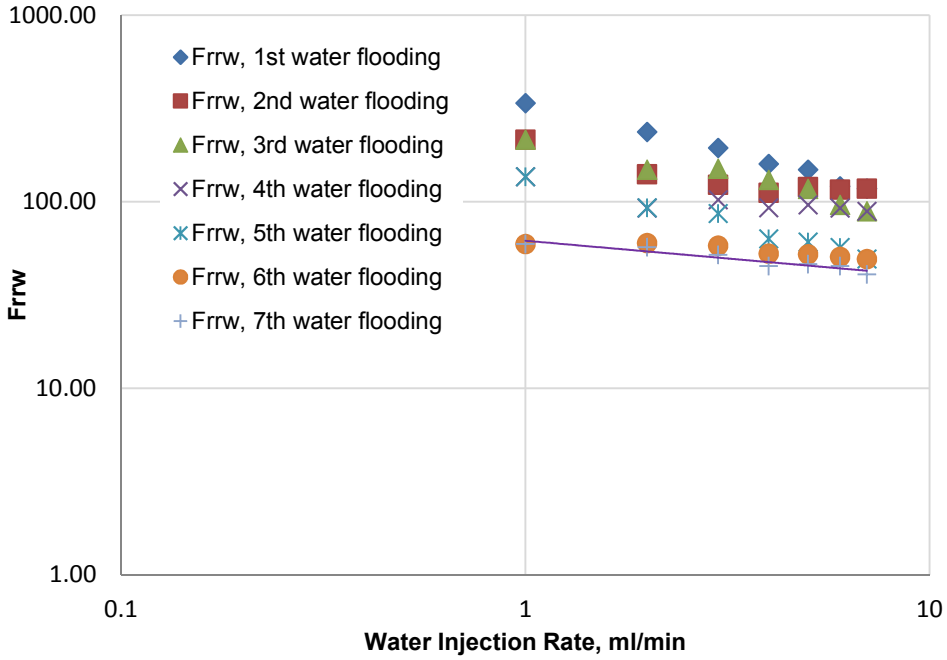

Figure 7.31—The residual resistance factor for a PPG concentration of 800 ppm.

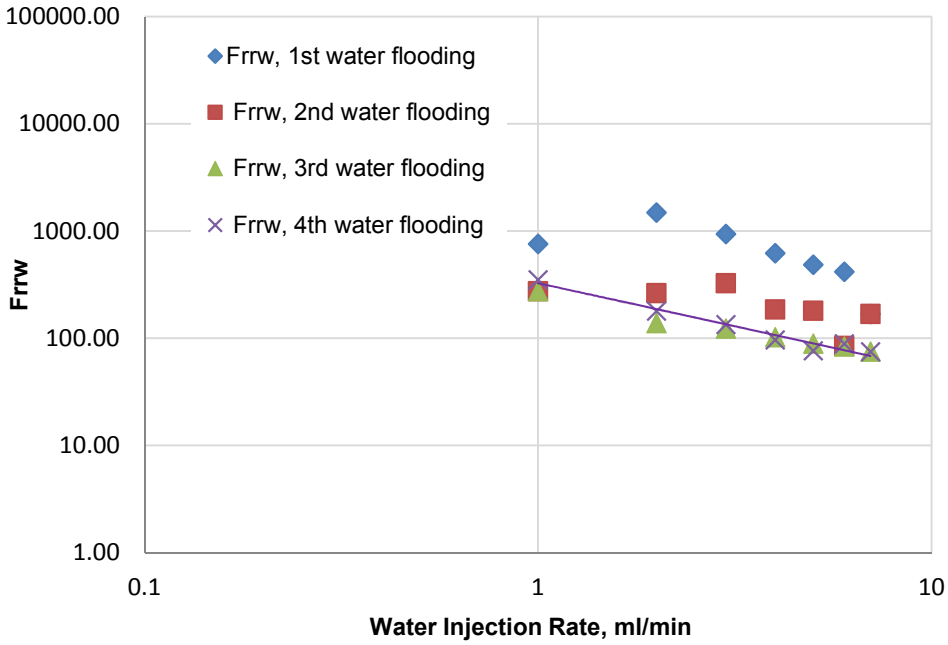

Figure 7.32—The residual resistance factor for a PPG concentration of 2000 ppm.

7.6.4.3. Effect of brine concentrations. Brine with concentrations of 0.05% and 1% NaCl were injected into the same PPG composition of brine to test the gel's resistance to different water salinities (see Figure 7.33 and 7.34, respectively). Injection flow rates from low-to-high and high-to-low were used to inject brine into sand. These repeated injection rates were run to investigate the effect of brine concentration on gel washout mechanisms. Six brine cycles with 0.05% NaCl were injected into the sand pack. The first few injection pressures began to increase, fluctuating with the increased injection rates. The water continued to inject until the fifth and sixth flooding were performed. At those flooding, injection pressure did not change too much with repeated water cycle.

Equivalently, injection pressure measured for 1% NaCl was increased, fluctuated, and finally overlapped with previous injection pressures after additional water cycles were injected.

The injection pressures measured for a brine concentration of 1% NaCl were greater than the injection pressures measured for brine a concentration of 0.05% NaCl at all of the injection flow rates. The injection pressure recorded for a 0.05% NaCl was 167 psi at the injection rate of 7 ml/min; it was 315 for 1% NaCl.

In contrast, larger injection water cycles were required to achieve stability for a 0.05% NaCl than were required for a 1% NaCl. Six water cycles of 0.05% NaCl were injected into sand pack model while only four cycles of 1% NaCl were injected.

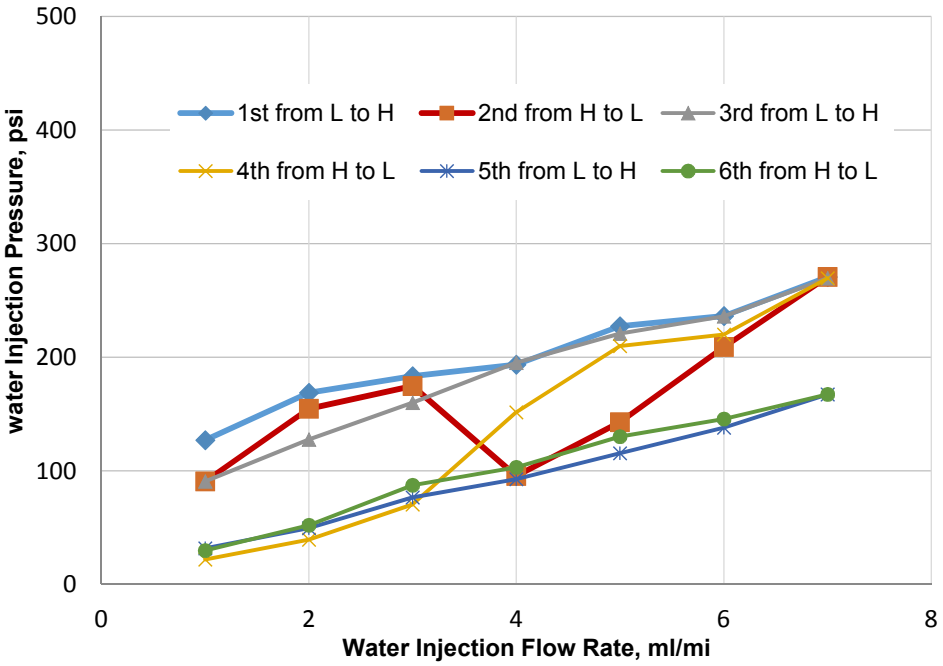

Figure 7.33—The water injection pressure for a brine concentration of 0.05%.

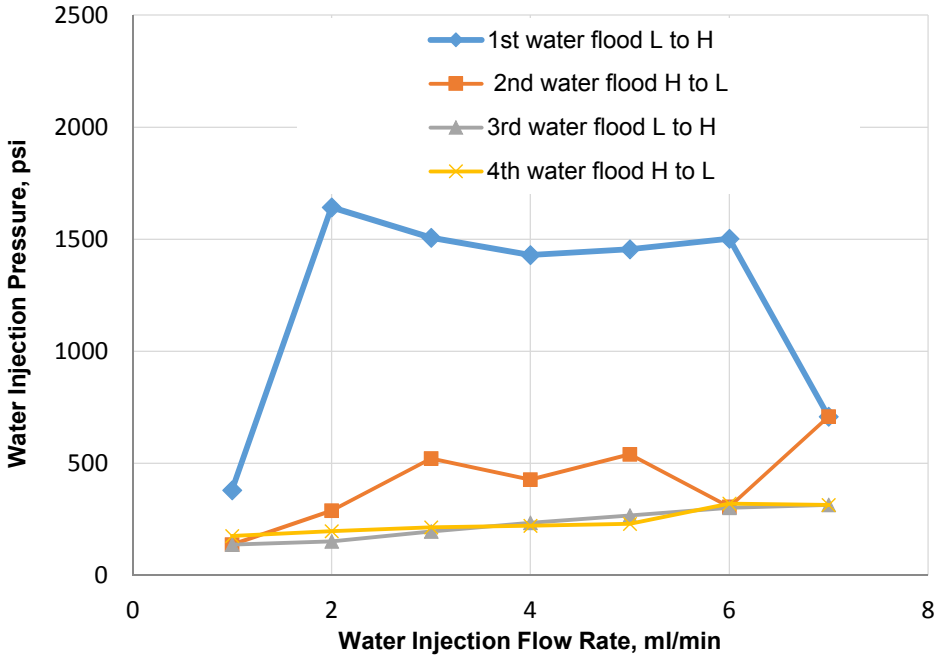

Figure 7.34—The water injection pressure for a brine concentration of 1%.

The residual resistance factors for two brine concentrations (0.05% and 1% NaCl) were calculated and plotted in Figures 7.35 and 7.36 respectively. The different cycles that run were based on the brine concentrations. Six cycles were run with the 0.05% and four cycles were run with the 1%. When 0.05% NaCl was injected, the first three cycles show a normal trend for Frrw trend behavior. The Frrw decreased with increased injection flow rates. But when the sand pack flushed with forth water the trend change. The Frrw increased with injection flow rates during the last three cycles. The Frrw determined for a brine concentration of 0.05% NaCl was less than the Frrw determined for a brine concentration of 1% NaCl at all of the injection flow rates. The Frrw determined for a 0.05% NaCl was 28 in a flow rate of 7 ml/min. The Frrw determined for 1% NaCl at this flow rate was 75. The power law equation was used to fit the Frrw determined at the last water cycle.

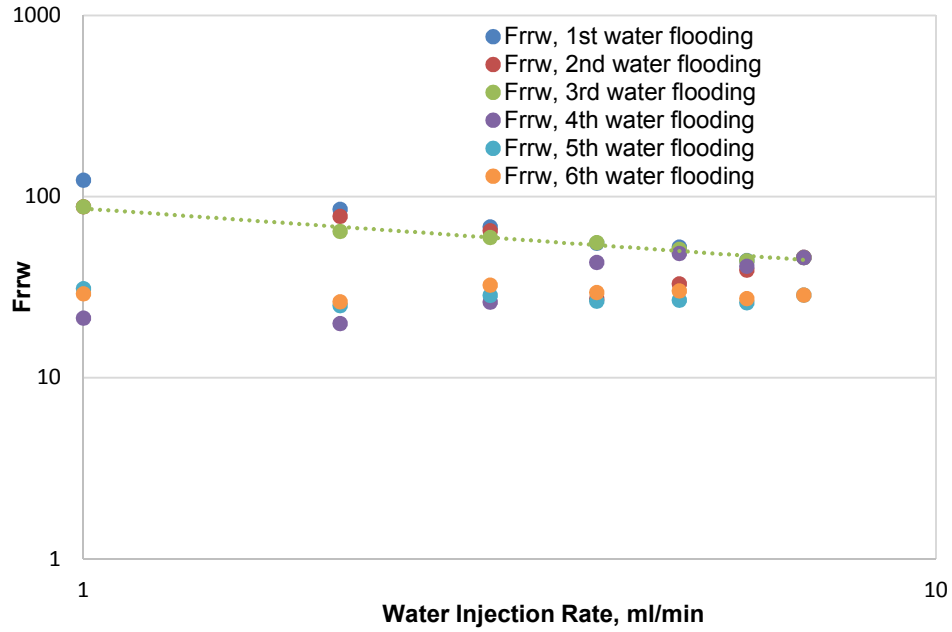

Figure 7.35—The residual resistance factor for a brine concentration of 0.05%.

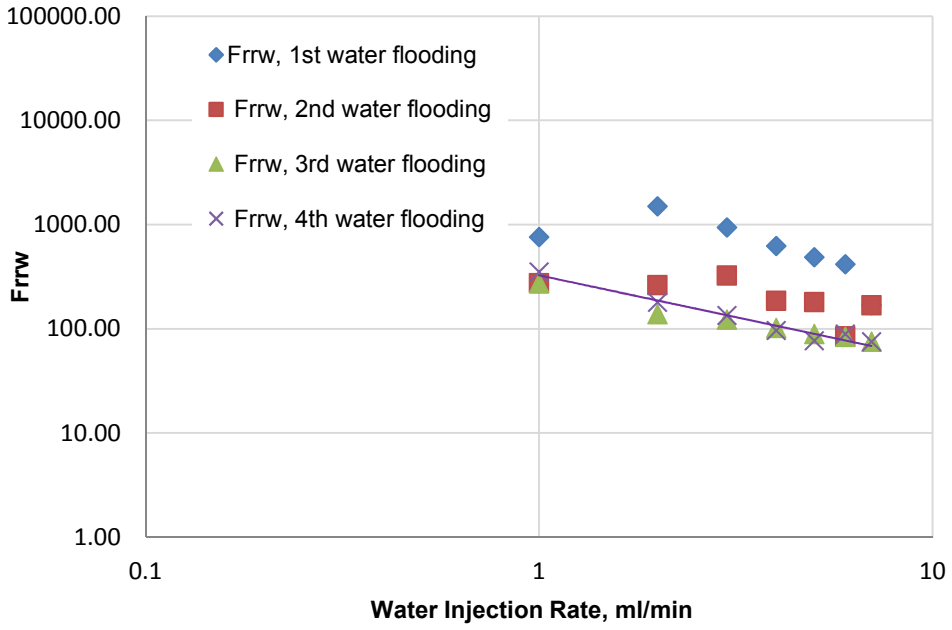

Figure 7.36—The residual resistance factor d for a brine concentration of 1%.

7.6.4.4. Effect of particle size. Two particle sizes (150 and 75 microns) were used to determine the effect of particle size in resisting the water flow through high permeability sand (see Figure 7.37 and 7.38, respectively). The water injection pressure for the water cycles increased and fluctuated during the water injection rate. The water injection pressure recorded for the 150 micron was substantially greater than the water injection pressure recorded for the 75 micron at all injection rate. The injection pressure recorded for the 150 micron was 2089 psi at a flow rate of 7 ml/min. The injection pressure recorded for the 75 micron at this flow rate was 314 psi. These findings revealed that the water flow through a larger particle was more restricted than the flow through a smaller particle in the same sand permeability sand.

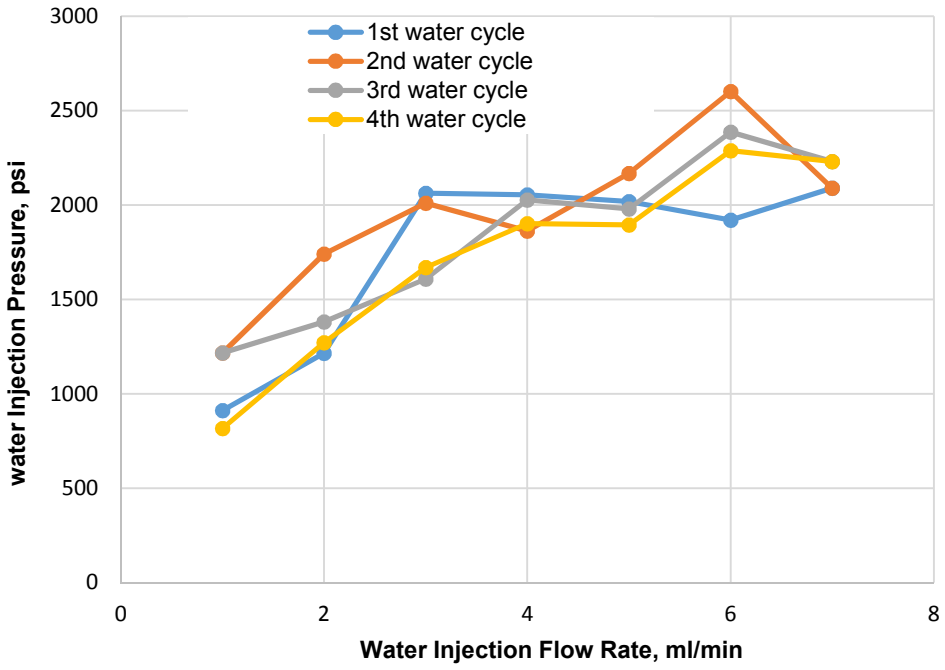

Figure 7.37—The water injection pressure for a 150 micron PPG.

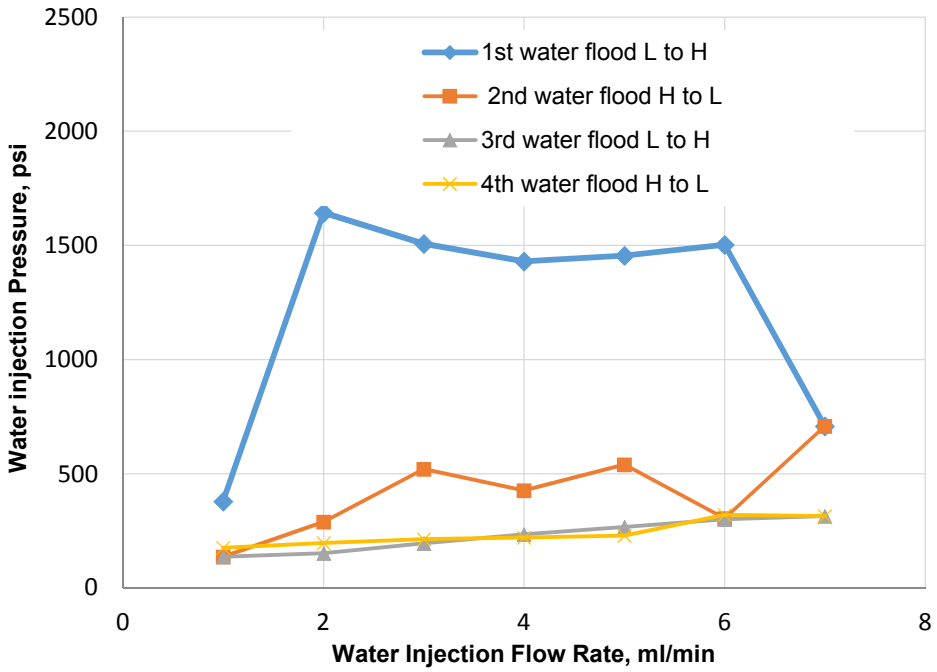

Figure 7.38—The water injection pressure for 75 micron PPG.

The residual resistance factor for both 75 and 150 micron PPGs were plotted in Figures 7.39 and 7.40 as a function of the injection flow rate. The Frrw for both particle sizes decreased as the injection flow rate increased. The significant decrease in Frrw was determined at the early injection rate. When the injection flow rate exceeded 4 ml/min, the Frrw became less dependent on injection flow rates. The Frrw decreased from 961 to 706 when injection flow rate increased from 1 to 2 ml/min in 150 micron PPG. It decreased slightly from 457 to 408 when injection flow rates increased from 6 to 7 ml/min.

The Frrw determined for a large particle size was larger than the Frrw determined for a small particle size during all of the injection rate. The Frrw determined at 150 microns was 408 at injection rate of 7 ml/min. The Frrw determined at 75 microns,

however, was 74. The power law equation was used to fit the Frrw determined at the last water cycle.

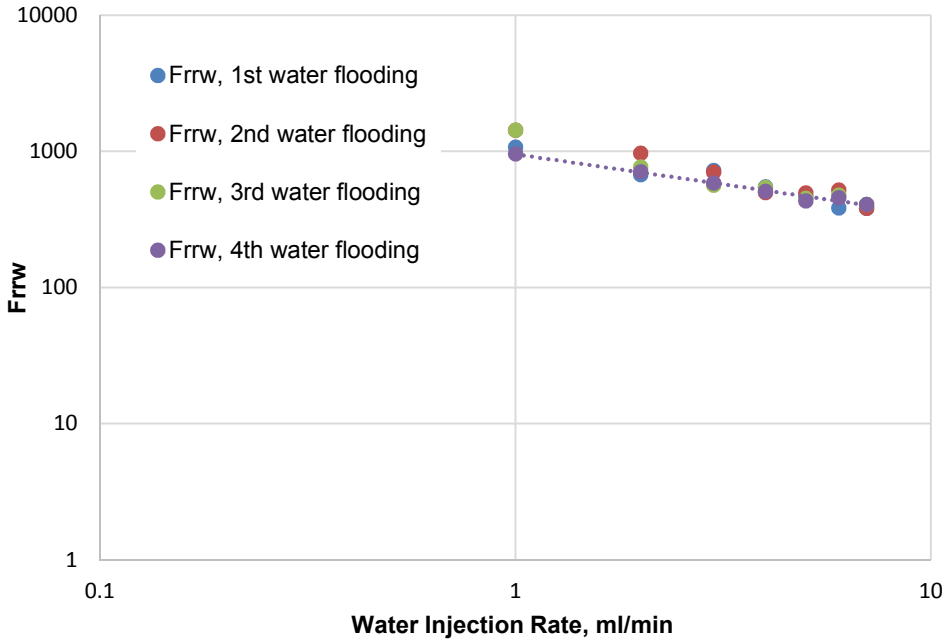

Figure 7.39—The residual resistance factor for a 150 micron PPG.

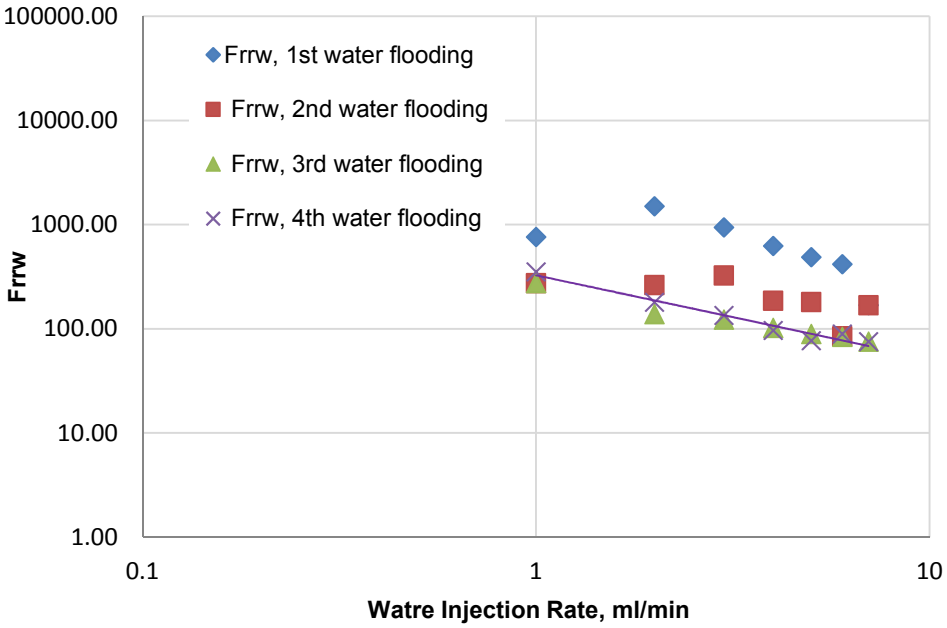

Figure 7.40—The residual resistance factor for a 75 micron PPG.

7.6.5. Residual Resistance Factor Correlations. The residual resistance factors shown in Figures 7-27, 7-28, 7-31, 7-35, and 7-39 have a very good relationship with injection flow rates when they plotted on log-log plots. This relationship was expressed using the power law equation as listed in the Table 7.6. Equation shown in the Table were fitted for the last water injection cycle.

Table 7.6—Fitting equation for residual resistance factor as a function of flow rate.

Effect	Value	Fitting Equations	R^2
Effect of K	K=26.5 Darcy	$Frrw= 326.16\ q^{-0.803}$	0.96
	K=65.4 Darcy	$Frrw= 42.165\ q^{-0.183}$	0.98
Gel concentration	800 ppm	$Frrw= 61.847\ q^{-0.191}$	0.91
	2000 ppm	$Frrw= 326.16\ q^{-0.803}$	0.96
Brine concentrations	0.05% NaCl	$Frrw= 86.024\ q^{-0.336}$	0.97
	1%NaCl	$Frrw= 326.16\ q^{-0.803}$	0.96
Effect of particle size	150 micron	$Frrw= 953.89\ q^{-0.443}$	0.98
	75 micron	$Frrw= 326.16\ q^{-0.803}$	0.96

7.6.6. PPG Blocking to Water Flow. The Frrw was defined early as the ratio of water phase permeability before and after particle gel treatment. Blocking efficiency to water flow refers to the percentage of permeability reduction. The stabilized water injection pressures measured at injection flow rate of 2 ml/min were used to calculate Frrw and blocking efficiency.

Table 7.7 shows the blocking efficacy to water flow determined for the effects of sand permeability, gel concentration, brine concentration, and particle size. PPG blocking

to water flow was too high for all the effects. It reached 90% and above, which indicates that PPG can be used efficiently to plug the large pore throat sizes/channels exist within the super-k permeability features. This high unvaried percentage of blocking was reached because sufficient PPG volume was injected into the sand pack model.

Table 7.7—A blocking efficiency to water flow determined at 2 ml/min.

Effect		Water Injection Pressure before PPG (psi)	PPG Injection Pressure (psi)	Water Injection Pressure after PPG (psi)	FRRW	PPG Blocking (%)
Effect of Permeability	26.5 Darcy	1.1	1680	197.5	179.5455	99.44304
	65.4 Darcy	0.15	27.1	1.6	10.66667	90.625
Gel Concentration	800 ppm	0.4	183.5	21	52.5	98.09524
	2000 ppm	1.1	1680	197.5	179.5455	99.44304
Brine Concentrations	0.05% NaCl	1.9	856	52.2	27.47368	96.36015
	1%NaCl	1.1	1680	197.5	179.5455	99.44304
Effect of Particle Size	75 micron	1.1	1680	197.5	179.5455	99.44304
	150 micron	1.8	2545.4	1272.1	706.7222	99.8585

7.6.7. Oil Recovery and Water Cut Measurements. The effect of PPG on increasing oil recovery and decreasing water production was discussed in the following subsections.

7.6.7.1. Effect of unconsolidated sandstone permeability. Two different ranges of sand pack permeability were used to determine the effect of sand permeability on oil recovery and water cut measurements (see Figures 7.41, 7.42, 7.43, and 7.44). Water was flooded at an injection flow rate of 2 ml/min into the sand pack's permeability. The oil

recovery increased and reached stability after 1% NaCl was injected approximately 5 PV. of The oil recovery increased as the permeability increased during the first water flooding. The oil recovery reached approximately 70% for a permeability of 26.5 Darcy and approximately 80% for a permeability of 65.4 Darcy. A sharp increase occurred in the water cut measurement during the first water flooding. The water cut fluctuated with a range of 90% before it became stable at approximately 99% at the end of the first water flooding process.

The PPG that was swollen in 1% NaCl with a concentration of 2000 ppm was injected at the same flow rate (2 ml/min). A considerable amount of oil increased when PPG's were being injected. The oil recovery increased above 20% incrementally for both permeabilities during the PPG injection. The oil recovery increased by 24% after 15 PV of PPG injection in permeability of 26.5 Darcy. The oil recovery increased by 15% after 18 PV PPG injection in permeability of 65.9 Darcy. The total oil recovery after the PPG injection was complete was above 95% for both permeabilities. The water cut decreased during the PPG injection, finally reaching 80%. This reduction in water cut increased the amount of oil produced from the sand pack models.

A second water flooding was performed after the PPG treatment was complete to determine whether or not any oil could be recovered from the sand pack. Approximately 5 PV of brine was injected into the sand packs. A negligible amount of oil was produced during this flooding. The total oil recovery obtained before, during, and after PPG treatment reached above 90% an increase of approximately 20% of that recovered during the PPG treatment.

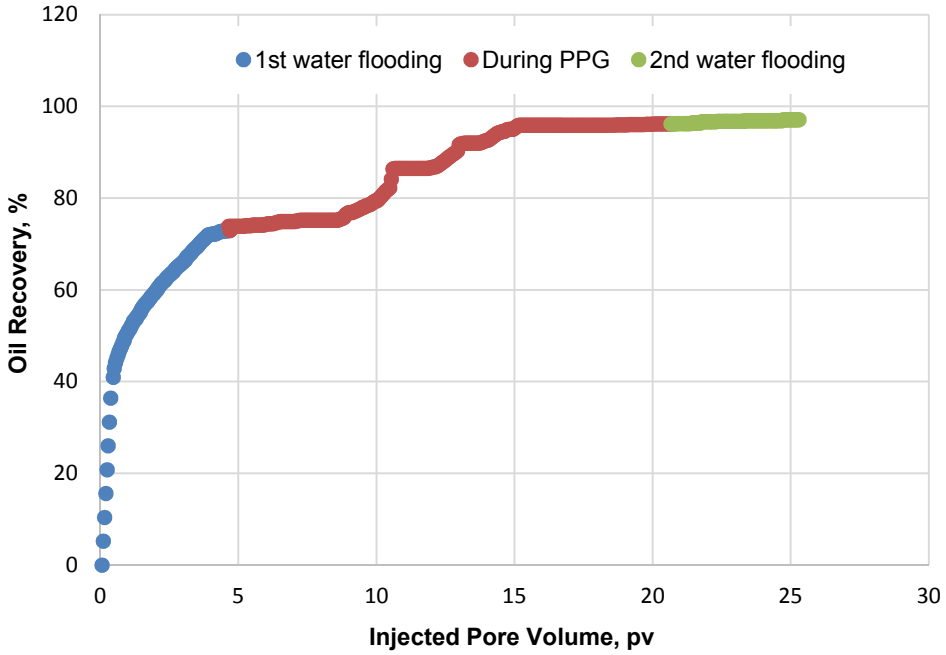

Figure 7.41—Oil recovery for a permeability of 26.5 Darcy.

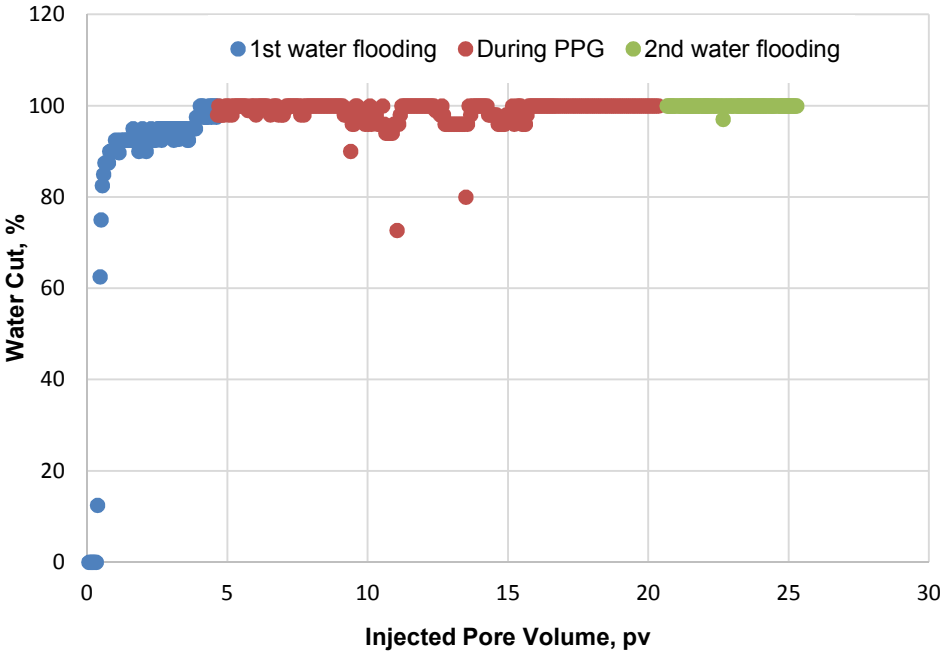

Figure 7.42—Water cut for a permeability of 26.5 Darcy.

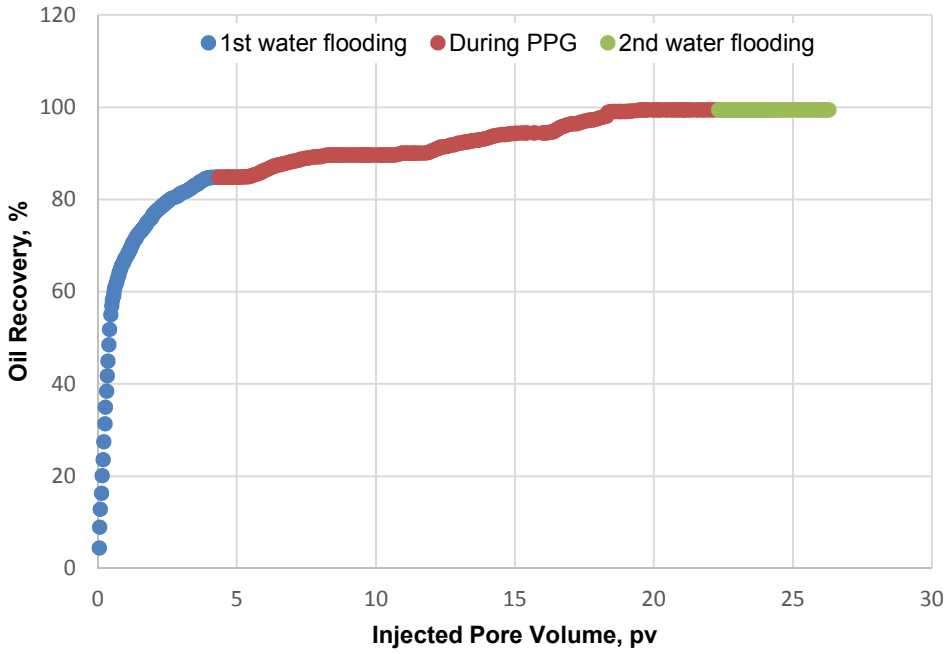

Figure 7.43—Oil recovery for a permeability of 65.4 Darcy.

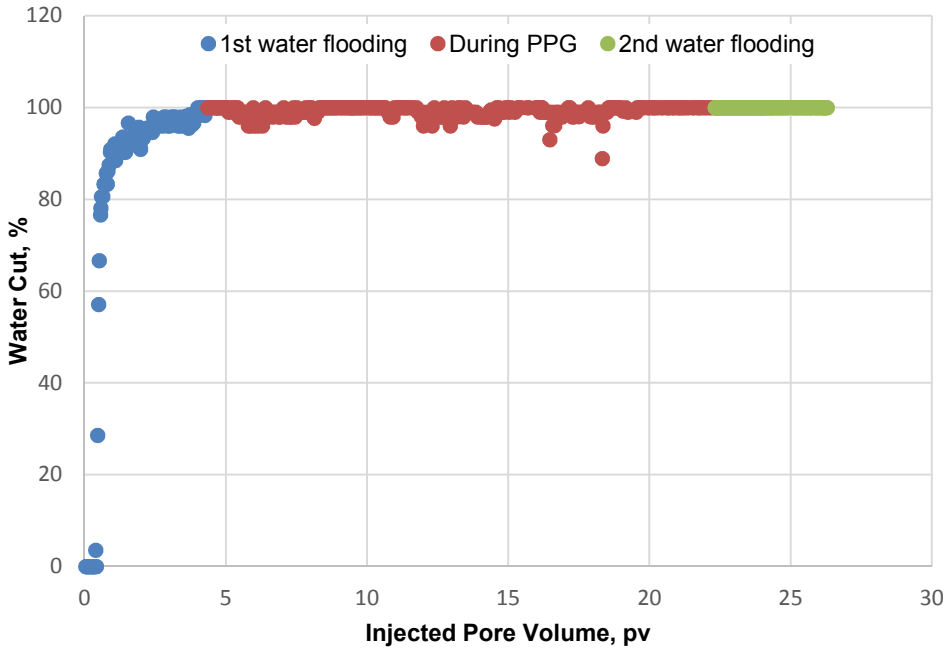

Figure 7.44—Water cut for a permeability of 65.4 Darcy.

7.6.7.2. Effect of gel concentrations. Two different ranges of PPG concentrations were used to test the effect of gel concentration on oil recovery and water cut measurements (Figures 7.45, 7.46, 7.47, and 7.48). Both sand packs used in this evaluation had the same average permeability with approximately 26.5 Darcy. Each sand pack was first flooded with 1% NaCl at an injection flow rate of 2 ml/min. The oil recovery increased substantially at the early injection pore volume before it became stable at the end of the water flooding process. Oil recovery reached approximately 70% after approximately 5 PV of water injection. The water cut increased sharply to reach approximately 99% during the end of this water flooding process.

The PPGs that were swollen in 1% NaCl with concentrations of 800 and 2000 ppm were injected into the sand packs after the water flooding was complete. The PPG were then injected with injection flow rates of 2 ml/min until the gel produced at effluent. The oil recovery during this treatment increased by approximately 25% for both concentrations. The oil recovery determined for both PPGs concentration were almost equal. The PPG injection pore volume, however, were varied. The oil recovery increased by 28% in 800 ppm after 42 PV of PPG were injected. The oil recovery increased by 24% in 2000 ppm after 15 PV of PPG were injected. This similarity in oil recovery indicates that different PPG concentrations can achieve same the oil recovery though different injection pore volumes are required. The water cut during the PPG injection decreased, reaching 80% before it increased again to 90% at the end of the PPG injection.

Water was recycled again at the same injection flow rate. Approximately 3 to 5 pore volumes of water were injected again though a very small amount of oil was obtained. The final oil obtained from the two sand pack models reached a similar

recovery (more than 90%). A larger PPG volume was, however, required for PPGs with smaller concentrations.

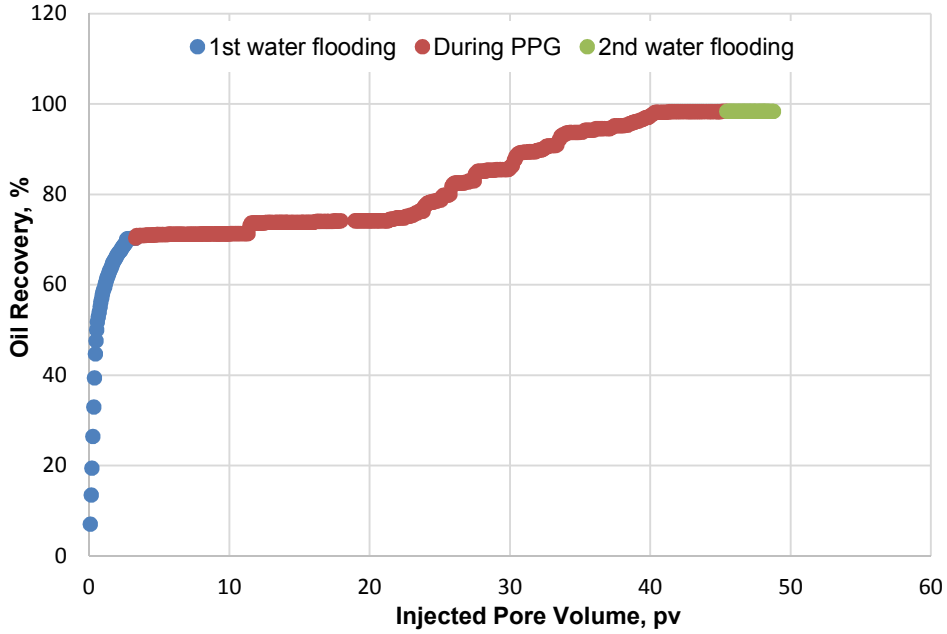

Figure 7.45—Oil recovery for a PPG concentration of 800 ppm.

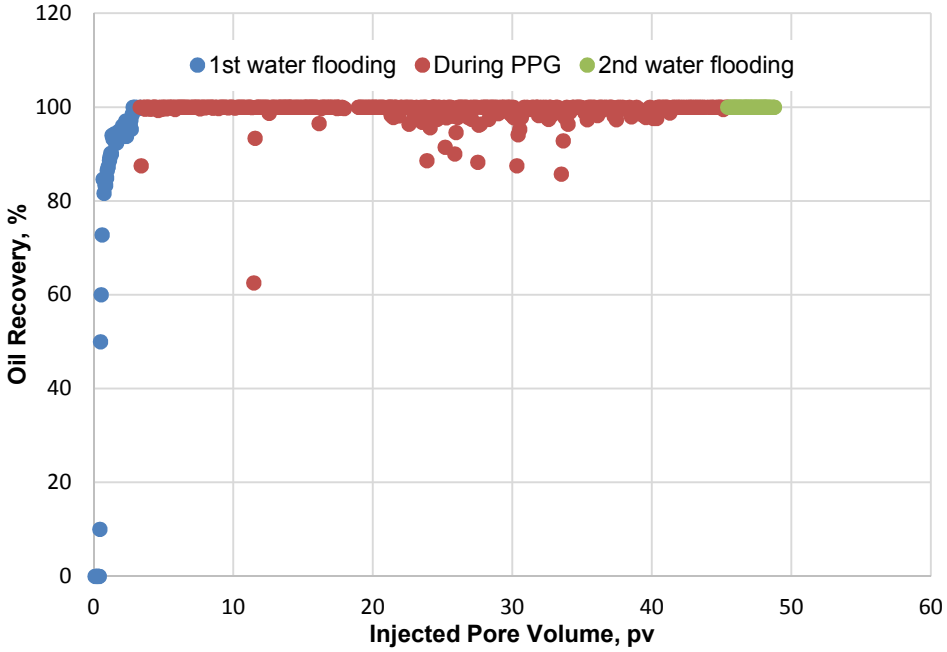

Figure 7.46—Water cut for a PPG concentration of 800 ppm.

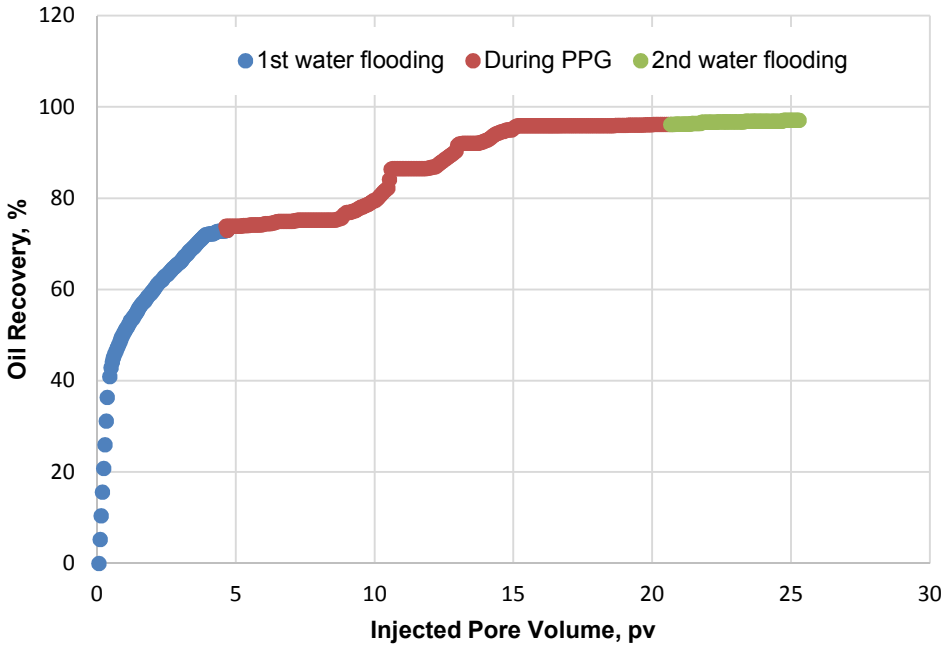

Figure 7.47—Oil recovery for a PPG concentration of 2000 ppm.

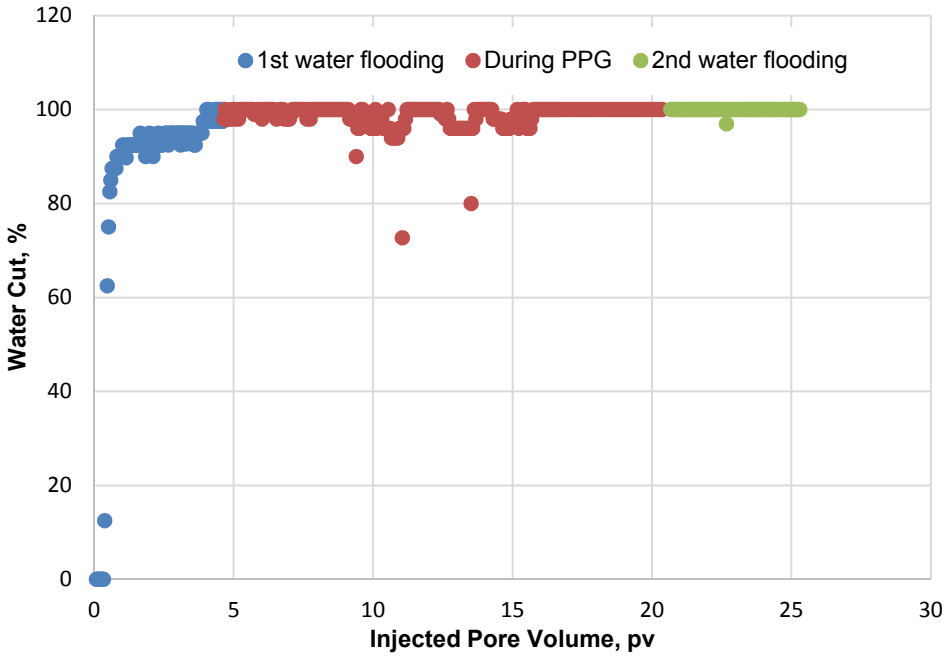

Figure 7.48—Water cut for a PPG concentration of 2000 ppm.

7.6.7.3. Effect of brine concentration. Two different ranges of brine concentration were selected for the experiments. Brine concentrations of a 0.05% and a 1% NaCl were used to prepare swollen PPGs for injection purposes. The brine was injected through the sand packs had a permeability of 26.5 Darcy. The brine was injected at an injection flow rate of 2 ml/min into the oil saturated sand pack. The oil recovery increased during the water flooding process to approximately 70% (see Figures 7.49 and 7.51). The water cut increased significantly reaching approximately 99% at the end of the water flooding mechanism (see Figures 7.50 and 7.52). The water injection continued until no oil was produced from effluent. A approximately 4 PV of 0.05% and 4 PV of 1% were injected into the sand packs. The PPGs that were swollen in 0.05% and 1% were injected into sand packs at the same injection rate (2 ml/min). The oil recovery increased by approximately 20% during the injection process. This increased, however, required different PPG injection pore volume. The PPGs that were swollen in a low brine concentration required less injection pore volume than did the PPGs swollen in high brine concentration to achieve the same incremental oil recovery factors. An approximately 6 PV of PPGs swollen in 0.05% increased oil recovery by 22%. Approximately 15 PV of PPGs swollen in 1% increased oil recovery by 24%. Water cut during the injection swollen PPGs decreased to around 80% and assist to increase oil recovery.

The sand packs were flushed again with brine to determine whether or not any oil recovery could be recovered. A small amount of oil was produced during the second water flooding cycle. The water cut continued to increase at a high percentage after a high percentage of oil was recovered during the PPG treatment. The final amount of oil recovered after the gel treatment was above 90%.

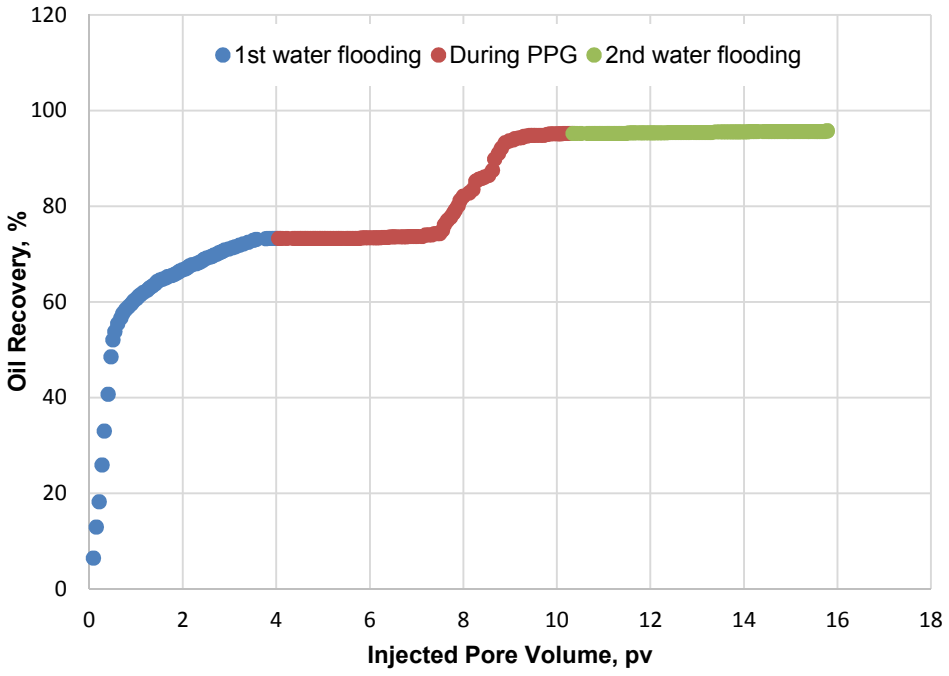

Figure 7.49—Oil recovery for a PPG swollen in 0.05%.

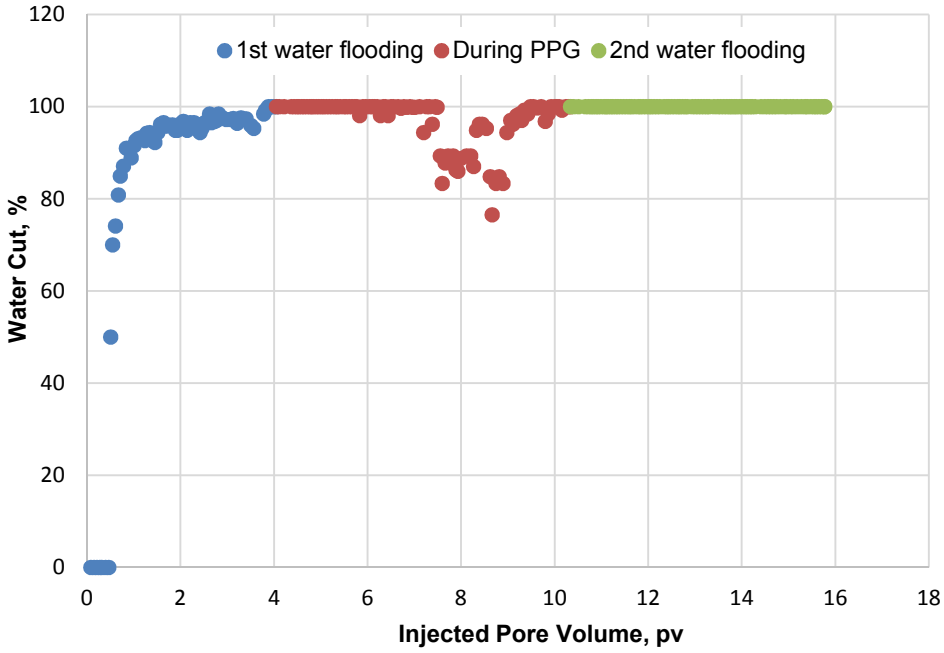

Figure 7.50—Water cut for a PPG swollen in 0.05%.

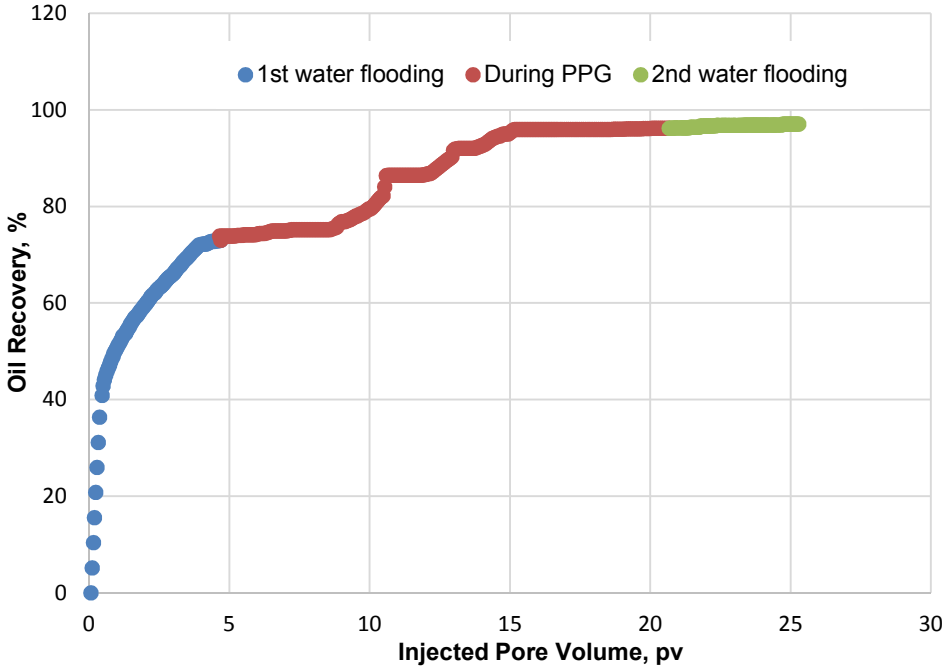

Figure 7.51—Oil recovery for a PPG swollen in 1 %.

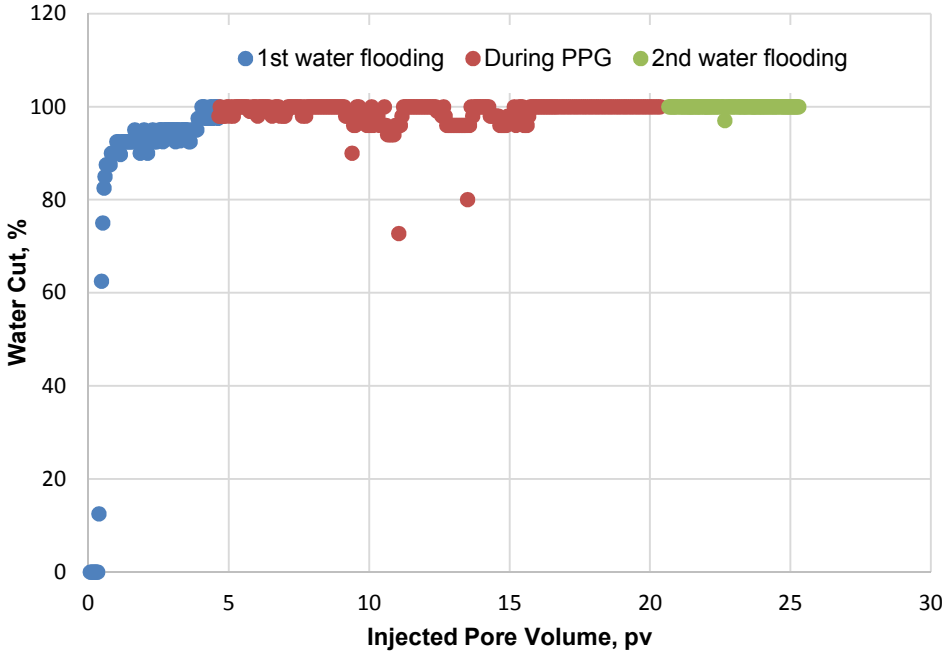

Figure 7.52—Water cut for a PPG swollen in 1 %.

7.6.7.4. Effect of particle size. Two different sizes of PPG were used to study the effect of particle size on the oil recovery and water cut measurements (see Figures 7.53, 7.54, 7.55, and 7.56). These PPGs were swollen in a 1 % NaCl concentration and injected through a sand pack permeability of 26.5 Darcy. Approximately 70% of oil recovered during the first water flooding. The water cut increased sharply as the water injection increased, reaching approximately 99% at the end of the water injection processes.

Both 75 and 150 micron PPG were injected at 2 ml/min through the sand packs. A considerable amount of oil was produced during these injections. The oil recovered when the 75 micron PPGs were injected increased by approximately 25%. It increased by 28% when 150 micron PPGs were injected. This a similar oil recovery required a different PPG injection pore volume. Large PPG sizes required a higher injection pore volume than did small PPG sizes. A approximately 35 PV of 150 micron PPG s were injected to recover 28%. Approximately 15 PV of 75 micron PPGs were injected to recover 25%. The water cut decreased during the PPGs injection to approximately 80%.

Water flooding was again conducted after the PPG injection to determine whether or not any oil could be produced. A negligible amount of oil was produced during this injection process. Water cut increased again during the second water flooding reaching approximately 99%. The final oil recovery after the gel treatment reached above 90%. A larger amount of PPGs were required for large particle size than did for smaller particles size.

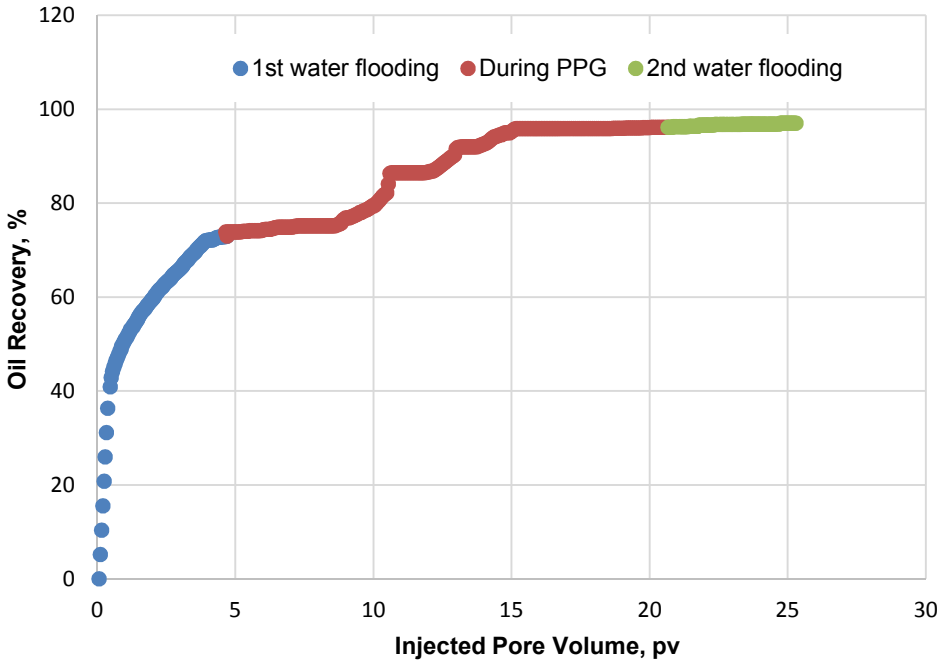

Figure 7.53—Oil recovery for a PPG size of 75 microns.

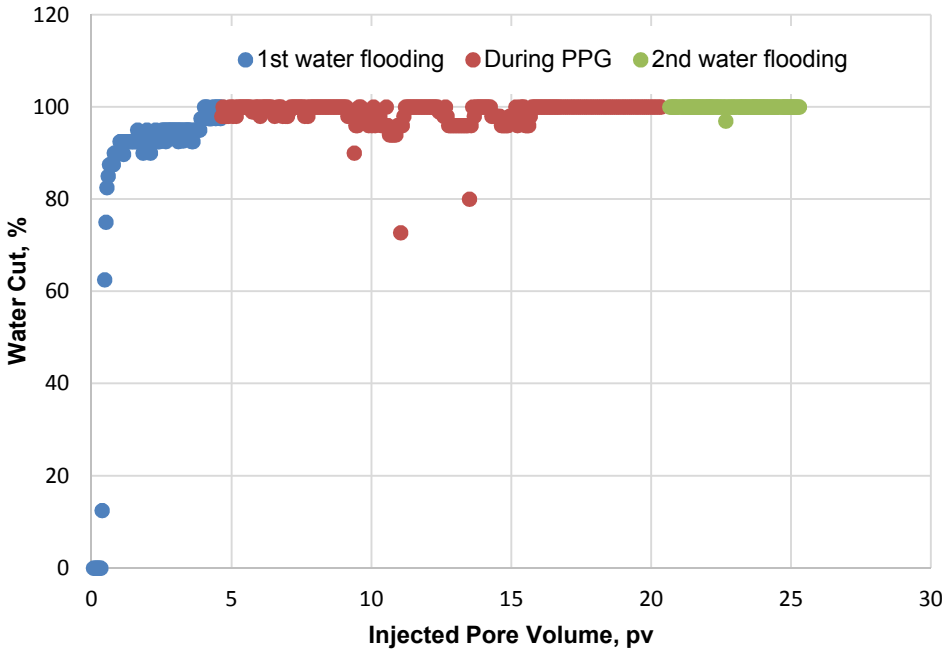

Figure 7.54—Water cut for a PPG size of 75 microns.

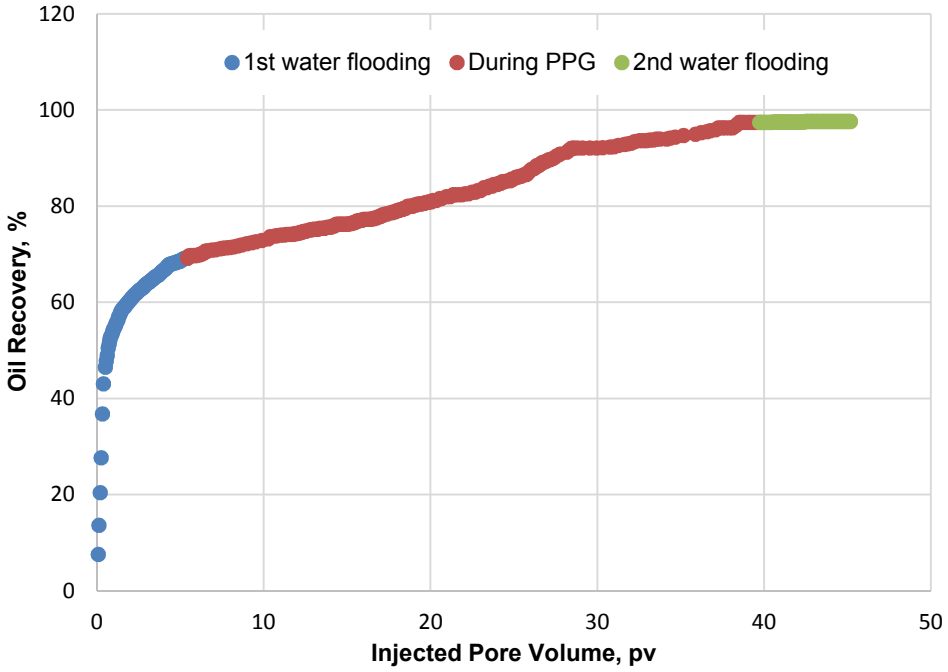

Figure 7.55—Oil recovery for a PPG size of 150 microns.

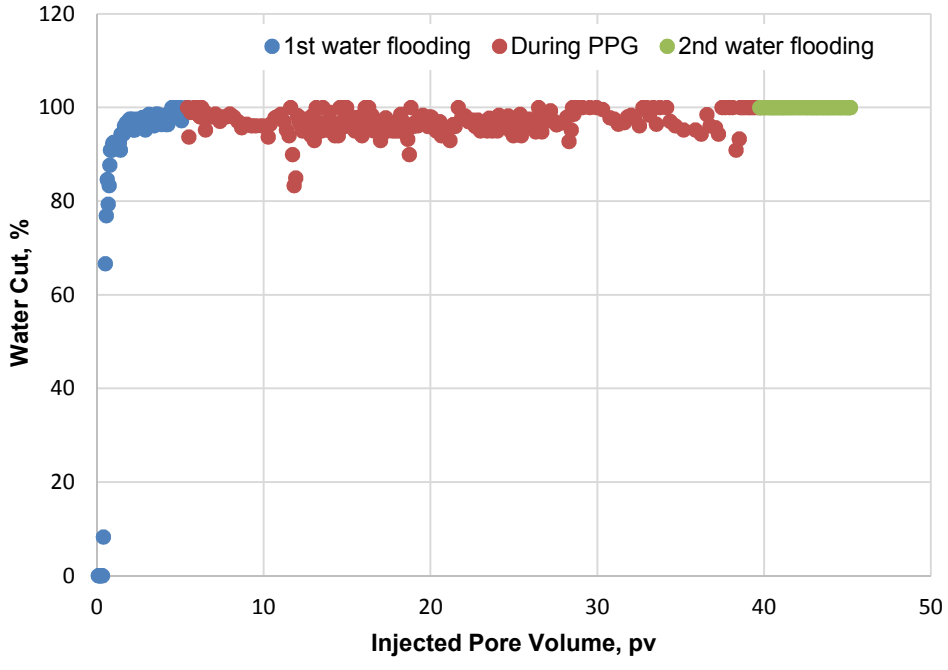

Figure 7.56—Water cut for PPG size of 150 microns.

7.6.8. Preformed Particle Gel Resistance to Water and Oil Flow. The sand pack model was saturated again with oil after the PPG injection. The water was injected next to determine the effect of PPG on oil and water flow. The results obtained for the effect studies of permeability, PPG concentration, brine concentration, and gel size are presented in the following subsections.

7.6.8.1. Effect of unconsolidated sandstone permeability. Two different ranges of permeability were used to investigate PPG's ability to reduce the permeability of water more than the permeability of oil. The residual resistance factor to water (Frrw) and the residual resistance factor to oil (Frro) were each used to determine the PPG's effect on blocking efficiency to water and oil flow, respectively. The Frrw is compared to Frro as a function of the fluid injection flow rate in Figure 7.56. Multiple cycles of water were injected to create Frrw1 and Frrw 2. The Frrw1 is a measurement of the blocking efficiency after the gel treatment was complete. The Frrw2 is measurement of the blocking efficiency after the gel treatment was complete and the sand pack was saturated again with oil.

Both the Frrw and the Frro decreased as the injection flow rates increased. They decreased substantially at the early injection flow rates and became independent when the injection rates increased. The Frrw was much greater than the Frro during all of the injection flow rates. This finding indicate that PPG reduce the water permeability much higher than the oil permeability. The Frrw1 was 560 and Frro was 26 at injection flow rate of 1 ml/min. A similar mechanism for a permeability of 65.4 Darcy in which the Frrw was much larger than the Frro during all the injection flow rates as it illustrated in Figure 7.58.

Both the Frrw and the Frro were plotted as a function of injection flow rates for both permeabilities (see Figures 7.59 and 7.60, respectively). The low permeability had a higher Frrw and a higher Frro than did a high permeability. The Frrw determined for a permeability of 26.5 Darcy was 560 at injection rate of 1ml/min. The Frrw determined for a permeability of 65.4 was 17 at same injection rate. The Frro determined for a permeability of 26.5 Darcy was 26 at injection rate of 1ml/min while the Frro determined for a permeability of 65.4 was 6.

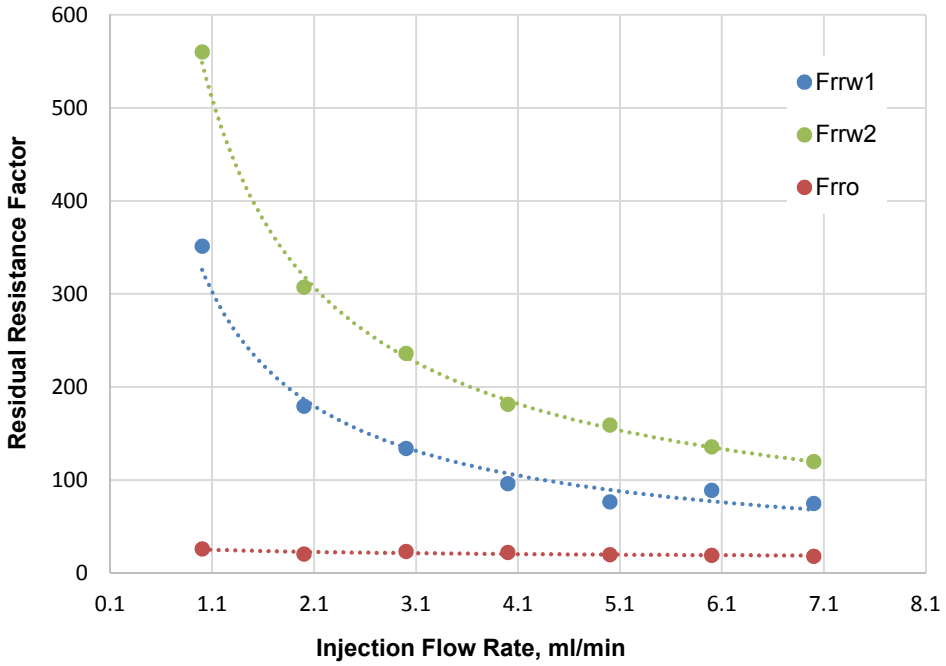

Figure 7.57—Frrw and Frro at a permeability of 26.5 Darcy.

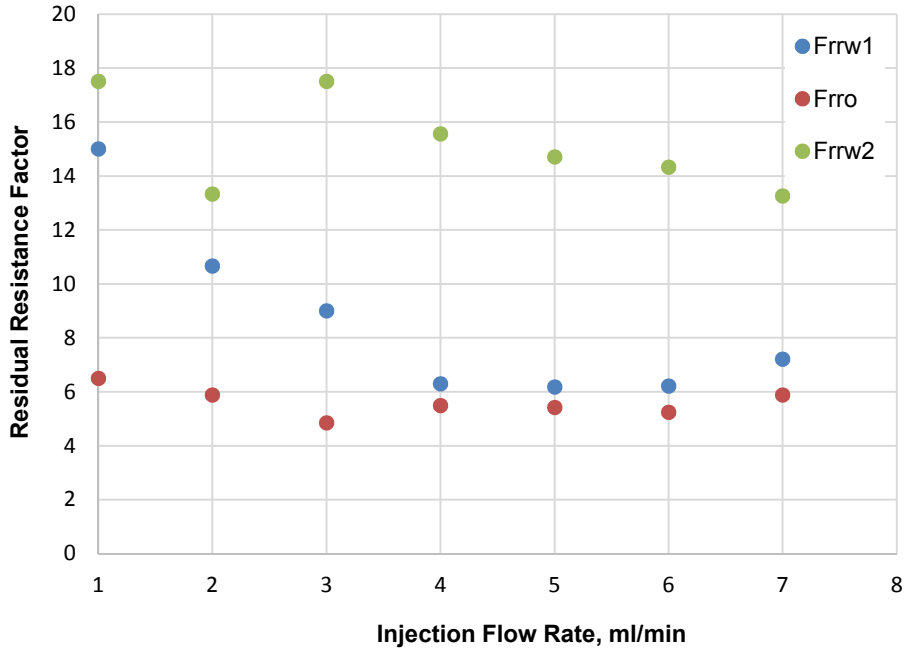

Figure 7.58— Frrw and Frro at a permeability of 65.4 Darcy.

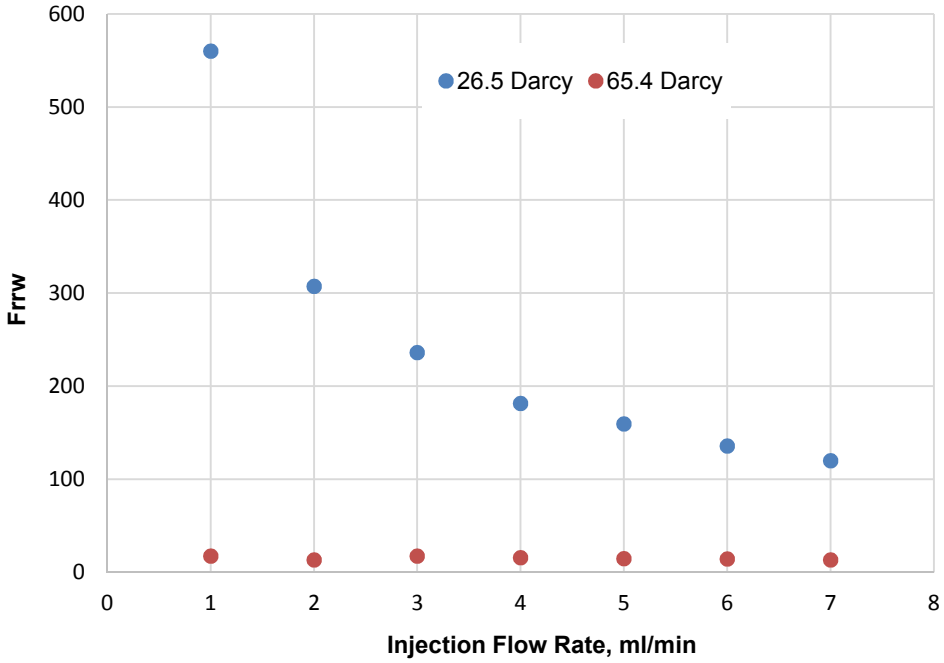

Figure 7.59—Compare residual resistance factor to water at a permeability effect.

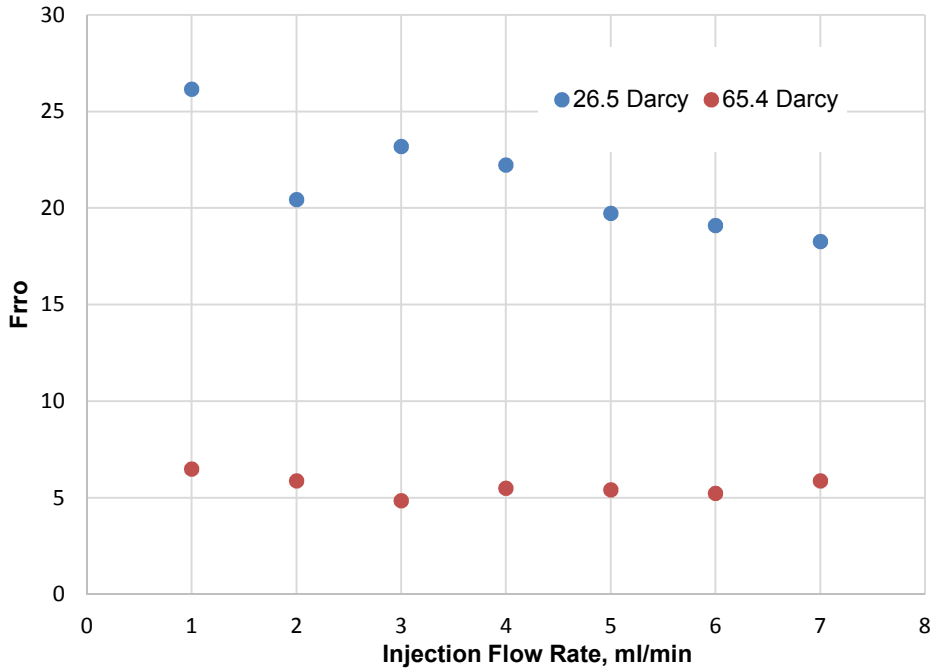

Figure 7.60—Compare residual resistance factor to oil at permeability effect.

7.6.8.2. Effect of gel concentrations. Multiple cycles of water and oil were performed to test the effect of a PPG concentration on the gel blocking efficiency to water and oil flow. The PPG concentration of 800 ppm and 2000 ppm were used in these investigations. The result after 2000 ppm of PPG were injected through a sand pack of 26.5 Darcy are illustrated in Figure 7.61. Both the Frrw and the Frro determined as a function of fluid injection flow rates; both decreased as the injection flow rates increased. The Frro determined during each of injection oil rates was less than the Frrw. The results that were obtained when 800 ppm PPGs were injected through the same sand pack permeability are illustrated in Figure 7.62. Again, both decreased as the injection flow rates increased. The Frro was much smaller than the Frrw all of the injection rates. Frrw 1 and Frrw 2 show insignificant change during the water injection. Thus, the oil flow did not decrease the blocking water efficiency too much.

The Frrw is compared to the Frro as a function of the PPG concentration in Figure 7.63 and 7.64. These results indicate that both the Frrw and the Frro obtained for a high concentration PPG were greater than the Frrw and the Frro obtained for a low concentration PPG. At injection rate of 1 ml/min, Frrw determined for PPG concentration of 2000 ppm was 560. While, the Frrw determined for PPG concentration of 800 ppm was 70 at same injection rate. Additionally, Frro determined for a PPG concentration of 2000 ppm was 26 at injection rate of 1 ml/min. While, the Frro determined for a PPG concentration of 800 ppm was 18 at same injection rate. These results also reveal that the PPG concentration did not have a significant impact on the Frro (as compared to the Frrw). In contrast to the permeability effect, the Frro was less influenced by change in the PPG concentration.

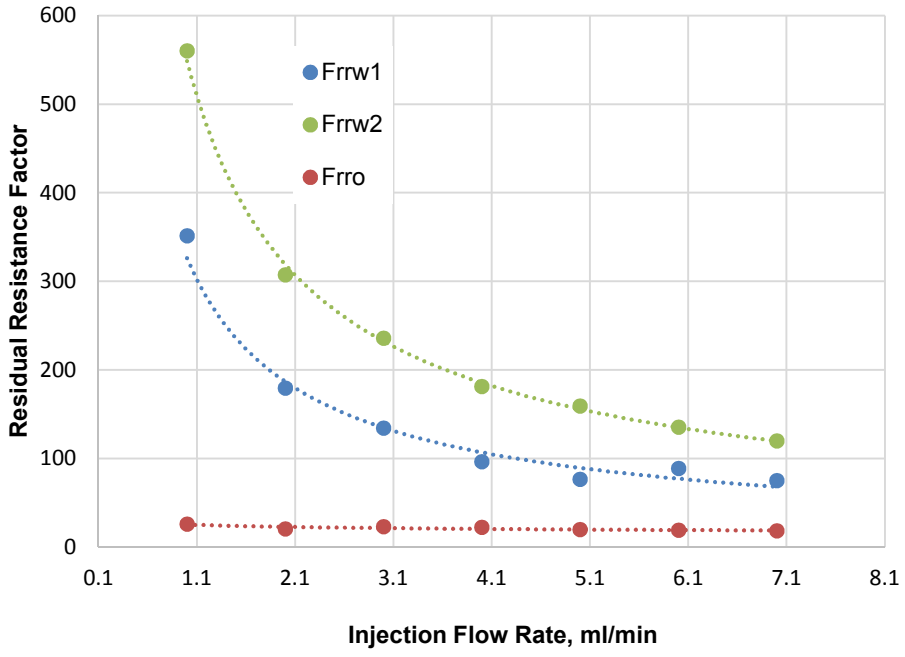

Figure 7.61—Residual resistance factor to water and oil at 2000 ppm PPG.

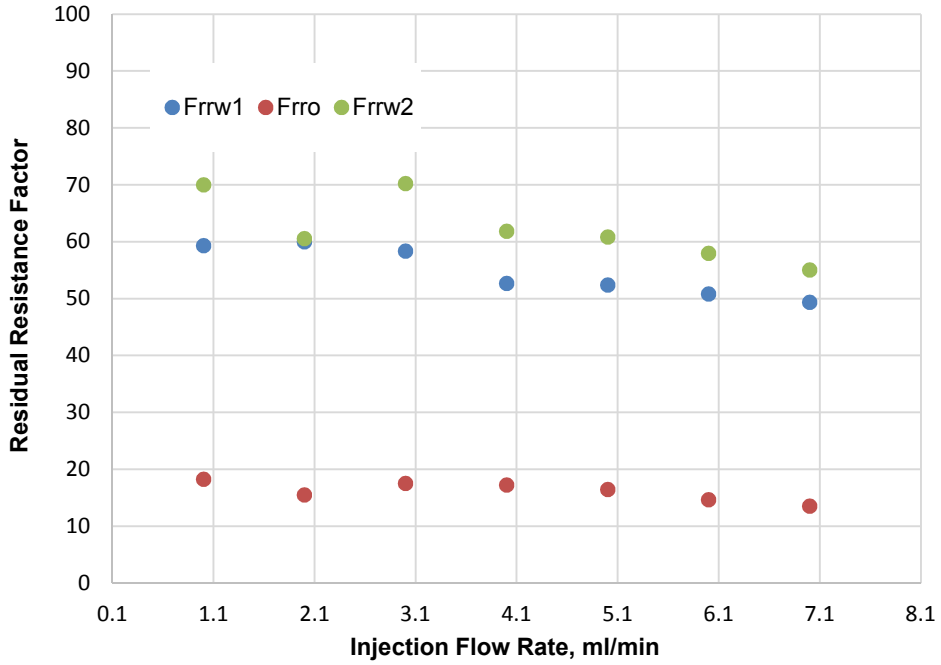

Figure 7.62—Residual resistance factor to water and oil at 800 ppm PPG.

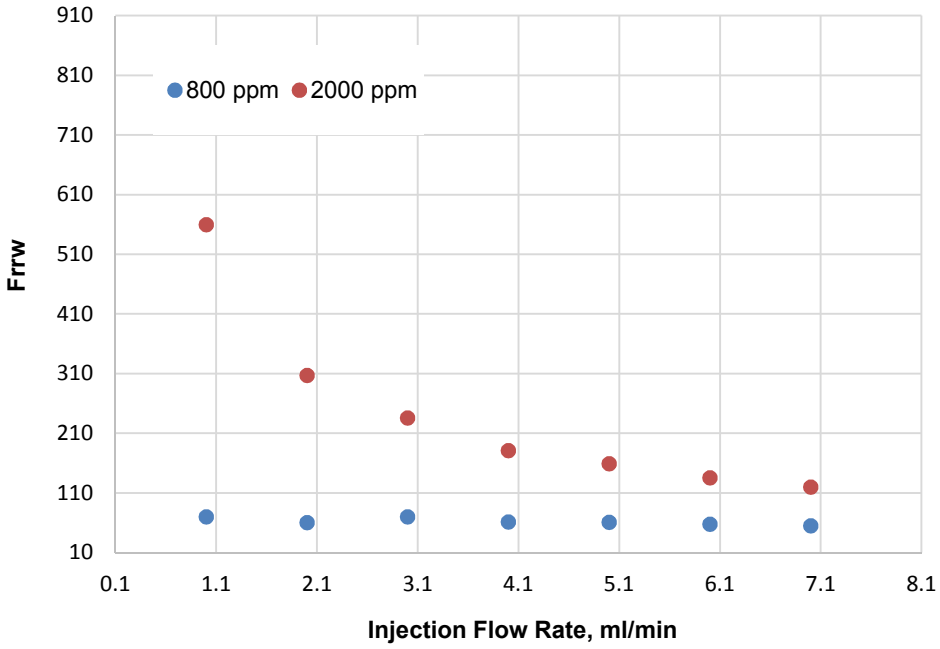

Figure 7.63—Residual resistance factor to water at PPG concentration effect.

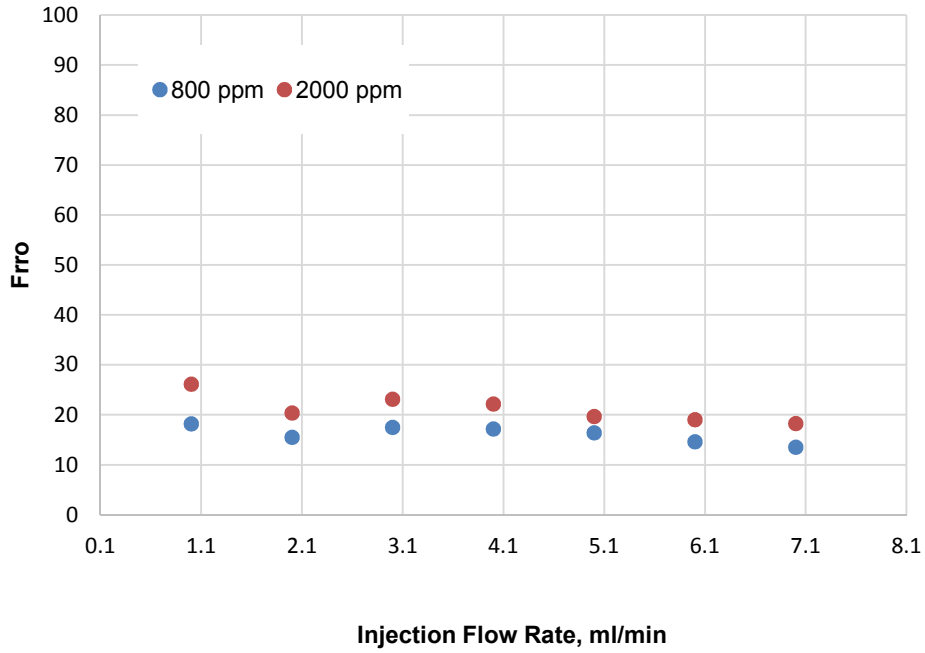

Figure 7.64—Residual resistance factor to oil at PPG concentration effect.

7.6.8.3. Effect of brine concentration. The brine concentration was carefully selected to test the blocking efficiency for water and oil flow. Both 0.05% NaCl and 1% NaCl solutions were used to prepare the PPGs to inject in a sand pack permeability of 26.5 Darcy. The Frrw and the Frro determined after flushed sand pack with multiple water and oil cycles are illustrated in Figure 7.65.

The Frrw during all of the injection flow rates was greater than the Frro. Additional water cycles of water were performed after the second oil injection. The Frrw remained greater than the Frro. These results also revealed that the Frrw and the Frro each as the injection rate increased. This decrease was more obvious during the first injection flow rates. A Similar trend was observed for the gel swollen in 1% NaCl (see Figure 7.66); the Frrw still larger than the Frro through different water cycles.

The Frrw is compared to the Frro as a function of the brine concentration in Figures 7.67 and 7.68. These results reveal both the Frrw and the Frro obtained for a high brine concentration were greater than the Frrw and the Frro obtained for a low brine concentration. The Frrw determined for a gel swollen in brine concentration of 1% NaCl was 560 at injection rate of 1 ml/min; the Frrw determined for a brine concentration of 0.05% was 69 at this flow arte. The Frro determined for a gel swollen in brine concentration of 1% NaCl was 26 at injection rate of 1 ml/min. The Frro determined for brine concentration of 0.05% was 14 at this flow arte. These results also reveal that the brine concentration had a great impact on both the Frro and the Frrw than did either the permeability or the gel concentrations.

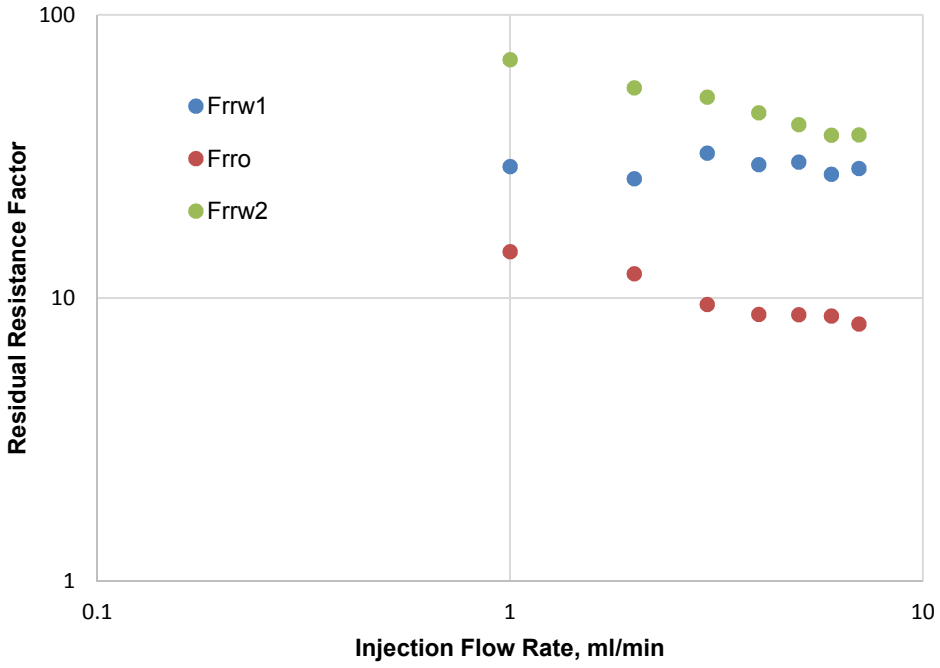

Figure 7.65— Frrw and Frro for a brine concentration of 0.05%.

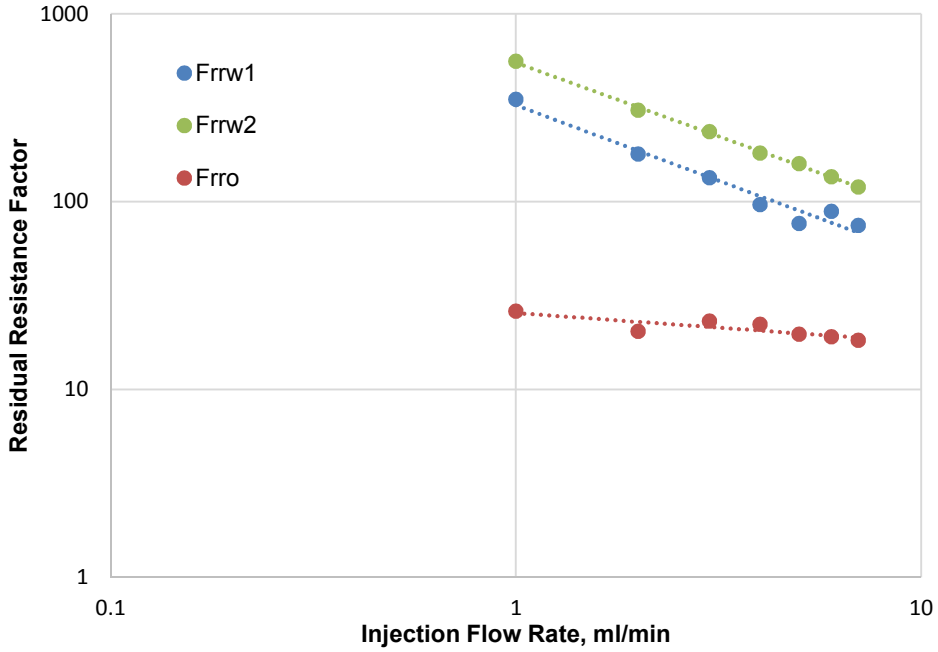

Figure 7.66— Frrw and Frro for a brine concentration of 1% .

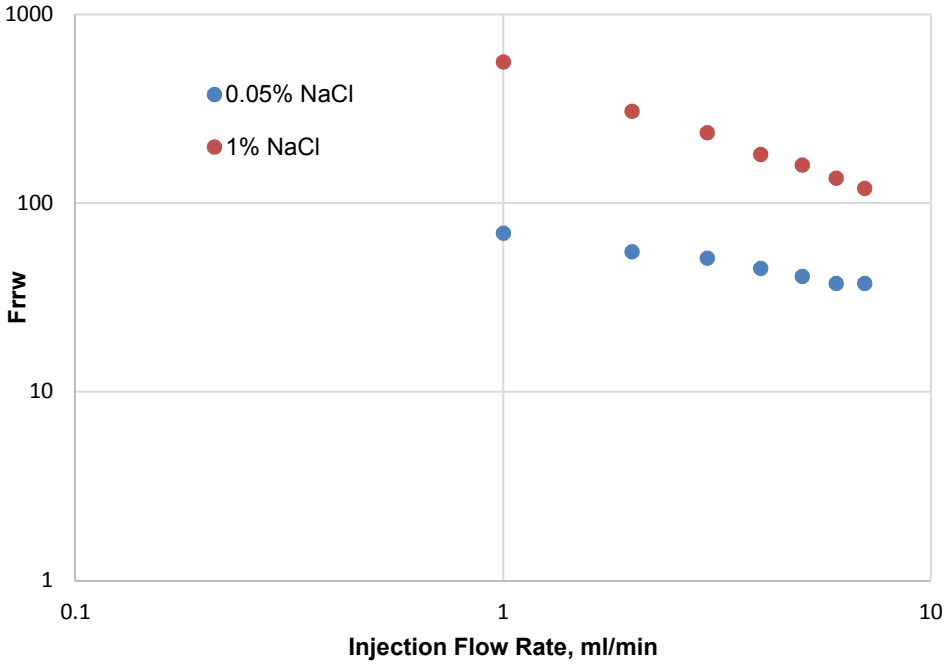

Figure 7.67—The residual resistance factor to water for a brine concentration effect.

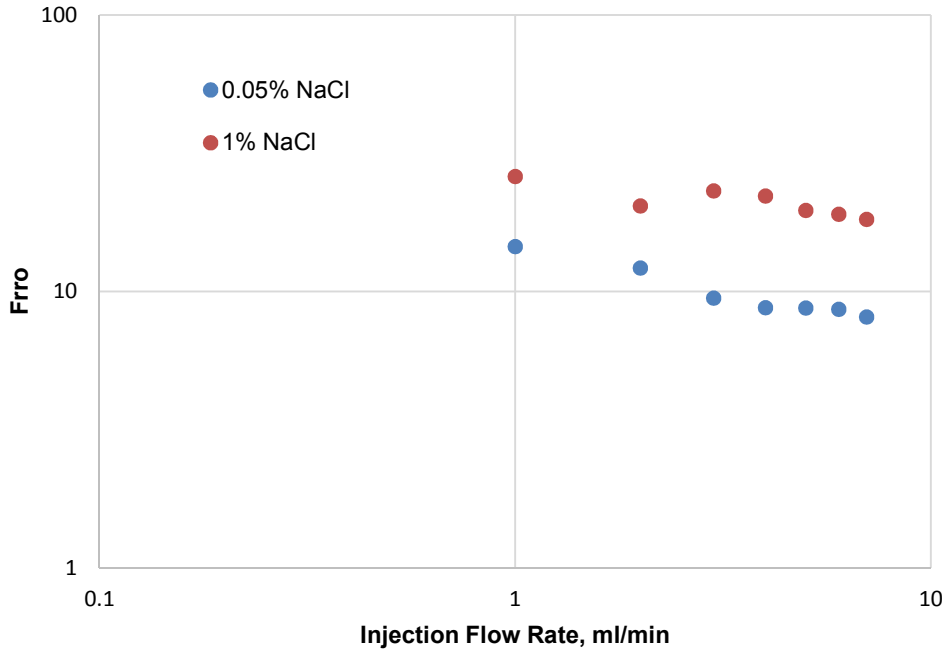

Figure 7.68—The residual resistance factor to oil for a brine concentration effect.

7.6.8.4. Effect of particle size. Particle gel sizes were used to determine the affect of PPG size on the blocking efficacy to water and oil flow. Multiple cycles of 1% NaCl and 37cp oil were injected through a sand pack permeability of 26.5 Darcy. The Frrw determined during multiple water injections was greater than the Frro during all of the injection flow rates (see Figure 7.69 and 7.70, respectively). Additional water cycles were performed after the sand was saturated with oil. The Frrw remained greater than the Frro. A similar decreased was observed for the Frrw and the Frro when the injection flow rates increased. The Frrw is compared to the Frro a function of particle size in Figure 7.71 and 7.72, respectively. In general, both the Frrw and the Frro obtained for a large particle size were greater than the Frrw and the Frro obtained for a small particle size. Particle size, however, had an insignificant impact on the particle size as compared with

previous effects. Both the Frrw and the Frro determined for 75 microns differed little from than the Frrw and the Frro determined 150 microns.

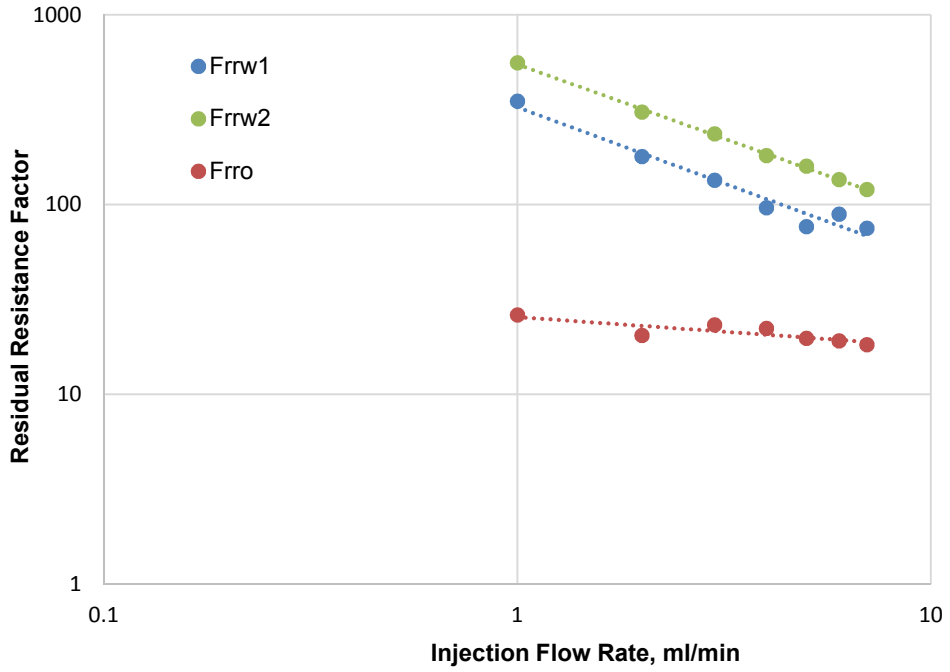

Figure 7.69—The residual resistance factor to water and oil for 75 microns.

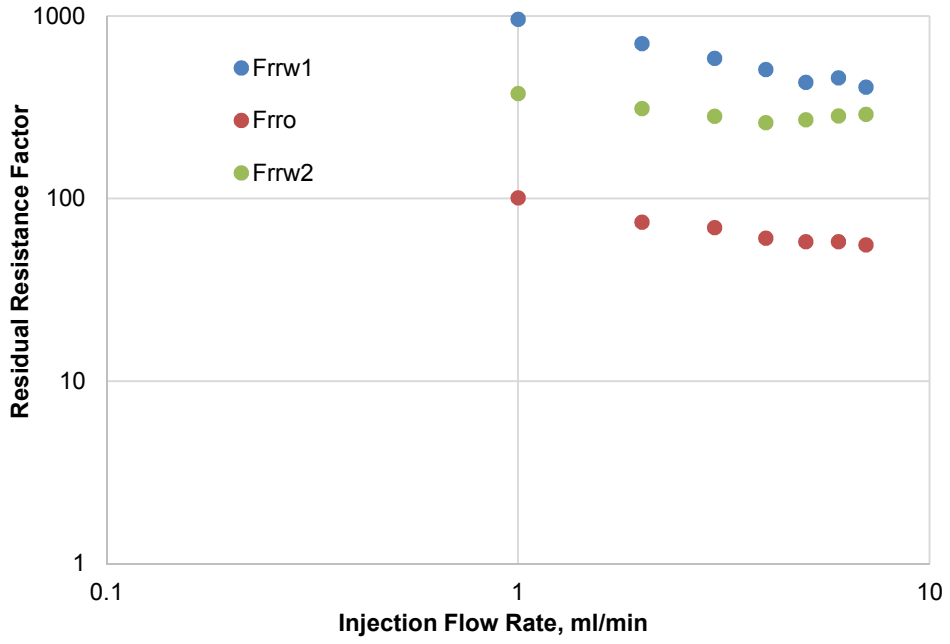

Figure 7.70—The residual resistance factor to water and oil for 150 microns.

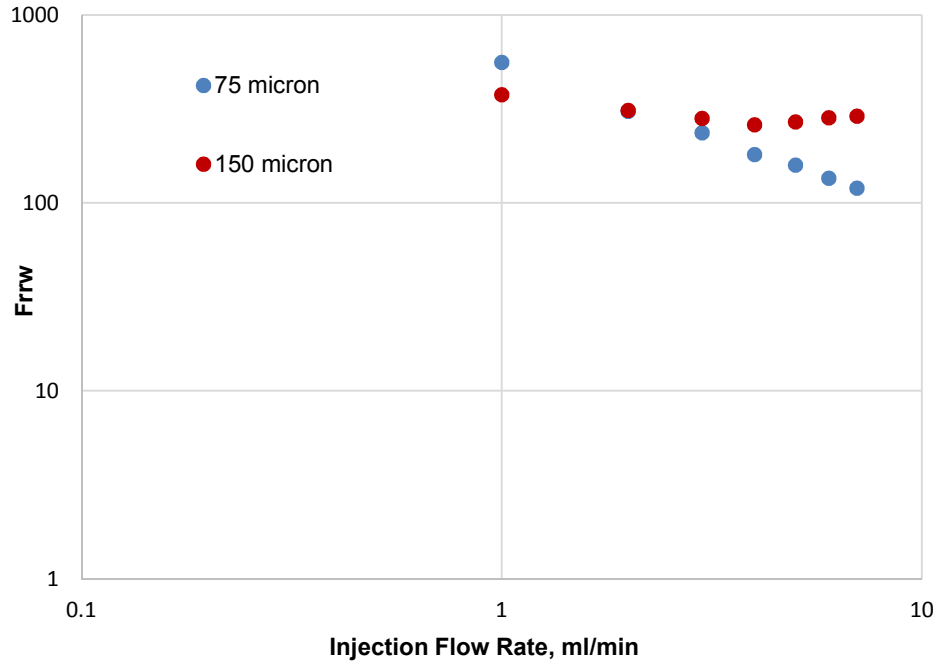

Figure 7.71—The residual resistance factor to water for a PPG size effect.

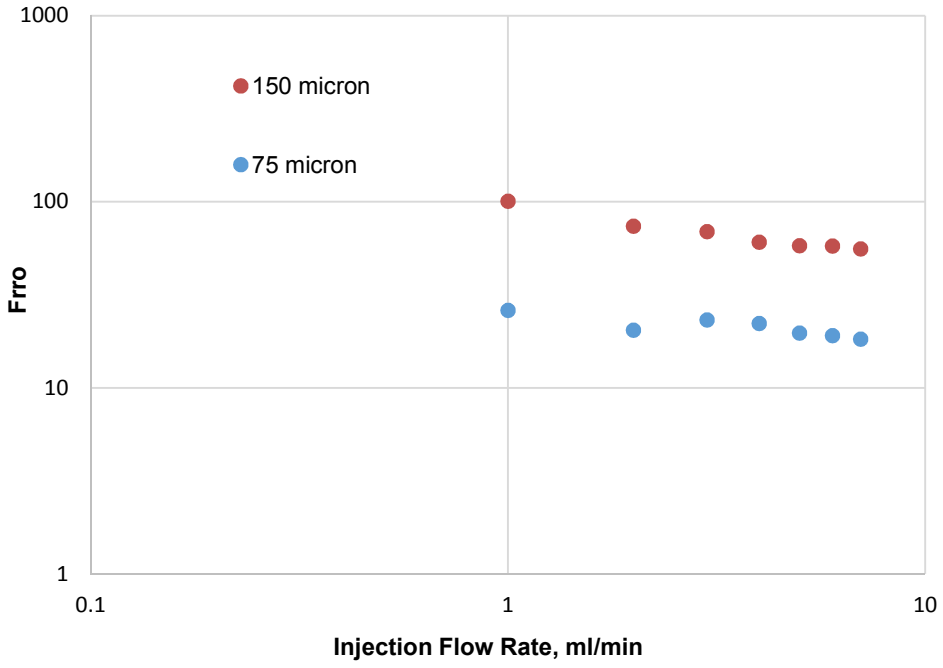

Figure 7.72—The residual resistance factor to oil for a PPG size effect.

7.7. CONCLUSION

A number of factors that affect PPG transport and resistance to water/oil flow through super-K sand permeability were intensively examined in this section. The effect of PPG to increase oil recovery and reduce water cut was also investigated. The following conclusions can be drawn from the research:

- In field applications, it is very common that operators often concern about particle size for better injection performance. Contrary to the conventional concepts in PPGs treatment practices, we found that PPGs injection was more sensitive to the PPGs strength than PPGs size.
- The results show fully swollen gel particles have better injectivity than partially swollen particles with larger diameter size; particle strength is more dominant particle movement than particle size. Injection pressure increased as the PPGs concentration, water salinity, and gel particle size increased.
- Large PPG injection pore volume was required to reach effluent when used high water salinity, big particle sizes, and low PPGs concentration.
- PPGs transport through super K permeability exhibited four patterns based on both the visual analyses and the threshold pressure gradient measurements as follows: pass; broke and pass; broke, entrapment, and pass; and broke, entrapment, and plug.
- After the PPGs injection process completed, cycles of saline water were injected into sand pack to test PPGs resistance to water flow. PPGs blocking efficiency to water flow were increased as the PPGs strength, PPGs size, and PPGs concentration increased.

- Large oil recovery incremental, usually reached around 20%, noticed during the PPGs injection treatment. Oil recovery during PPGs injection was varied and based on PPGs injection pore volume, PPGs concentration, and PPGs strength. Oil recovery increased as the PPGs slug volume and PPGs concentration increased but it was less sensitive to the increase in gel strength and particle size.
- After the PPGs injection process completed, cycles of saline water and oil were injected into sand pack to test PPGs resistance to water and oil flow. PPGs reduced the permeability to water much greater than did for the permeability to oil during all the injection flow rates.

8. GEL PROPAGATION AFFECT ON NON-CROSS FLOW HETEOGENITY RESERVOIR

8.1. INTRODUCTION

Preformed particle gel were used as a diversion agent to correct permeability heterogeneity present in mature oil fields. The factors affecting the PPG's ability to increase oil recovery and decrease water production in non-cross flow heterogeneity reservoirs are discussed in the following section.

8.2. OBJECTIVES AND TECHNICAL CONTRIBUTIONS

This work was conducted in an attempt to study the behavior of a micron-size PPGs propagation through both high and low permeabilities by evaluating the following:

- Study the effect of permeability contrast ratio on the oil recovery factor before, during, and after PPG treatment.
- Determine the injection profile change after the gel treatment for both low and high permeabilities.
- Compare the oil recovery and water cut results obtained during the initial water flooding with results obtained after PPG treatment.
- Determine the oil produced from low permeability/un-swept zones after PPG treatments are introduce.
- Determine the blocking efficiency to water flow after the heterogeneity sand pack model is treated with PPGs.

- The ratio between the high permeability and low permeability zones is an important factor to be considered during PPG treatment. Understanding this factor helps improve a PPG's ability to increase the vertical sweep efficiency from un-swept low permeability zones.

8.3. EXPERIMENTAL DESCRIPTION

The following are descriptions of the materials and equipments which used to conduct the heterogeneity experiments.

8.3.1. Preformed Particle Gel. A superabsorbent polymer was used as a PPG to conduct these experiments. Dry particles with a mesh size of 170-200 (90-75 microns) were swollen in a 1% Sodium Chloride (NaCl) brine concentration. Gel concentrations of 2000 ppm was used.

8.3.2. Brine Concentration and Oil Viscosity. A 1 wt% NaCl solution was used for brine flooding and to prepare swollen PPGs. Heavy oil with a viscosity 195 cp at 70 °F was used to saturate the sand pack model.

8.3.3. Magnetic Stirring Vessel. An accumulator with a 1200 ml capacity and a maximum adjusted impeller speed of 1800 r/min was used to inject PPGs into a high permeability sand pack model. The impeller was placed at the bottom of the accumulator to keep the PPG dispersed in brine before it was injected into the model.

8.3.4. Sand Packs. Three sizes of silica sand were used to obtain different permeability contrasts between the models. Mesh sizes of 18-20, 50-60, and 100-120 were used to obtain low and high permeability sand packs. Silica sand was packed into two separate tubes that have the same length and area. The silica sand's size distribution as determined through sieving test is listed in Table 8.1.

Table 8.1—Size distribution of silica sand.

Sieves (mesh)	Size (microns)
18-20	1000-850
50-60	300-250
100-120	150-125

8.4. EXPERIMENTAL SETUP

The experimental setup used in this experiment is depicted in Figure 8.1. Two the same dimensions tubes with (20 cm in length and 2.7 cm in diameter) were used to contain the silica sand pack. Two horizontal (parallel in position tubes) were packed with different sand grains to emulate the permeability contrast present in reservoirs. A syringe pump was used to inject suspended PPG, brine, and oil from accumulators into the sand pack models. Two pressure transducers were mounted in front of each sand pack model to acquire the injection pressure change during the brine flooding and gel treatment processes. The test tubes was kept at the outlets of each sand pack to collect the volume of the effluents. The collected volume was used to determine gel penetration into each sand packs permeability.

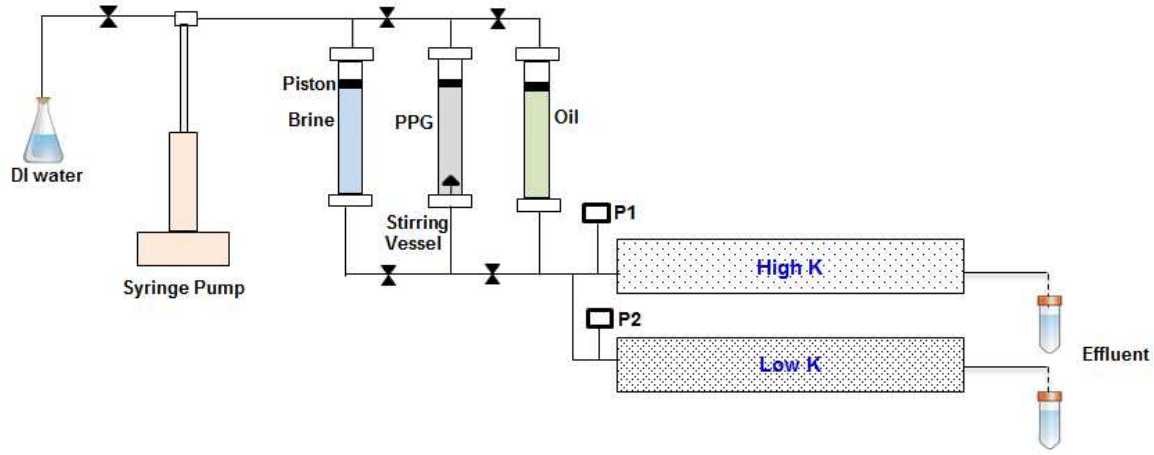

Figure 8.1—A schematic diagram of the non-cross flow experiment apparatus.

8.5. EXPERIMENTAL PROCEDURES

Parallel sand pack tests were used to simulate the non-cross flow heterogeneities present in oil reservoirs. The ratio between the high permeability and low permeability layers is an important factor to be considered during PPG treatment. Three experiments were conducted with varying layer permeability contrast ratio as a part of this parallel heterogeneity study. The permeability contrast ratio was between the high permeability and low permeability zones as follows: 44, 20, and 4.

The high permeability sand pack was kept nearly constant for all the three experiments. The low permeability sand pack, however, was varied. The rationale of keeping low permeability varied was to investigate the PPG's blocking efficiency in a high permeability zone at different permeability ranges. This study was investigated by evaluating the injection pressure, oil recovery factors, water cut, and injection profile obtained for each permeability ratio contrast.

The following subsections are the procedures used to carry out the experiments. They are briefly explained as follow:

8.5.1. Preparing and Saturating Sand Pack Models. A vibrator machine Was used to prepare the different sizes of silica sand so that the desire sand pack permeability could be obtained. A screen filter was fastened at the end each tube to prevent migrating sand during the flooding processes. Sand grains were added and vibration was used until the entire tubes was filled. The sand pack models were then vacuumed for at least 6 hr. The sand packs was fully saturated next with 1% NaCl to determine pore volume, porosity, and permeability. The sand pack models were each continued flushed with brine at different injection flow rates to ensure the model was 100% saturated with brine.

Heavy oil viscosity was injected from the accumulator into each sand pack at a rate of 1 ml/min. The oil was injected until no water was produced and the injection pressure became stable. The brine volume produced was recorded to determine the oil in place and the irreducible water saturation for each sand pack model.

The permeability, pore volume, porosity, irreducible water saturation, and original oil in place obtained for each experiment are summarized in Table 8.2.

Table 8.2—The sand pack properties for different permeability contrast ratio.

Case #	Permeability Contrast Ratio	Permeability (Darcy)	Pore Volume (gm)	Porosity (%)	Swi (%)	OIIP (cc)
1	44	High 22.1	41.87	34.84	26	30.8
		Low 0.5	24.9	20.72	12	21.8
2	20	High 22.4	32.60	30.72	27	21.93
		Low 1.1	35.40	33.35	18	32.60
3	4	High 21.7	35.7	33.64	25	26.70
		Low 6.2	39.60	37.31	8	36.60

Finally, the sand pack permeabilities (low and high) were connected to each other (as illustrated in Figure.8.1) and the first water flooding process was began.

8.5.2. First Water Flooding. A 1% NaCl was injected into both low and high permeabilities at a rate of 1 ml/min to simulate secondary oil recovery conditions. Oil and water productions from each permeability was recorded separately for every 3 ml,. The brine was injected into the sand packs until no oil was produced and the brine injection pressure became stable. Both oil recovery and water cut were determined for the low and the high sand pack permeabilities during the first water flooding.

The PPGs that had been swollen in 1% NaCl with a concentration of 2000 ppm were injected into the sand packs at a rate of 1 ml/min after the first water flooding processes was complete. The volumes of oil and water production at outlet were monitored during an injection 0.5 PV of PPG. The gel injection pressure was also recorded to determine the gel propagation's response into low and high permeabilities.

8.5.3. Second Water Flooding. A 1% NaCl was injected again at same injection rate after PPG treatment to test the gel blocking efficiency for high permeability. The PPG performance as a diverting agent to improve oil recovery from low permeability (un-swept zones) was also determined. Brine was also injected until no oil was produced at the outlets and the injection pressure became stable.

The above procedures were all repeated for the three experiments conducted. The oil recovery factor, the water cut, and the injection profile were each determined for the low and the high permeability sand pack models.

8.6. RESULTS AND ANALYSIS

The injection pressure, the oil recovery, the water cut, and the injection profile results obtained for the three permeability contrast ratios are discussed systematically as follow.

8.6.1. Injection Pressure Measurements. The injection pressures of the first water flooding, PPG injection, and second water flooding of the three layer permeability contrast ratios are plotted in Figures 8.2, 8.3, and 8.4. All three injection pressures changed in similar manner. These changes are discussed in the following subsections.

8.6.1.1. First water flooding. The injection pressure's drop was slightly different At each low and high permeability. These differences were related to the differences in permeability between the layers. Water was injected until the injection pressure became stable. The pressure became stable for both k when approximately 2 PV of brine was injected. Most of the water injection pressure for the three permeability contrasts became stable at approximately 0.5 psi.

8.6.1.2. PPG treatment. The PPG injection pressure rose significantly more than the previous injection pressure during water flooding. It increased sharply in both the low and the high permeability layers. PPG injection pressure was less obvious in low permeability layers than in high permeability. This finding indicates that a considerable amount of PPGs flew into high permeability layers and a small amount of gel particles flew into low permeability layers. The PPG injection pressure for most permeability contrasts were above 5 psi (approximately 10 times more than the pressure recorded during the first water flooding). The PPG injection pressure did not became stable because only 0.5 PV of PPG was injected.

8.6.1.3. Second water flooding. Water was injected again after the PPG was injected to determine the effect of PPG on the injection pressure measured at the low and high permeability. The blocking efficacy of PPG to water flow in low and high permeability layers were also obtained. The water injection pressure began to decline, becoming stable after approximately 0.5 PV water was injected. The second water injection pressure was compared to the first water flooding. This injection pressure was still much larger for all of the water injection pore volumes. The injection pressure increased between 5 to 20 times more than the injection pressure recorded before PPG treatment. The injection pressure for both the low and the high permeabilities changed little during the water flooding process. The first case of heterogeneity layer, however, the injection pressure for the high permeability was slightly larger than the low permeability layer.

8.6.1.4. Effect of permeability contrast ratio. A comparison between the injection pressures changes for the different permeability contrast layers as a function of the injection pore volume is illustrated in Figure 8.5. The injection pressure drop in all of the tested permeability contrast layers began nearly at the same range each time. The injection pressure rose sharply when 0.5 PV of PPG was injected. The injection pressure for case # 3 was much lower than the pressure recorded for both cases # 1 and # 2. This trend occurred because too much PPG volume suspension was transported into the low permeability packs (case #3) producing a higher degree of blocking in these zones. The permeability contrast in case # 3 also had less heterogeneity than did the other two cases, creating more uniform brine distribution flew into the low and high permeability layers.

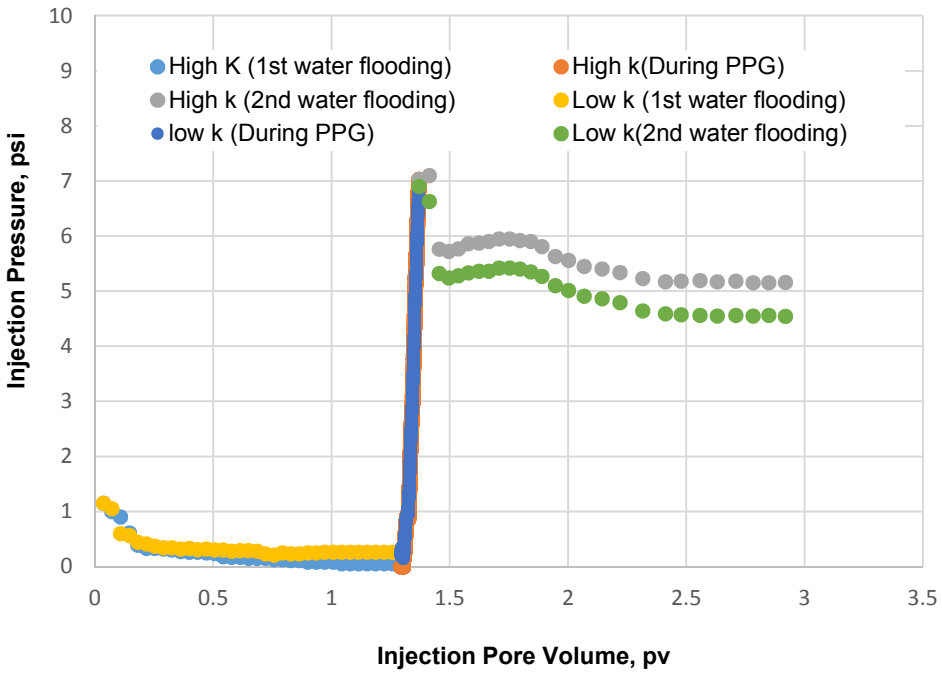

Figure 8.2—Injection pressure measurement for case # 1.

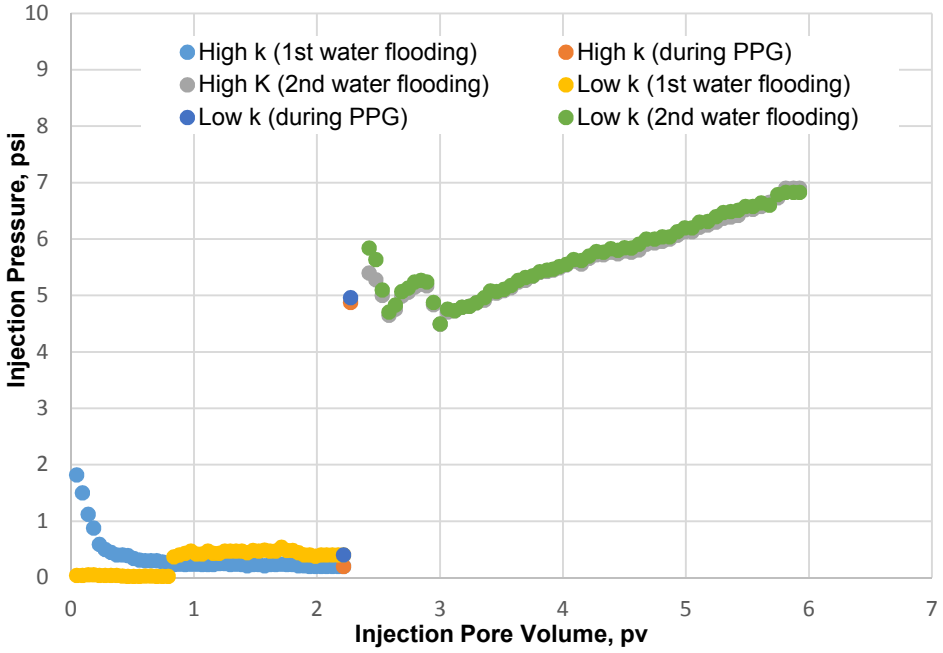

Figure 8.3—Injection pressure measurement for case # 2.

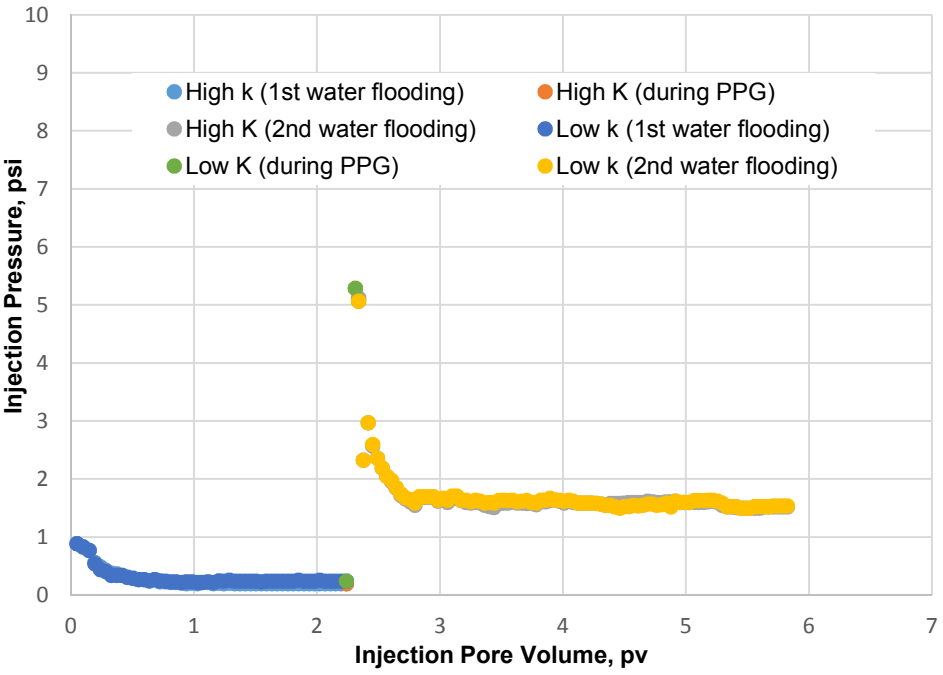

Figure 8.4—Injection pressure measurement for case # 3.

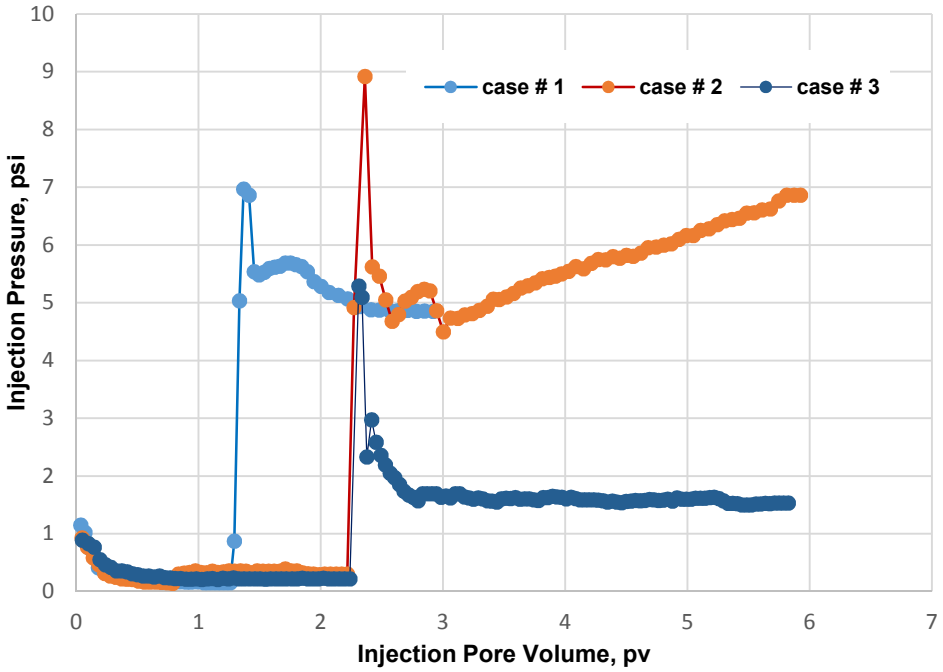

Figure 8.5—The injection pressures for the different permeability contrast ratios.

8.6.2. Water Cut Measurements. The water cut curves of the first water flooding, the PPG injection, and the second water flooding of the three layer permeability contrasts are plotted in Figures 8.6, 8.7, and 8.8. All five water cut curves changed in a similar manner.

8.6.2.1. First water flooding. Large differences in the water cut were observed between the low and high permeability packs during the first water flooding. This flooding was primarily transported through high permeability layers. The water cut in the high permeability zones was higher than 90%. The water cut in the low permeability was between a negligible percentage and 0% (as indicated by water cut curves). This finding typically happens to water flooding in heterogeneous reservoirs when large areas of low permeability zones are untouched during the secondary recovery mechanisms.

8.6.2.2. PPG treatment. The water cut in low permeability layers began to increase when PPG were injected into the heterogeneity model. The water cut in the low permeability zones rose significantly more than during the previous water flooding. The fractional flow reached 100% in case #1 and between 10% and 40% in cases # 2 and # 3. The total water cut declined at the end of the PPG injection in both the low and the high permeability layers as illustrated in Figures 8.6, 8.7, and 8.8. The water cut decreased to below 50% for all of the tested permeability contrasts. This decline in water cut indicates that PPGs can effectively block the water channels and divert the water floods to displace oil from low permeability layers.

8.6.2.3. Second water flooding. The water cut began to decrease in the high permeability layers and increase in the low permeability layers when the water flooding was resumed. The water cut in the low permeability layers fluctuated during the first few pore volumes. It fluctuated between approximately 70% and 80% in the beginning. It rose above 90% at the end of water flooding. The total water cut reduced by approximately 20% in all the treated permeability layers ratios.

The water cut in the low permeability layers was significantly higher than that in the high permeability layers during the second water flooding in case# 3. The water cut in the high permeability layer became 0%. It became higher than 80% in the low permeability layer. Reversions in the water cut because most of the injected PPG was propagated through high permeability layers, blocking the injected water flow's paths.

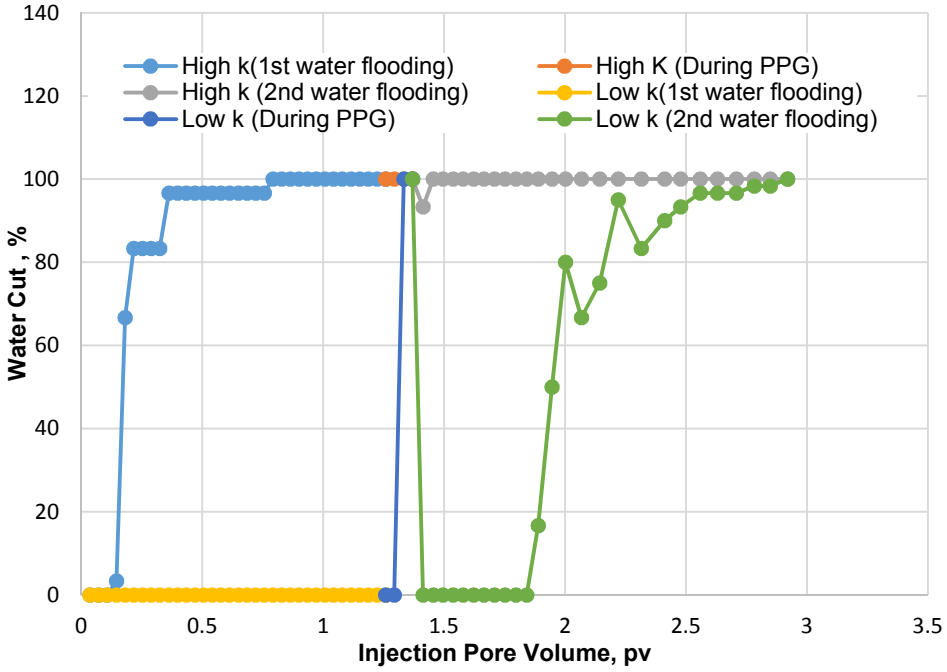

a) Water cut for each low and high permeability**.**

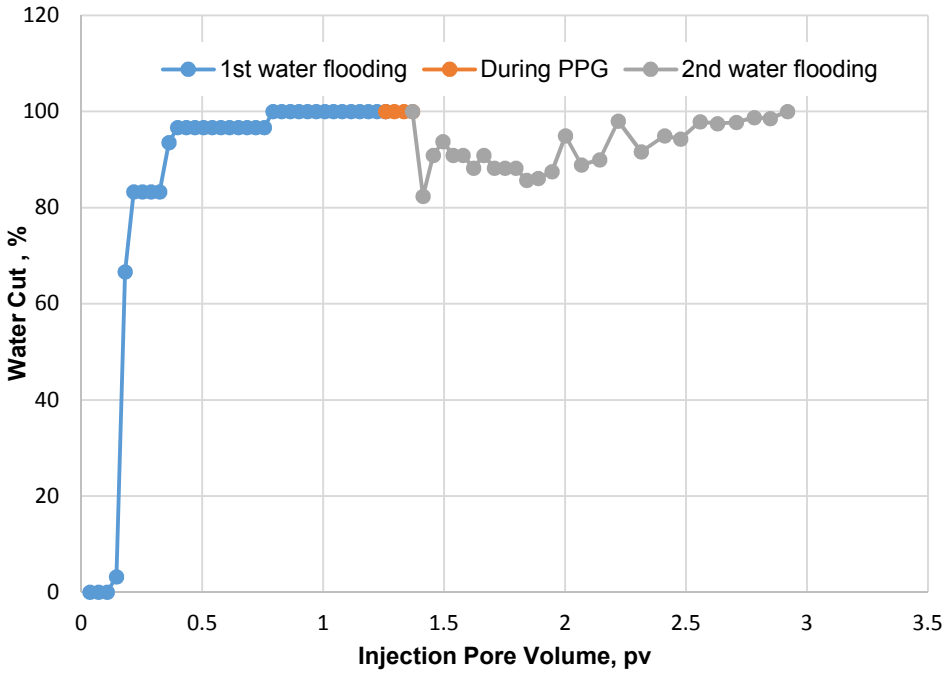

b) Water cut for total permeability model**.**

Figure 8.6—The water cut measurements for case #1.

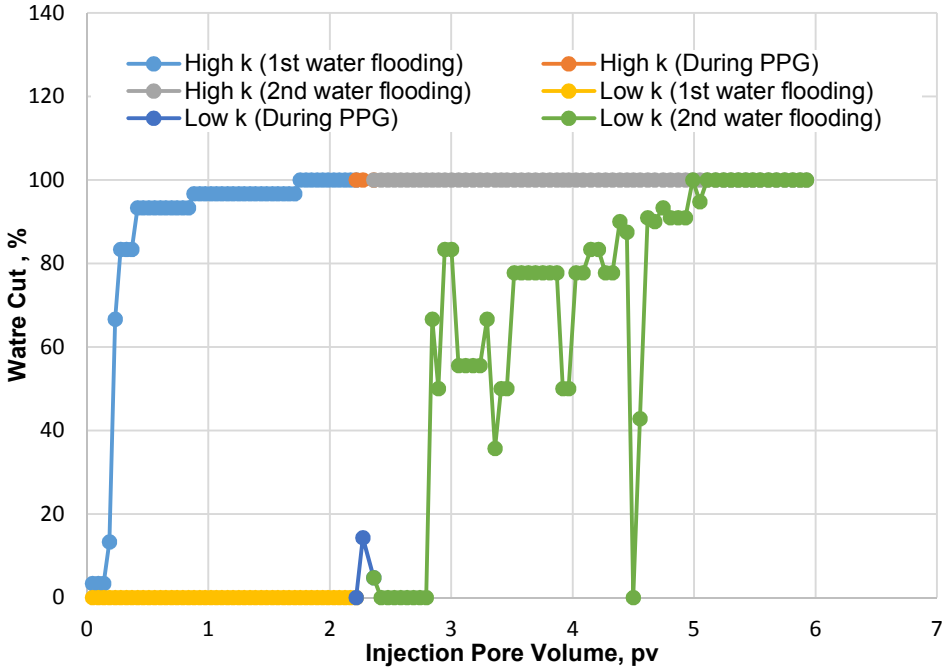

a) Water cut for each low and high permeability.

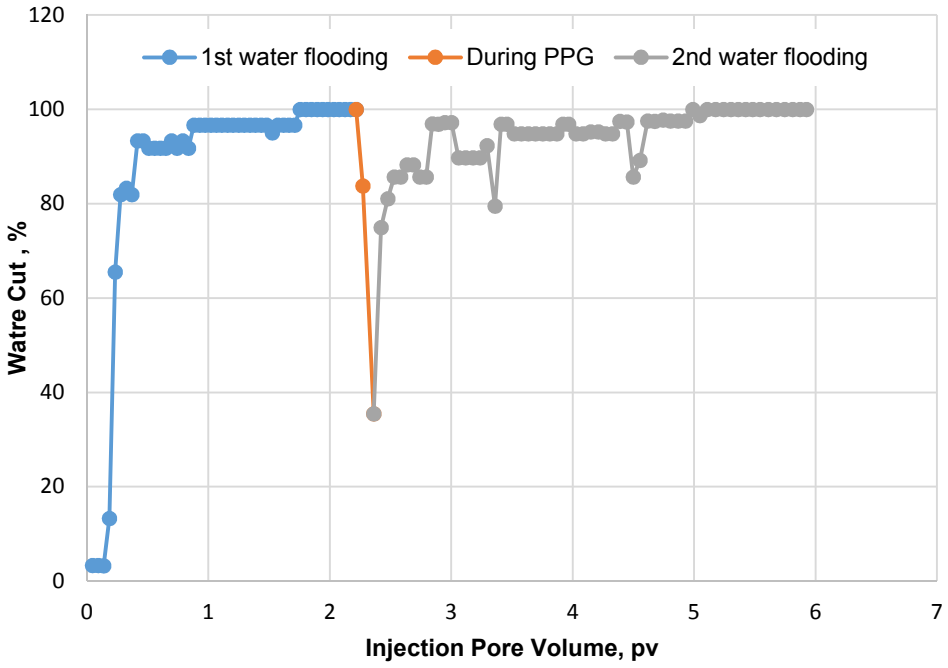

b) Water cut for total permeability model.

Figure 8.7—The water cut measurements for case #2.

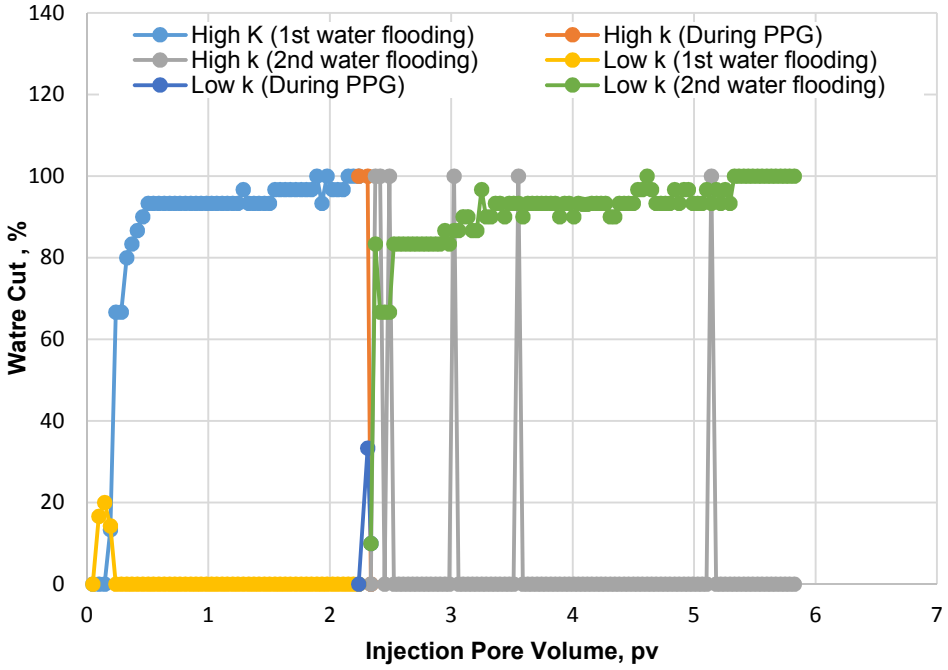

a) Water cut for each low and high permeability.

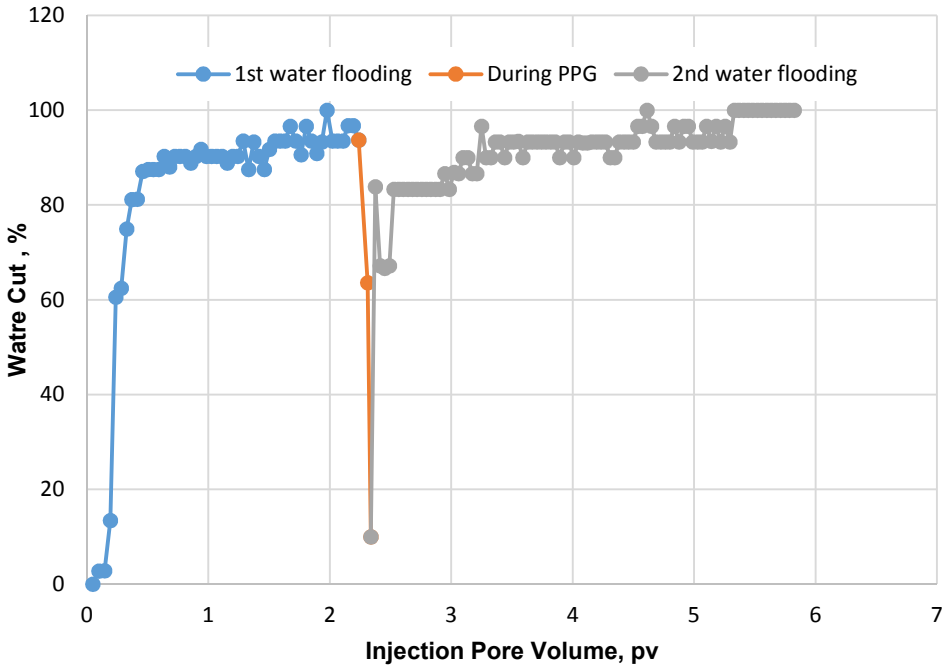

b) Water cut for total permeability model.

Figure 8.8—The water cut measurement for case #3.

8.6.3. Oil Recovery Measurements. The oil recovery curves of the first water flooding, the PPG injection, and the second water flooding of the three layer permeability contrasts are plotted in Figures 8.9, 8.10, 8.11, 8.12, 8.13, and 8.14. The oil recovery was determined for low, high, and total permeabilities as a function of pore volume injection.

In the initial water flooding stage, a large volume of oil was recovered from high permeability compared to a very small volume of oil was recovered from low permeability sand layers (Figures 8.9, 8.11, and 8.13). The recoverable oil volume from the low permeability layer decreased substantially as the sand pack's permeability contrast ratios increased. The recovery factors for the permeability contrast ratios of 4, 20, and 44 were 20, 1.9, and 0.9, respectively. A larger amount of water injection was flew through the high permeability than it was through low permeability. Therefore, low oil recovery was obtained from the low permeability layers. Nearly all of the injected water was diverted into high permeability layers during this stage. More than 4 PV of water was injected through high permeability layers. In contrast, less than 0.1 PV of water was injected through the low permeability layers.

The cumulative oil recovery of the high permeability layer (upper curve), the total oil recovery (middle curve), and the low permeability layer (lower curve) is illustrated in Figures 8.10, 8.12, and 8.14. The oil recovery of the high permeability layers during the first water flooding was higher than that in the low permeability layers. The oil recovery reached approximately 70% in the high permeability; it reached approximately 7% in the low permeability layers. As a result, the high permeability contrast ratio created a large remaining oil saturation in low permeability layers.

The oil produced from the low permeability layers did not reach the level of oil produced from the high permeability layers. The sweep efficiency of the heterogeneity improved and oil recovered from the low permeability began to rise during PPG injection. The oil recovered from the low permeability layer increased substantially more than that recovered from the high permeability layers. The recovery factor obtained from the low permeability layer at permeability contrast ratios of 4, 20, and 44 increased to 30, 18, and 3, respectively. This oil production increase from low permeability layer indicates the PPGs diverted most of the water injection flow to low permeability layers.

A significant amount of oil recovery was recovered from the low permeability layers during the second water flushing. A large amount of PPG suspension remained in the high permeability layers, helping reduce the permeability contrast between layers. PPGs also helped improve sweep efficiency of the heterogeneity layers and increased the amount of recovered oil from the low permeability layer during the second water flooding. The oil recovered from the low permeability layer rose substantially more than it did in the high permeability layers. The recovery factor obtained from the low permeability layer at a permeability contrast ratio of 4, 20, and 44 was increased to 93, 61, and 38, respectively. This significant increase in oil recovery reveals the PPGs efficiency in blocking high permeability layers and diverting most of the water flooding flow to low permeability layers.

The oil that was recovered from the low permeability layers increased, approaching the amount of the total oil recovery that was revealed, during the second water flooding (see Figures 8.10, 8.12, and 8.14). The oil that was recovered from a low permeability layer was slightly higher than the amount of oil recovered from a high

permeability layer at the end of second water flooding when the permeability contrast ratio was 4. The oil recovered from a low permeability layer reached 93 % at the end of the flooding mechanisms. The oil recovered from the high permeability layer reached 80 %. Thus, PPGs can effectively increase the oil recovered from rich low permeability layers.

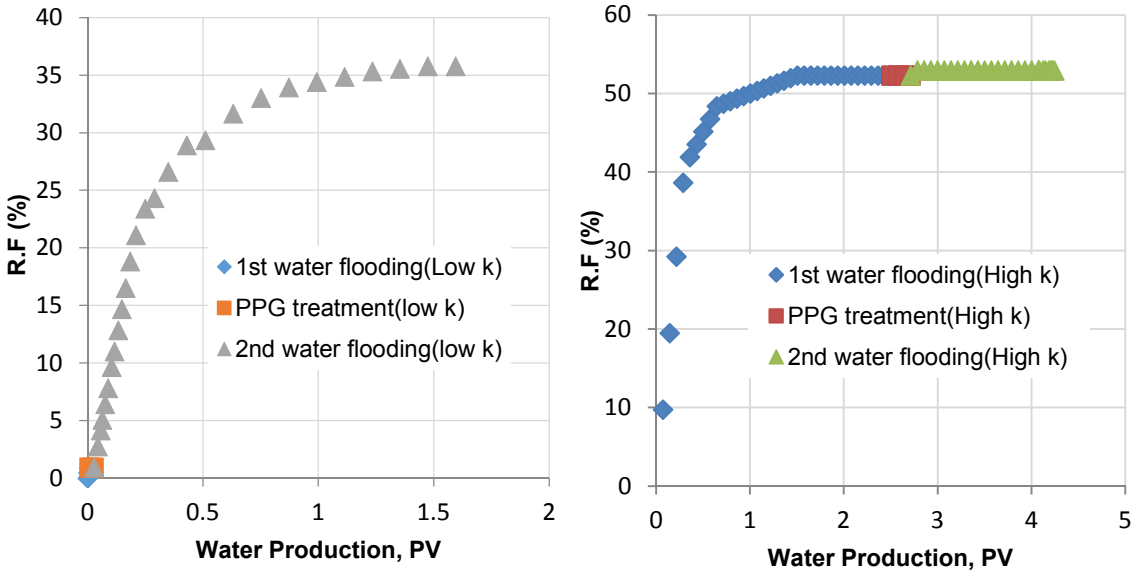

a) Oil recovery for a low k (0.5 Darcy). b) Oil recovery for a high k (22.1 Darcy).

Figure 8.9—The oil recovery measurements for case # 1.

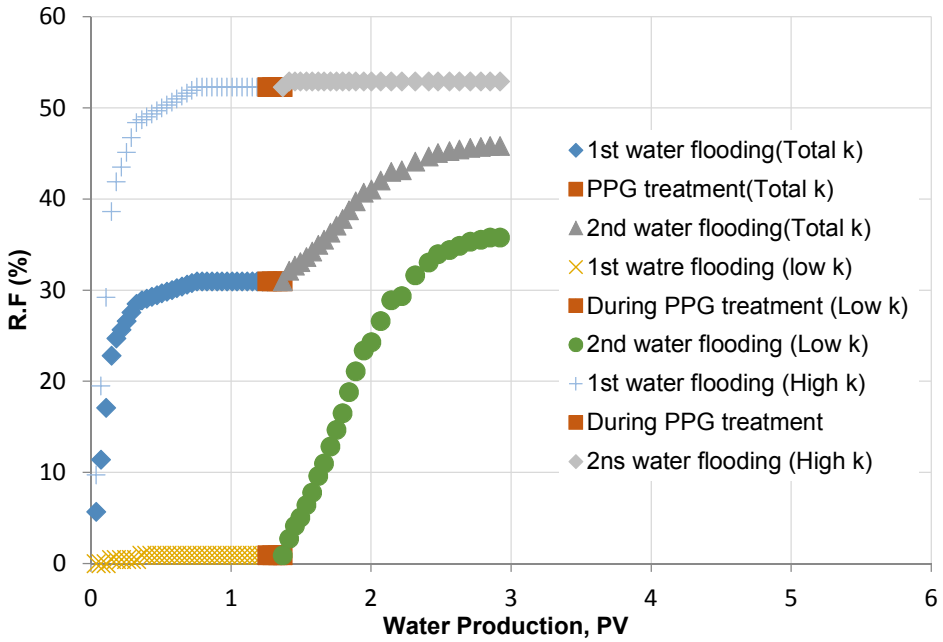

Figure 8.10—The oil recovery for low, high, and total permeabilities for case # 1.

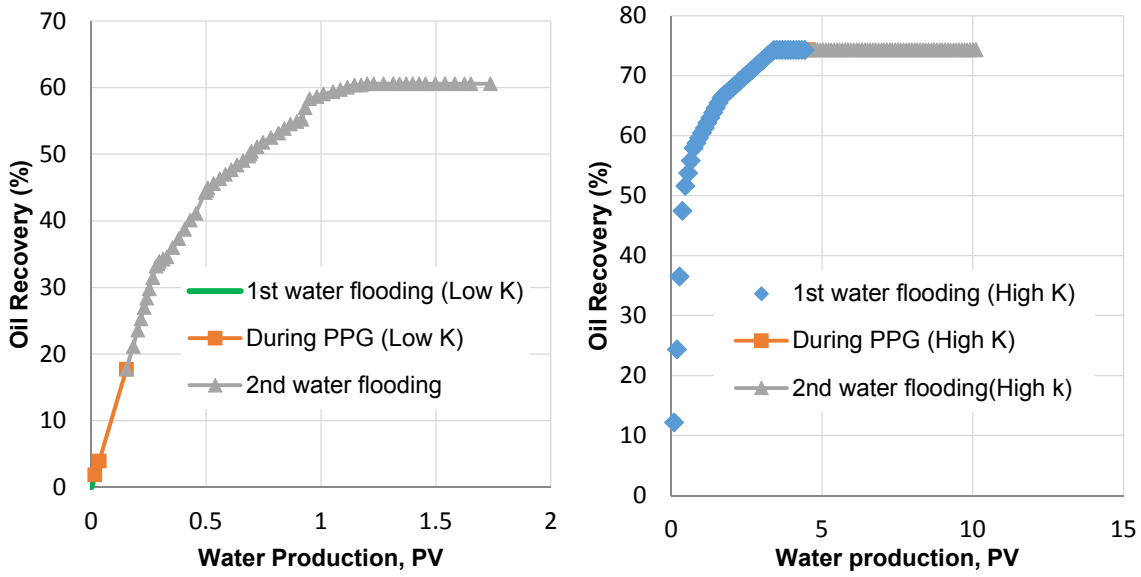

a) Oil recovery for a low k (1Darcy). b) Oil recovery for a high k (20 Darcy).

Figure 8.11—The oil recovery measurements for case # 2.

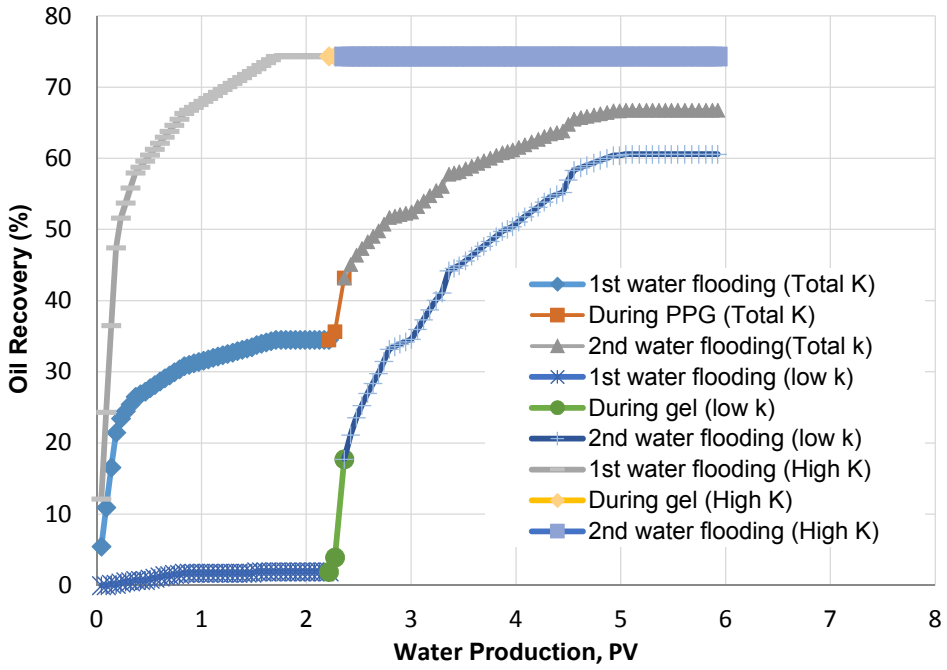

Figure 8.12—The oil recovery for low, high, and total permeabilities for case #2.

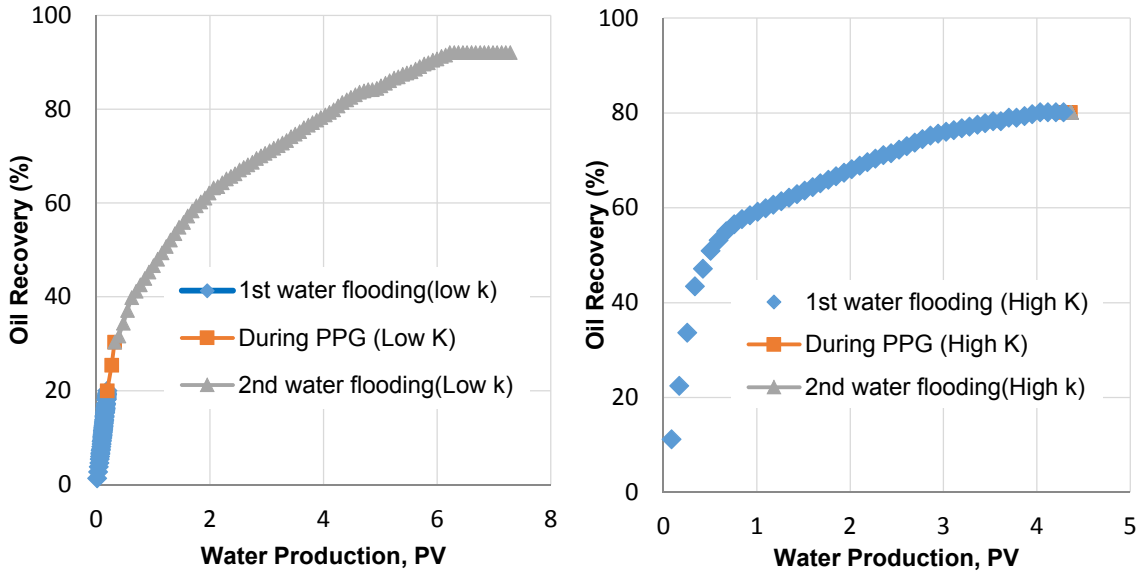

a) Oil recovery for a low k (6.1 Darcy). b) Oil recovery a high k (22 Darcy).

Figure 8.13—The oil recovery measurements for case # 3.

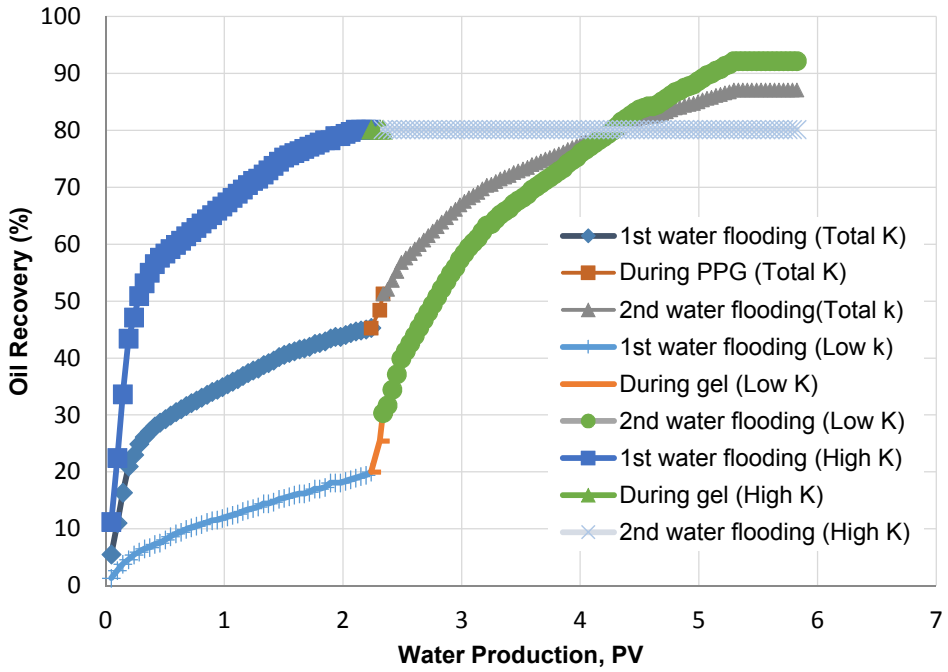

Figure 8.14—The oil recovery for low, high, and total permeabilities for case #3.

8.6.4. Effect of Permeability Contrast Ratio. The results of the permeability contrast ratio of 44, 20 and 4 were compared to study one another the effect of the non-cross flow heterogeneous formations on cumulative oil production. This comparison was carefully monitored before, during, and after the PPG injection. The results help to understand at which permeability ratio oil recovery was increased the most. They also help to determine at which permeability ratio, PPG was more applicable to improve sweep efficiency in low permeability formations.

The oil recovery results obtained for each permeability contrast ratio during the first water flooding, during the PPG injection, and after the second water flooding are listed in Table. 8.3. Both the final oil recovery and the ratio of incremental recovery recorded for every permeability contrast are listed in this Table as well. The ratio of

incremental oil recovery was calculated based on ratio of the oil recovery increase from low and high permeabilities. The incremental ratio results were used to determine at which permeability ratio PPGs are more efficient at increasing the amount of recovered oil from low k.

The results indicate that amount of oil that can be obtained from the whole flooding mechanisms. This smaller permeability contrast (less heterogeneous reservoirs) produced more uniform injection water distribution than did the higher permeability contrast ratio. The final oil recovery obtained from a low permeability layer was 93% when permeability contrast ratio was 4, while it was only 38% when permeability contrast was ratio 44. As a result, the amount of the total oil recovered from both low and high permeability layers reached 88% and 47%, respectively.

The results obtained for the ratios of the incremental oil recoveries (low permeability to high permeability) indicate that the higher permeability contrast produce a larger oil recovery than did the lower permeability contrast. Thus, the PPGs ability to increase the amount of oil recovered from a low permeability zones increased as the permeability contrast ratio increased. The ratios of the incremental oil recoveries was 4.6 (93/20) for a permeability ratio of 4, 31.5 (60/1.9) for a permeability ratio of 20, and 40 (36/0.9) for a permeability ratio of 44. These results revealed that as the reservoir become more heterogeneous, PPGs ability to improve sweep efficiency and recover oil from low permeability become more obvious and effective.

Table 8.3—A summary permeability contrast ratio.

Permeability Contrast Ratio	Permeability, Darcy	Oil recovery (%)			Oil Incremental Recovery	Ratio of Incremental Recovery	Total Oil Recovery,%
		1st Water Flooding	PPG Treatment	2nd Water Flooding			
44	High 22.1	52.2	52.2	52.2	1	40	45.8
	Low 0.5	0.9	0.9	36	40		
20	High 22.4	74	74	74	1	31.5	66.7
	Low 1.1	1.9	1.9	60	31.5		
4	High 21.7	80	80.1	80.2	1	3.9	86
	Low 6.2	20	31.7	93	4.6		

8.6.5. Improve Injection Profile. Injection is one of the most common reservoir problems created by reservoir heterogeneity. The production/injection flow percentage was used in this study to evaluate injection profile change as a result of PPG treatments. This flow is the ratio of the total production volume of oil and water obtained from each permeability layer to the total brine injection volume. This parameter helps clarify how the injection profile changes as a result of PPG treatments. It provides a quantitative value of how much fluid is produced during the first water flooding, during the PPG, and after the second water flooding. The production profile change between the low and high permeability sand pack was calculated as.

$$Injection\ profile = (\frac{Vp}{Vi}) \times 100 \quad \text{..... (8.1)}$$

where V_p is the cumulative volume of total fluid produced at each permeability and Vi is the cumulative volume of total water injected.

When production profile increased to 100% means injection water flew through that permeability layer started to increase. If production profile was decreased to less than 100% means water injection through that permeability layer started to decrease. If the production profile equals 100% all of the total water injected flew through the permeability layer. The injection profile curves of the first water flooding, the PPG injection, and the second water flooding of the three layer permeability contrast are plotted in Figures 8.15, 8.16, and 8.17. All the three production profiles had similar changes. A poor injection profile was identified during the first water flooding for all of the low permeability layers. A high production profile trend was identified for the high permeability layers. The injection profile was less than 5% in the low permeability layers; it was above 80% in high permeability layers. Thus, more than 80% of the total water injection that was used in the first water flooding was transported into the high permeability layers. This large water injection transported explains the high amount of remaining oil saturation that was not produced from low permeability zones.

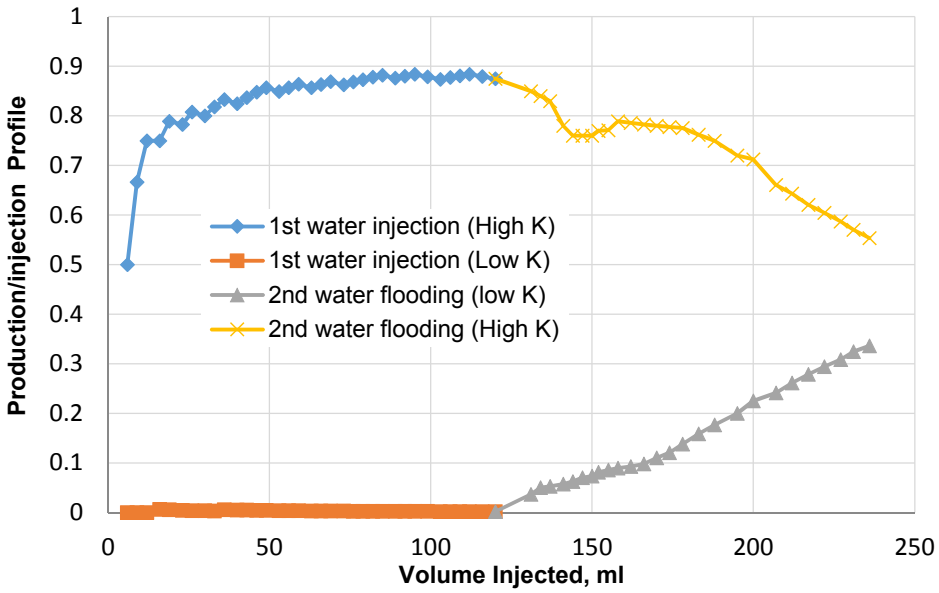

Figure 8.15—The injection production profile for a permeability contrast ratio of 44.

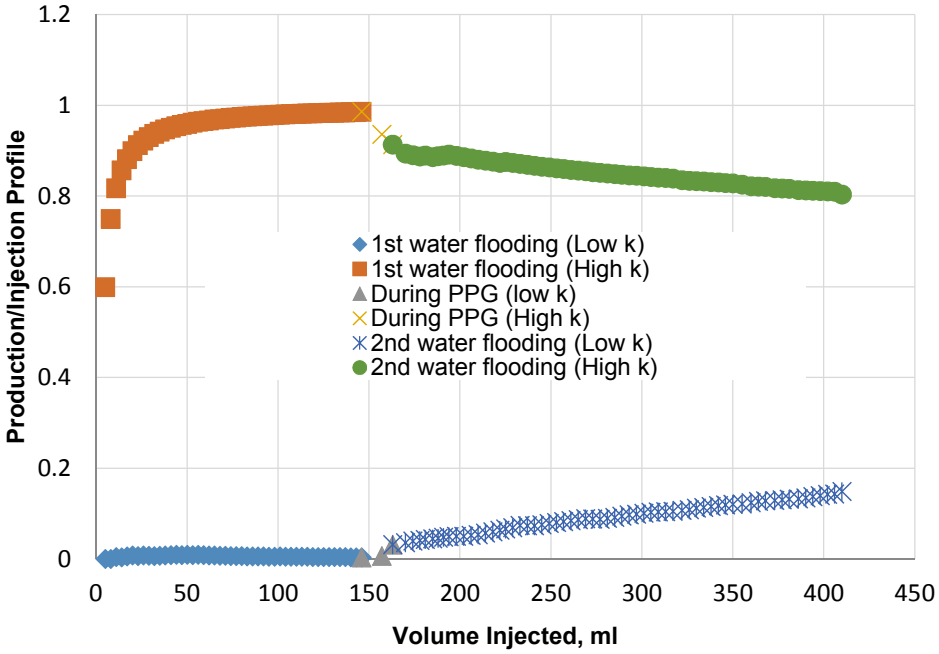

Figure 8.16—The injection production profile for a permeability contrast ratio of 20.

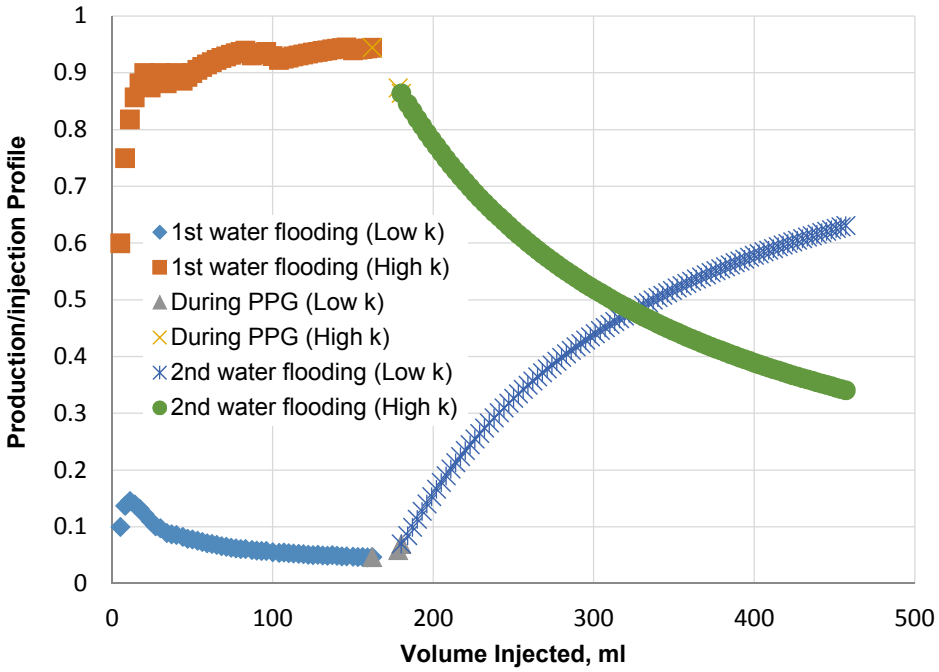

Figure 8.17—The injection production profile for a permeability contrast ratio of 4.

The injection profile began to improve in the low permeability layers once the PPGs injected into the heterogeneous permeability. The injection profile in the high permeability declined by approximately 10% while it increased in the low permeability by approximately 3 %. The profile change indicates that the PPG plugged the high permeability zone gradually and diverting the water injection to low permeability layers.

The injection profile was significantly improved after the PPG treatment was complete. It began to increase in the low permeability layer during the second water flooding; it began to decrease in the high permeability layers. Thus, the PPG effectively diverted most of the injection water to sweep the large oil remaining in the low permeability layers. The injection profile in the low permeability layers reached an average between 15 and 60%. It decreased to 30 and 50% in high permeability layer.

Several cases (a permeability contrast of 4) the injection profile in the low permeability layer was improved significantly more than in the high permeability layers, reaching 63% in the low permeability and 34 % in the high permeability. This difference in injection profiles was a result of the permeability contrast effect; the low permeability contrast had a higher injection profile than the others. Therefore, PPG can effectively divert more than 60% of the water injection into the low permeability layers.

The final injection profile percentages determined both before and after the PPG treatment are listed in Table 8.4. A significant improvement in the water injection volume in low permeability layers occurred as a result of the PPG injection.

Table 8.4—The final production improvements for the three permeability contrasts.

Permeability Contrast Ratio	Permeability, Darcy	Injection Profile,%	
		1st Water Flooding	2nd Water Flooding
44	High 22.1	88	55
	Low 0.5	0.1	33.6
20	High 22.4	83	80
	Low 1.1	0.5	15
4	High 21.7	90	34
	Low 6.2	5	63

8.7. CONCLUSION

This section was focusing on evaluate the use of PPG to improve the conformance control in non-heterogeneity formations. Three different ranges of permeability contrast were tested. Water cut, oil recovery, and injection profile were determined. The following are the main conclusions drawn from this section:

- The effect of PPG on improving sweep efficiency and recovering more oil from low permeability became more obvious and effective as the sand pack model became more heterogeneous.
- Oil recovery from the low permeability sand packs improved significantly after the PPG injection was complete. The oil recovery incremental was strongly dependent on the permeability contrast ratio.
- The oil recovery incremental from that was obtained from the low permeability was larger than that obtained from the high permeability. The

oil recovery incremental ratio revealed better oil improvement at a large permeability contrast ratio.

- Injection profile improved significantly after the PPG treatment. In some cases (e.g., permeability contrast of 4) the injection profile in low permeability was improved much larger than in high permeability layers. It reached approximately 63% in the low permeability and approximately 34 % in the high permeability.

9. GEL PROPAGATION EFFECT ON CROSS FLOW HETEROGENITY RESERVOIRS

9.1. INTRODUCTION

To make the research more robust and to provide a deep understanding of the effect of heterogeneity on oil recovery mechanisms during water flooding, the research was extended to study also the cross-flow heterogeneity problems. Various scenarios of crossflow heterogeneity presented in mature oil field reservoirs were investigated. Preformed particle gels (PPGs) were also evaluated for their ability to increase the amount of oil recovered from crossflow heterogeneous formations after they were flooded with water.

9.2. OBJECTIVES AND TECHNICAL CONTRIBUTIONS

This study was conducted in attempt to investigate the behavior of micron PPG propagation through unconsolidated sandstones. These cores have interaction flow communication between their layers. The objective can be met by evaluating the following:

- Determine whether or not the oil recovery improved after the PPG was injected into the heterogeneity sand pack model.
- Evaluate the gel's ability to plug water injected into high permeability zones.
- Study the effect of PPG slug pore volume on improving oil sweep efficiency.

- Evaluate the factors that influences a PPG's ability to reduce the water cut during water flooding processes.
- Evaluate the use of hydrochloric acid to treat the gel filter cake formed on the surface of low permeability zones during a PPG injection. Evaluate this acid treatment based on both the injection pressure behavior and the oil recovery improving.
- The results gathered from this study will be tremendously beneficial when designing a PPG injection. They will clarify the PPG mechanisms needed to divert the water injection to produce more oil from un-swept zones. The results gathered from this study can be used to build a numerical simulator that matches the field application use. The knowledge obtained from both the cross flow heterogeneity sand pack investigation and a previously homogenous sand pack investigation will provide a clear vision of a PPG design and select a best well candidate for conformance control treatment.

9.3. EXPERIMENTAL DESCRIPTION

9.3.1. Preformed Particle Gel. A superabsorbent polymer was used as a PPG to conduct these experiments. Dry particles with a mesh size of 170-200 (90-75 micron) were swollen in a 1% NaCl brine concentration. Gel concentrations of 2000 ppm were used.

9.3.2. Brine Concentration and Oil Viscosity. A 1 wt% Sodium Chloride (NaCl) solution was used for brine flooding and to swell PPG. Oil with a viscosity 37 cp at 70 °F was used to saturate the sand pack model.

9.3.3. Magnetic Stirring Vessel. An accumulator with a 1200 ml capacity and a maximum adjusted impeller speed of 1800 r/min was used to inject PPGs into the high permeability sand pack model. An impeller was placed at the bottom of the accumulator to keep the PPGs dispersed in brine before they were injected into the model.

9.3.4. Sand Pack. Two sizes of silica sand were used to obtain different permeabilities. Both a 18-20 and 80-100 mesh sizes were used to obtain high and low permeabilities, respectively. A vibrator was used to pack the silica sand into the model. The size distribution of the silica sand used in the experiments, as determined by a sieving test is listed in Table 9.

Table 9.1—Size distribution of silica sand.

Sieves (mesh)	Size (microns)
18-20	1000-850
80-100	180-150

9.4. EXPERIMENTAL SETUP

The experimental setup used in this experiment is illustrated in Figure 9.1. It was constructed of a stainless steel round tube with a diameter of 2 inches and 1 ft length with 3 different pressure taps was assigned to monitor fluid and PPG flow. A round hole perforated screen tube with diameter less than 1 inch was inserted inside the stainless steel round tube. Large sand grains (18-20 mesh size) were poured first inside the stainless steel around the perforated screen tube. Fine sand grains (80-100 mesh size) were then poured inside the perforated screen. A vibrator was used for both sizes to

enhance sand packing inside the model. A syringe pump was used to inject suspended PPG, brine, and oil from accumulators to the crossflow heterogeneity model. Pressure transducers were mounted in front and along the sand pack model to acquire the injection pressure change during brine flooding and gel treatment processes. The test tubes were kept at the outlet to collect the volume of the oil and water productions.

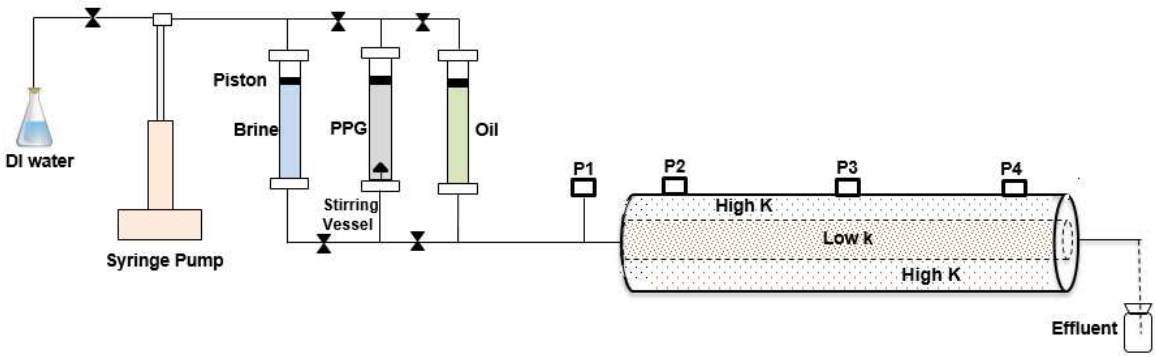

Figure 9.1—The cross flow heterogeneity apparatus.

9.5. EXPERIMENTAL PROCEDURES

The procedures followed during the non-cross flow heterogeneity experiments are described briefly here.

9.5.1. Preparing and Saturating Sand Pack Models. A vibrator machine was used to prepare different sizes of silica sand do that the desire sand pack permeability can be obtained. Large sand grains 18-20 were used to provide a high permeability of approximately 30 Darcy. An 80-100 mesh size was used to provide a low permeability of approximately 0.5 Darcy. Begin pouring the sand grains inside and around the perforated tube after fastened the end with screen filter to prevent migrating sand during flooding processes. The sand was poured and vibration was used until the entire tube was filled

with sand. The sand pack models were then vacuumed for at least 2 hr before they were fully saturated with a 1% NaCl solution. The pore volume and porosity of the whole cross-flow model were determined. Sand pack models were flushed with brine at different injection flow rates (1, 2, 4, and 6 ml/min) to ensure the model was 100% saturated with brine.

Oil viscosity with 37cp was injected from accumulator into the cross flow sand pack model at a rate of 1, 2, 4, 6, and 8 ml/min. Oil was injected until desirable connate water saturation was achieved. Table 9.2 summaries heterogeneity sand pack parameters obtained for the five performed experiments before starting with first water flooding process.

Table 9.2—A summary of the cross flow heterogeneity sand pack's properties.

Effects		Pore volume (gm)	Porosity (%)	Swi (%)	OIIP (cc)
PPG slug volume	0.5 PV	247.5	39.9	28.1	160.9
	3 PV	253	40	29.6	178.1
	5.5 PV	251.5	40	29.8	176.3
heterogeneity level	Large un-swept	244	39	28.7	173.8
	Less heterogeneity	214	34.5	10.6	191.3

9.5.2. First Water Flooding. A 1% brine NaCl solution was injected into the crossflow heterogeneity model at a rate of 2 ml/min to simulate secondary oil recovery conditions. Oil and water productions at effluent were recorded at every 3 ml. The brine was injected until no oil was produced and the brine injection pressure became stable. Overall, 3 PV of brine injection was sufficient to ensure no oil was produced at effluent., Both oil recovery and water cut were determined during the first water flooding.

9.5.3. PPG Treatment. Swollen PPG dispersed in 1% NaCl with a concentration of 2000 ppm was injected into sand packs at rate of 2 ml/min after completing the first water flooding processes. PPGs were injected in different values of pore volume to evaluate their effect on the oil recovery incremental. The volume of oil and water production at the outlet as well as PPG injection pressure was recorded for each experiment.

9.5.4. Second Water Flooding. Brine was injected again at the same injection flow rate after the PPG treatment was complete, to test the gel blocking efficiency for high permeability (swept zones from first water flooding). It also to determine the oil recovery incremental from the un-swept zones. Brine was also injected until no oil was produced at the outlets and the injection pressure became stable. Approximately 3 PV of brine was also injected so that could be compared to the results obtained to the results obtained from the first water flooding.

These procedures were repeated for each experiment. The oil recovery factor, water cut, and injection pressure were each determined during the water flooding and PPG treatments.

9.6. RESULTS AND ANALYSIS

9.6.1. Effect of PPG Slug Volume. Three volume ranges of PPG were used to test the affect of PPG injection pore volume on the oil sweep efficiency. PPG was injected in very small amounts (0.5 PV) so that only the sand pack face was treated. A simple sketch is given in Figure 9.2 that simplifies the injection and placing process 0.5 PV of PPGs into the planned target zone.

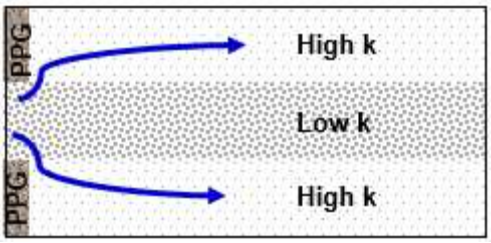

Figure 9.2—Inject 0.5 PV of PPG and its use to divert the water injection flow.

The second PPG volume slug was increased until it reached the first segment of the sand model. Approximately 3 PV of a PPG injection pore volume was used to reach the first segment of the sand model. A pressure reading from the first pressure sensor was used to locate the PPG propagation's length. A simple sketch is given in Figure 9.3 that simplifies the injection and placing 3 PV of PPGs into the planned target zone.

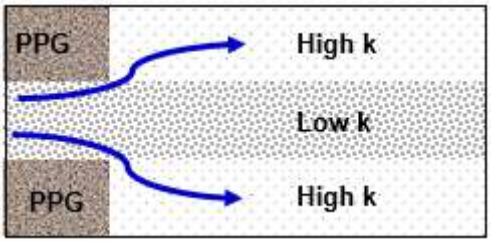

Figure 9.3—Inject 3 PV of PPG and its use to divert water injection flow.

The third PPG slug volume was used to investigate PPGs deep penetration affect when gel was injected until it reached the second sand pack segment. Approximately 5.5 PV of a PPG injection pore volume was used to reach the second sand segment section. A simple sketch is given in Figure 9.4 that simplifies the injection process, placing 5.5 PV of PPGs into the planned target zone.

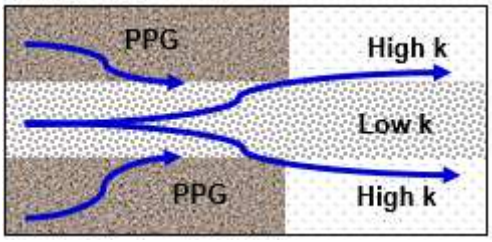

Figure 9.4—Inject 5.5 PV of PPG and its use to divert water injection flow.

9.6.1.1. PPG slug volume of 0.5 PV. Water was injected at rate of 2 ml/min into a heterogeneity model. A large amount of oil (Figure 9.5) was recovered and continued to increase until reach maximum oil recovery at 63%. A 3PV of a 1% NaCl solution was injected to reach the maximum oil recovery. Water cut as indicated in Figure 9.6 was also increased accordingly. It continued to increase until the end of the first water cycle. At the end of injecting the 3PV, the oil recovery stopped increasing and the water cut reached 100%. The injection pressure during the first water flooding recorded as a function of injection pore volume as shown in Figure 9.7. The injection pressure during this cycle was very low and fluctuating between 0.07 and 0.12 psi before it became stable at 0.08 psi. This pressure indicates the water was easily injected into and through the high permeability zone and sweeping most of the oil from this permeability.

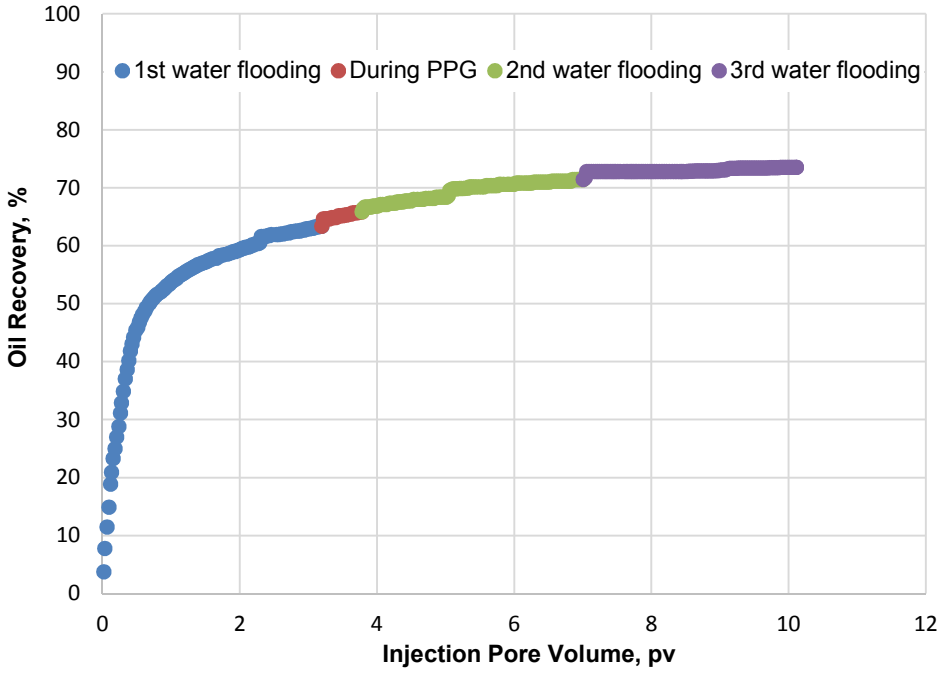

Figure 9.5—Oil recovery during water flooding and a PPG injection of 0.5 PV.

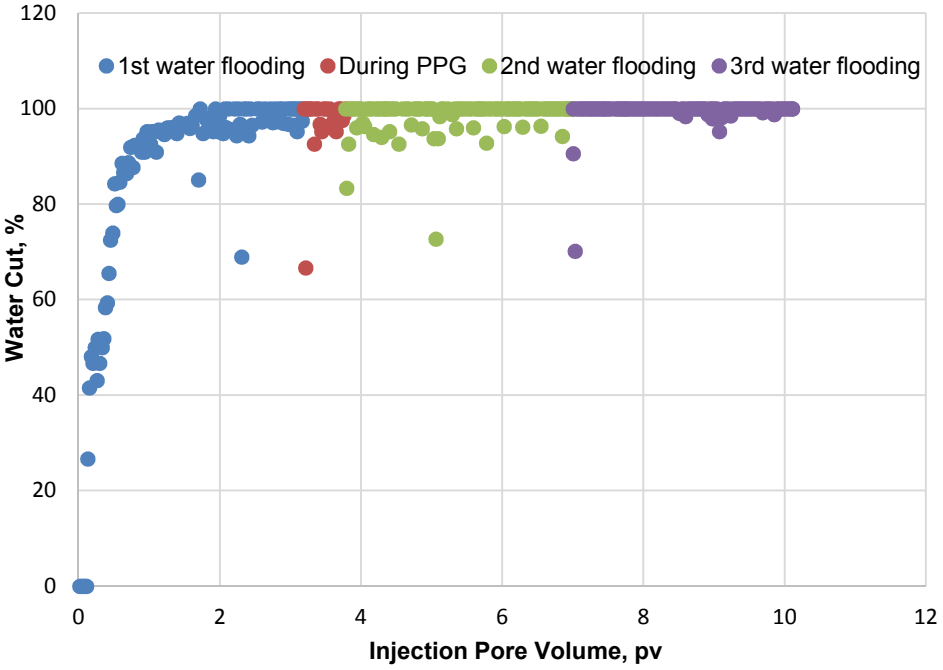

Figure 9.6—Water cut during water flooding and a PPG injection of 0.5 PV.

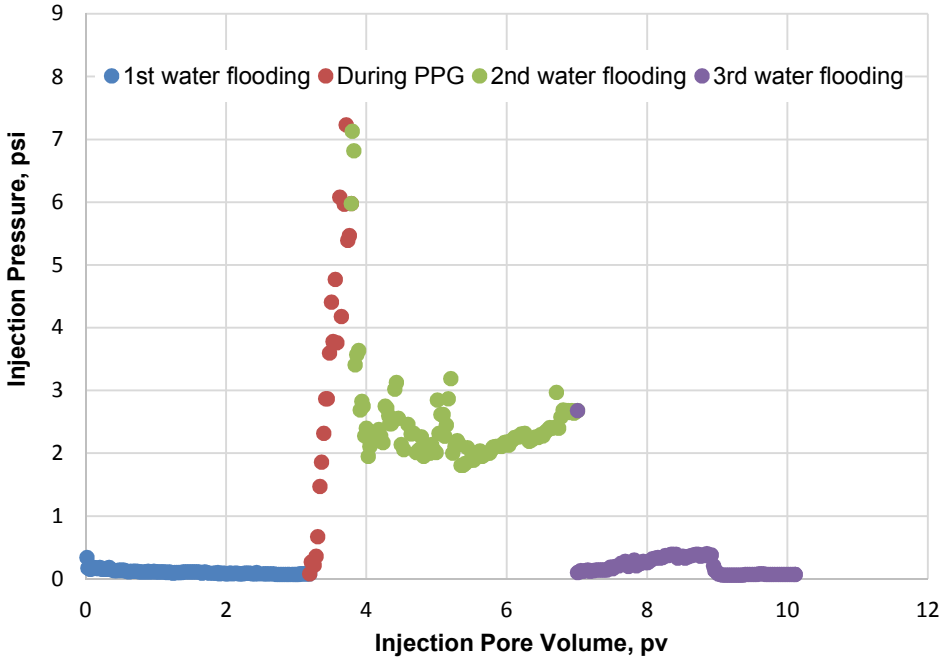

Figure 9.7—Injection pressure during water flooding and a PPG injection of 0.5 PV.

A PPG with a concentration of 2000 ppm was injected at the same injection flow rates (2 ml/min) for consistency purposes. Only 0.5 PV was injected into the model after the first water flooding process was complete. During this treatment an increase of oil recovery was noticed. The amount of oil increased by approximately 4% to reach approximately 67% of total oil recovered. Water cut measurements indicated a decrease in water production during the gel injection, allowing the oil production to increase. The water cut was reduced by a percentage range between 5 and 8%.

A significant change occurred in the injection pressure measurements during the gel injection; the injection pressure increased significantly, despite the small injection volume of PPG that was used. It increased 50 times greater than did the water injection pressure recorded during the first water stage injection. It peaked at 7 psi at the end of

the gel treatment process. This significant increase indicates the PPG effectively plugged the high preamble paths present within the sand pack.

Water was flooded again at the same injection flow rate to determine how much oil could be recovered after the gel treatment. This second water flooding was also used to test the PPGs blocking efficiency to water flow. Water injected until no oil was produced at effluent. Approximately 3 PV of water was injected which was similar to water injection pore volume used in the first water flooding. The oil recovery increased considerably during this water cycle. It continued to increase until it reached a stable recovery at 71%. This recovery revealed that approximately 5% of the recovery incremental was produced after the gel treatment. This incremental percentage illustrates PPG's ability to divert the water injection into an un-swept area to recover more oil. The water cut continued to change; this decrease was not stable during the second water flooding. The water cut returned to a 100% measurement level at the end of the water injection. The injection pressure dropped significantly (from 7 psi to around 2 psi) during the early injection pore volume of the second water flooding. It continued to fluctuate between 2 psi and 3 psi before it became stable at the end of the injection mechanism (at 2.6 psi). Despite this reduction in pressure, this water injection pressure remained greater than the water injection pressure recorded during the first water flooding. The injection pressure became stable in 2.68 psi in the second water flooding which was greater than stable injection pressure (0.08 psi) recorded during the first water flooding.

A small percentage volume of PPGs was likely propagated into the small permeability zones reducing its permeability. This reduction could decrease the amount of oil produced from this zones. Therefore, a syringe was used to flush a small amount of

acid, approximately 6 ml of 10% HCl volume into the sand pack face. The sand model was maintained for 24 hr for acid soaking purposes. The third water cycle was injected at the same injection flow rate (2 ml/min) to test the oil recovery and to evaluate the effect of HCl on PPG blocking efficiency. The amount of oil recovered increased slightly by approximately 2% oil incremental to reach 73.5% at the end of the water flooding. The acid stimulation mitigated/removed the gel particle filter cake, increasing the amount of oil recovered from low permeability zones. The water cut changed very little during this third water cycle staying at 100%. A noticeable change occurred in the injection pressure. This pressure decreased sharply from 2.68 psi to 0.13 psi after the acid treatment was complete. This pressure was almost similar to the original injection pressure before performed the gel treatment. The injection pressure increased slightly to 0.21 psi. A similar water injection pore volume (3 PV) was injected, decreasing the injection pressure until it became stable at 0.07 psi. The stable injection pressure obtained during the third water flooding revealed that HCl can be used to achieve a 100% water permeability retained.

This highly improve in permeability after the acid treatment indicate a good fit to couple the gel treatment with acid treatment to recover more oil from both high and low permeability zones.

9.6.1.2. PPG slug volume of 3 PV. The heterogeneity model was oil saturated according to the standard core flooding procedure. Water was then injected at 2 ml/min to determine the amount of oil recovered during the first water flooding. Water flooding continued until no oil was produced at effluent. A large amount of oil was recovered (see Figure 9.8) and continued to increase until reach maximum oil recovery at 57%. A 3PV

of 1% NaCl was injected to achieve the maximum oil recovery. Water cut (as indicated in Figure 9.9) was also increased accordingly and increased until the end of the first water cycle. At the end of injecting the 3PV, the oil recovery levelled and water cut reached 100%. The injection pressure during the first water flooding recorded as a function of the injection pore volume is given in Figure 9.10. The injection pressure during this cycle was very low becoming stable at 0.01 psi. This significant low pressure indicates the brine moved easily through the high permeability zone.

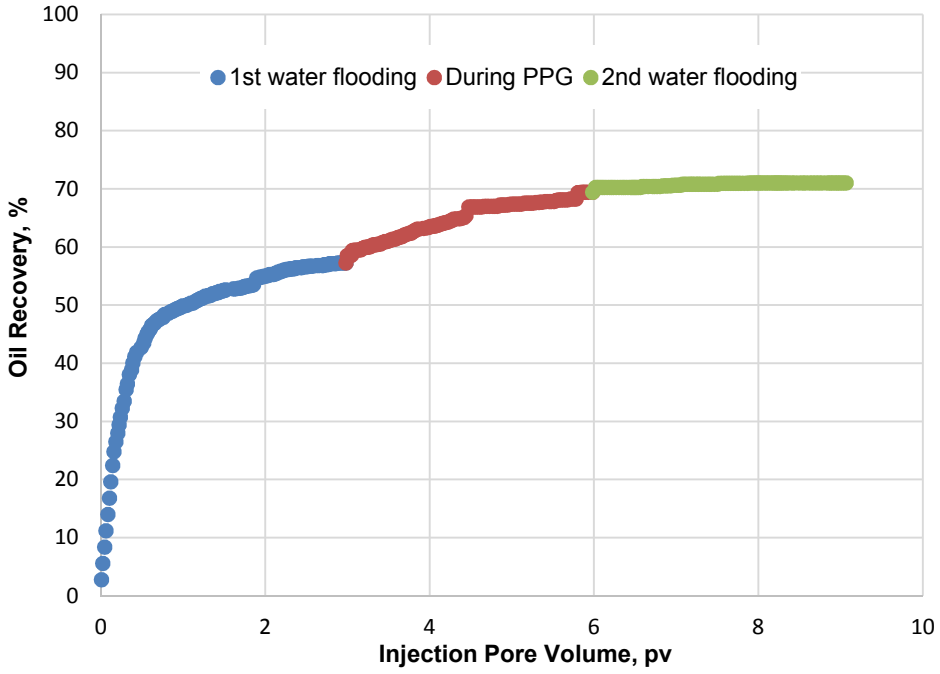

Figure 9.8—Oil recovery during water flooding and PPG injection of 3 PV.

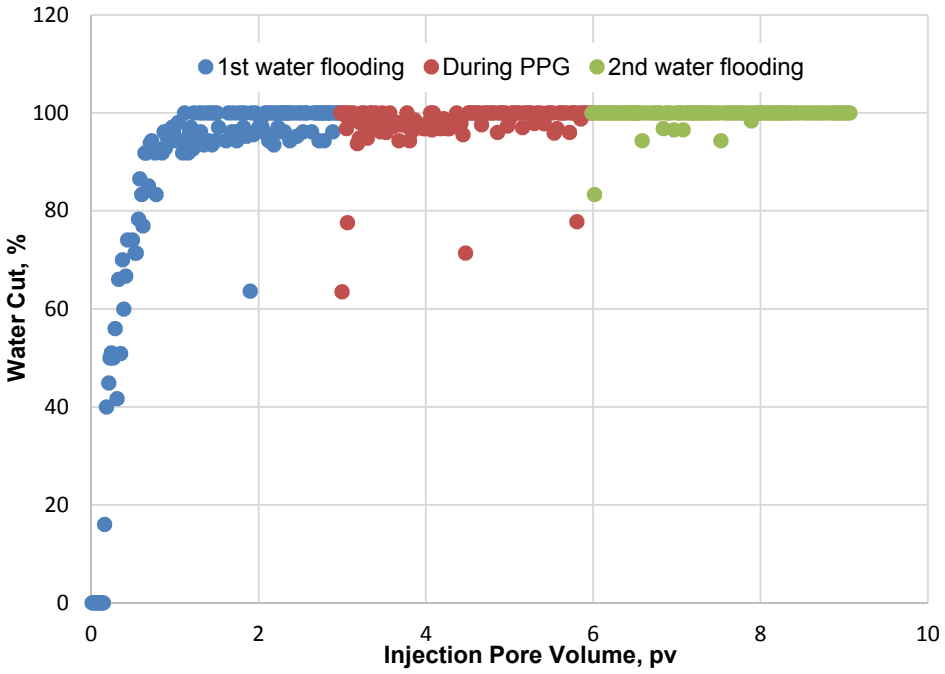

Figure 9.9—Water cut during water flooding and PPG injection of 3 PV.

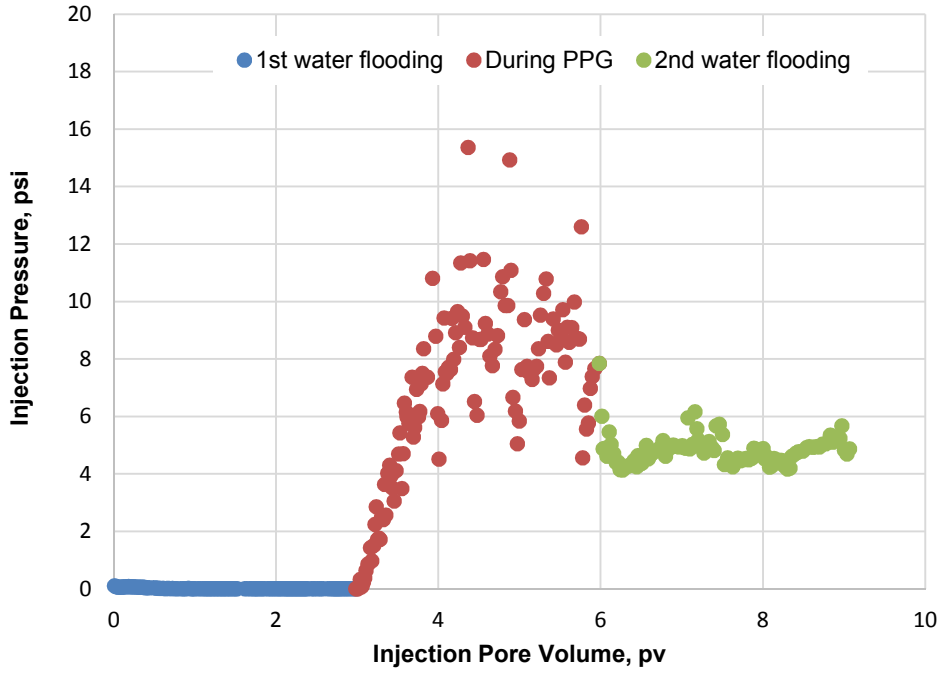

Figure 9.10—Injection pressure during water flooding and PPG injection of 3 PV.

Swollen PPGs in a 1% NaCl solution with a concentration of 2000 ppm were injected at the same injection flow rates (2 ml/min) for consistency purposes. A 3 PV of swollen suspended PPG was injected into the model after the first water flooding was complete. A considerable increase in oil recovery occurred during this treatment. This increase began at approximately 13% and peaked at approximately 70%. The water cut measurements indicate water production rate decreased in during the gel injection. The water cut was reduced by between 5 and 8%. A significant change in the injection pressure measurements occurred during the gel injection. The injection pressure increased significantly more during this treatment than it did during the previous water flooding. The injection pressure peaked at 15 psi during the gel treatment while the injection pressure before the gel treatment was only 0.01psi. This significant increase in injection pressure reveals that PPG's can effectively plug the high preamble paths within sand pack.

A second cycle of water was performed after the gel treatment at the same injection flow rate. Water continued to inject until no oil produced at effluent, around 3 PV was injected which was similar to water injection pore volume performed in the first water flooding. The oil recovery increased slightly during this water cycle. The oil recovery became stable at 71%. Water cut continued to change; it fluctuated and reached 100% water cut again at the end of the flooding process. The injection pressure dropped significantly to 4 psi during the early injection pore volume of the second water flooding. It fluctuated between 4 psi and 5 psi becoming stable at the end of the injection mechanism at 4.5 psi. This decrease in injection pressure, however, still greater than the water injection pressure recorded during the first water flooding. The injection pressure

became stable at 4.5 psi during the second water flooding while it became stable at 0.01 psi during the first water flooding.

9.6.1.3. Deep penetration treatment. The first water cycle was performed at an injection rate of 2 ml/min. A significant amount of oil (Figure 9.11) was recovered reaching a maximum oil recovery of 63%. A 3 PV of a 1% NaCl was injected during this cycle. Water cut (as indicated in Figure 9.12) increased sharply during the early water injection stage, reaching 100% at the end of the first water cycle. The injection pressure during the first water flooding recorded as a function of the injection pore volume is given in Figure 9.13. The injection pressure stable during this cycle was a very low at 0.07 psi.

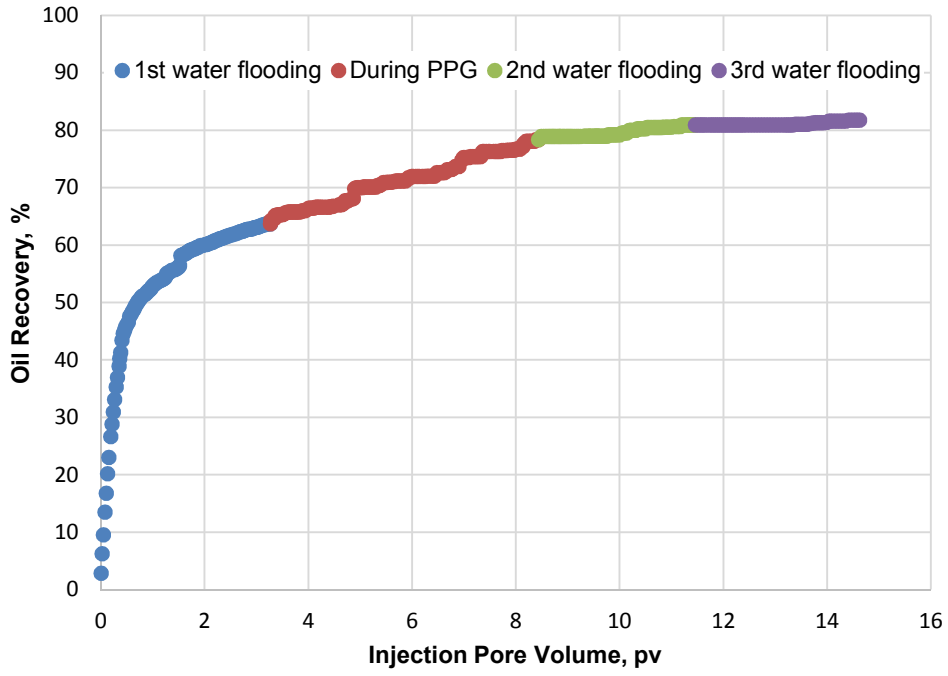

Figure 9.11—Oil recovery during water flooding and PPG injection of 5.5 PV.

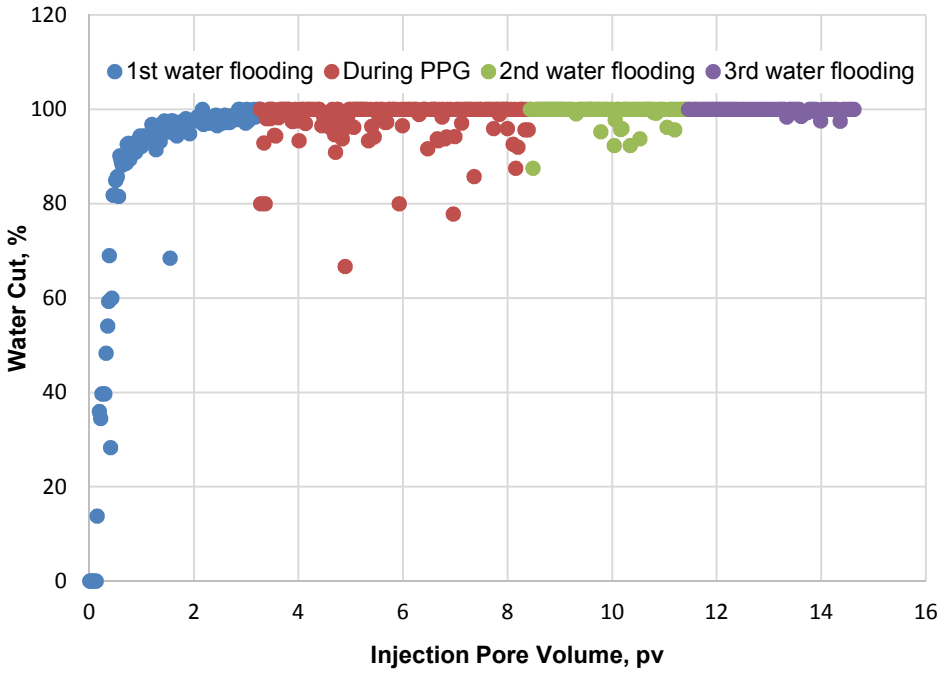

Figure 9.12—Water cut during water flooding and PPG injection of 5.5 PV.

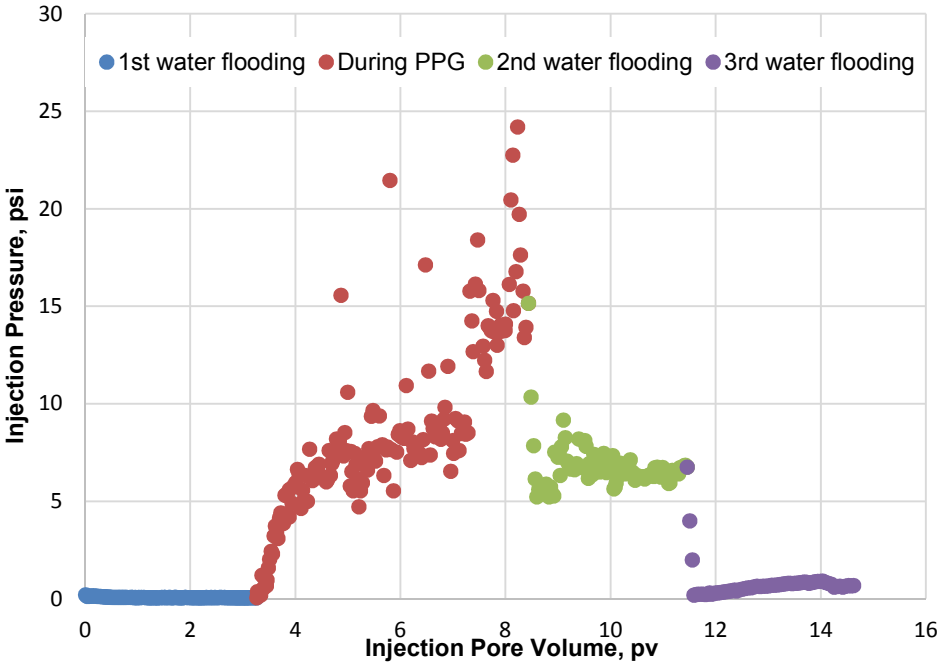

Figure 9.13—Injection pressure during water flooding and PPG injection of 5.5 PV.

PPGs were injected deep into the sand pack at a rate of 2 ml/min until they reached the second section. They reached the second section after 5 PV was injected into the heterogeneity sand pack model. During this treatment a substantially increase in oil production was noticed. The oil production increased by approximately 16% to reach a total of approximately 79%. The water cut decreased 5 to 20% during the gel injection indicating the injected water was consumed to recover more oil. The injection pressure measurements increased significantly to around 24 psi during the gel injection. This finding reveals that increasing the PPG injection pore volume significantly increased the injection pressure.

A second batch of water cycles was injected at the injection flow rate of 2 ml/min to test both the oil recovery increase and the water flow resistance after the gel treatment. Approximately 3 PV of water was injected until no oil was produced at effluent. The oil recovery increased by around 2% before becoming stable at 81%. The water cut continued to change reaching 100% water cut at the end of the second water flooding. The injection pressure dropped significantly to approximately 5 psi during the early injection pore volume of the second water flooding. It became stable at the end of the injection mechanism at 6.4 psi. This decrease in injection pressure, however, was still greater than the water injection pressure recorded during the first water flooding.

A syringe was used to flush 6 ml of 10% HCl volume into the sand pack face. The sand model was maintained for 24 hr for acid soaking purposes. A third cycle of water was injected at the same injection flow rate (2 ml/min). The oil recovery increased slightly by approximately 1.5% oil incremental to reach to 81.7% at the end of the water flooding process. The water cut changed very little during this water cycle and continuing

at a level of 100%. The injection pressure decreased sharply after the acid treatment was complete, decreasing to 0.27 psi. It decreased to almost similar to the original injection pressure before performed the gel treatment. The injection pressure became stable at 0.68 psi after a similar water injection pore volume (3 PV) was injected. The stable injection pressure obtained during the water flooding show that HCl can achieve 100% water permeability retained.

The increase in the injection pressure that occurred during the last few injection pore volumes, in particularly at PV of 11 likely occurred because PPG began to re-swell again. The gel particle size increased increasing the injection pressure. Imqam et al. (2014) noted that PPGs will re-swell again after an acid treatment is complete when they are touched again with the same brine concentration. Imqam et al. (2014) also found that this increase in swelling volume is limited. It remains substantially smaller, however, than the original swelling volume.

Table 9.3 summaries the results obtained for the effect of the PPG slug volume. The results gathered from three experiments indicate that on averaged 60% of the oil recovery could be produced during the first water flooding. After PPG injection, oil recovery improved. The oil recovery gained both during and after the PPG treatment varied with gel slug volume. The oil recovery increased as the PPG injection pore volume increased. It did not increase linearly with the PPG injection volume. The Oil recovery percentage increased by 12.7% during PPG injection at 0.5 PV of PPG during the second water flooding. This percentage increased to 24% after the PPG slug volume increased to 3. But when PPG injection pore volume increased to 5.5, oil recovery did not increase substantially as compared to a PPG volume of 3.

The most of the oil production was occurred during the PPG injection, this indicate that PPG injection not only reduce the large channels but also divert the injection aqueous phase to produce more oil. This mechanism caused to have the majority of incremental oil recovery percentage gained during PPG injection.

Table 9.3—A summary of oil recovered during water flooding and PPG injection.

PPG slug volume, PV	Oil recovery (%)			Total oil recovery, %	Oil incremental recovery, %
	1st water flooding	PPG treatment	2nd water flooding		
0.5	63	2.5	5.5	71	12.7
3	57.3	12.2	1.5	71	24
5.5	63.4	14.6	2.5	80.5	27

9.6.2. Effect of Heterogeneity Sweep Volumes. This section discusses two scenarios of heterogeneity shapes/levels within formations. The first model present results of injected PPG when large un-swept volume/low permeability is greater than swept area volume/high permeability. This model design experiment differs than previous three experiments. Here, the high permeability layer was surrounded by low permeability layers. Figure 9.14 show a simple sketch cartoon to simplify inject and place 3 PV of PPG into the large un-swept planned target zone.

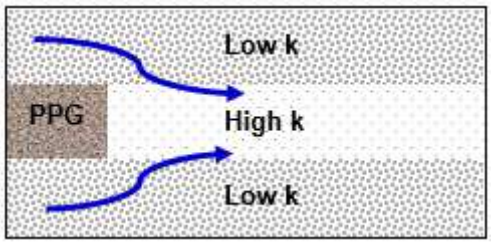

Figure 9.14—PPG injection into large un-swept heterogeneity model.

The second scenario depicts the results obtained for the model with less heterogeneity sand pack in which large volume of low permeability/un-swept zones dominated the model. Figure 9.15 show a simple sketch cartoon to simplify inject and place 3 PV of PPG into the less heterogeneity sand pack model.

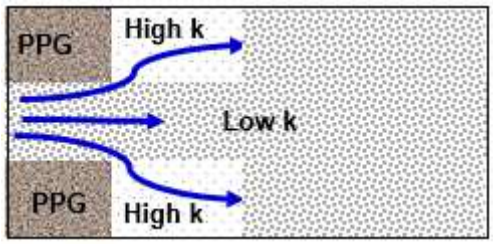

Figure 9.15—PPG injection into less heterogeneity model.

9.6.2.1. Large un-swept volume. The first batch of water was injected into the heterogeneity model at an injection rate of 2 ml/min. The oil recovery (Figure 9.16) increased sharply during the early stages of water injection pore volume. It continued to increase until reaching a maximum oil recovery of 58%. During this flooding cycle a 3PV of 1% NaCl solution was injected. The water cut (as indicated in Figure 9.17) also increased and fluctuated until reaching 100% at the end of the water injection cycle. The injection pressure during the first water flooding recorded as a function of the injection pore volume (as shown in Figure 9.18) was very low becoming stable at 0.1 psi.

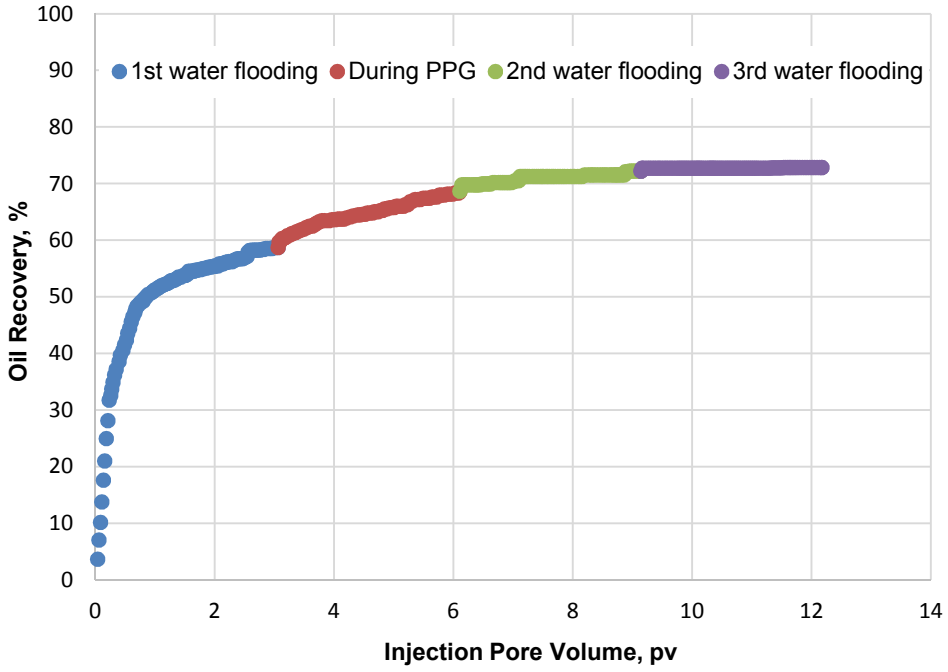

Figure 9.16—Oil recovery determined from a large un-swept heterogenity model.

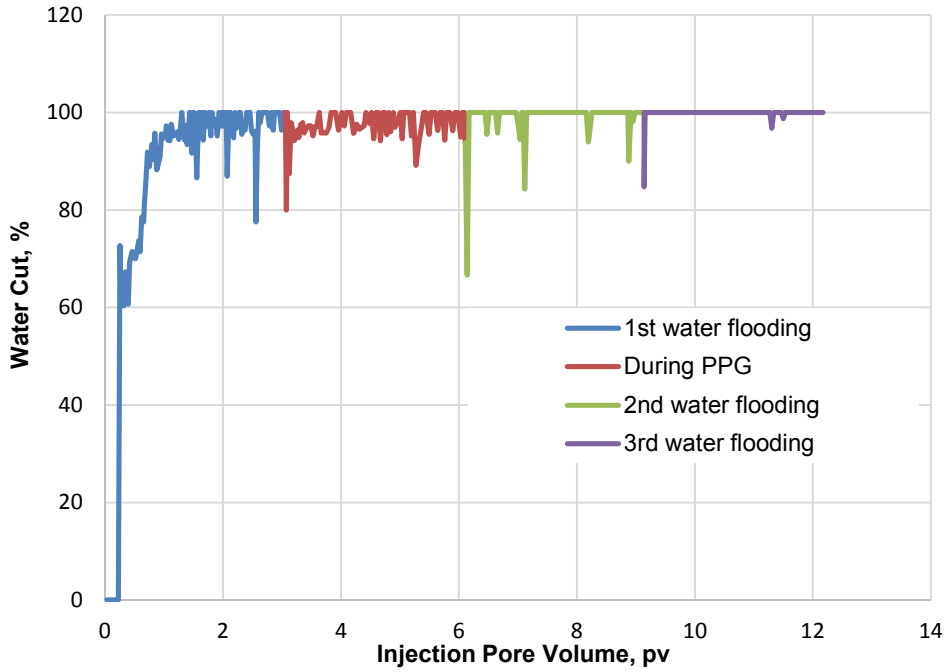

Figure 9.17—Water cut determined from a large un-swept heterogenity model.

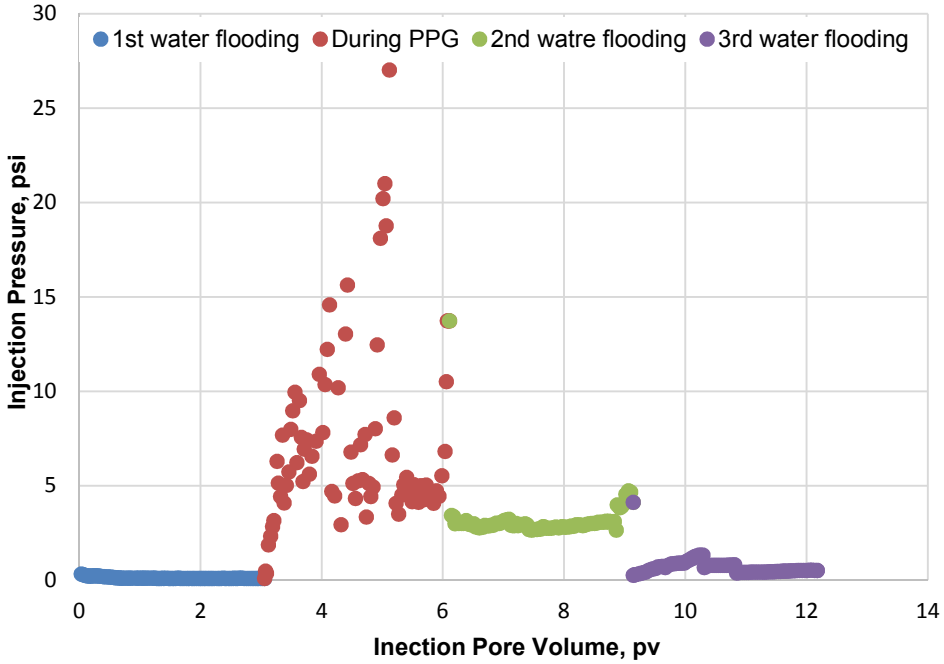

Figure 9.18—Injection pressure measured from large un-swept heterogenity model.

PPGs with a concentration of 2000 ppm were injected at injection flow rates of 2 ml/min for consistency purposes. A 3 PV of swollen PPGs was injected into the model after the end of the first water flooding. The amount of oil recovered increased during this treatment. Oil production increased by approximately 10% to reach around 68% of the total oil recovery. The water cut dropped during the gel injection to between 5 and 20%. The injection pressure increased significantly peaking at approximately 27 psi during the gel treatment.

Water was injected again after the gel treatment at the same injection flow rate (2 ml/min). It continued to inject until no oil was produced at effluent. Approximately 3 PV of water was injected which was similar to water injection pore volume during the first water flooding. The oil recovery increased by 4% reaching the total stable recovery at

72%. This incremental percentage illustrates the PPG's ability to divert the water injection into an un-swept area to recover more oil. The water cut continued to change though most of the measurements were recorded at 100%. The injection pressure dropped significantly to approximately 2.7 psi during the early injection pore volume of the second water flooding. It became stable at the end of the injection mechanism at 2.65 psi. This decrease in injection pressure, however, remained greater than the water injection pressure recorded at the first water flooding. In the first water flooding, the injection pressure became stable at 0.1 psi while in the second water flooding injection pressure became stable at 2.65 psi.

A small amount of acid approximately 6 ml of 10% HCl volume was injected into the sand pack face by a syringe. The sand pack model was maintained 24 hr for acid soaking purposes. Water was injected again at same injection flow rate (2 ml/min). The oil recovery increased slightly by around 0.6 % oil incremental to reach 72.8% at the end of the water flooding process. The water cut changed very little compared with previous flooding. The injection pressure decreased sharply after the acid treatment was complete decreasing from 2.65 psi to 0.48 psi. The stable injection pressure was similar to the original injection pressure before performed the gel treatment. The injection pressure during the first water flooding was 0.1 psi and during the third water flooding was 0.49 psi.

9.6.2.2. A model with less heterogeneity. Water was injected at 2 ml/min into a heterogeneity model. A large amount of oil (as shown in Figure 9.19) was produced during this injection cycle. The oil recovery increased becoming stable at 54%. A 3 PV of a 1% NaCl solution was injected during this flooding cycle. The water cut (as indicated in Figure 9.20) also increased as the injection pore volume increased before becoming stable at 100% water cut. The injection pressure during the first water flooding was recorded as a function of the injection pore volume (see Figure 9.21). The injection pressure during this cycle was a quite low and becoming stable at 0.48 psi.

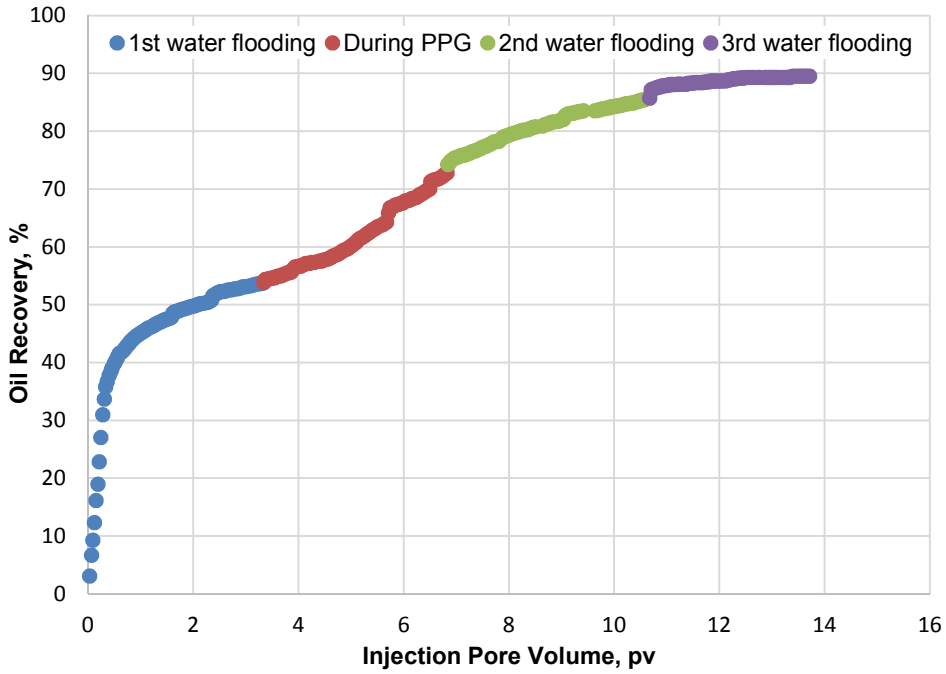

Figure 9.19—Oil recovery determined from a model with less heterogenity.

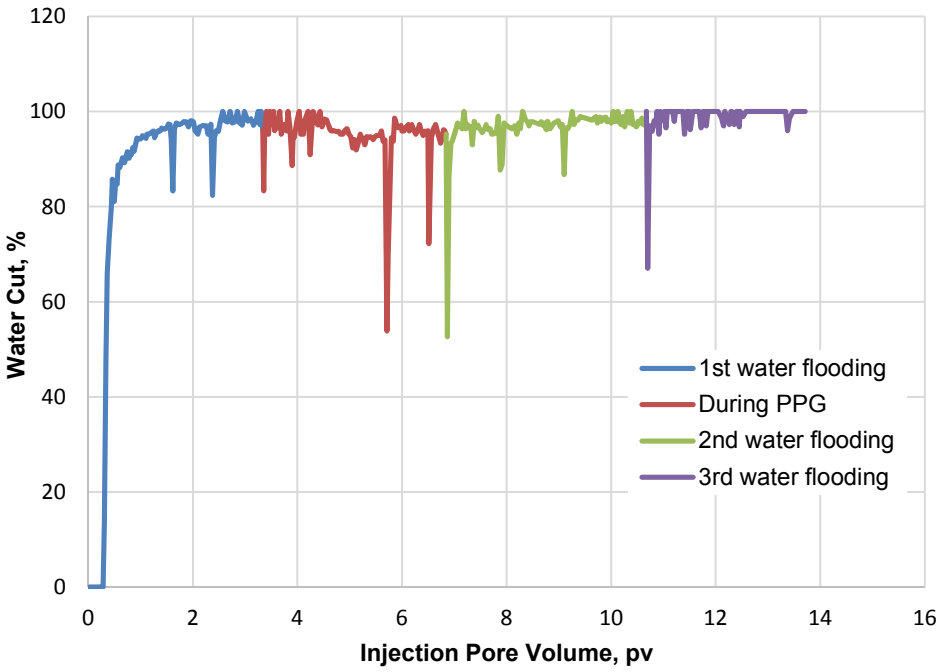

Figure 9.20—Water cut determined from a model with less heterogenity.

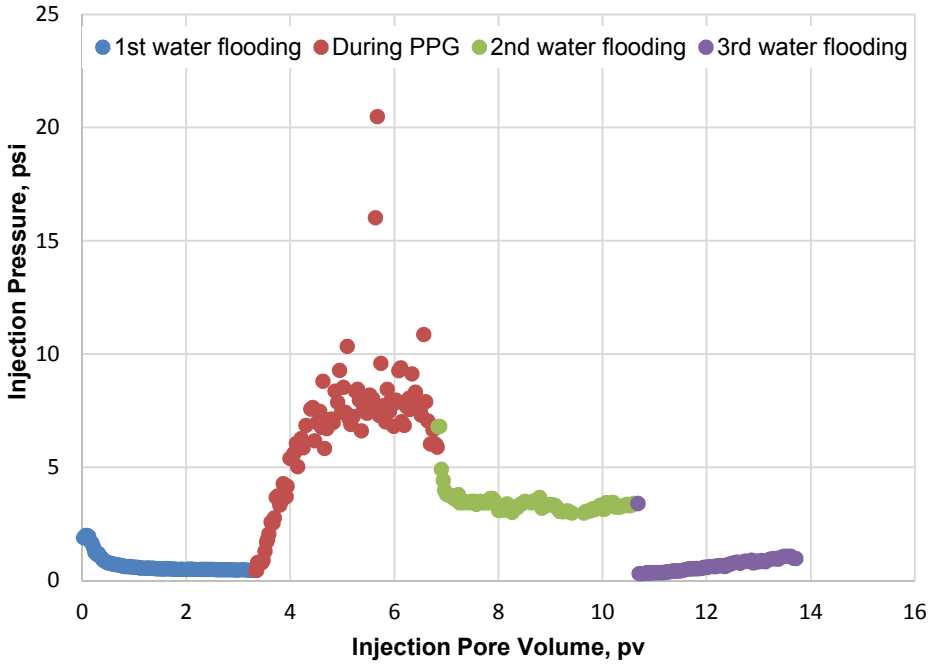

Figure 9.21—Injection pressure determined from a model with less heterogenity.

PPGs with a concentration of 2000 ppm were injected at the injection flow rates (2 ml/min). A 3 PV was injected into the model after the first water flooding process was complete. During this injection treatment a substantially increase of oil recovery was observed. The amount of oil increased by approximately 20% to reach approximately 74% during this injection treatment. A very clear trend of water cut reduction was achieved during this PPG injection treatment. It was reduced by between 5 and 50%. The water cut remained at an average of 93% until the gel treatment was complete. The injection pressure measurements changed significantly during the gel injection process peaking at 20 psi. This increase in pressure is much greater than the injection pressure recorded during the first water flooding.

A second water flooding was performed after the PPG injection treatment was complete. Water was injected at flow rate of 2 ml/min. This injection was continued until no oil was produced at effluent. Approximately, 3 PV of water was injected which was similar to the water injection pore volume during the first water flooding. The oil recovery increased considerably during this water cycle. It continued to rise until reaching a stable recovery at 85% (equivalent to 6% incremental of oil production). The water cut decreased between 97% and 95% during the injection pore volume. The injection pressure dropped significantly to approximately 3 psi during the early injection pore volume of the second water flooding. It became stable at 3.34 psi at the end of injection mechanism. This decrease in injection pressure, however, was still greater than the water injection pressure recorded during the first water flooding. In the first water flooding, the injection stable pressure was 0.48 psi; it was 3.34 psi during the second water flooding.

A around 6 ml of 10 % HCl volume was injected into the sand pack face by a syringe and the sand model soaked for 24 hr. Water was injected again after the soaking period at same injection flow rate (2 ml/min). The amount of oil recovery was increased slightly by approximately 4 % oil incremental to reach 89.5 % at the end of the water flooding. The water cut increased during the water injection cycle into 100% at the end of injection processes. The injection pressure decreased sharply after the acid treatment dropping to 0.44 psi. The injection pressure declined to the original injection pressure before performed the gel treatment. The injection pressure increased slightly and became stable at 0.99 psi after injected similar water injection pore volume (3 PV).

9.7. DISCUSSION

The results obtained in section 8 indicate that PPG was not only propagated into a high permeability layers, but also there was a portion of PPG propagated into low permeability. PPG propagated into low permeable zones in the cross flow heterogeneity model might be more pronounced.

This section discusses also the acid effect on the conformance control results determined after PPG injection. The injection pressure measured, as shown in Table 9.4, at sand face during the multiple water flooding were used to determine the effect of PPG on reducing water permeability and to determine the effect of HCl on improving conformance results after gel treatment. Blocking efficiency after gel and acid treatments were measured for the effects PPG slug volume and heterogeneity sweep volume.

Results indicated that PPG blocking efficiency reached 90% and above during most of the experiment. The PPG blocking at the sand face was unaffected by the gel

injection pore volume as the blocking efficiency remained above 96%. The effect of HCl on the sand face's blocking efficiency was varied; it was dependent on the gel injection/heterogeneity sweep volumes. Blocking efficiency was significantly affected by the PPG injection pore volume; it was reduced below 0% when a small pore volume (0.5 PV) of PPGs was injected. While, at PPG injection of 5.5 PV conformance results did not hurt too much, it decreased from 98.9% to 89.7%. In real world, where large volume of PPG is injected compared to small volume of acid used, this lab results indicated that conformance control results would not hurt too much after the sand heterogeneity flushed with HCl stimulation.

Table 9.4—A summary for blocking efficiency after PPG and HCl treatments.

Experiments		Injection pressure, psi				Frrw		Blocking Efficiency %	
		Before PPG	During PPG	After PPG	After HCl	After PPG	After HCl	After PPG	After HCl
PPG slug volume, PV	0.5	0.08	7	2.68	0.07	33.5	0.87	97	-14.2
	3	0.01	15	4.5	-	450	-	99.7	-
	5.5	0.07	24	6.4	0.68	91.4	9.71	98.9	89.7
heterogeneity sweep volume	Large un-swept	0.1	27	2.65	0.49	26.5	4.9	96.2	79.5
	Less heterogeneity	0.48	20	3.34	0.99	6.95	2.06	85.6	51.5

9.8. CONCLUSION

This section is discussing the use of PPG to improve the conformance control in cross flow heterogeneity formations. Five experiments were conducted successfully performed to investigate the effects of PPG injection volume and formation sweep

volume on oil recovery improve, water cut decrease, and injection pressure performance. The following conclusions were drawn from this section:

- Oil recovery improved significantly both during and after the PPG injection. This increase was related to the PPG injection pore volume and the formation sand sweep volume.
- Oil recovery increased as the PPG injection volume increased. This increase, however, was not linear.
- The PPG injection increased oil recovery by an average of 20%. This amount increased as the sand sweep volume decreased.
- Water cut measurements indicate the water production rate decreased during the gel injection, increasing the amount of recovered oil from the heterogeneity sand model. The water cut was reduced by a percentage of between 5 and 20% during most of the experiments.
- The injection pressure increased considerably during the PPG injection. It decreased during the second water flooding remained higher than the injection pressure measured before the PPG treatment.
- The injections when combined PPG with HCl treatments can potentially improve conformance control. The HCl treatment did not significantly influence the PPG treatment.
- Water injection cycles were performed after the acid treatment and improved in oil production was noted during these cycles. Oil recovery increased between 1 and 5% after the acid treatment which imply continued enhancement in low permeability sweep layers.

10. A COMBINATION OF STIMULATION AND CONFORMANCE TREATMENT TO IMPROVE OIL RECOVERY

10.1. INTRODUCTION

In the existence of non-cross flow heterogeneity between the low and high permeability layers, a considerable amount of PPG injection volume propagated into high permeable zones and plug it. However, still small amount of PPG form a gel filter cake on the surface of low permeable zones during PPG injection (Figure 10.1).

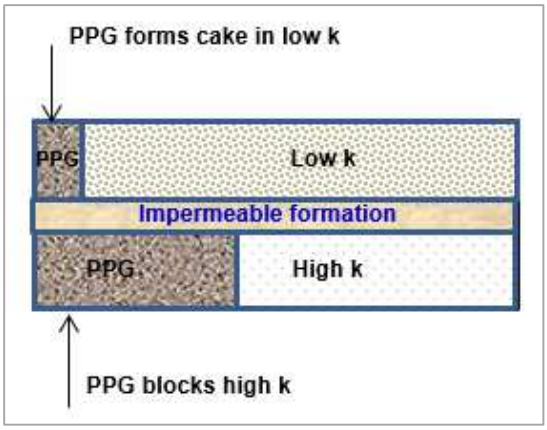

Figure 10.1—Gel filter cake formed on low permeability zones.

Section 4 was focused only on combined PPG with HCl acid to remove gel filter cake in homogenous single low permeability core formation. Therefore, this current section presents an additional work results obtained from new experiment models. It aims to determine the effectiveness of combining HCl acid and PPG to gain a better conformance control results in heterogeneous core formations.

PPG was injected into large permeability zones (thief zones) to reduce their permeability and then divert the injection water to recover more oil from un-swept low-permeable zones. Acid was then pumped into heterogeneity model to remove the gel cake formed after gel treatment. The combined technologies increased the oil production from both low and high permeability cores. This current work was also extended to assess the possible side effect of acid treatment on reducing the gel-blocking efficiency in high-permeability cores.

The new model was tested by investigating two parallel formations having low and high permeabilities. The high permeability sand pack had permeabilities above 10 Darcy while the low permeabilities sand pack had permeabilities less than 1 Darcy.

10.2. OBJECTIVES AND TECHNICAL CONTRIBUTIONS

This work was conducted in an attempt to study the mechanisms of combined conformance control and stimulation treatments to produce more oil from un-swept low permeability zones by evaluating the following:

- Compare the oil recovery results obtained from the heterogeneity model before and after introduce the gel treatment with results obtained after HCl acid treatments.
- Evaluate the acid effectiveness to remove the gel cake formed on the surface of the low permeable layer.
- Study the change in water injection pressure after both permeability layers treated with acid.

- Investigate the effect of HCl on gel blocking efficiency to water flow. This investigation was performed by determining the residual resistance factor to water for the high permeable zones.
- Results from this study will promote the use of PPG for conformance control application, where the concern for PPG treatment was damaging low permeable zone. This concern was eliminated by flushing zones with an economic volume amount of HCl.

10.3. EXPERIMENTAL DESCRIPTION

10.3.1. Preformed Particle Gel. A superabsorbent polymer was used as a PPG to conduct these experiments. Dry particles with a mesh size of 170-200 (90-75 microns) were swollen in a 1% Sodium Chloride (NaCl) brine concentration. Gel concentrations of 2000 ppm was used.

10.3.2. Brine Concentration and Oil Viscosity. A 1 wt% of NaCl solution was used for brine flooding. It was also used to prepare swollen PPGs. Heavy oil with a viscosity 195 cp at 70 °F was used to saturate the sand pack model.

10.3.3. Hydrochloric Acid (HCl). HCl from Fisher Scientific was diluted with distilled water to obtain a concentrations of 10%. A 0.1 PV of HCl acid was flushed into the non-cross flow heterogeneity model and model was kept soaked for 12hr.

10.3.4. Magnetic Stirring Vessel. An accumulator with a 1200 ml capacity and a maximum adjusted impeller speed of 1800 r/min was used to inject PPGs into high and low permeability sand pack model. The impeller was placed at the bottom of the accumulator to keep the PPG dispersed in brine before injected into the model.

10.3.5. Sand Pack. Three sizes of silica sand were used to obtain different permeability contrasts between models. A 18-20, 50-60, and 100-120 mesh sizes were used to obtain low and high permeability sand packs. Silica sand was packed into two separate tubes that had the same length and area.

10.4. EXPERIMENTAL SETUP

The experimental setup used in this experiment is illustrated in Figure 10.2. It constructed of two same tubes dimensions (with 20 cm in length and 2.7 cm in diameter) used to contain the silica sand pack. Two horizontal (parallel in position) tubes were packed with different sand grains to emulate the permeability contrast present in reservoirs. A syringe pump was used to inject suspended PPG, brine, oil, and HCl from the accumulators into the sand pack models. Two pressure transducers were mounted in front of each sand pack model to acquire the injection pressure change during the brine flooding and the gel treatment processes. The test tubes were mounted at the outlets of each sand pack to collect the volume of the fluid produced.

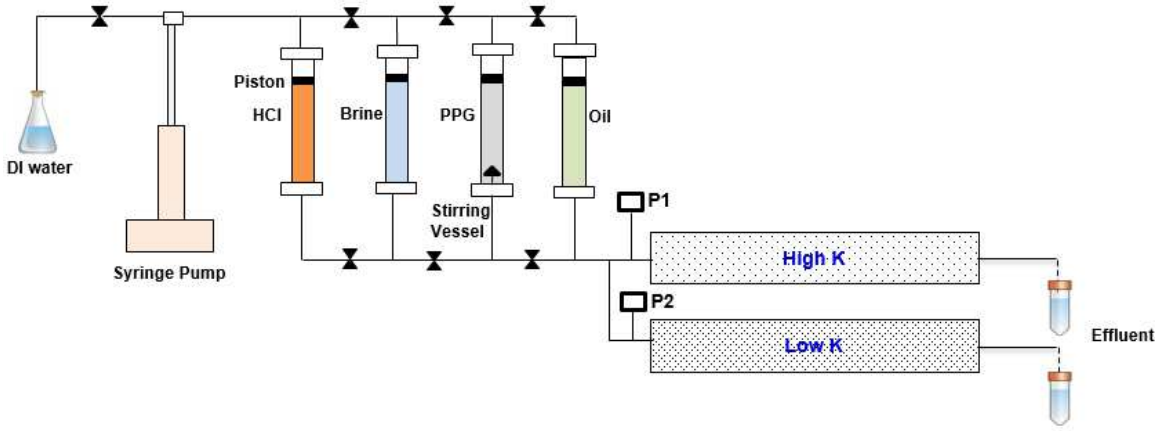

Figure 10.2—Combined PPG with HCl experiment apparatus.

10.5. EXPERIMENTAL PROCEDURES

The procedures for carrying out the non-cross flow heterogeneity experiments were briefly described as follows:

10.5.1. Preparing and Saturating Sand Pack Models. A vibrator machine Was used to prepare the different sizes of silica sand to get the desire sand pack permeability. Sand pack models were vacuumed for at least 6 hr. It was then fully saturated with 1% NaCl to determine pore volume, porosity, and permeability.

Heavy oil viscosity was injected from the accumulator into each sand pack at a rate of 1 ml/min. Oil was injected until no water was produced and injection pressure became stable. Both sand pack permeability (low and high) layers were connected to each other as shown in Figure 10.2 and the water flooding cycles were began as follows.

10.5.2. First Water Flooding. A 1% NaCl was injected into both low and high permeability layers at rate of 1 ml/min to simulate secondary oil recovery conditions. During the first water flooding, both oil recovery and water cut were determined for the low and the high sand pack permeability.

10.5.3. PPG Treatment. A 0.5 PV of swollen PPGs in 1% NaCl with a concentration of 2000 ppm were injected into the sand packs at rate of 1 ml/min. Oil and water productions volume were collected at effluent. Gel injection pressure was also monitored.

10.5.4. Second Water Flooding. A 1% NaCl was injected again at same injection rate after PPG treatment to examine the gel blocking efficiency to high permeability. PPG performance to improve oil recovery from low permeability was also determined.

10.5.5. HCl Soak Treatment. A very small amount of 10% HCl was injected into both sand packs model for mitigating the gel cake formed on surface of low permeability sands. A 0.1 PV was injected at 1 ml/min into sand packs. The model was remained for acid soaking purpose for 12 hr.

10.5.6. Third Water Flooding. Same brine concentration was injected again at 1 ml/min after the soaking HCl time. The injection pressure was monitored during the third water flooding to determine the effect of HCl on minimizing/removing gel cake on low permeability zones. The injection pressure also measured for high permeability to determine any side effect on the blocking efficiency of PPG to the high permeability zones. Fluid productions at each sand pack was collected during the water flooding. Brine was injected until no oil produced at outlets and injection pressure became stable.

The above procedures were repeated for each experiment. The oil recovery factor and injection pressure were both determined for the low and the high permeability sand pack models.

10.6. RESULTS AND ANALYSIS

10.6.1. Injection Pressure Measurements. The injection pressure of the first water flooding, the PPG injection, the second water flooding, and the third water flooding of the three layer permeability contrast are plotted in Figures 10.3,10.4, and 10.5.

The injection pressure drop measured for the low and high permeability layers was a little bit low. The pressure became stable for both permeabilities when approximately 2 PV of brine was injected. Most of the water injection pressure for the three permeability contrast became stable at approximately 0.5 psi.

PPG pressure increased sharply in the both low and high permeability layers. It was, however, less in low permeability layers. This finding indicate that a considerable amount of PPG flew into the high permeability layers and a small amount of gel particles flew into the low permeability layers. The PPG injection pressure for most permeability contrasts reached above 5 psi (approximately 10 times increased than pressure recorded in first water flooding).

During the second water injection, water injection pressure was declined after the PPG treatment. It became stable after approximately 0.5 PV of water injection. The second water injection pressure was still greater than injection pressure measured during the first water flooding. The injection pressure after PPG injection pressure was increased between 5 and 20 times.

The third water cycle was injected after the HCl was injected and soaked into the non-cross flow heterogeneity. The water injection pressure declined sharply at the early stage of the third water injection. At this early water injection pore volume, the injection pressure was dropped into the original injection pressure. The injection pressure began gradually increased when the water injection pore volume increased. This increase in pressure was due to the PPG re-swelling mechanisms (Imqam et al. 2014). The injection pressure continue to rise until finally became stable. In most cases, pressure became stable after 2 PV water injection. The injection pressure was lower than previous injection pressure recorded in the second water flooding at the end of third water flooding.

The injection pressure measured for the high permeability layer was still higher than the injection pressure measured for the low permeability layers. Thus, HCl was effectively used to reduce the gel damage caused to low permeability layers. It had less effect on the conformance control results for the high permeability layers.

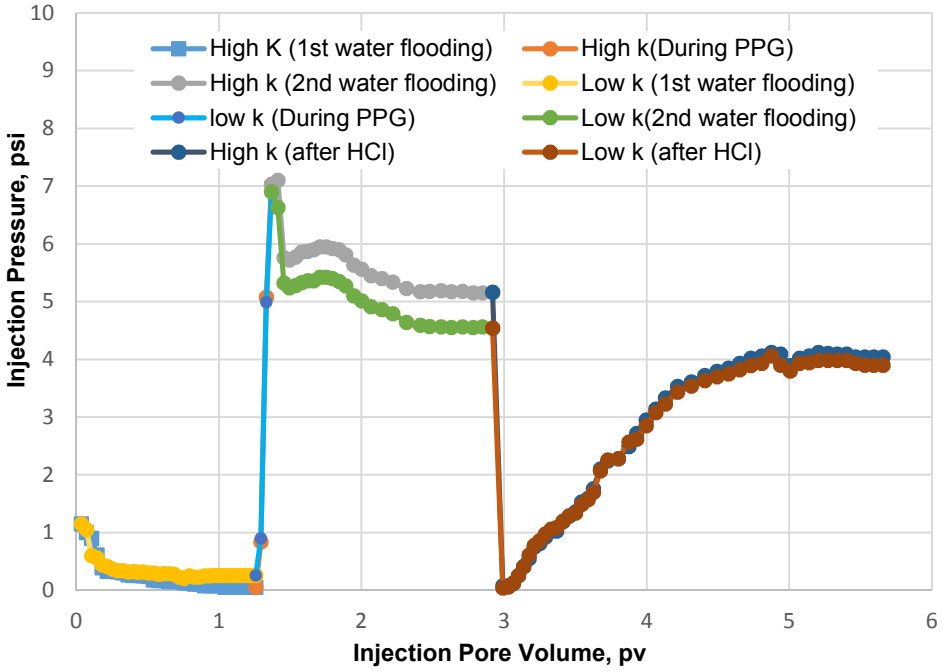

Figure 10.3—Injection pressure for permeability contrast ratio of 44.

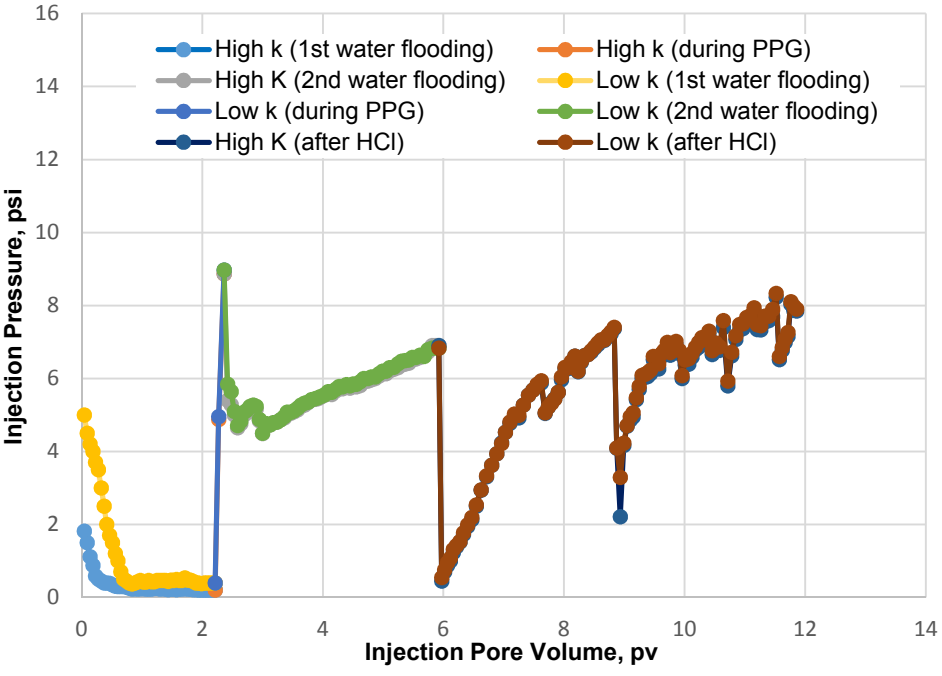

Figure 10.4—Injection pressure for permeability contrast ratio of 20.

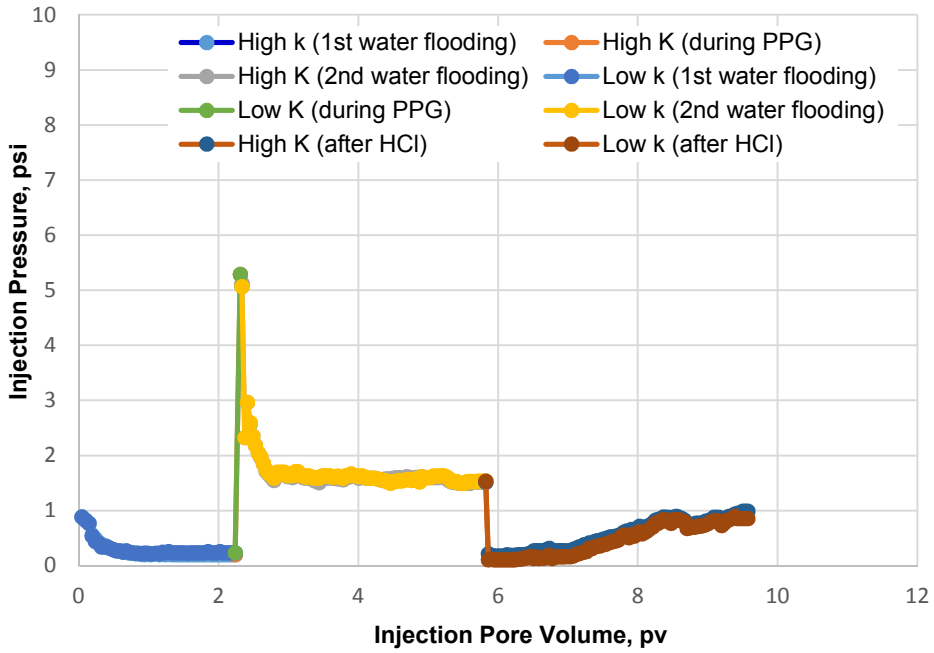

Figure 10.5—Injection pressure for permeability contrast ratio of 4.

10.6.2. Oil Recovery Measurements. The oil recovery curves of the first water flooding, the PPG injection, and the second water flooding of the three layer permeability contrast are plotted in Figures 10.6, 10.7, and 10.8. The oil recovery was determined for low and high permeability layers as a function of pore volume injection.

In the initial water flooding stage, a large volume of oil was recovered from the high permeability layers while a very small volume of oil was recovered from the low permeability layers. The recoverable oil volume from the low permeability decreased substantially as the permeability contrast ratios of sand packs increased. The recovery factors for permeability contrast ratios of 4, 20, and 44 were 20, 1.9, and 0.9, respectively.

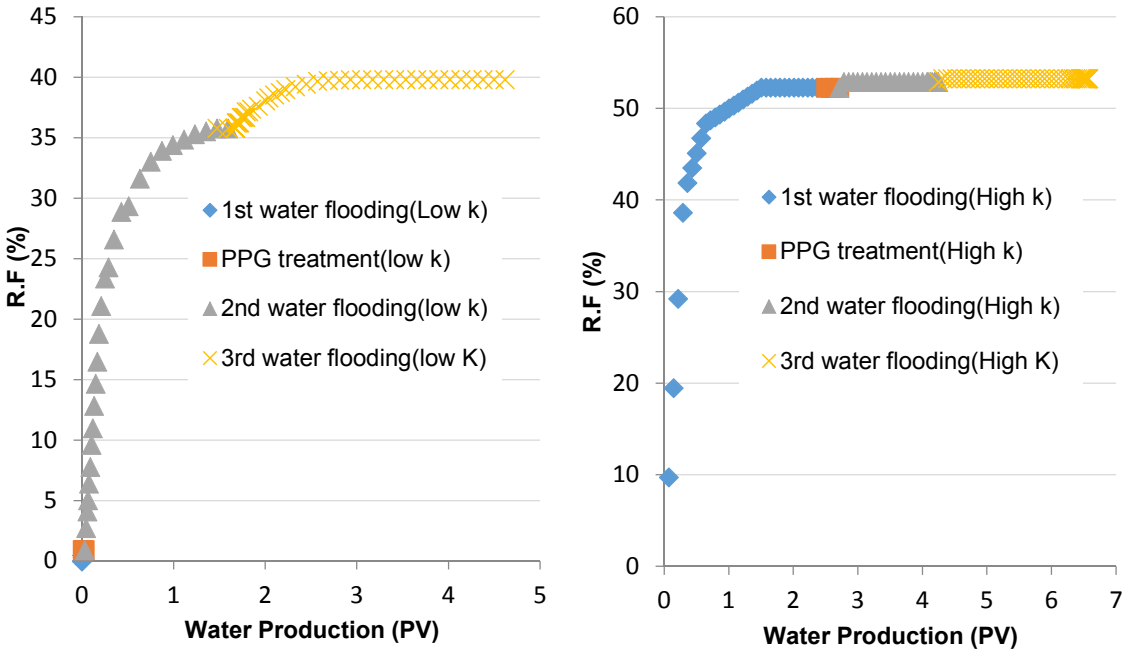

a) Oil recovery for Low k (0.45 Darcy) **b) oil recovery for High k (20 Darcy)**

Figure 10.6—Oil recovery for permeability contrast ratio of 44.

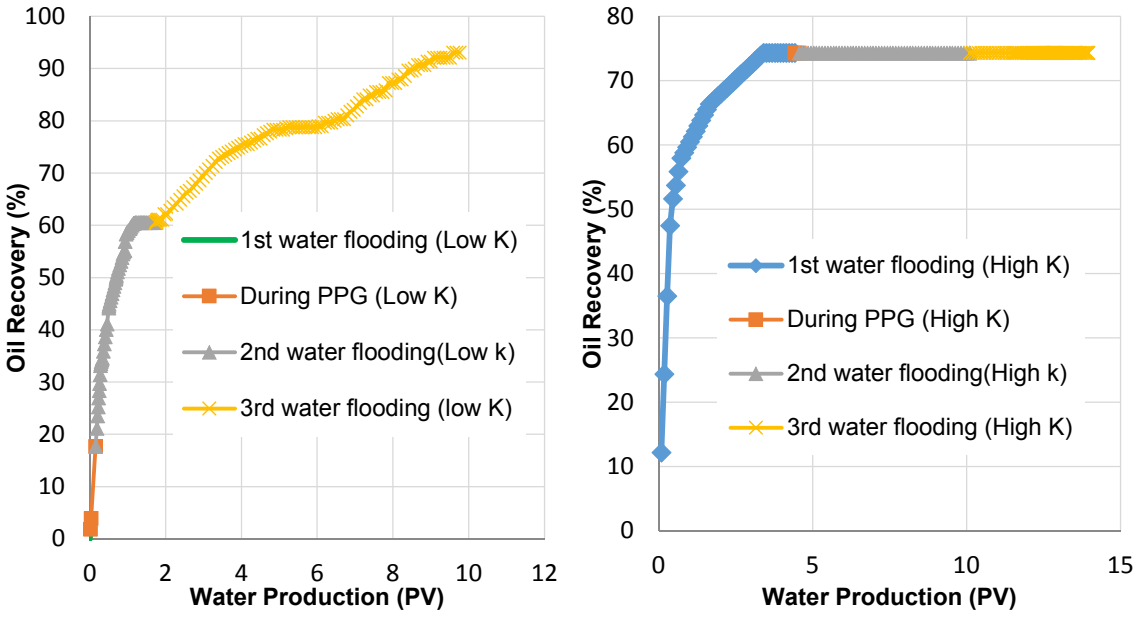

a) Oil recovery for Low k (1Darcy) **b) Oil recovery for High k (20 Darcy)**

Figure 10.7—Oil recovery for permeability contrast ratio of 20.

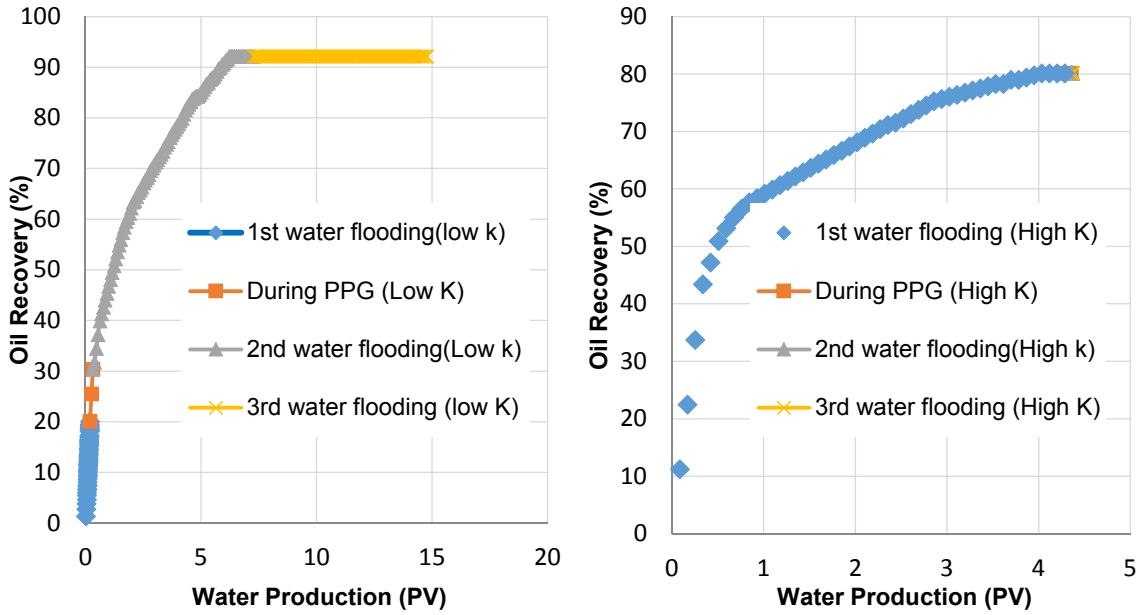

a) Oil recovery for Low k (6.1 Darcy) **b) Oil recovery High k (22 Darcy)**

Figure 10.8—Oil recovery for permeability contrast ratio of 4.

During PPG injection, the sweep efficiency of the heterogeneity improved and the oil recovered from the low permeability began to increase. The oil recovered from the low permeability layers increased substantially more than that recovered from the high permeability layers. The recovery factors obtained from the low permeability at permeability contrast ratios of 4, 20, and 44 were increased to 30, 18, and 3, respectively.

Large amount of PPG stayed in high permeability layers helping reduce the permeability contrast between layers. PPGs improve sweep efficiency of the heterogeneity layers and increased the amount of oil recovered from the low permeability during the second water flooding. The oil recovery in low permeability rose substantially more than it did in the high permeability layers. The recovery factor obtained from the

low permeability layers at permeability contrast ratios of 4, 20, and 44 was increased to 93, 61, and 38, respectively.

Third water flooding was performed to identify if there were any oil can be produced from the treated low permeability layers. A considerable amount of oil was produced during the third water flooding after acid stimulation. The oil produced from the low permeability layers was greater than the oil produced from the high permeability layers. The oil recovery increased by 5 to 30% for permeability contrast ratio of 44 and 20, respectively. In the permeability contrast ratio of 4, the water injection could not gain any oil improve from both the low permeability layer and the high permeability layers. This change in oil recovery could be explained as a result of the different gel damage level/percentage caused to the low permeability layers. The injection pressures measurement indicated a large increased in the injection pressure for large contrast permeability ratio. While a small injection pressure was for the low contrast permeability ratio. The higher damage ratio would be formed in large permeability contrast ratio than that in small permeability contrast ratio. This damage was caused by propagating gel particle into the low permeability layers. It formed a gel cake into their sand surfaces. Consequently, such damage decreased the chance to produce more oil from these zones during the second water flooding. As the gel cake was removed by the acid stimulation, oil began to produce from these stimulated layers as shown in the large permeability contrast ratio.

10.6.3. Evaluate PPG Blocking to High and Low Permeabilities. The obtained results indicated that PPG not only propagated to seal the high permeability layers, but also there was a portion of PPG propagated into low permeability layers as well. This section discusses the effects of PPGs on reducing both low and high permeabilities layers during a gel treatment. These effects can be investigated by measuring the low permeability and high permeability layers before and after the PPGs treatment. Blocking efficiency provides a quantitative percentage values on the permeability reduction created by PPG injections. The blocking efficiency results used to determine whether or not large amounts of gel was propagated into low permeability layers.

Water injection stable pressure measured before and after the PPG treatment were used to determine the PPG's blocking in both high and low permeability sand packs (see Table 10.1). The results indicate that the PPG's blocking efficiency was larger in the high permeability layers than it was in the low permeability layers. At a permeability contrast ratio of 44, the blocking efficiency was 99% in the high permeability layers and 94% in the low permeability layers. The blocking efficiency was consistence with the oil recovery results; it increased as the permeability contrast ratio increased. Therefore, better conformance results would be achieved for sever heterogeneity formations.

The results gathered also indicate that the low permeability sand pack was hurt during the PPG injection. Hydrochloric acid was soaked near the sand face to mitigate the gel blocking to low permeable sand. Based on previous study (Imqam et al. 2015), very small amount of HCl could be used to remove gel filter cake damage. Therefore, a 0.1 PV of 10% HCl was soaked into the cross flow heterogeneity model. The third water flooding was injected at a rate of 1 ml/ min to determine the improvement in low

permeability. The Pressure data shown in Table 10.1 (fifth column) was measured during the third water flooding after the acid stimulation. PPG blocking to the low permeability was reduced for all permeability contrast ratios. This reduction was more visible in the permeability ratio of 4; it decreased by approximately 10% after the sand was soaked with acid. The PPGs blocking efficiency in the high permeability layers was, however, reduced insignificantly. This insignificant change indicates that HCl influences on the conformance results obtained for the high permeability layers was very little.

Table 10.1—A PPG's water blocking efficiency after PPG and HCl.

Permeability Contrast Ratio	Absolute Permeability (Darcy)	Pressure			Frrw		Blocking Efficiency, %	
		before Gel	after Gel	after Acid	after Gel	after Acid	After Gel	after Acid
44	High 22.1	0.05	5.16	4.04	103.2	80.8	99	98.7
	Low 0.5	0.26	4.54	3.9	17.4	15	94	93
20	High 22.4	0.2	6.83	6.7	34.15	33.5	97	97
	Low 1.1	0.4	6.83	6.7	17.07	16.7	94	94
4	High 21.7	0.2	1.52	0.99	7.6	4.95	86	79
	Low 6.2	0.24	1.53	0.86	6.37	3.58	84	72

10.7. CONCLUSION

This section examined the effectiveness of combined PPG and HCl to improve oil sweep efficiency and study the side effect of HCl on the PPG blocking efficiency to the high permeability layers. The following conclusion can be drawn from this section.

- A considerable oil recovery incremental was observed from the low permeability layers after the acid treatment. HCl mitigated the gel filter cake formed on low permeability and as a result oil recovery was improved.
- PPG blocking to the high permeability sand was larger than PPG blocking to the low permeability sand. The blocking efficiency was increased with increased in the permeability contrast ratio.
- Hydrochloric acid was able to mitigate the PPG blocking to the low permeability. It's capability to mitigate the gel filter cake was improved when the permeability ratio was increased. HCl did not hurt too much the conformance result in the high permeability.

11. A COMBINATION BETWEEN CONFORMANCE TREATMENT AND MOBILITY CONTROL TO IMPROVE OIL RECOVERY

11.1. INTRODUCTION

Gel treatments have a very different objective than the traditional polymer flooding. However, both treatments were ultimately intended to improve sweep efficiency. In the traditional polymer flood, we want to see the injected the polymer solution penetrates as far as possible into the low permeability un-swept zones. In contrast, in gel treatment, we want to see the gel penetrates as far as possible into high permeability and much less into low permeability.

Therefore, a heterogeneity model was built from two parallel tubes have the same diameter and length packed with different sand grain sizes. It was built to emulate the low and high permeabilities layers in reservoirs. PPG was injected to plug high permeability swept zones and then polymer was injected to recover more oil from the low permeability un-swept zones.

11.2. OBJECTIVES AND TECHNICAL CONTRIBUTIONS

This work was aimed to study the mechanism of combined three technologies, namely conformance control, stimulation treatments, and mobility control to produce more oil from swept and un-swept zones by evaluating the following:

- Compare oil recovery obtained from heterogeneity model before and after introduced the gel treatment with results obtained after polymer flooding.

- Study the effect of water injection pressure after the polymer flooding for both high and low permeabilities.
- Determine the water cut change during the four water flooding: initial water flooding, second water flooding after gel treatments, third water flooding after acid treatments, and forth water flooding after polymer flooding.
- Results obtained from this study will prompt using PPG as conformance material with polymer to correct the heterogeneity and improve the mobility to increase oil recovery from both swept and un-swept formations.

11.3. EXPERIMENTAL DESCRIPTION

11.3.1. Preformed Particle Gel. A superabsorbent polymer was used as a PPG to conduct these experiments. Dry particles with a mesh size of 170-200 (90-75 microns) were swollen in a 1% Sodium Chloride (NaCl) brine concentration. Gel concentrations of 2000 ppm was used.

11.3.2. Brine Concentration and Oil Viscosity. A 1 wt% NaCl solution was used for brine flooding. It was also used to prepare swollen PPGs. Heavy oil with a viscosity 195 cp at 70 °F was used to saturate the sand pack model.

11.3.3. Hydrochloric Acid (HCl). HCl was diluted with distilled water to obtain a concentrations of 10%. A 0.1 PV (High K) of HCl acid was injected to be soaked near the sand face for both k.

11.3.4. Polymer. High molecular weight polyacrylamide (FLOPAAM 3630 S, 18 million Dalton) from SNF Floerger company was used. Polymer concentration was 1000 ppm prepared in 1% NaCl brine.

11.3.5. Magnetic Stirring Vessel. An accumulator with a1200 ml capacity and A maximum adjusted impeller speed of 1800 r/min was used to inject PPGs into a high permeability sand pack model. The impeller was placed at the bottom of the accumulator to keep PPG dispersed in brine before it was injected into the model.

11.3.6. Sand Packs. Three sizes of silica sand were used to obtain different permeability contrasts between the models. Mesh sizes of 18-20, 50-60, and 100-120 were used to obtain low and high permeability sand packs. Silica sand was packed into two separate tubes that had the same length and area.

11.4. EXPERIMENTAL SETUP

The experimental setup used in this experiment is shown in Figure 11.1. It constructed of two same tubes dimensions (20 cm in length and 2.7 cm in diameter) were used to contain the silica sand pack. Two horizontal (parallel in position) tubes were packed with different sand grains to emulate the permeability contrast exist in reservoirs. A syringe pump was used to inject suspended PPG, brine, oil, HCl, and polymer from the accumulators into the sand pack models. Two pressure transducers were mounted in front of each sand pack model to acquire the injection pressure change during the brine flooding and gel treatment processes. The test tubes were kept at the outlets of each sand pack to collect the volume of the fluid produced at the effluents.

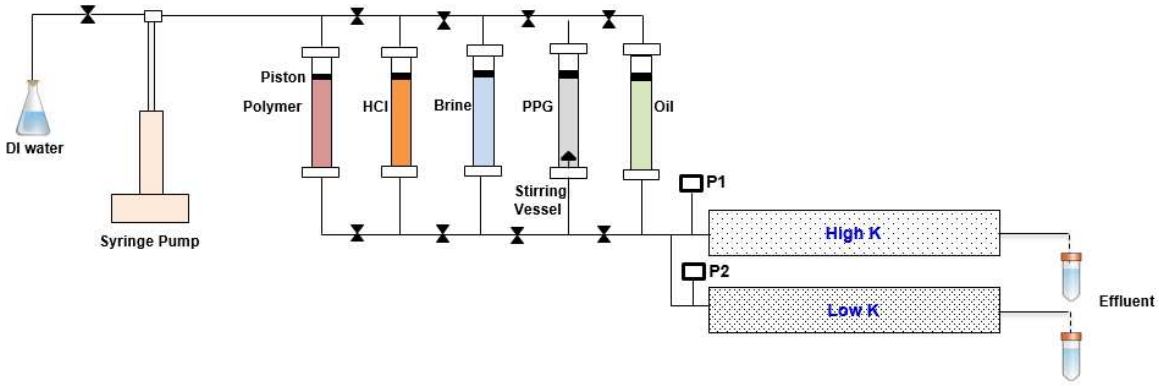

Figure 11.1—Schematic diagram of combined treatment techniques apparatus.

11.5. EXPERIMENAL PROCEDURES

The procedures for carrying out the non-cross flow heterogeneity experiments were briefly described as follows:

11.5.1. Preparing and Saturating Sand Pack Models. A vibrator machine was used to prepare the different sizes of silica sand so that the desire sand pack permeability could be obtained. Sand pack models were vacuumed for at least 6 hr. It then fully saturated with 1% NaCl to determine pore volume, porosity, and permeability.

Heavy oil viscosity was injected from the accumulator into each sand pack at a rate of 1 ml/min. Oil was injected until no water was produced and the injection pressure became stable. Both sand pack permeabilities (low and high) are connected to each other as shown in Figure 11.1 and then water flooding cycles began as follows.

11.5.2. First Water Flooding. A 1% NaCl was injected into both low and high permeabilities at a rate of 1 ml/min to simulate secondary oil recovery conditions. During the first water flooding, both oil recovery and water cut were determined for low and high sand pack permeability layers.

11.5.3. PPG Treatment. Swollen PPGs in 1% NaCl with a concentration of 2000 ppm were injected into the sand packs at a rate of 1 ml/min after the first water flooding processes were complete. During 0.5 PV of PPG injection treatment, volume of oil and water production were collected. The gel injection pressure was also recorded to determine the gel propagation response into low and high permeability layers.

11.5.4. Second Water Flooding. A 1% NaCl was injected again at the same injection rate after PPG treatment to test the gel blocking efficiency for high permeability. Oil recovery measurements from low permeability or un-swept zones were also determined.

11.5.5. HCl Soak Treatment. A very small amount of 10% HCl was injected into both sand packs model for mitigating the gel cake formed on surface of low permeability sands. A 0.1 PV was injected at 1 ml/min into the sand packs. Sand packs was kept for 12hr for HCl soaking purpose.

11.5.6. Third Water Flooding. A 1% brine concentration was injected again at 1 ml/min after the soaking HCl time period. The injection pressure was monitored during the third water flooding to determine the effect of HCl on minimizing/removing gel cake from low permeability zones. Fluid production at each sand pack effluents was collected during the water flooding.

11.5.7. Polymer Flooding. Polymer was injected into both sand packs at 1 ml/min. A 1 PV of polymer was injected. The injection pressure and fluid production at effluent were both recorded during polymer flooding.

11.5.8. Final Water Flooding. The final patches of water flooding was injected at 1 ml/min into both sand packs after polymer flooding. The injection pressure, oil recovery, and water production were all recorded for each sand pack permeability. Brine was continued injected until no oil produced at outlets and injection pressure became stable.

The above procedures were all repeated for each experiment. The oil recovery factor, the water cut, and the injection pressure were each determined for the low and the high permeability sand pack models.

11.6. RESULTS AND ANALYSIS

11.6.1. Oil Recovery Measurements. The oil recovery curves of the water flooding recycles, the PPG injection, and the polymer flooding of the three layer permeability contrast are plotted in Figures 11.2, 11.3 and 11.4. The oil recovery was determined for low and high permeabilities as a function of the pore volume injection.

In the initial water flooding stage, a large volume of oil was recovered from high permeability layers compared to a very small volume of oil was recovered from low permeability layers. The recoverable volume from the low permeability layers decreased substantially as the sand pack permeability contrast ratios increased.

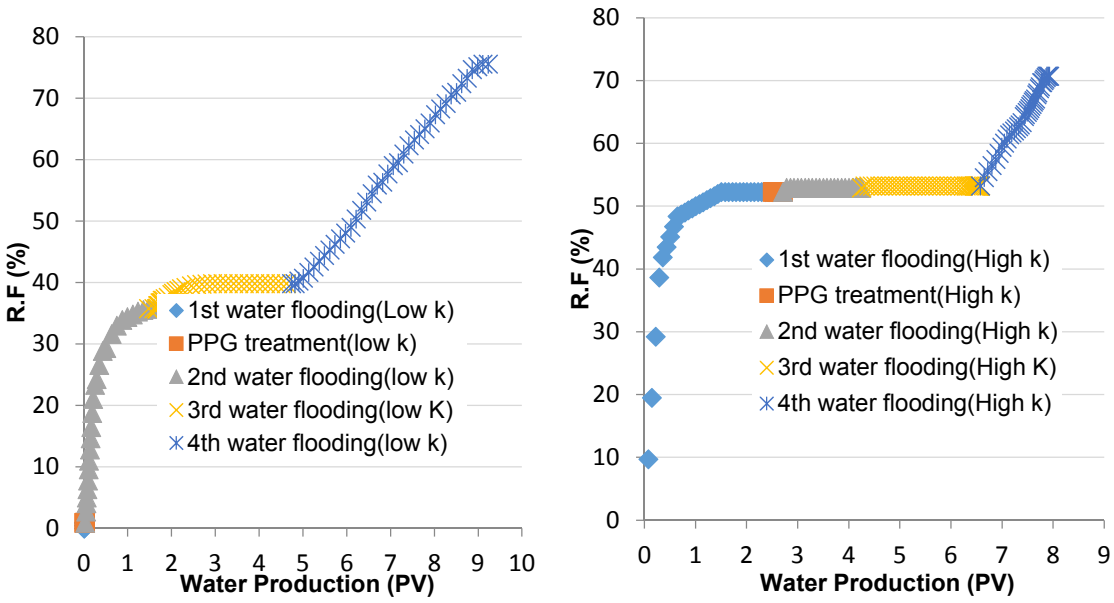

a) Low permeability of 0.5Darcy. b) High permeability of 20 Darcy.

Figure 11.2—Oil recovery for permeability of 0.5 Darcy and 20 Darcy.

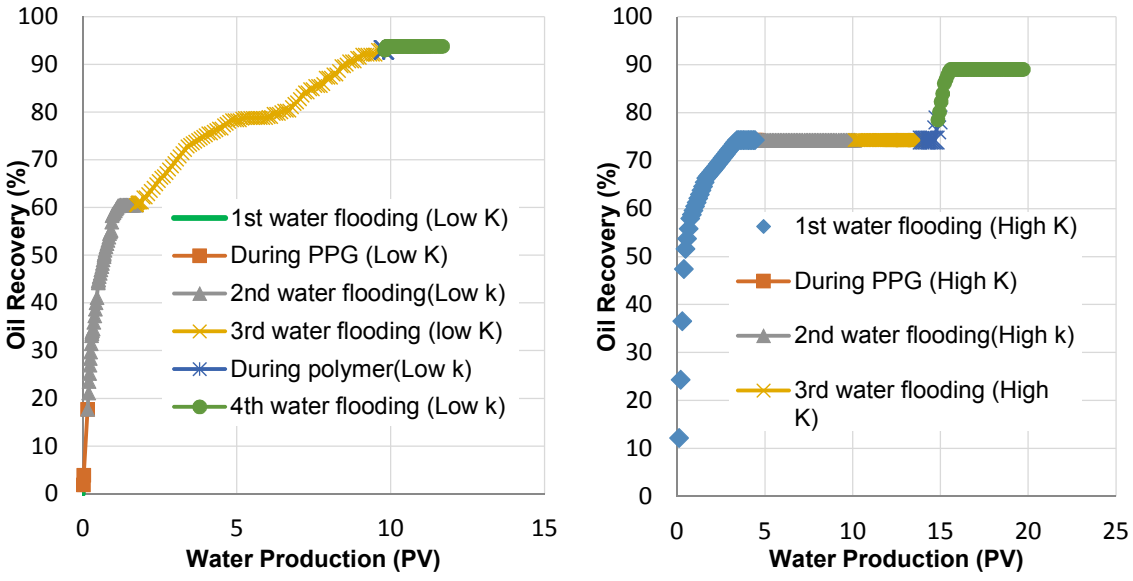

a) Low permeability of 1 Darcy. b) High permeability of 20 Darcy.

Figure 11.3—Oil recovery for permeability of 1 Darcy and 20 Darcy.

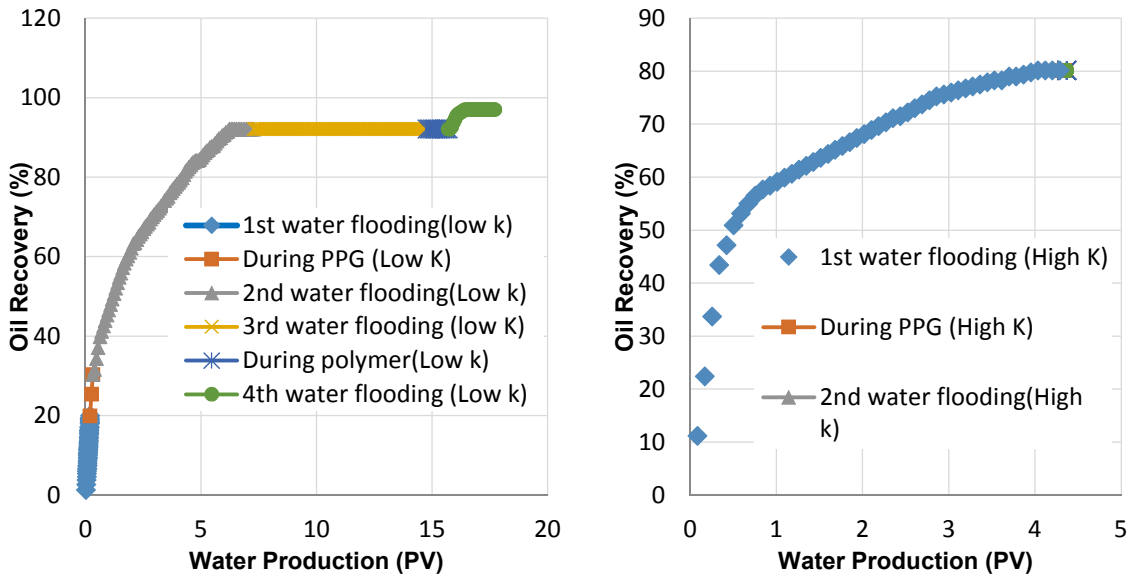

a) Low permeability of 6.1 Darcy. b) High permeability of 21 Darcy.

Figure 11.4—Oil recovery for permeability of 6.1 Darcy and 21 Darcy.

During PPG injection, the sweep efficiency of the heterogeneity improved and oil recovered from low permeability began to rise in low permeability layers. The oil recovered from low permeability increased substantially more than that recovered from high permeability layers. The recovery factor obtained from low permeability at permeability contrast ratio of 4, 20, and 44 was increased to 30, 18, and 3, respectively.

A large amount of PPG remained in the high permeability layers helping reduce the permeability contrast between layers. This PPGs also helped to improve sweep efficiency of the heterogeneity layers and increase the amount of oil recovered from the low permeability during the second water flooding. The oil recovered from low permeability rose substantially more than it did in the high permeability layers. The

recovery factor obtained from the low permeability at permeability contrast ratio of 4, 20, and 44 was increased to 93, 61, and 38, respectively.

Results also show a considerable amount of oil was produced during the third water flooding after the acid stimulation. Oil produced from the low permeability layers was much greater than the oil produced from the high permeability layers. Oil recovery increased by 5 to 30% for the heterogeneity models which have permeability contrast ratio of 44 and 20, respectively.

The oil recovery did not increased too much during polymer flooding for both low and high permeability. For instance, in permeability ratio of 22, oil recovery increase was approximately 5% from high permeability. This low percentage might be occurred because of the small polymer volume injected into the sand faces.

Final water cycle was injected into the heterogeneity model to determine the efficiency of combined PPG with polymer to increase oil recovery. A significant increase in the oil recovery was noticed during the fourth water flooding for both low and high permeabilities layers. In most permeability contrast ratios, a higher oil recovered was from low permeability layers than it was in high permeability layers. In permeability contrast ratios of 44, 20, and 4 the oil recovered incremental from the low permeability layers was 35, 2, and 5%, respectively while, in high permeability was 17, 11, and 0%, respectively.

At the end of this final cycle of water flooding, the final oil recovered from most permeability contrast ratios reached 80% from each low and high permeability layers. Most interestingly, the oil recovered from the low permeability layers was exceed the oil recovered from the high permeability layers.

11.6.2. Water Cut Measurements. The water cut curves obtained during the water flooding cycles, the PPG injection, and the polymer flooding of the three layer permeability contrasts are plotted in Figures 11.5, 11.6, and11.7.

During the first water flooding, large differences in the water cut were observed between the low and the high permeability packs. As shown by water cut curves, the water cut in the high permeability was higher than 90% while, in the low permeability packs was between negligible percentage and 0%.

As PPG started to inject into non cross flow heterogeneity model, the water cut in low permeability layers began to increase. The water cut in the low permeability rose significantly more during this water flooding than the previous water flooding.

When the water flooding is resumed again, the water cut began to decrease in the high permeability layers and increase in the low permeability layers. Water cut was fluctuated between approximately 70 and 80% in the beginning. It rose above 90% at the end of water flooding.

Water was injected again into the non-cross heterogeneity model after the acid treatment. Water cut was not effected too much with acid treatment.

Reduction in water cut was observed in both high and low permeabilities layers in the permeability ratio of 20 during the polymer flooding. The water cut dropped to 80% when the sand pack model was flooded with high viscous polymer. Other permeability ratios did not show any reduction in water cut.

A final patches of water injection were performed after the polymer flooding. A considerable dropped in water cut was determined for the permeability ratio of 44. Water cut decreased for both high and low permeability layers. Water cut decreased to 88, 75,

and 86% for the permeability ratios of 44, 20, and 4, respectively. It returned back into 100% at the end of water flooding processes. Decrease in water cut from high permeability layers was less than water cut decrease from the low permeability layers. These drops in water cut caused an increase of oil recovery from these layers.

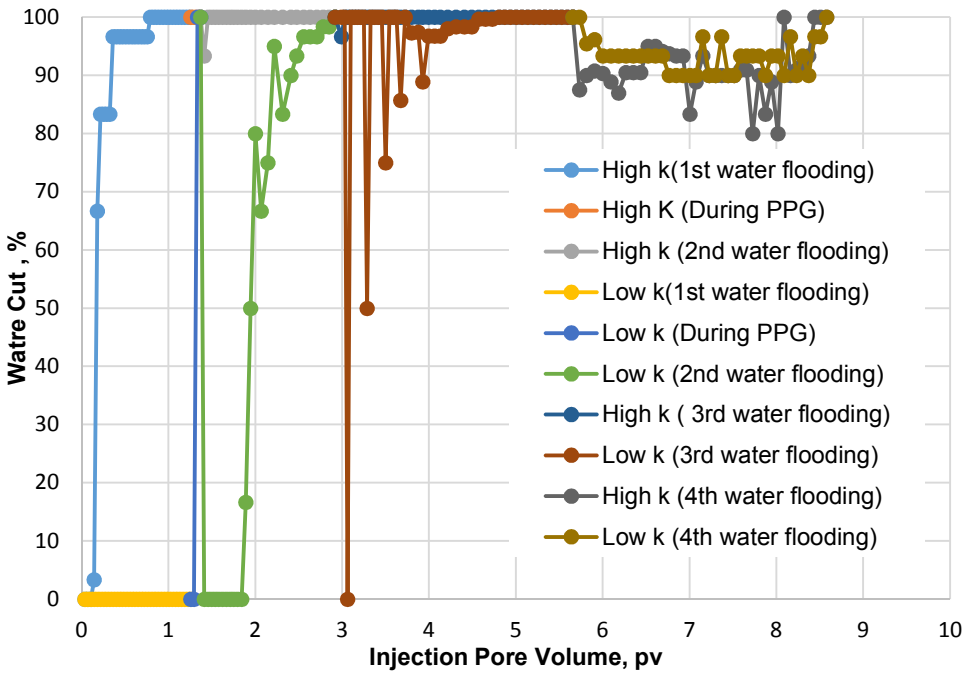

Figure 11.5—Water cut for permeability of 0.5 Darcy and 20 Darcy.

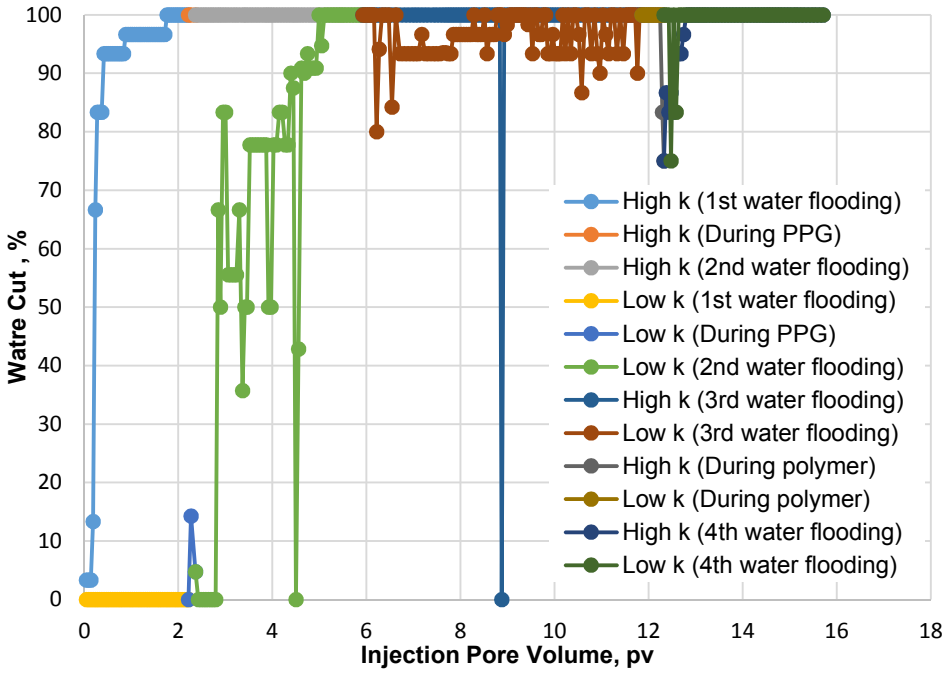

Figure 11.6—Water cut for permeability of 1 Darcy and 20 Darcy.

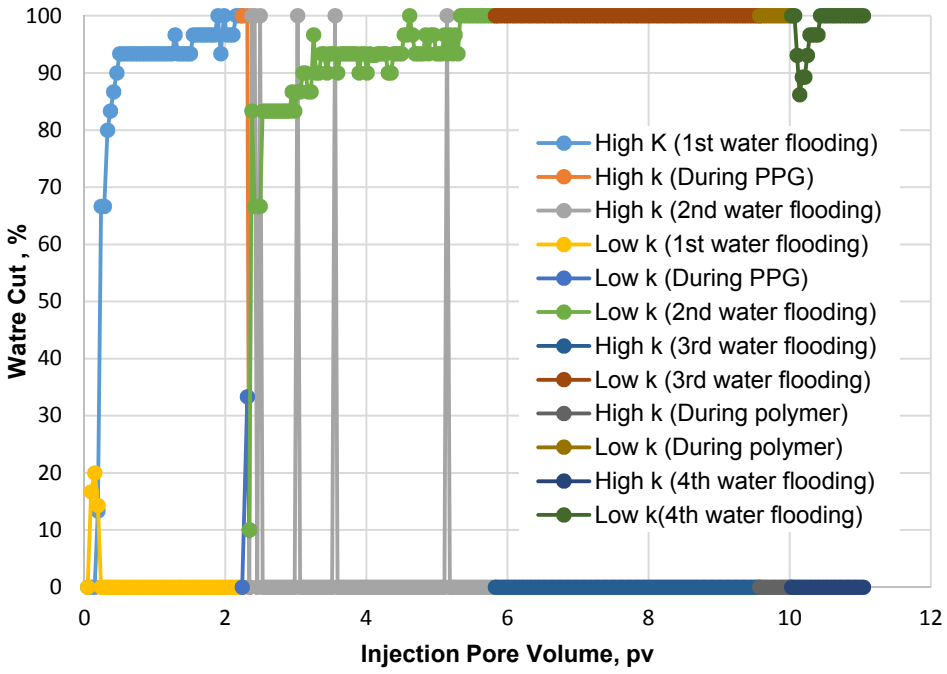

Figure 11.7—Water cut for permeability of 6.1 Darcy and 20 Darcy.

11.6.3. Injection Pressure Measurements. The injection pressures during the water flooding cycles, the PPG injection, and the polymer flooding of the three layer permeability contrast are plotted in Figures 11.8, 11.9, and 11.10.

The pressure drop during the first water flooding was slightly different at each the low and high permeability. These differences in pressure is expected because the difference in permeability between the layers.

The PPG injection pressure rose significantly more than the previous water flooding. It increased sharply in the both the low and the high permeability layers. It was less in low permeability layers.

During the second water flooding, water injection pressure began to decline after the PPG treatment. It became stable after around 0.5 PV. The second water injection pressure, however, was higher than injection pressure recorded during the first water flooding.

Polymer was injected into both the non-cross flow heterogeneous permeability layers. The injection pressure for all the permeability contrast ratios was increased much higher than the injection pressure measured during the prior water flooding.

The final water cycles was performed after polymer flooding was complete. The injection pressure declined for all the permeability contrast ratios. In the permeability contrast ratio of 44, injection pressure was higher than pressure recorded at prior water flooding. But it was similar to pressure change in the second water flooding. While, in permeability contrast of 4, injection pressure was in the same pressure change with

injection pressure measured in the prior water flooding. At the end of final water flooding, the injection pressure get back to the original pressures.

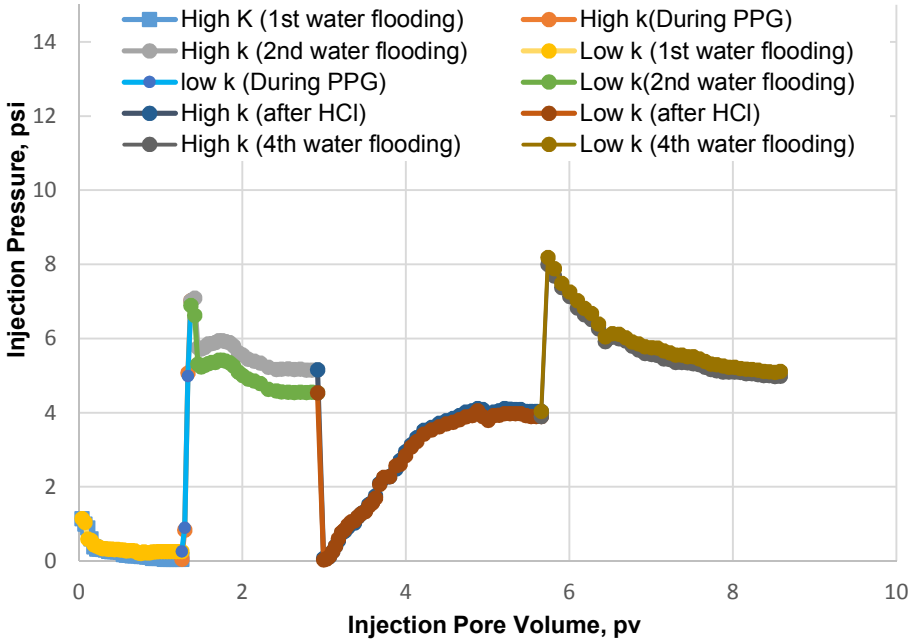

Figure 11.8—Injection pressure for permeabilities 0.4 Darcy and 20 Darcy.

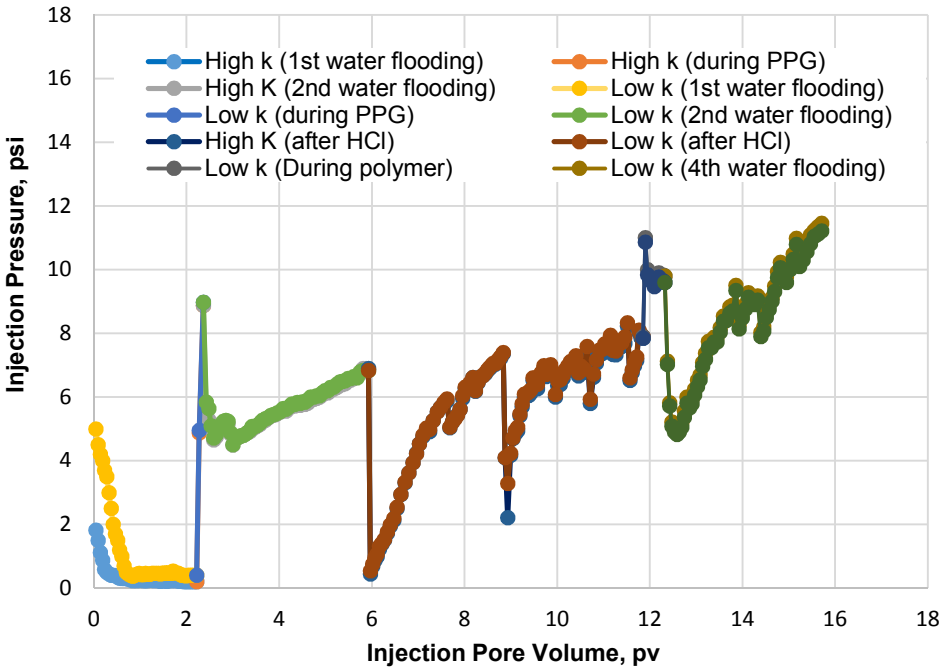

Figure 11.9—Injection pressure for permeabilities 1 Darcy and 20 Darcy.

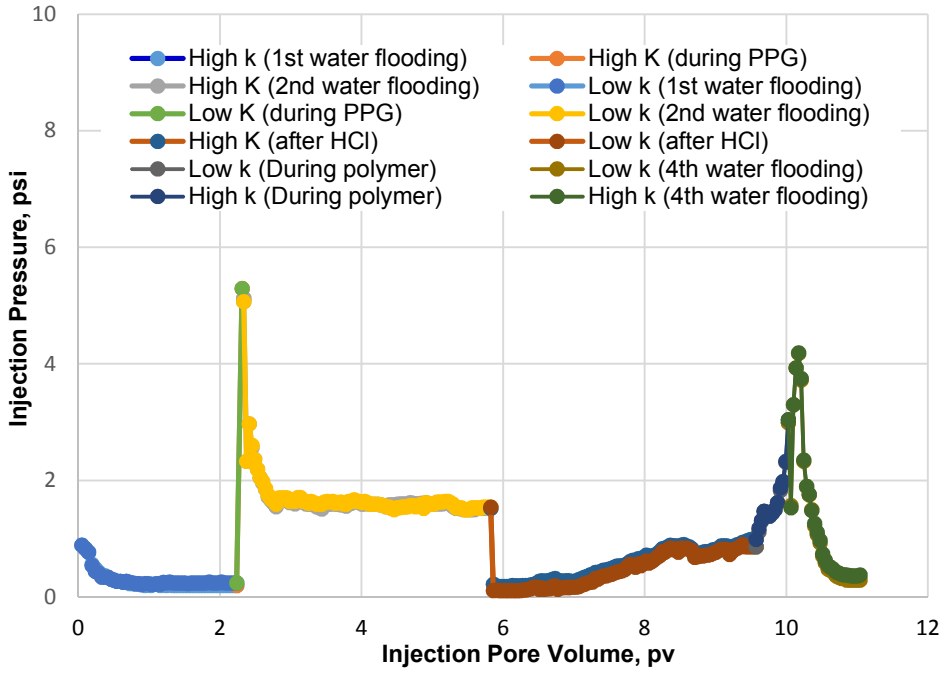

Figure 11.10—Injection pressure for permeabilities 6.1 Darcy and 21 Darcy.

11.7. CONCLUSION

- Combined PPG with polymer enhanced the oil recovered from both low and high permeability layers but more oil recovered was in low/un-swept layers. Oil recovery increased by approximately 25% from the low permeability layer and approximately 10% from the high permeability layers.
- Water cut decreased for both high and low permeability layers after polymer flooding. But water cut reduction from the low permeability layers was more pronounced than it was from the high permeability layers.
- The injection pressures measured after polymer flooding for all the permeability contrast ratios were greater than injection pressure measured after acid treatment but they were still close or less than injection pressure measured after PPG treatment.

12. CONCLUSIONS & RECOMMENDATIONS

12.1. CONCLUSIONS

This dissertation provide an extensive laboratory work to evaluate PPG treatment as a cost effective method to control excessive unwanted water production and improve sweep oil efficiency. The study provide a comprehensive evaluation work on PPGs injection, mechanisms, and placement in different porous media models namely: fractures, conduits, channels, super-K permeability cores, heterogeneity cores, and low permeability cores. The research involved using PPG as a conformance control material with other techniques such as stimulation treatment using Hydrochloric acid and Mobility control using polymer. The major findings collected during this study are sorted below based on the discussed topics as follow:

i. **Effect of a Gel Pack on Oil and Water Flow**. A swollen PPG was placed in a large channel and cycles of brine and oil were injected through the gel to evaluate PPGs resistance to water flow.

- PPGs formed a gel pack permeability with in channel rather than fully blocking it. Gel resistance to water flow improved when larger particles and stronger gel strengths were selected. The PPG pack was compressible; its compressibility decreased as the load pressure increased
- PPG pack permeability measurements taken at different brine concentrations, particle sizes, and oil viscosities were not followed Darcy law. Instead, the measurements revealed that the PPG was velocity dependent, followed a

nonlinear relationship. PPG permeability was dependent on not only the velocity of the brine injected but also the elasticity index of the gels used.

- Particles reduced the permeability to water much more than that to oil. The particle gels were less resistant to high viscosity oil than they were to low viscosity oil.

ii. **Evaluate The Effectiveness of Using Acid to Remove Gel Cake.** In this topic, the factors effect on forming gel damage cake, the interaction between PPG and HCl, and the permeability reduction and the retained after gel and acid treatments were all evaluated.

- PPG formed a permeable surface gel cake on the low-permeability cores. The formation of a gel cake significantly reduced the permeability when the brine concentration was low and the rock permeability was high.
- Hydrochloric acid effectively removed the gel cake damage that formed on low-permeability zones.
- The PPGs did not swell significantly after the HCl treatment when they were flushed with different cycles of brine. This low swelling ratio decreased the PPG's chance of damaging low-permeable cores.

iii. **Particle Gel Propagation through Open Conduits.** Swollen PPGs in different brine concentrations were injected into different internal diameters to determine the passing/blocking criteria for PPG injection.

- Two new empirical correlation models were successfully developed to predict both the PPG resistance factor and the stable injection pressure.

- Weak gels can be injected into large particle openings ratio with relative small increase in injection pressure compared to strong gels. Weak gels broke into small sizes allowing them to pass through easily.
- PPG strength impacted the injectivity significantly more than did the particle opening ratio. Its size was reduced when it moved through the conduits due to dehydration and breakdown.

iv. **Disproportionate Permeability Reduction through Conduits.** In this subject, different cycles of brine and oil were injected through PPG filled closed fractures. It aims to determine how much PPG reduced water permeability much greater than oil permeability.

- The permeability reduction factor to water became 100 to 1700 times greater than the permeability reduction factor to oil.
- A different disproportionate permeability reduction mechanisms of the particle gel was investigated. The gel strength greatly affected the DPR and is an important parameter that should be considered in PPG design.

v. **Micron-size Particle Gel Propagation through Super K Permeability Systems.** A suspended swollen PPG was injected into super k sand pack models to monitor gel propagations and performance to increase oil recovery and decrease water production.

- Fully swollen gel particles have a better injectivity than partially swollen particles with larger diameter sizes; particle strength is more dominant particle movement than particle size.

- A large PPG injection pore volume was needed to reach effluent when high water salinities, big particle sizes, and low PPG concentration were used.
- The PPGs reduced the permeability to water much more than they reduced the permeability to oil during all of the injection flow rates. Its blocking efficiency to water flow increased significantly as the PPGs strength, size, and concentration increased.
- A large oil recovery incremental, typically reached near 20%, occurred during the PPGs injection treatment. Oil recovery during the PPGs injection varied according to the PPGs injection pore volume, concentration, and strength.

vi. **Gel Propagation Effect on Non-Cross Flow Reservoir Heterogeneity.** This topic discussed the effect of use PPG to correct the non-cross flow heterogeneity problems to improve sweep efficiency and increase oil recovery from un-swept/low permeability formations.

- Large incremental oil recovery from low permeability sand pack after PPGs treatment. This increase in oil recovery was strongly dependent on the permeability contrast ratio.
- The use of PPG to correct non cross flow heterogeneity problem became more effective when the sand pack permeability layers became more heterogeneous.

vii. **Gel Propagation Effect on the Cross Flow Reservoir Heterogeneity**. A novel experiments were used to evaluate the use of the diversion materials using PPG to improve oil recovery in cross flow heterogeneity formations. An acid treatment using HCl was involved in the evaluation process to mitigate the gel filter cake formed on the low permeability zone.

- A significant increase was noticed in oil recovery during PPG treatment. Oil recovery increased was dependent on the changes that occurred in PPG slug and the heterogeneity level between layers.
- A stimulation treatment was used after PPG treatment retained the injection pressure to the original situation, before the PPG treatment was introduced.

viii. **A Combination of Stimulation and Conformance Treatments to Improve Oil Recovery.** This part of research introduced the use of combing HCl and PPG to improve conformance control results obtained from the non-cross flow heterogeneity formations. HCl proposed to remove gel filter cake formed on surface of low k during gel treatment to increase oil recovery during post water flushes process.

- The HCl was used successfully to mitigate the gel filter cake formed. The gel blocking efficiency in the large permeability cores did not hurt too much with acid treatment.
- The amount of oil recovered typically reached 5% after the acid treatment. This increase in oil production caused by increased the amount of water injection into low permeability.

ix. **A Combination of Conformance Treatments and Mobility Controls to Improve Oil Recovery.** This work investigated the useful techniques of combining PPG with polymer to improve oil recovery from both low and high permeability zones. The PPGs were injected into high permeability zones to improve the sweep efficiency in low permeability zones and polymer was injected next to further increase oil production from both low and high permeability.

- The combination techniques show a very good promising results where oil recovery in some experiments increased to more than 20% from low permeability cores.

12.2. RECOMMENDATIONS FOR FUTURE WORK

The ultimate objective of this dissertation was to provide a comprehensive and systematic study into designing better particle gel treatments intended for use in large permeability features such as fractures and high permeability streaks to increase oil recovery and reduce water production. The following are suggestions for future work to extend the outcomes of the current research:

- During this study PPG was investigated heavily in both open fractures and super-K permeability systems. Additional work is needed to determine factors that affects a PPGs injections and placement through closed fractures features.
- Further work is need to evaluate PPG use to correct the non-cross flow heterogeneity problems. The impact of gel strength, concentration, and slug volume should be investigated.
- The current work introduced combing PPG with other techniques such as stimulation and mobility controls. However, further investigation should be performed to better understand oil recovery changes when polymer are used either alone or in combination with gel.

BIBLIOGRAPHY

Al-Anazi, H.A. and Sharma, M.M. 2002. Use of pH Sensitive Polymer for Conformance Control. Paper SPE 73782 presented at the International Symposium and Exhibition on Formation Damage Control, Lafayette, Louisiana, USA, 20–21 February.doi: 10.2118/73782 M.

Al-Sharji, H.H., Grattoni, C.A., Dawe, R.A., and Zimmerman, R.W. 1999. Pore-Scale Study of the Flow of Oil and Water through Polymer Gels. Paper SPE 56738 presented at the SPE Annual Technical Conference and Exhibition, Houston, 3–6 October. DOI: 10.2118/56738-MS.

Bai, B., Li, L., Liu, Y., Liu, H., Wang, Z., and You, C. 2007a. Preformed particle gel for Conformance Control: Factors Affecting its Properties and Applications. SPE Res Eval & Eng 10 (4): 415–421. SPE-89389-PA. Doi: 10.2118/89389-PA.

Bai, B., Liu, Y., Coste, J.-P., and Li, L. 2007b. Preformed particle gel for Conformance Control: Transport Mechanism through Porous Media. SPE Res Eval & Eng 10 (2): 176–184. SPE-89468-PA. Doi: 10.2118/89468-PA.

Bai, B., Wei, M., and Liu,Y. 2013. Field and Lab Experience with a Successful Preformed Particle Gel Conformance Control Technology. Presented at the SPE Production and Operation Symposium, Oklahoma City, 23-28 March. SPE-164511-MS. http://dx.doi.org/10.2118/164511-MS.

Bailey, B., Crabtree, M., Tyrie, J., Elphick, J., kuchuk, F., Romano, C., Roodhart, L. 2000. Water Control. *Oilfield Review* **12** (1): 30.

Benson I., Nghiem L.X., Bryant S.L., Sharma M.M. and Huh C.2007. Development and Use of a Simulation Model for Mobility/Conformance Control Using a pH-Sensitive Polymer. Paper SPE 109665 presented at SPE Annual Technical Conference and Exhibition, California, 11-14 November .doi: 10.2118/109665-MS.

Carr, M. and Yang, H. 1998. Evaluation for Polymer Damage Aids in Candidate Selection for Removal Treatment. Presented at the SPE Gas Technology Symposium, Calgary, 15-18 March. SPE 39785-MS. http://dx.doi.org/10.2118/39785-MS.

Crews, J. and Huang, T. 2010. New Remediation Technology Enables Removal of Residual Polymer in Hydraulic Fractures. Presented at the SPE Annual Technical Conference and Exhibition, Florence, 19-22 September. SPE 135199-MS.http://dx.doi.org/10.2118/135199-MS.

Chan, K.S 1995. Water Control Diagnostic Plots. Presented at the SPE Annual Technical Conference and Exhibition, Dallas, 22-25 October. SPE 30775-MS.http://dx.doi.org/10.2118/30775-MS.

Chauveteau, G. and A. Zaitoun 1981. Basic rheological behavior of xanthan polysaccharide solutions in porous media: Effects of pore size and polymer concentration. Enhanced oil recovery: proceedings of the third European Symposium on Enhanced Oil Recovery: 197-212.

Chauveteau, G., Tabary, R., Renard, M., and Omari, A. 1999. Controlling In-Situ Gelation of Polyacrylamides by Zirconium for Water Shutoff. Paper SPE 50752 presented at the SPE International Symposium on Oilfield Chemistry, Houston, 16–19 February. Doi: 10.2118/50752-MS.

Chauveteau, G., Omari, A., Tabary, R., Renard, M., Veerapen, J., and Rose, J. 2001. New Size-Controlled Microgels for Oil Production. Paper SPE 64988 presented at the SPE International Symposium on Oilfield Chemistry, Houston, 13–16 February. Doi: 10.2118/64988-MS.

Chauveteau, G., Tabary, R., le Bon, C., Renard, M., Feng, Y., and Omari, A. 2003. In-Depth Permeability Control by Adsorption of Soft Size-Controlled Microgels. Paper SPE 82228 presented at SPE Euro-pean Formation Damage Conference, The Hague, 13–14 May. Doi: 10.2118/82228-MS.

Coste, J.-P., Liu, Y., Bai, B., Li, Y., Shen, P., Wang, Z., and Zhu, G. 2000. In-Depth FLuid Diversion by Pre-Gelled Particles. Laboratory Study and Pilot Testing. Paper SPE 59362 presented at the SPE/DOE Improved Oil Recovery Symposium, Tulsa, 3–5 April. Doi: 10.2118/59362-MS.

Dong H.Z; Fang, S.F; Wang, D.M; Wang, J.Y; Liu, Z; Hou, H. 2008. Review of Practical Experience &Management by Polymer Flooding at Daqing. Paper SPE 114342 presented at the SPE/DOE Improved Oil Recovery Symposium, Tulsa, 19–23 April. Doi: 10.2118/114342-MS.

Elsharafi, M. and Bai, B. 2012. Effect of Weak Preformed Particle Gel on Unswept Oil Zones/Areas during Conformance Control Treatments. *Ind. Eng. Chem. Res*. **51** (35): 11547–11554. Doi**:** 10.1021/ie3007227.

Environmental Protection Agency. 2000. Profile of the Oil and Gas Extraction Industry. EPA/310-R-00-004.

Frampton, H., Morgan, J.C., Cheung, S.K., Munson, L., Chang, K.T., and Williams, D. 2004. Development of a Novel Water flood Conformance Control System. Paper SPE 89391 presented at the SPE/DOE Symposium on Improved Oil Recovery, Tulsa, 17–21 April. Doi: 10.2118/89391-MS.

Ganguly, S., Willhite, G.P., Green, D.W., and McCool, C.S. 2001. The Effect of Fluid Leak off on Gel Placement and Gel Stability in Fractures. Paper SPE 64987 presented at the SPE International Symposium on Oilfield Chemistry, Houston, 13–16 February. DOI: 10.2118/64987-MS.

Ganguly, S., Willhite, G.P., Green, D.W., and McCool, C.S. 2003. Effect of Flow Rate on Disproportionate Permeability Reduction. Paper SPE 80205 presented at the SPE International Symposium on Oilfield Chemistry, Houston, 5–7 February. DOI: 10.2118/80205-MS.

Garmeh R., Izadi M., Salehi M., Romero J.L., Thomas C.P. and Manrique E.J.2011 .Thermally Active Polymer to Improve Sweep Efficiency of Water Floods: Simulation and Pilot Design Approaches. Paper SPE 144234 presented at Enhanced Oil Recovery Conference, Kuala Lumpur, 19-21 July. Doi: 10.2118/144234-MS.

Grattoni, C.A., Al-Sharji, H.H., Yang, C., Muggeridge, A.H., and Zimmerman, R.W. 2001. Rheology and Permeability of Crosslinked Polyacrylamide Gel. Journal of Colloid and Interface Science 240: 601-607.doi:10.1006/jcis.2001.7633.

Green, Don and Willhite, Paul. 1998. 545 pp.; Softcover. SPE Textbook Series Vol. 6. ISBN: 978-1-55563-077-5. Society of Petroleum Engineers

Halliburton. 2002. Water Management Manual. H03349. V1.12/02.

Hill, F., Monroe, S., and Mohanan, R. 2012. Water Management—An Increasing Trend in the Oil and Gas Industry. Presented at the SPE/EAGE European Unconventional Resources Conference and Exhibition, Vienna, 20-22 March. SPE-154720-MS, http://dx.doi.org/10.2118/154720-MS.

Huh, C., Choi, S.K., and Sharma, M.M. 2005. A Rheological Model for pH-Sensitive Ionic Polymer Solutions for Optimal Mobility-Control Applications. Paper SPE 96914 presented at the SPE Annual Technical Conference and Exhibition, Dallas, 9–12 October. Doi: 10.2118/96914-MS.

Imqam, A., Bai, B., Al-Ramadan, M. Wei, M., Delshad, M., Sepehrnoori, K. 2014. Preformed Particle Gel Extrusion through Open Conduits during Conformance Control Treatments. SPE-169107-PA. http://dx.doi.org/10.2118/169107-PA.

Imqam, A., Bai, B. 2015. Optimizing the strength and size of preformed particle gels for better conformance control treatment. *Fuel Journal;* **148:** 178–185. http://dx.doi:10.1016/j.fuel.2015.01.022.

Imqam, A., Bai, B., Xiong, C., Wei, M., Delshad, M., Sepehrnoori, K. 2014. Characterizations of Disproportionate Permeability Reduction of Particle Gels through Fractures. Paper SPE 171531 presented at the SPE Asia Pacific Oil & Gas Conference and Exhibition held in Adelaide, Australia, 14–16 October. http://dx.doi.org/10.2118/171531-MS

Imqam, A., Elue, H., Muhammed, F., Bai, Baojun. 2015. Hydrochloric Acid Applications to Improve Particle Gel Conformance Control Treatment. Paper SPE- 172352 presented at the SPE Nigeria Annual International Conference and Exhibition, 5-7 August, Lagos, Nigeria. http://dx.doi.org/10.2118/172352-MS.

Imqam, A, Bai, B. 2015. Preformed Particle Gel Propagation through Super-K Permeability and its Resistance to Water Flow during Conformance Control. Paper SPE 176429 accepted to present at the SPE Asia Pacific Oil & Gas Conference and Exhibition held in Bali, Indonesia, 20–22 October.

Kosztin, B., Ferdiansyah, E., Zadjali, F., Al-Sharji, H., Al-Ma'amari, K., Al-Salmani, S. 2012. Joint Stimulation-Water Shut-off Technology Leads to Extra Oil from Mature Fields. Presented at the SPE North Africa Technical Conference and Exhibition, Cairo, 20-22 February. SPE 149658-MS. http://dx.doi.org/10.2118/149658-MS.

Krishnan, P., Asghari, K., Willhite, G., McCool, C., Green, D., and Vossoughi, S. 2000. Dehydration and Permeability of Gels Used in In-Situ Permeability Modification Treatments. Paper SPE 59347 presented at the SPE/DOE at Improved Oil Recovery, Tulsa, 3–5 April. DOI: 10.2118/59347-MS.

Larry W. Lake. 1989. Enhanced Oil Recovery. Englewood Cliffs, NJ: Prentice Hall, 550 pp. ISBN, 0132816016, 9780132816014.

Liang, J.-T., Lee, R.L., and Seright, R.S. 1993. Gel Placement in Production Wells. SPEPF 8 (4): 276–284; Trans., AIME, 295. SPE-20211-PA. DOI: 10.2118/20211-PA.

Liang, J.-T., Sun, H., and Seright, R.S. 1995. Why Do Gels Reduce Water Permeability More Than Oil Permeability? SPERE 10 (4): 282–286; Trans., AIME, 299. SPE-27829-PA. DOI: 10.2118/27829-PA.

Liang, J., and Seright, R.S. 1997. Further Investigations of Why Gels Reduce kw More Than ko. Paper SPE 37249 presented at the 1997 SPE International Symposium on Oilfield Chemistry, Houston, Texas, 18-21 February.

Liu, Jin., and Seright. R.S. 2000. Rheology of Gels Used For Conformance Control in Fractures. Paper SPE 59318 presented at Improved Oil Recovery Symposium, Tulsa, Oklahoma, 3-5 April. DOI: 10.2118/59318-MS.

Liu, Y, Bai, B., and Shuler, P.L. 2006. Application and Development of Chemical-Based Conformance Control Treatments in China Oil Fields. Paper SPE 99641 presented at the SPE/DOE Symposium on Improved Oil Recovery, Tulsa, 22–26 April. DOI: 10.2118/99641-MS.

McCool, C.S., Li, X., and Willhite, G.P. 2009. Flow of a Polyacrylamide/Chromium Acetate System in a Long Conduit. SPE Journal 14(1): 54-66. SPE 106059-PA. DOI: 10.2118/106059-PA.

Mahdavinia, G.R., Pourjavadi, A., Hosseinzadeh, H., Zohuriaan, M. 2004. Modified Chitosan 4. Superabsorbent Hydrogels from Poly (Acrylic Acid-co-acrylamide) Grafted Chitosan with Salt- and pH-responsiveness Properties. *Eur Polym J*; **40**: 1399-1407. doi:10.1016/j.eurpolymj.2004.01.039.

Morgan N.: "Pop Goes the Polymer", BP Frontiers (December 2007), pp. 6-9.

Nguyen, T.Q. 2004. Effect of Composition of a Polyacrylamide-Chromium(III) Acetate Gel on the Magnitude of Gel Dehydration and Disproportionate Permeability Reduction. Paper SPE 89404 presented at the SPE/DOE Fourteenth Symposium on Improved Oil Recovery, Tulsa, 17–21 April. DOI: 10.2118/89404-MS.

Pritchett, J., Frampton, H., Brinkman, J., Cheung, S, Morgan, J., Chang, K.T., Williams, D., and Goodgame, J. 2003. Field Application of a New In-Depth Water flood Conformance Improvement Tool. Paper SPE 84897 presented at the SPE International Improved Oil Recovery Conference in Asia Pacific, Kuala Lumpur, 20–21 October. Doi: 10.2118/84897-MS.

Ohms, D., McLeod, J., Graff, C., Frampton, H., Morgan, J., Cheung, S., Yancey, K., Chang, K. 2009. Incremental Oil Success From Waterflood Sweep Improvement in Alaska. Paper SPE 121761 presented in International Symposium on Oilfield Chemistry, Woodlands, 20-22 April. http://dx.doi.org/10.2118/121761-MS.

Reddy, B.R. 2013. Laboratory Characterization of Gel Filter Cake and Development of Non-oxidizing Gel Breakers for Zirconium Crosslinked Fracturing Fluids. Presented at the SPE International Symposium on Oilfield Chemistry, Woodlands, Texas, 8-10 April. SPE-164116-MS. http://dx.doi.org/10.2118/164116-MS.

Richard, B., Crystal, L., Tim, S., Steven, W. 2014.Combining Conformance Treatment with Mobility Control Increases Enhanced Recovery Factor. Paper SPE 169046 presented at the SPE SPE Improved Oil Recovery Symposium, Tulsa, 12-16April. Doi: 10.2118/169046-MS.

Roussennac, B., Toschi, C. 2010. Brightwater Trial in Salema Field (Campos Basin, Brazil).Paper SPE 131299 presented SPE EUROPEC/EAGE Annual Conference and Exhibition held in Barcelona, Spain, 14–17 June. http://dx.doi.org/10.2118/131299-MS.

Rousseau, D., Chauveteau, G., Renard, M., Tabary, R., Zaitoun, A., Mallo, P., Braun, O., and Omari, A. 2005. Rheology and Transport in Porous Media of New Water Shutoff/Conformance Control Microgels. Paper SPE 93254 presented at the SPE International Symposium on Oilfield Chemistry, Houston, 2–4 February. Doi: 10.2118/93254-MS.

Rubinstein, M., Dobrynin, A.V., and Joanny, J.F. 1996. Elastic Modulus and Equilibrium Swelling of Polyelectrolyte Gels. *Macromolecules*, **29** (1): 398–406. **DOI:** 10.1021/ma9511917.

Sarwar, M.U., Cawiezel, K.E., and Naser-El-Din, H.A. 2011. Gel Degradation Studies of Oxidative and Enzyme Breakers to Optimize Breaker Type and Concentration for Effective Break Profiles at Low and Medium Temperature Ranges. Presented at the SPE Hydraulic Fracturing Technology Conference and Exhibition, Woodlands, Texas, 24-26 January. SPE-140520-MS. http://dx.doi.org/10.2118/140520-MS.

Seright, R.S. 1998. Improved Methods for Water Shut-off. Annual Report (U.S. DOE Report DOE/PC/91008-4), U.S.DOE Contract DE-AC22-94PC91008.

Seright, R.S. 1988. Placement of Gels to Modify Injection Profiles. Paper SPE 17332 presented at the SPE/DOE Enhanced Oil Recovery Symposium, Tulsa, 16–21 April. DOI: 10.2118/17332-MS.

Seright, R.S. and Liang, J.1994. A Survey of Field Applications of Gel Treatments for Water Shutoff. Paper SPE 26991 presented at the SPE III Latin American & Caribbean Petroleum Engineering Conference, Buenos Aires, April 27-29.

Seright, R.S. 1999a. Mechanism for Gel Propagation through Fractures. Paper SPE 55628 presented at the SPE Rocky Mountain Regional Meeting, Gillette, Wyoming, 15–18 May. DOI: 10.2118/55628-MS.

Seright, R.S. 1999b. Using Chemicals to Optimize Conformance Control in Fractured Reservoirs. First Annual Report, Contract No. DE-AC26-98BC15110, U.S. DOE, Washington D.C. (September 1999) 24.

Seright, R.S. 1995. Reduction of Gas and Water Permeabilities Using Gels. SPEPF 10 (2): 103–108; Trans., AIME, 299. SPE-25855-PA. DOI: 10.2118/25855-PA.

Seright, R.S. 1997.Use of Preformed Gels for Conformance Control in Fractured Systems. SPE production & facilities 12 (1): 59-65.SPE-35351-PA. DOI: 10.2118/35351-PA.

Seright, R.S. 2001. Gel Propagation through Fractures. SPEPF 16(4): 225-231. SPE –PA. DOI: 10.2118/74602-PA.

Seright, R.S., Lane, R.H., and Sydansk, R.D. 2001. A Strategy for Attacking Excess Water Production. Paper SPE 70067 presented at the SPE Permian Basin Oil and Gas Recovery Conference, Midland, 15-16 May. doi: 10.2118/70067-MS.

Seright, R.S. 2002. Conformance Improvement Using Gels. First Annual Report, Contract No. DE-FC26-01BC15316, U.S. DOE, Washington D.C. (September 2002) 43–59.

Seright, R.S. 2003. Washout of Cr(III)-Acetate-HPAM Gels From Fractures. Paper SPE 80200 presented at the SPE International Symposium on Oilfield Chemistry, Houston, 5-7 February. DOI: 10.2118/80200-MS.

Seright, R.S. 2006. Optimizing Disproportionate Permeability Reduction. Paper SPE 99443 SPE/DOE Symposium on Improved Oil Recovery, Tulsa, 22-26 April. DOI: 10.2118/99443-MS.

Seright, R.S. 2009. Disproportionate Permeability Reduction With Pore-Filling Gels. SPE*J* 14 (1): 5-13.SPE-99443-PA. DOI: 10.2118/99443-PA.

Smith, D., Giraud, M., Kemp, C., McBee, M., Taitano, J., Winfield, M., Portwood J.T., and Everett, D. 2006. The successful Evolution of Anton Irish Conformance Effort. Paper SPE 103044 presented at SPE Annual Technical Conference and Exhibition, San Antonio, 24-27 September. DOI: 10.2118/103044-MS.

Sydansk, R.D., and Moore,P.E. 1992.Gel Conformance Treatments Increase Oil Production in Wyoming.Oil and Gas Journal 40-45.

Sydansk , R.D.,Xiong, Y., Al-Dhafeeri,A., Schrader, R., and Seright, R.S. 2005. Characterization of Partially Formed Polymer Gels for Application to Fractured Production Wells for Water–Shutoff Purposes.SPE Prod & Fac 20 (3): 240-249.SPE-89401-PA. DOI: 10.2118/89401-PA.

Turner, B. and Zahner, R. 2009. Polymer Gel Water-Shutoff Applications Combined with Stimulation Increase Oil Production and Life of Wells in the Monterey Formation Offshore California. Presented at the SPE Western Regional Meeting, San Jose, California, 24-26 April. SPE-121194-MS. http://dx.doi.org/10.2118/121194-MS.

Yanez P.A.P., Mustoni J.L., Relling M.F., Chang K.T., Hopkinson P. and Frampton H.2007. New Attempt in Improving Sweep Efficiency at the Mature Koluel Kaike and Piedra Clavada Water flooding Projects of the S. Jorge Basin in Argentina. Paper SPE 107923 presented at Latin American and Caribbean Petroleum Engineering Conference, Buenos Aires, 15-18 April .doi: 10.2118/107923-MS

Yang, C., Grattoni, C.A., Muggeridge, A.H., and Zimmerman, R.W. 2002 .Flow of water through channels Filled with Deformable Polymer Gels. Journal of Colloid and Interface Science 250: 466-470.doi:10.1006/jcis.2002.8325.

Wang, Y. and Seright, R.S.2006. Correlating Gel Rheology with Behavior during Extrusion through Fractures. Paper SPE 99462 presented at SPE/DOE Symposium on Improved Oil Recovery, Tulsa, 22-26 April. DOI: 10.2118/99462-MS.

Willhite, G.P. 2002. Mechanisms Causing Disproportionate Permeability in Porous Media Treated With Chromium Acetate/HPAAM Gels. SPEJ 7 (1): 100–108. SPE-77185-PA. DOI: 10.2118/77185-PA.

Wilton, R., and Asghari, K. 2007. Improving Gel Performance in Fractures: Chromium Pre-Flush and Overload. Journal of Canadian Petroleum Technology 46(2) : DOI: 10.2118/07-02-04.

Zaitoun, A. and Kohler, N. 1988. Two-Phase Flow through Porous Media: Effect of an Adsorbed Polymer Layer. Paper SPE 18085, SPE Annual Conference and Exhibition, Houston, TX, USA, October 2-5. http://dx.doi.org/10.2118/18085-MS

Zaitoun, A., Tabary, R., Rousseau, D., Pichery, T., Nouyoux, S., Mallo, P., and Braun, O. 2007. Using Microgels to Shut Off Water in a Gas Storage Well. Paper SPE 106042 presented at the SPE International Symposium on Oilfield Chemistry, Houston, 28 February–2 March. Doi: 10.2118/106042-MS**.**

Zaitoun, A., Makakou, P., Blin, N., Al-Maamari, R.S., Al-Hashmi, A.R., Abdel-Goad, M., Al-Sharji.H.H. 2012. Shear Stability of EOR Polymers. SPE Journal 17(2): 335-339. SPE-141113-PA. DOI: 10.2118/141113-PA.

Zaitoun, A., Bertin, H., and Lasseux, D. 1998. Two-Phase Flow Property Modifications by Polymer Adsorption. Paper SPE 39631 presented at the SPE/DOE Improved Oil Recovery Symposium, Tulsa, 19–22 April. DOI: 10.2118/396.

Zhang, H., and Bai, B. 2011. Preformed particle gel Transport through Open Fracture and its Effect on Water Flow. SPE Journal 16(2): 388-400. SPE-129908-PA. DOI: 10.2118/129908-PA.

Zhao, P., Zhao, H., Bai, B., Yang, X. 2004. Improved Injection Profile by Combing Plugging Agent Treatment and Acid Stimulation. Presented at the SPE Improved Oil Recovery Symposium, Tulsa, Oklahoma, 17-21 April. SPE-89394-MS. http://dx.doi.org/10.2118/89394-MS.

Zhao, Y.., Su, H., Fang, L., Tan, T. 2005. Superabsorbent Hydrogels from Poly (Aspartic acid) with Salt-, Temperature- and pH-responsiveness Properties. *Polym J* **46**: 5368–5376. doi:10.1016/j.polymer.2005.04.015.

VITA

Abdulmohsin Hussain Imqam is from Asabaa City, Libya. He received his BS in petroleum engineering from Sirte University, Libya in May 2004. After graduation, he worked as a petroleum engineer for two and half years in National Oil Corporation (NOC). While employed with NOC, Imqam enrolled in the Master's degree program in petroleum engineering at Tripoli University (formerly Al-Fatah University). He received his MS in June 2008.

Imqam has experience in both academia and industry. He served as a senior lecturer in the Petroleum Engineering Department at Gharian University for one year and half. He taught production engineering, reservoir engineering, and fluid mechanics classes. Imqam also worked as reservoir/production engineer in different companies for four years.

Imqam joined University of Missouri Science and Technology for his PhD in January 2011. He received both his PhD. in petroleum engineering and MS in engineering management in August 2015.

He was able to publish several journal and conference papers some of which are listed within the references.